LATERAL LOAD CAPACITY OF DRILLED SHAFTS IN JOINTED ROCK

by

Albert C. To

B.S., University of California, Berkeley (1997)

Submitted to the Department of Civil and Environmental Engineering
in partial fulfillment of the requirements for the degree of

Master of Science
in Civil and Environmental Engineering

at the

MASSACHUSETTS INSTITUTE OF TECHNOLOGY

May 1999

[June, 1999]

Signature of Author.....
Department of Civil and Environmental Engineering

Certified by.....
Herbert H. Einstein
Professor of Civil and Environmental Engineering
Thesis Supervisor

Accepted by.....
Andrew J. Whittle
Chairman, Department Committee on Graduate Studies

LATERAL LOAD CAPACITY OF DRILLED SHAFTS IN JOINTED ROCK

by

Albert C. To

Submitted to the Department of Civil and Environmental Engineering
on May 20, 1999 in partial fulfillment of the requirements for the Degree of Master of Science in Civil and Environmental Engineering

ABSTRACT

Large vertical (axial) and lateral loads often act on the heads of drilled shafts in jointed rock. In current design practice, the p-y curve method used in design of laterally loaded drilled shafts in soil is adopted in the design of such shafts in jointed rock. The p-y curve method treats the soil as a continuum. The continuum model is not applicable to jointed rock, in which the joints form blocks.

A new discontinuum model was developed in this thesis to determine the lateral load capacity of drilled shafts in a jointed rock mass with two and three joint sets. It contains two parts: a kinematic and a kinetic analysis. In the kinematic analysis, the removability theorem of a convex block is expanded to analyze the removability of a block intersecting a pile and the removability of a combination of blocks. Based on these removability theorems, a method was developed to select removable combinations of blocks using easily constructed 2-dimensional figures only.

In kinetics, each selected removable combination of blocks is analyzed with the limit equilibrium approach to determine the ultimate lateral load capacity. Although the analysis is similar to slope stability analysis, it is more complicated with the addition of a lateral force exerted by the pile and the vertical pile load exerted on the wedge. The analysis also considers the weight of the wedge, the shearing resistance along the joints, and the vertical pile load exerted on the wedge. Simple analytical relations were developed to solve for the ultimate lateral load capacity.

Thesis Supervisor: Herbert H. Einstein
Title: Professor of Civil and Environmental Engineering

ACKNOWLEDGEMENTS

This research was made possible through the sponsorship of the Federal Highway Administration (FHWA) and Massachusetts Highway Department (MHD). The help and advice of Ernest Helmut of MHD are greatly appreciated.

I would like to express my gratitude and appreciation to my advisor, Professor H. H. Einstein, for his guidance, support, and encouragement throughout the course of this research work and thesis writing.

I would also like to dedicate this thesis to my dear parents, Ho Kueng To and Siu Fun To, for their understanding and endless support and love.

CONTENTS

LIST OF FIGURES

LIST OF TABLES

CHAPTER 1

INTRODUCTION

1.1 INTRODUCTION

Drilled Shafts in jointed rock are frequently used when the layer of overburden soil is thin and/or the soil strength is low. Large vertical (axial) and lateral loads often act on the heads of the drilled shafts, and thus make the analysis of such shafts important. The method used in common practice to design laterally loaded rock-socketed shafts in jointed rock has adopted the p-y curve method used to design laterally loaded shafts in soil (Matlock, 1970; Amir 1986; Wyllie 1992; Gabr 1993). However, all the applications based on the p-y curve method assume that the soil is a continuum. The assumption is not applicable in jointed rock where joints cut across each other to form wedges. Current design methods do not consider the shearing resistance along the joints when the wedges are acted on by the laterally loaded shafts. Therefore, a new method needs to be developed to treat jointed rock as a discontinuum and to consider the effect of joints.

1.2 GOAL OF RESERACH

The goal of the research is to develop a discontinuum model to calculate the ultimate lateral capacity of drilled shafts in jointed rock. First, the kinematics of the wedges bounded by the joints and the pile is examined using the block theory (Goodman and Shi, 1985). Then the kinetics of the wedges is analyzed by the limit equilibrium approach.

1.3 ORGANIZATION

This introduction is followed by **Chapter 2,** which discusses kinematic analysis from a simple convex block to a non-convex block to a block intersecting a pile to a combination of blocks intersecting a pile. A 2-dimensional graphical method was developed to identify removable combinations of blocks in a rock mass with two and three joint sets. The selected removable combinations are analyzed with limit equilibrium in **Chapter 3**, the kinetics chapter. Finally, **Chapter 4** provides the summary, conclusions, and recommendations for further research.

CHAPTER 2

KINEMATICS

2.1 INTRODUCTION

Joints often exist in rocks in sets at various orientations and cutting across each other to form blocks or wedges. Wedge analysis deals with the stability of these blocks based strictly on their geometry with the following assumptions:

1. All the joint surfaces are perfectly planar.
2. Individual blocks are not deformable.
3. Joint surfaces extend entirely throughout a block.

In designing for the lateral capacity of drilled shafts in jointed rock, wedge analysis can be used to determine the removability of individual blocks close to the shaft. Then with other design parameters including the direction of the applied force, and friction and cohesion of the joints, different combinations of removable blocks can be selected for kinetics analysis.

2.2 REMOVABILITY THEOREM FOR A CONVEX BLOCK

In *Block Theory and Its Application to Rock Engineering* by Goodman and Shi (1985), the removability theorem of a convex block is presented. A block is convex if a straight line between any two points within the block does not intersect any space outside the block. If a straight line does intersect any space outside, the block is said to be non-convex. Figure 2.1 shows an example of a convex block and a non-convex block.

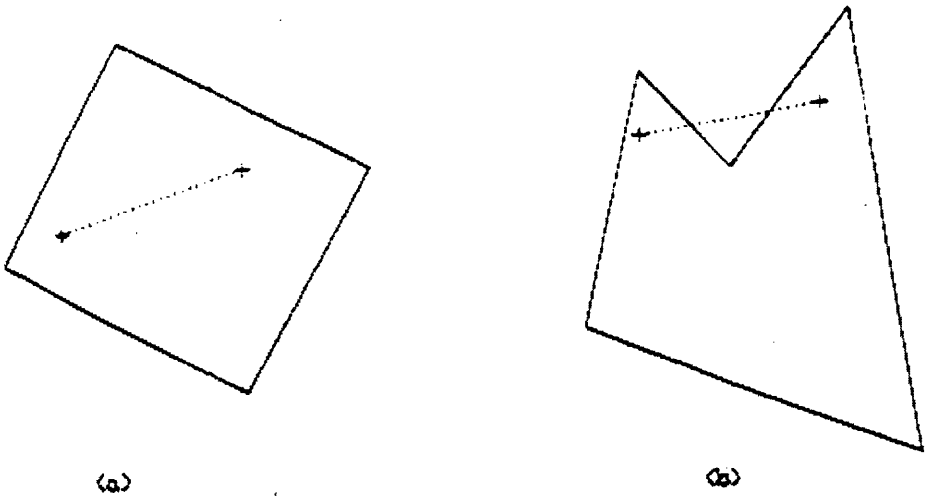

Figure 2.1 (a) A Convex Block; (b) A Non-Convex Block

A block pyramid (BP) is defined by joint-plane half-spaces only or together with free-surface half-spaces. The joint-plane subset of the half-spaces defining the block pyramid is denoted as the joint pyramid (JP). The space pyramid (SP) is defined as the free-surface half-spaces, which are also a subset of the block pyramid half-spaces. Thus, the block pyramid (BP) is the intersection of the joint pyramid (JP) and the space pyramid (SP). Figure 2.2 shows these joint-planes and their respective half-spaces.

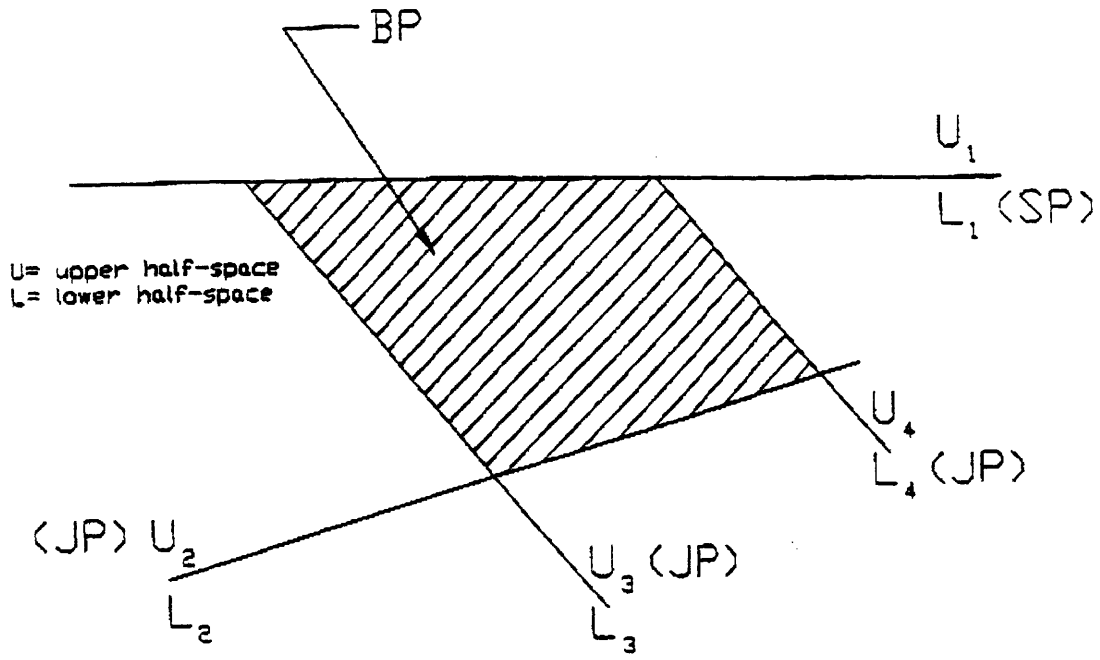

Figure 2.2 A Convex Block (BP) Defined by SP and JP, a Two-Dimensional Example

The criterion for the removability of a convex block is presented as follows:

$$BP = JP \bigcap SP = \varnothing \qquad (2.1)$$

and

$$JP \neq \varnothing \qquad (2.2)$$

Equation (2.1) states that the block pyramid (BP) is empty or finite and equation (2.2) states that the joint pyramid is not empty or infinite. Simply stated, a pyramid is empty if all the planes of the half-spaces defining the pyramid are shifted so that they intersect at a common point and there is no common intersection except this point among all the half-spaces of these planes. In addition to the above graphical method, the emptiness of a pyramid can also be determined by vector analysis or stereographic projections. Figure 2.3 and 2.4 show a two-dimensional example of a removable block and a non-removable block respectively and graphical proofs of their removability.

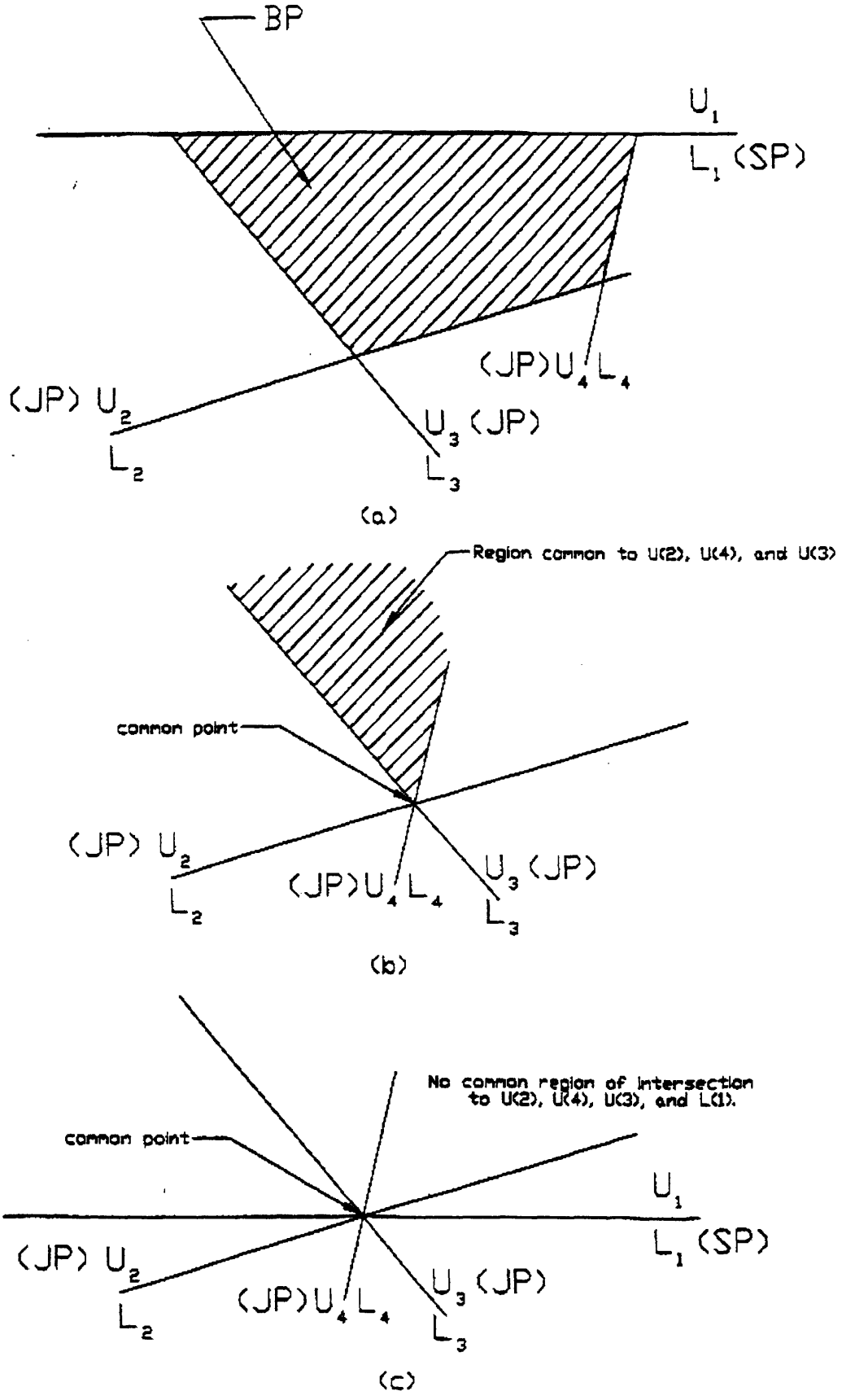

Figure 2.3 (a) A Removable Block; (b) Proof of JP's Non-Emptiness; (c) Proof of BP's Emptiness

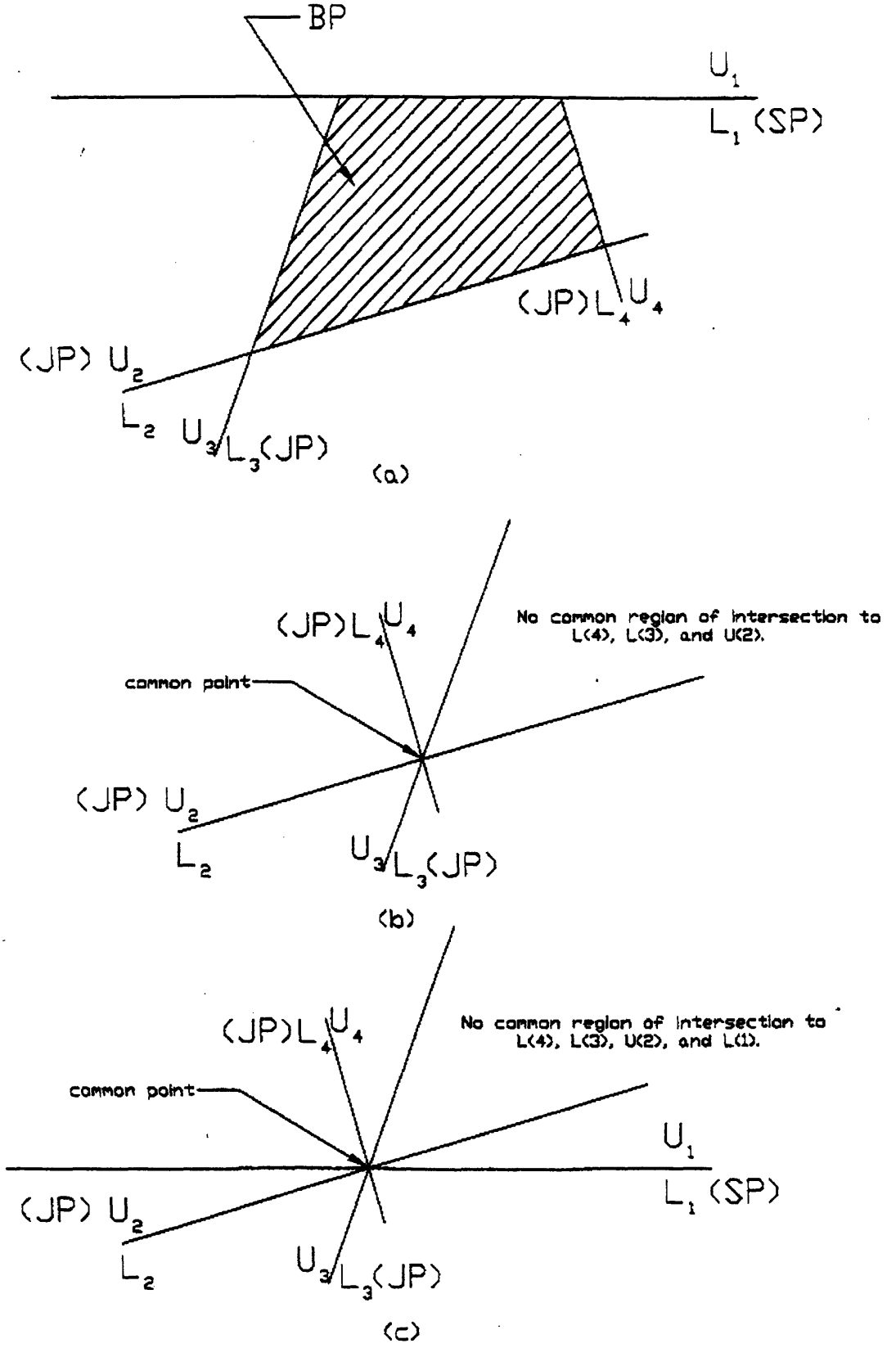

Figure 2.4 (a) A Removable Block; (b) Proof of JP's Emptiness; (c) Proof of BP's Emptiness

2.3 SHI'S THEOREM FOR REMOVABILITY OF A NON-CONVEX BLOCK

Shi (1982) states the removability theorem of a non-convex block as follows:

$$A_i \in B,\ i = 1,...,h \tag{2.3}$$

such that

$$\bigcup_{i=1}^{h} B(A_i) = B \tag{2.4}$$

where B is a non-convex block and $A_1, A_2, ..., A_h$ are convex blocks such that their union forms block B.

The criterion for the removability of a non-convex block is

$$JP(A_i) \bigcap SP(A_i) = \varnothing \tag{2.5}$$

and

$$JP(A_i) \neq \varnothing \tag{2.6}$$

Figure 2.5 shows a figure of a non-convex block B that is decomposed into three convex blocks $B(A_1)$, $B(A_2)$, $B(A_3)$, each is entirely within B. By intuition, the non-convex block B is removable, and the graphical proof is given in Figure 2.6. For each convex block, the JP is not empty because the graphical proof shows a common region for the intersection of the joint plane half-spaces. The BP, which is the intersection of JP and SP, is empty because the proof shows only one common point of intersection. With each convex block satisfying JP's non-emptiness and BP's emptiness, one can conclude that the non-convex united block is removable.

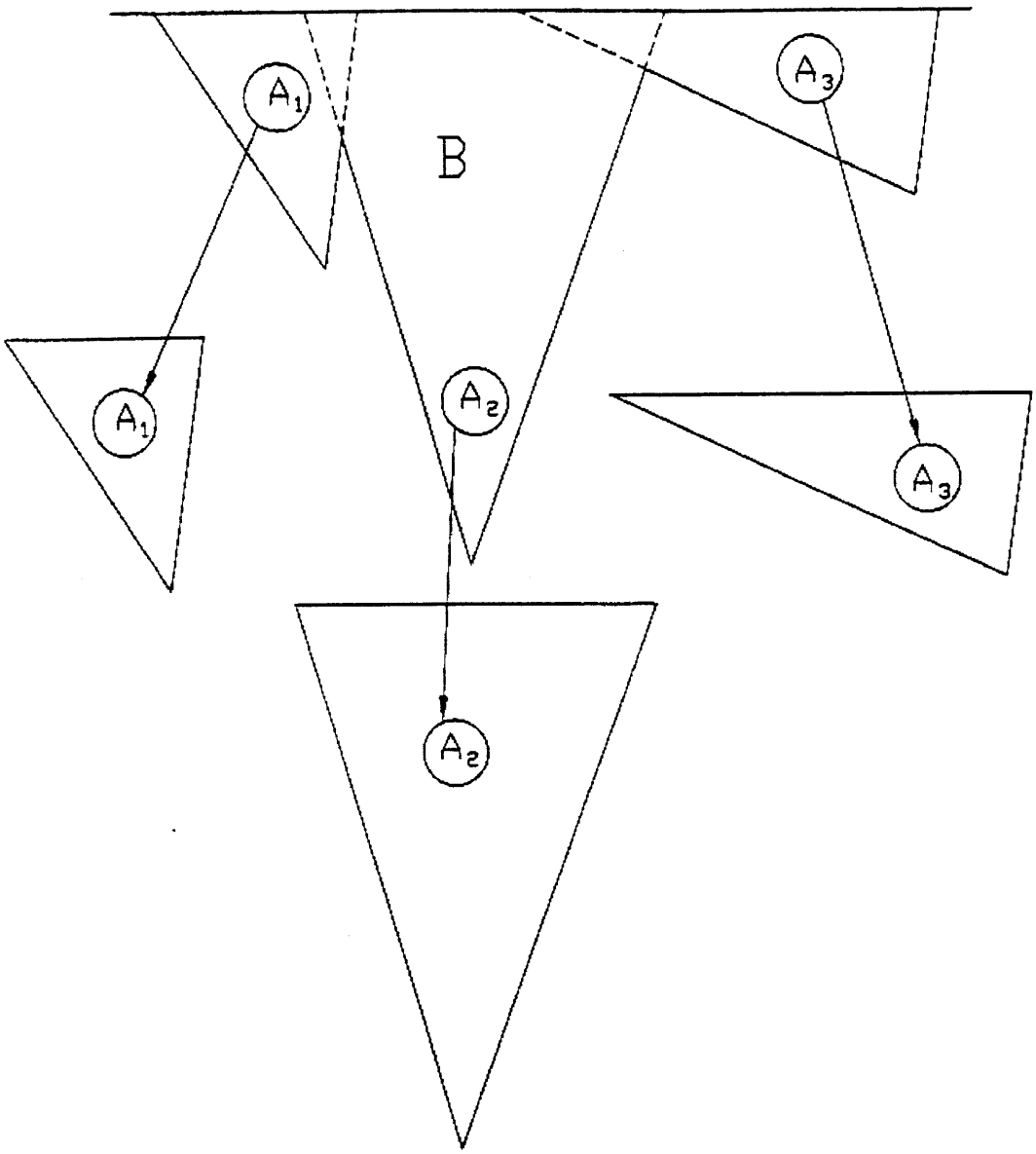

Figure 2.5 Decomposition of a Non-Convex Block

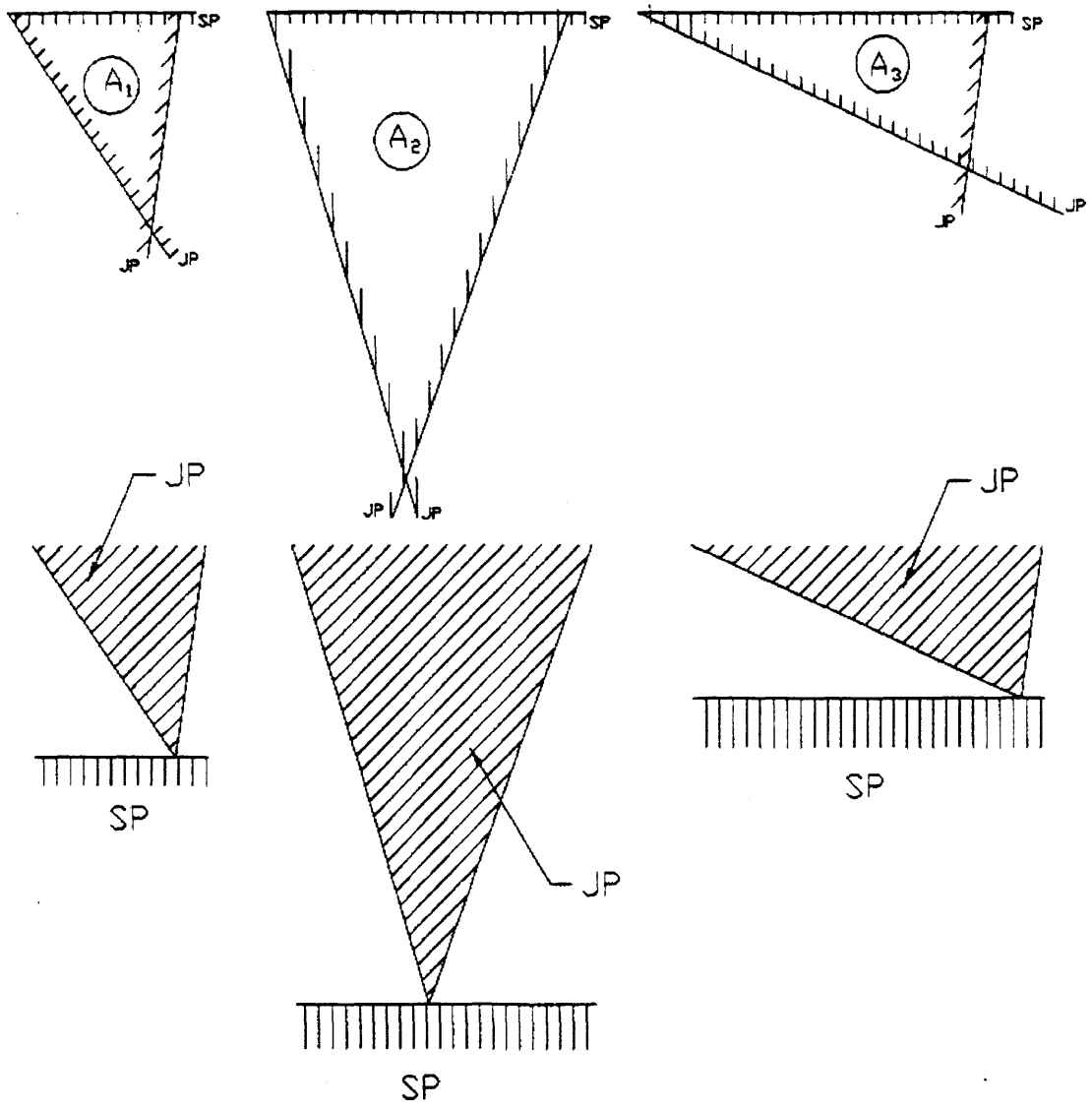

Figure 2.6 Proof of Non-Emptiness of JP and Emptiness of BP of Each Convex Block

2.4 REMOVABILITY OF A BLOCK BY A PILE

In *Block Theory and Its Application to Rock Engineering* by Goodman and Shi (1985), excavation of curved blocks of tunnels has been examined. This approach is similar to analyzing removability of a block by a pile. Since the boundary surface of a block that intersects a pile is a curved surface rather than a flat one, the curved surface is approximated by constructing m tangent planes as shown in Figure 2.7.

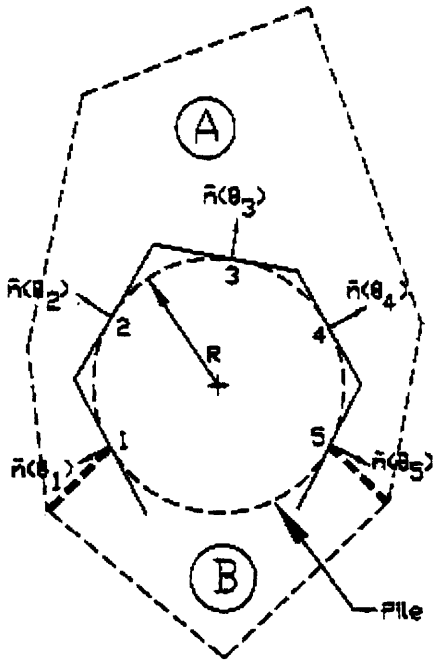

Figure 2.7 Approximation of the Curved Boundary by Five Tangent Planes

First, select m points along the curved boundary, and construct a tangent plane through each point with each tangent plane having a normal vector ň. In a clockwise procedure, denote the normal vectors as $\check{n}(\theta_1)$, $\check{n}(\theta_2)$,..., $\check{n}(\theta_m)$ where θ_i is the angle measured clockwise between $\check{n}(\theta_1)$ and $\check{n}(\theta_i)$. The key to this approximation technique is selecting enough points so that the intersection of the tangent planes can adequately represent the curved surface upon one's judgement.

The union of the upper half-spaces of these m tangent planes forms the pile pyramid (PP)

$$PP = \bigcup_{i=1}^{m} U((\check{n}(\theta_i)) = U(\check{n}(\theta_1)) \bigcup U(\check{n}(\theta_m)) \qquad (2.7)$$

as shown in Figure 2.8 where $U(\check{n}(\theta_i)$ is the upper half-space of the tangent plane defined by the normal vector $\check{n}(\theta_i)$.

For convenience of analyzing the emptiness of the joint pyramid (JP), the pile pyramid (PP) may be treated as a subset of the joint pyramid (JP).

$$PP \subset JP \qquad (2.8)$$

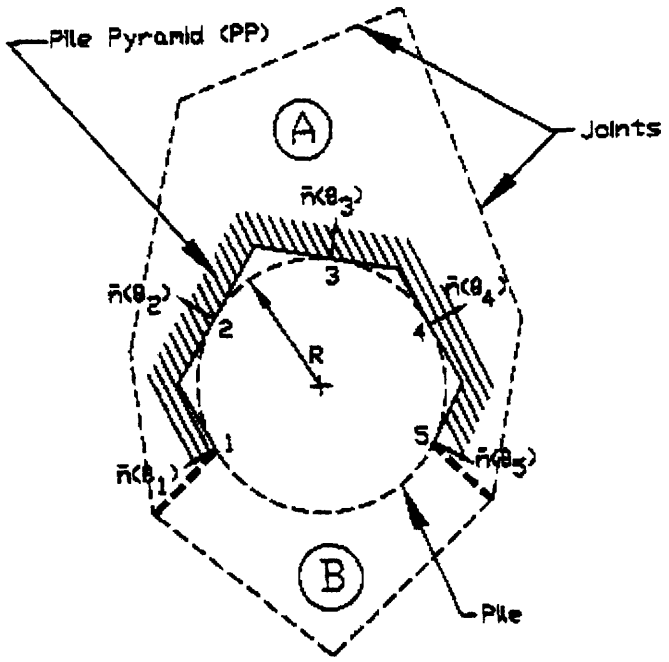

Figure 2.8 Illustration of a Pile Pyramid

Having defined the pile pyramid (PP), the criteria for the removability of a non-convex block that intersects a pile is

$$JP(C_i) \bigcap SP(C_i) = \varnothing \qquad (2.9)$$

and $$JP(C_i) \neq \varnothing \qquad (2.10)$$

and $$\theta_m - \theta_1 \geq 180^\circ \text{ (the "angle" criterion)} \qquad (2.11)$$

where

$$PP \subset JP \qquad (2.12)$$

$$C_i \in D,\ i = 1,...,h \tag{2.13}$$

such that

$$\bigcup_{i=1}^{h} D(C_i) = D \tag{2.14}$$

where D is a non-convex block and $C_1, C_2, ..., C_h$ are convex blocks such that their union forms block D.

The "angle" criterion (equation (2.11)) states that the angle between the normal vectors $\check{n}(\theta_1)$ and $\check{n}(\theta_m)$ must be greater than or equal to 180°. This new requirement allows a pile to move a block without the interference of other blocks around the pile. Figure 2.9 shows an example of a non-convex block (Block A) which satisfies the removability criteria above and another non-convex block (Block B) which satisfies the removability criteria above except the "angle" criterion; each block is in contact with a pile. It is apparent that Block B is non-removable because the pile is being blocked by Block A when the pile tries to move Block B. In contrast, there is no interference by Block B when the pile is moving Block A. Since Block A also satisfies the other criteria in the theorem above, it can be defined as a removable block.

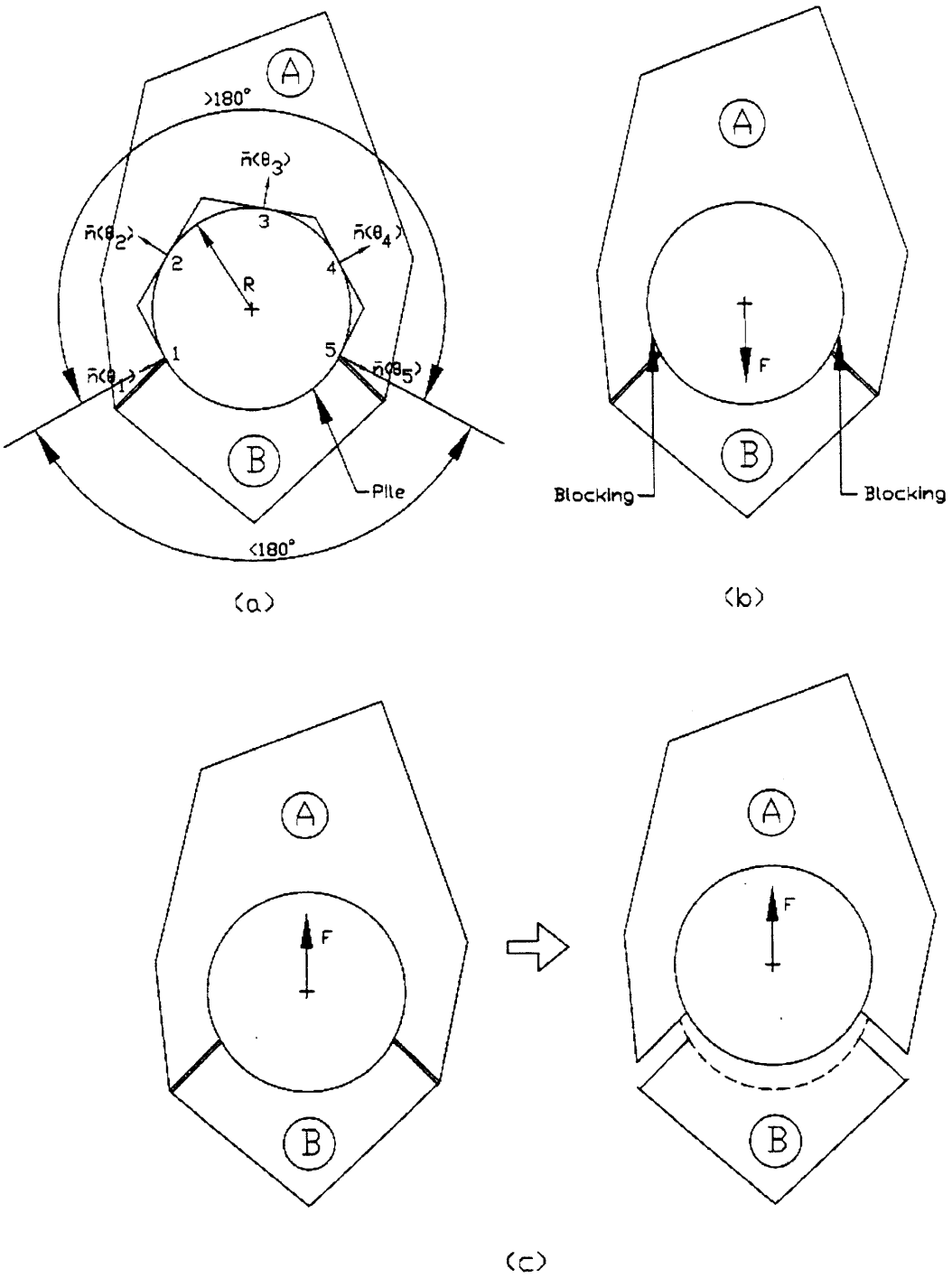

Figure 2.9 Illustration of the "angle" Criterion

2.5 2-DIMENSIONAL GRAPHICAL METHOD

To describe the removability of a combination of blocks, it is necessary to consider the interaction between the pile and its surrounding blocks, the interaction between adjacent blocks, and the direction of force. Since it is very difficult and time-consuming to check the removability of each individual block and it is not easy to gain complete geological information around the pile, some assumptions are made to simplify the problem. Joints in a joint set are assumed to be parallel to each other and have the same spacing, and thus removability can be determined easily. With this assumption, a graphical method can be used to identify combinations of removable blocks. The procedures for using the method and the reasoning underlying the method are presented below.

The 2-D graphical method uses descriptive geometry techniques. First, a plan view of the pile and its surrounding blocks formed by joints is needed, and this drawing is called a joint mesh. Second, a 2-D drawing showing the intersections between the blocks and the pile is used to identify removable blocks since the removal of a combination of blocks results from the interaction between the pile and the blocks intersecting the pile. This drawing is obtained by unfolding the surface of the pile into a plane and mapping all the intersecting joints onto it. This drawing is called a joint map on a pile and can be easily done with CAD programs such as AutoCAD or spreadsheet programs such as Excel. The procedures for making the figures and identifying each intersecting block and its joints are presented below by using CAD programs first and then by using spreadsheets:

1. Figure 2.10a shows the top view, front view, and the development of a pile and a joint. The top view of the pile is divided into 12 equal sectors numbered from 1 to 12. Each joint in the joint set is denoted by a letter (A,B,C,...) for identification purposes. In this example, the pile has a diameter of D and the joint set has a dip of 60 degrees and a horizontal spacing of s. The development of the pile can be thought of as unfolding a right cylinder into a rectangle. The length of the development is

πD. The development is divided into 12 equal sectors numbered from 1 to 12 corresponding to the numbers on the pile in the top view.

2. A hypothetical joint, shown as a dotted line in the figure, is drawn from the upper-left hand corner of the front view of the pile dipping at 60^{o}. This hypothetical joint will be a guide for drawing other joints. Every number on the pile is traced from the top view by the dashed lines to the hypothetical joint on the front view, then onto the corresponding lines on the development of the pile, as indicated by the arrows. When all the corresponding intersection points on the development are connected, the development of the joint is completed.
3. Since the shape of the development is identical for joints with identical dip, other joints can be copied above or below the initial joint development with the correct spacing. The complete development of the joint set is shown in Figure 10b. Such development is called joint map as indicated previously.

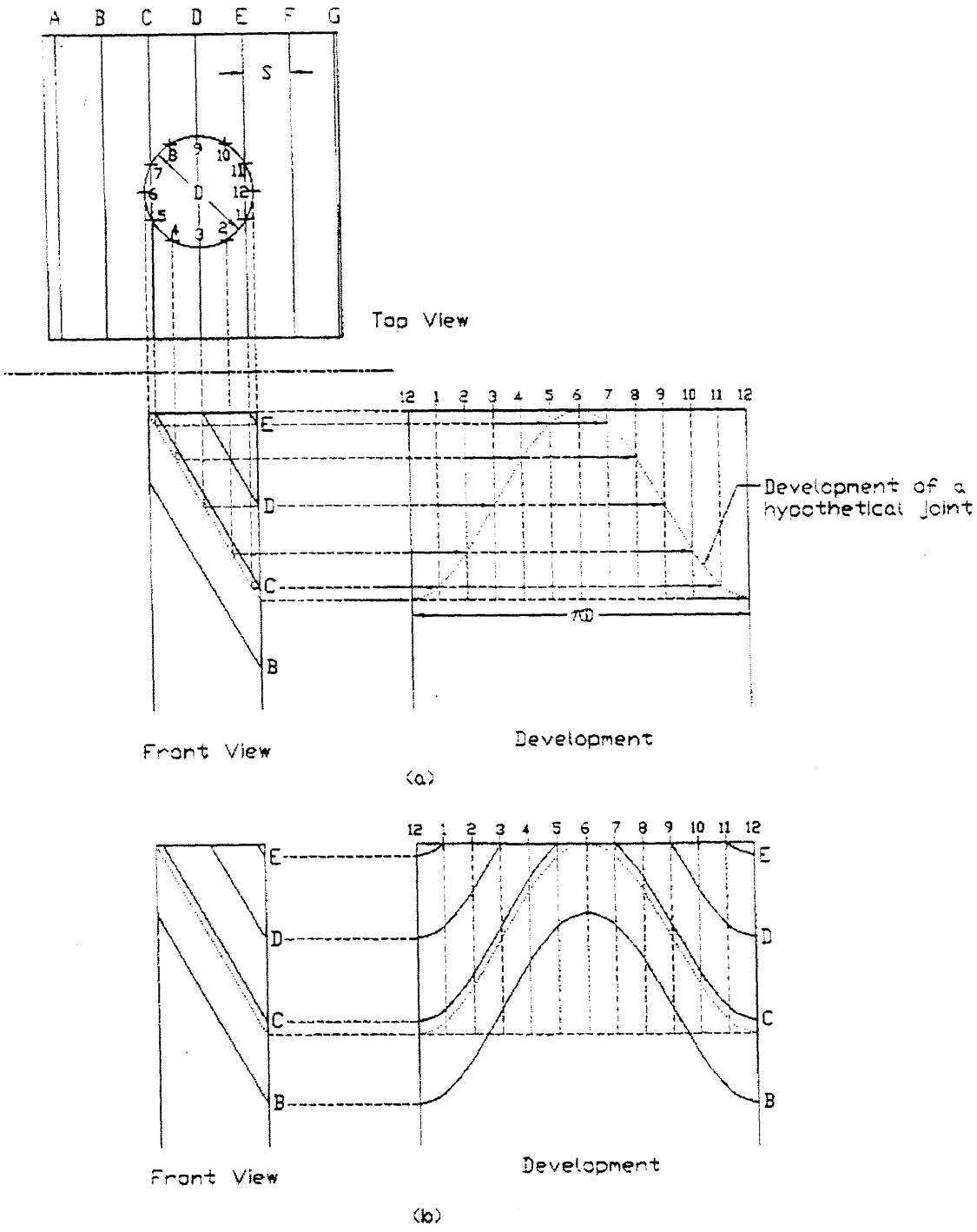

Figure 2.10 Development of a Joint Set on a Pile

When the development of two joint sets with different orientations is combined, the intersections between the blocks and the pile become visible. An example is shown in Figures 2.11 and 2.12, which are a joint mesh and joint map on a pile respectively of a rock mass with two joint sets. The two joint sets have the following orientations respectively: N-S, 30°E and E-W, 60°S. Each joint in the same joint set is denoted by a number or a letter. In Figure 2.12, joints cut across each other to form grids of different shapes. Each grid represents the intersection between a block and the pile. In a two-joint-set system, a block is always formed by a pair of adjacent joints from each joint set, and thus a block is denoted by combining the four codes of the bounding joints. Notice that grids are bounded by two to six joint segments because a block may be partially or entirely intersected by a pile. It is also important to understand the direction that the blocks are dipping. In this case, since one joint set is dipping east and the second is dipping south, the general dip direction of the blocks is southeast.

As shown in Figure 2.13, block 34NO intersects the pile entirely at two different locations because the block is broken into two parts when the pile is installed. Therefore, two grids of 34NO can be found on the joint map in Figure 2.12. Each grid is the area bounded by adjacent joints 3 and 4 from the first joint set and adjacent joints N and O from the second joint set. Block 34NO can be traced onto the surface mesh as grid 34NO, which is shown dotted in Figure 2.11. Since there are technically two separate blocks formed by the same four joints, the way to distinguish and denote them is as follows:

- The block that dips from the surface toward the pile and intersects the pile is called block 34NO(R) where R means removable, and the grid of block 34NO(R) is on the west half of the pile since the block dips southeastward. Since the west half of the pile is between numbers 3 to 9 of the pile in ascending order, grid 34NO(R) is found on the joint map in Figure 2.12 within this range of numbers.
- The other block that dips from the intersection away from the pile is called block 34NO(N) where N means non-removable, and the grid of block 34NO(N) is on the east half of the pile since the block dips southeastward. Since the east half of the pile is between numbers 9 to 3 of the pile in ascending order, grid 34NO(N) is found on the joint map in Figure 2.12 within this range of numbers.

The reason that one block is removable and the other is not will be discussed later.

The grid 45MN is more difficult to interpret because on the joint map it is bounded by two joint segments only. As shown in Figure 2.14, the actual block is bounded by four joints, but it intersects the pile only with two of the four joints. To describe the block, one needs to use all four joints and this is done as follows: if the bounding joint segment is concave up, the adjacent joint of the same joint set forming the block is the joint above it; if the bounding joint segment is concave down, the adjacent joint of the same joint set forming the block is the joint below it. Thus, the grid belongs to the block 45MN, which is bounded by adjacent joints 4 and 5 (concave up) and by adjacent joints M and N (concave down). Grid 45MN is shown dotted in Figure 2.11 and Figure 2.12.

4. For a system with more than two joint sets, the same procedures apply. Later in the thesis, an example of a three-joint-set system will be presented.

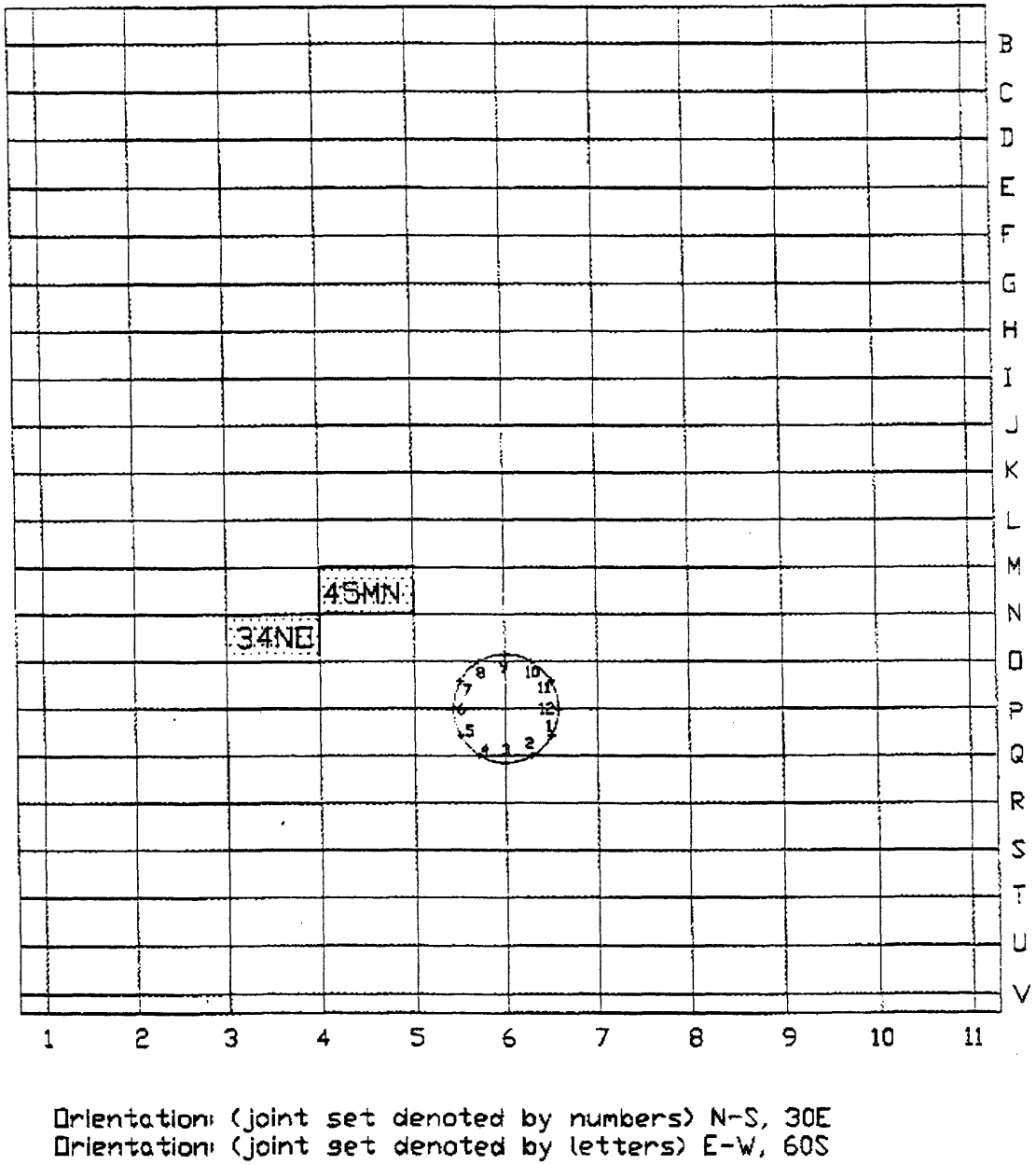

Figure 2.11 Surface Joint Mesh

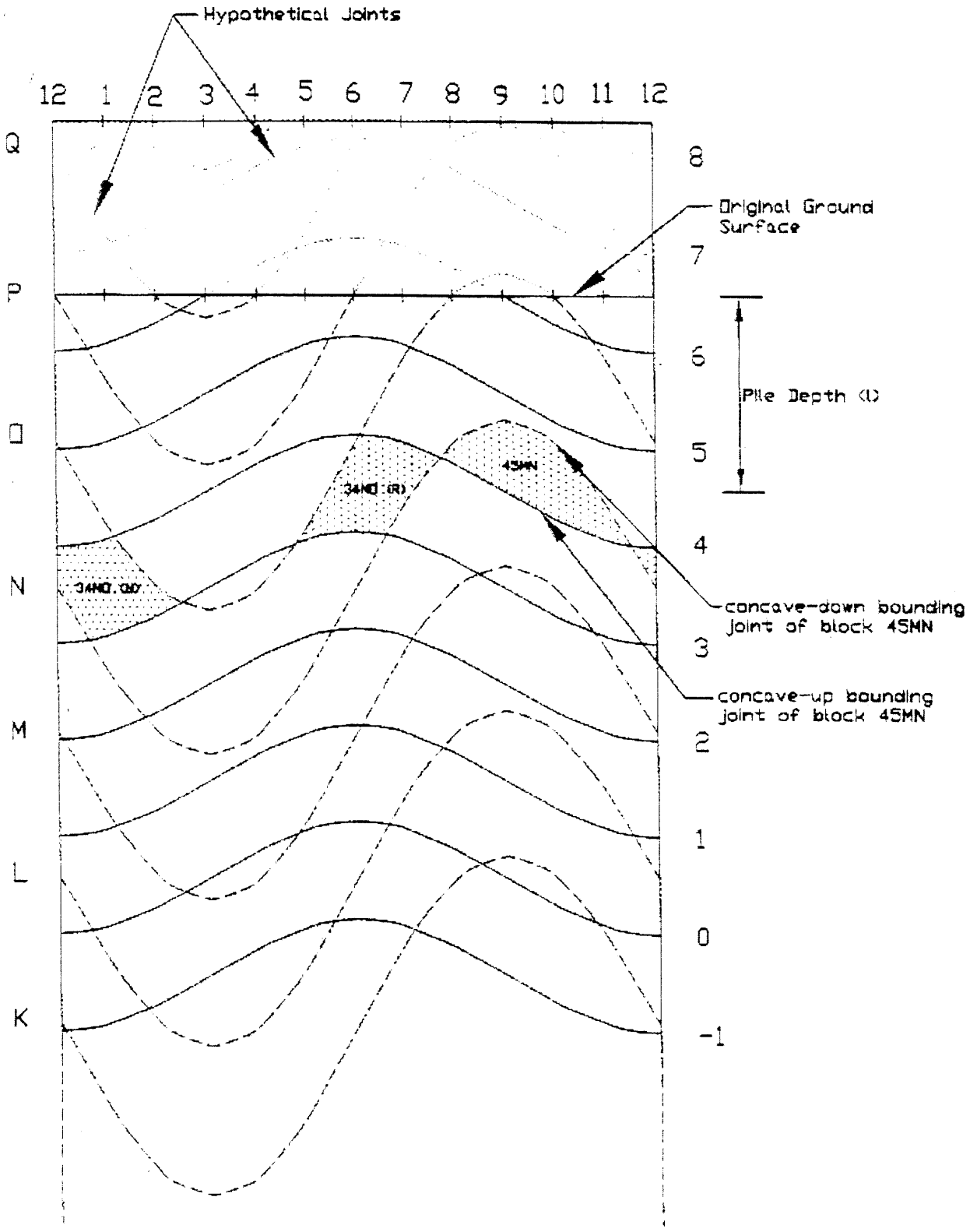

Figure 2.12 Joint Map on a Pile

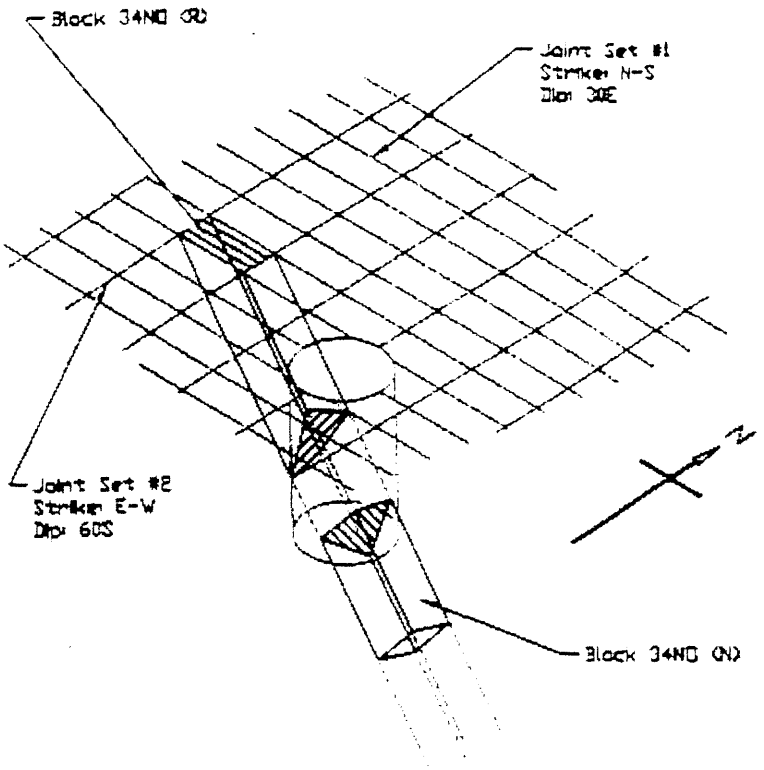

Figure 2.13 Block 34NO in 3D View

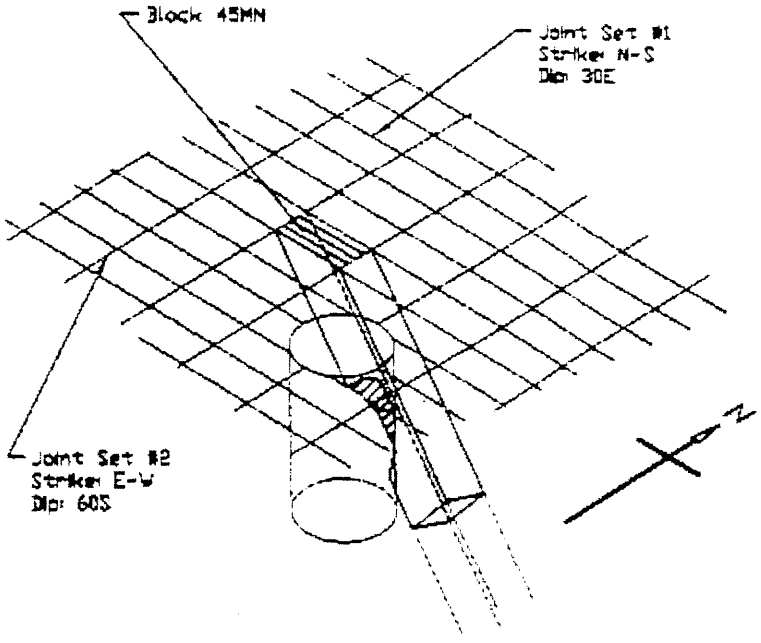

Figure 2.14 Block 45MN in 3D View

The spreadsheet method is proposed by Helmut Ernst from the Massachusetts Highway Department (MHD). In this method, joints are described by equations and can then be plotted in a spreadsheet program. The procedures are as follows

1. Define γ as the dip angle and β as the angle measured counterclockwise from the positive x axis to the strike line in the x-y-z coordinate system as shown in Figure 2.15. Define θ as the azimuth angle (0^{o}-360^{o}) beginning from the East (x-direction) in a clockwise direction, D as the diameter of the pile, and s as the horizontal spacing.
2. A joint on a surface mesh is described by the following linear equation in the x-y plane:

$$y=\tan\beta \bullet x+n \bullet s/\cos\beta \qquad (2.12)$$

where tan β is the slope of the joint and $s/\cos\beta$ is the distance between each joint in the y-direction as shown in Figure 2.16. n is a joint number, which is an integer and starts at 0 for the joint passing through the origin (0,0) or the center of the pile. For each increment of $\pm n$, the joint shifts a distance of $\pm n \bullet s/\cos\beta$ in the y direction. Thus, For n=1 and n=–1, the joint lies immediately above and below the n=0 joint respectively. An example of a surface joint mesh is shown in Figure 2.17 for a joint set with an orientation of N45°E, 45°SE.

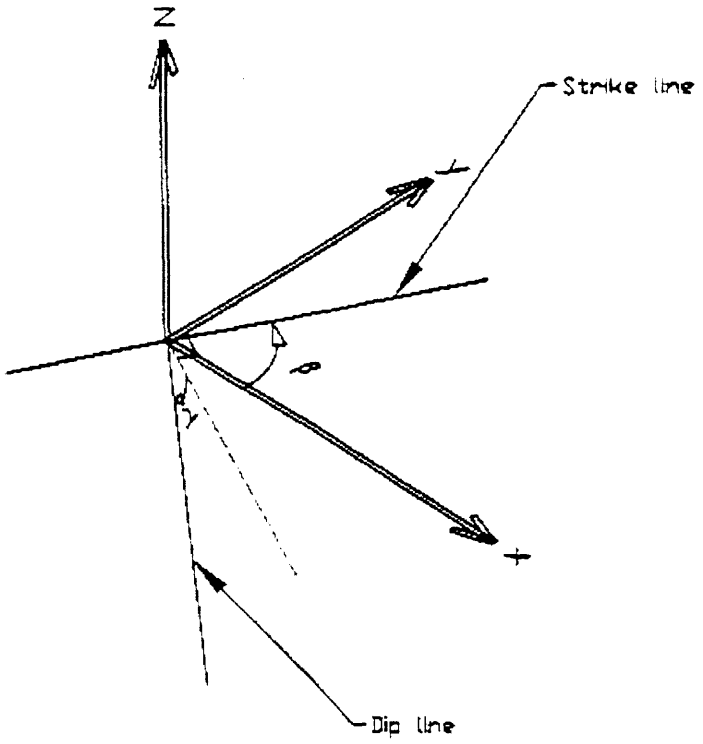

Figure 2.15 Dip and Strike Lines

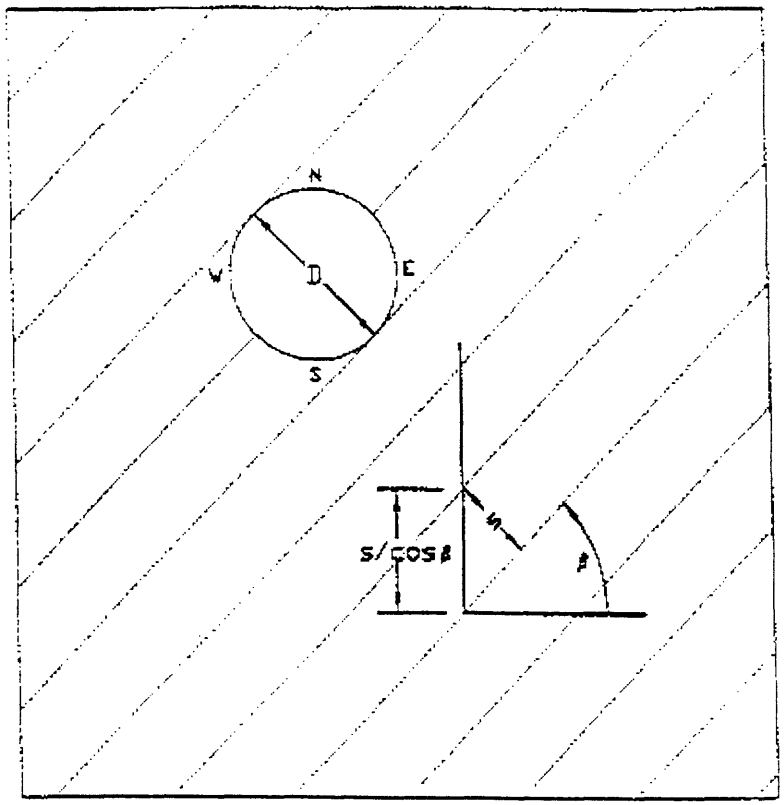

Figure 2.16 A Surface Mesh

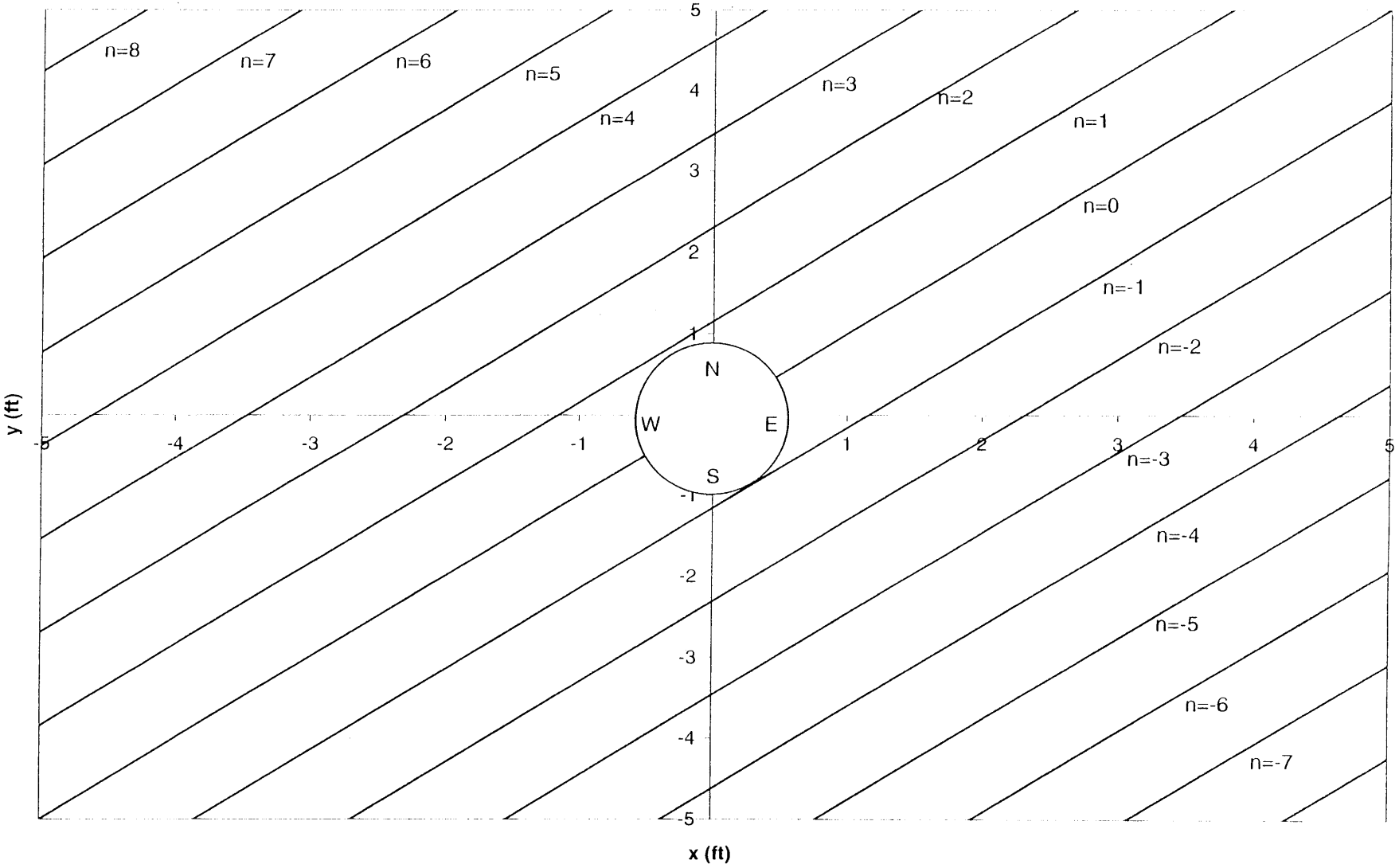

Figure 2.17 Construction of a Joint Mesh Using Spreadsheet

3. Since the intersection between a joint and a circular pile is a conic section as shown in Figure 2.18, the development of an intersection of a joint on a pile can be described by a sinusoidal function. The function is as follows:

$$z=0.5\bullet D\tan\gamma\bullet\cos(\theta+\beta-270^{o})-n\bullet s\bullet\tan\gamma \qquad (2.13)$$

where z is the vertical distance measured from a point on the joint to the surface, n is a joint number and is an integer, $D\tan\gamma$ is the distance between the maximum point and minimum point on the curve and $s*\tan\gamma$ is the vertical distance between adjacent joints as shown in Figure 2.19. For a particular D, γ, β, s, and n, by varying θ from 0^{o} to 360^{o}, a curve in the θ-z plane is generated for the development of an intersection between the joint and the pile shown as a solid curve in Figure 2.20. The variable n corresponds to the n used in equation (2.12); i.e., for n=0, the joint passes through the center of the pile. For each increment of $\pm$n, the joint development shifts a distance of $\pm n\bullet s\bullet\tan\gamma$ in the z direction. For example, as shown in Figure 2.20, the dashed curve has a joint number n=k, and thus it shifts a distance of $k\bullet s\bullet\tan\gamma$. An example of a joint map on a pile is shown in Figure 2.21 for the same joint set used above.

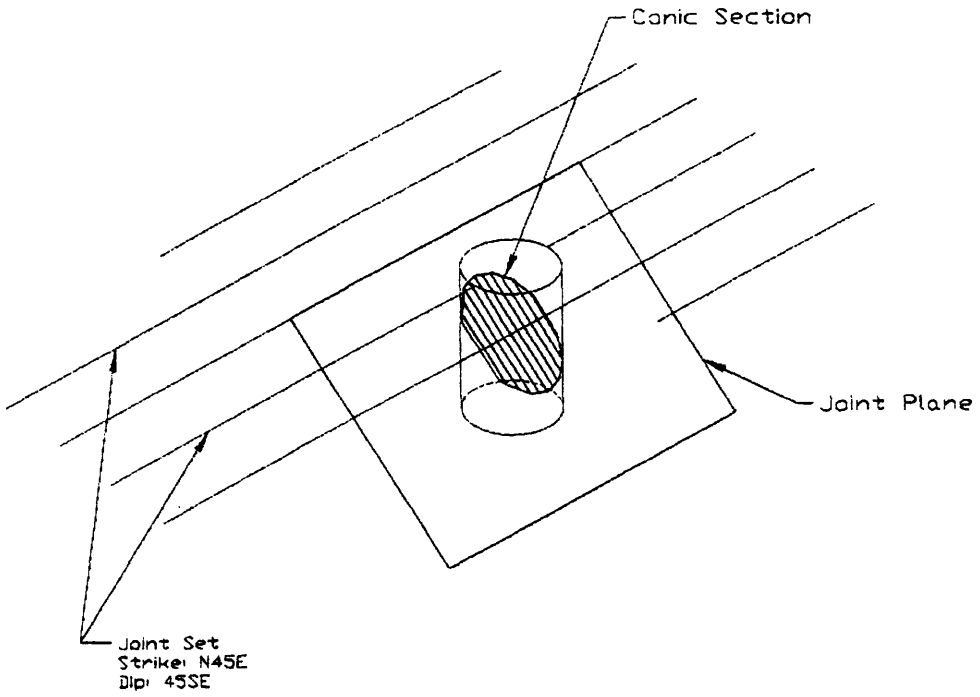

Figure 2.18 Intersection of a Joint on a Pile

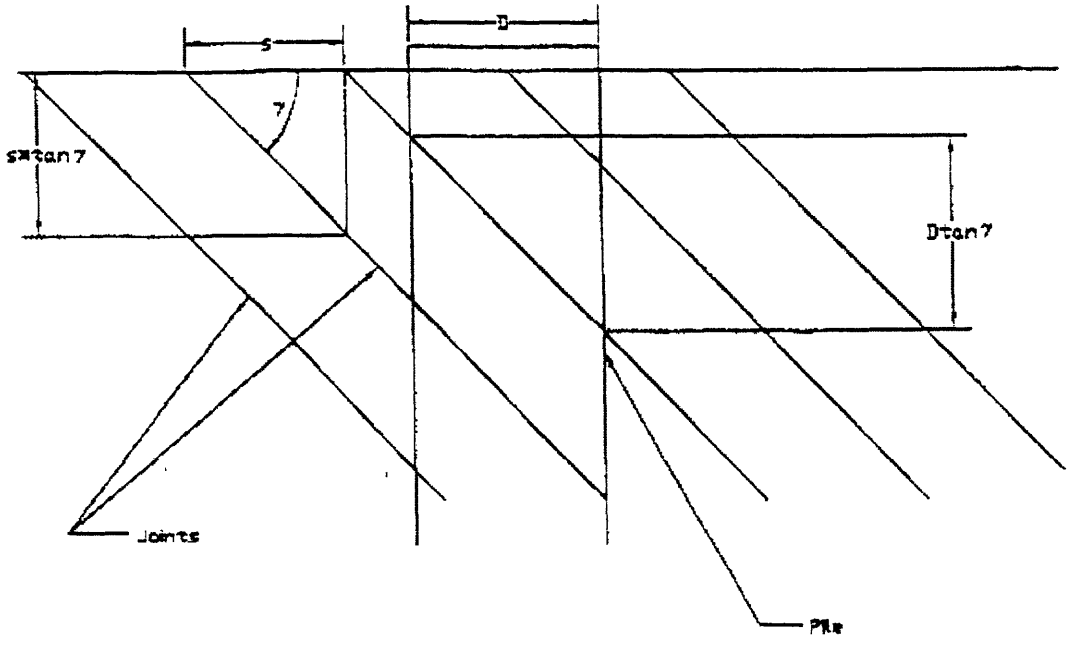

Figure 2.19 Cross Section (Perpendicular to the Joint Strike Line) of a Rock Mass

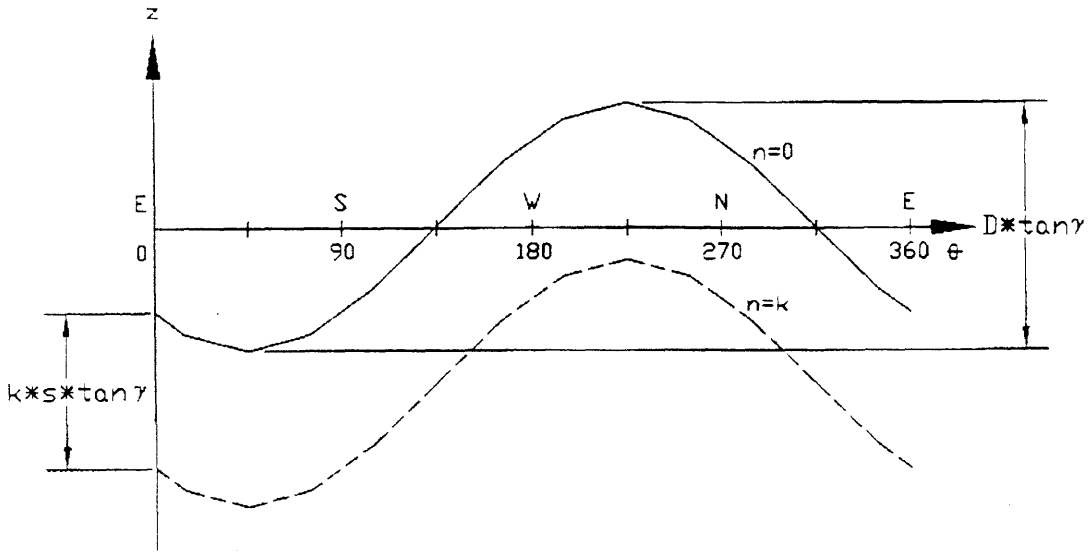

Figure 2.20 Joint Development on a Pile by Using Spreadsheets

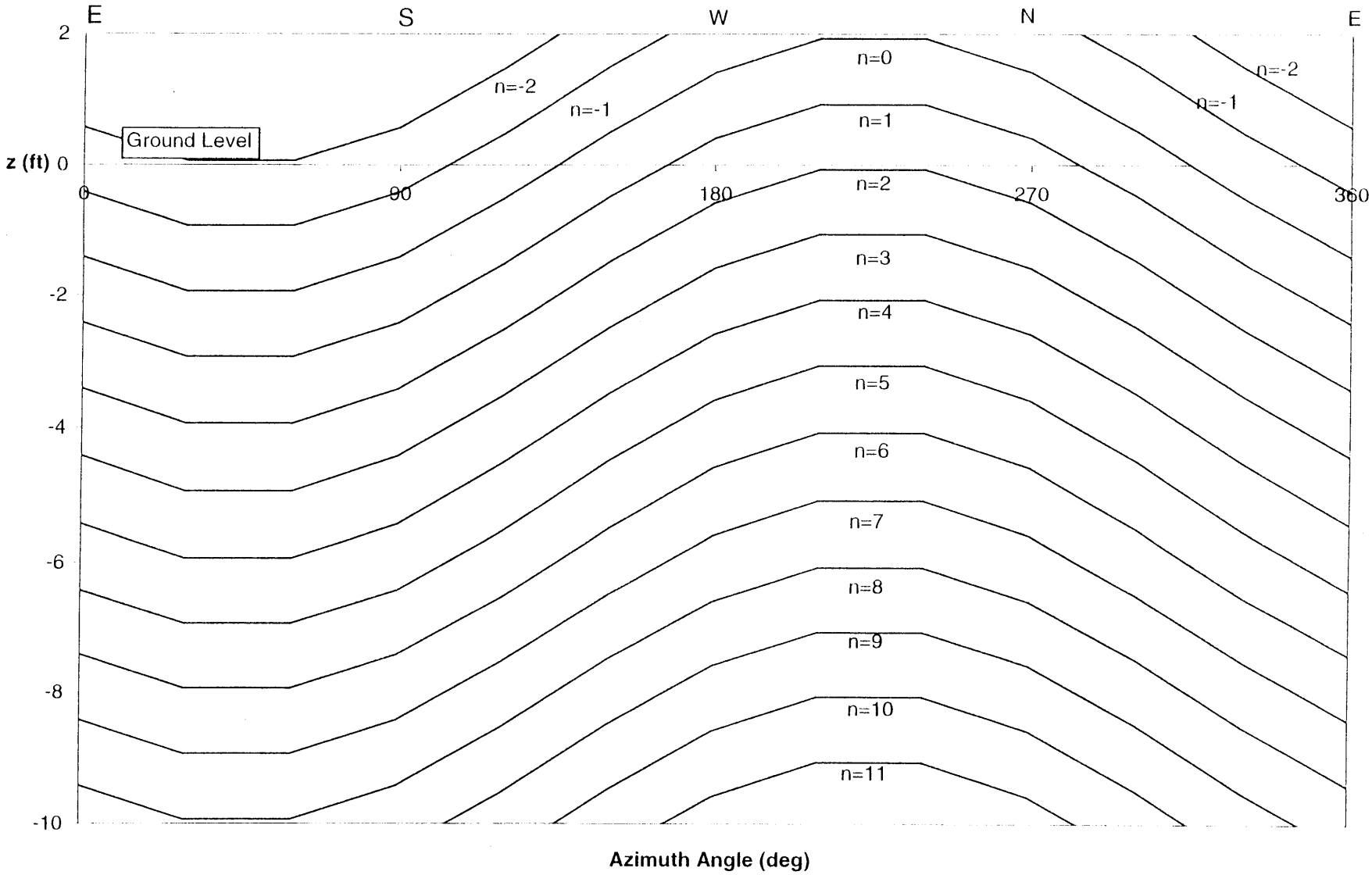

Figure 2.21 Construction of a Joint Map on a Pile by Using Spreadsheet

2.6 REMOVABILITY OF A COMBINATION OF BLOCKS BY A PILE

The removability theorem of a non-convex block and the removability theorem of a block by a pile are extended to the removability of a combination of blocks by a pile. According to the two theorems, a combination of blocks is removable if each individual block in the combination is removable and if the combination as a whole satisfies the "angle" criterion. Therefore, the removability theorem of a combination of blocks by a pile is as follows:

$$C_j \in D,\ j = 1,....h \tag{2.14}$$

such that

$$\bigcup_{j=1}^{h} D(C_j) = D \tag{2.15}$$

where D is a combination of blocks $C_1, C_2, ..., C_h$ such that their union forms D.

The criterion for the removability of a combination of blocks by a pile is

$$JP(C_j) \bigcap SP(C_j) = \varnothing \tag{2.16}$$

and $$JP(C_j) \neq \varnothing \tag{2.17}$$

and $$\theta_m - \theta_1 \geq 180^\circ \text{ (the "angle" criterion)} \tag{2.18}$$

Figure 2.22 shows a combination of seven removable blocks $C_1, C_2, \ldots, C_7$ and the normal vectors $\check{n}(\theta_1), \ldots, \check{n}(\theta_7)$ of the approximated tangent planes of the pile. The "angle" criterion requires that a combination of blocks must encompass at least half of the pile at any depth, not only on the surface. Notice that blocks C_2, C_3, C_4, and C_5 satisfy the "angle" criterion on the surface because they encompass more than half of the pile. However, Figure 2.23 shows a 3D view of this same combination of removable blocks not satisfying the angle criterion at all depths. Notice that when the pile is moving these removable blocks, other blocks around the pile block its way out. Thus, this combination of blocks C_2, C_3, C_4, and C_5 is not removable.

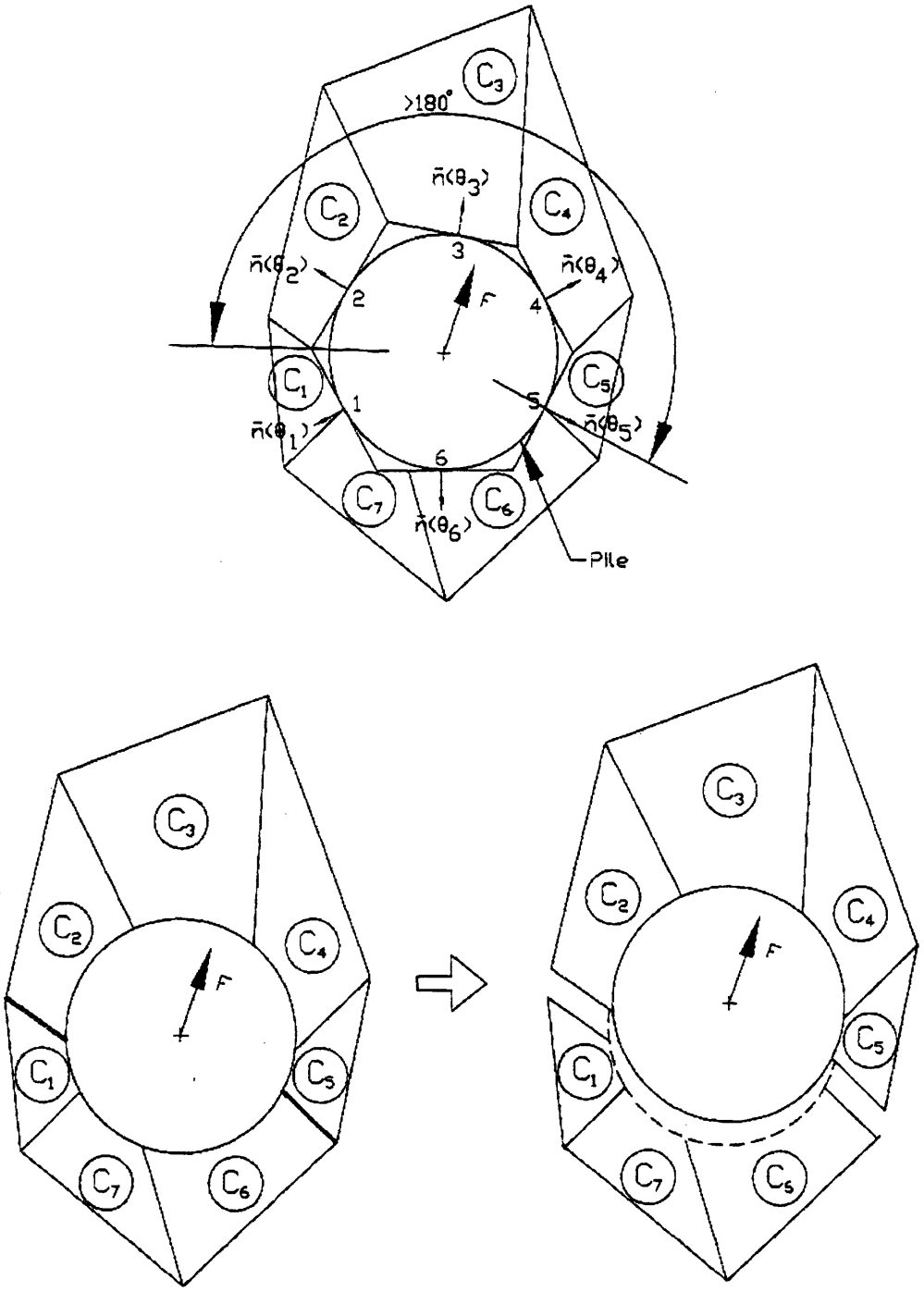

Figure 2.22 Illustration of the "angle" Criterion

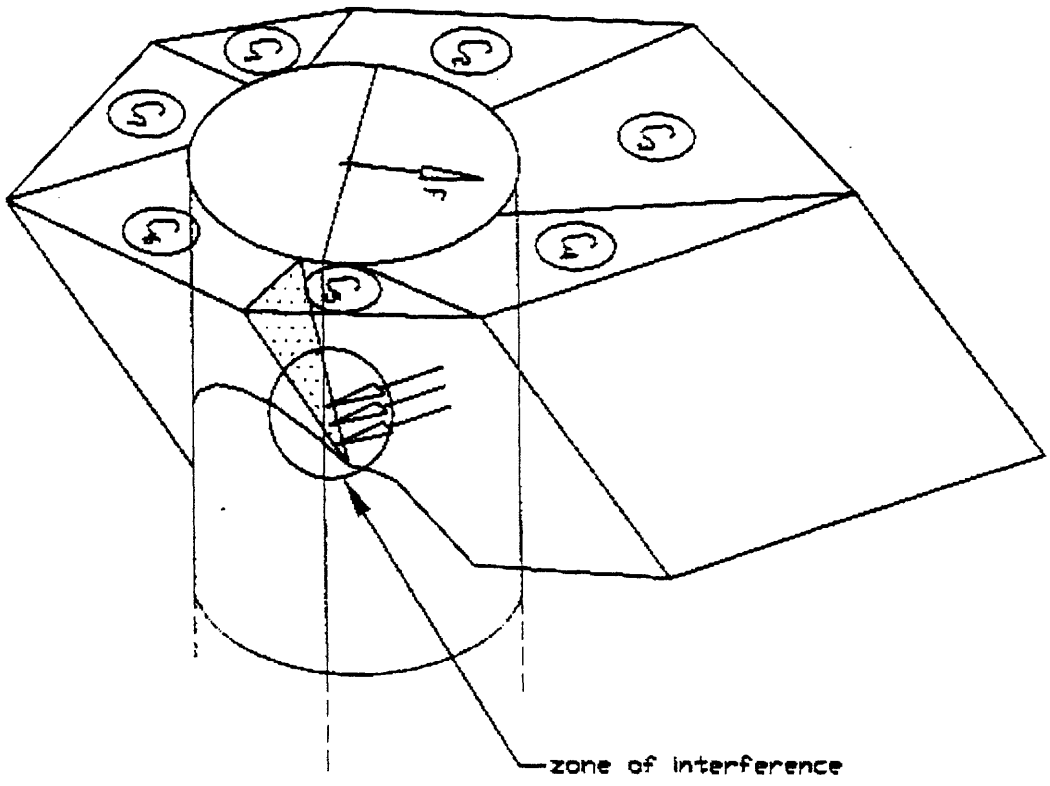

Figure 2.23 Illustration of the "angle" Criterion in 3D View

The direction of the lateral force is critical in the identification of the combination of removable blocks. As shown in Figure 2.24, when a force acts on a pile, only half of the pile in front of the force acts on the blocks, and the pile surface that applies force onto the blocks is called the area of influence. This area of influence is geometrically defined as the half pile surface that is cut off by a vertical plane perpendicular to the force direction. In the identification of removable combination of blocks by using joint map, only the blocks that intersect the area of influence are selected. This satisfies the "angle" criterion mentioned before because it requires that a combination of blocks must encompass at least half of the pile.

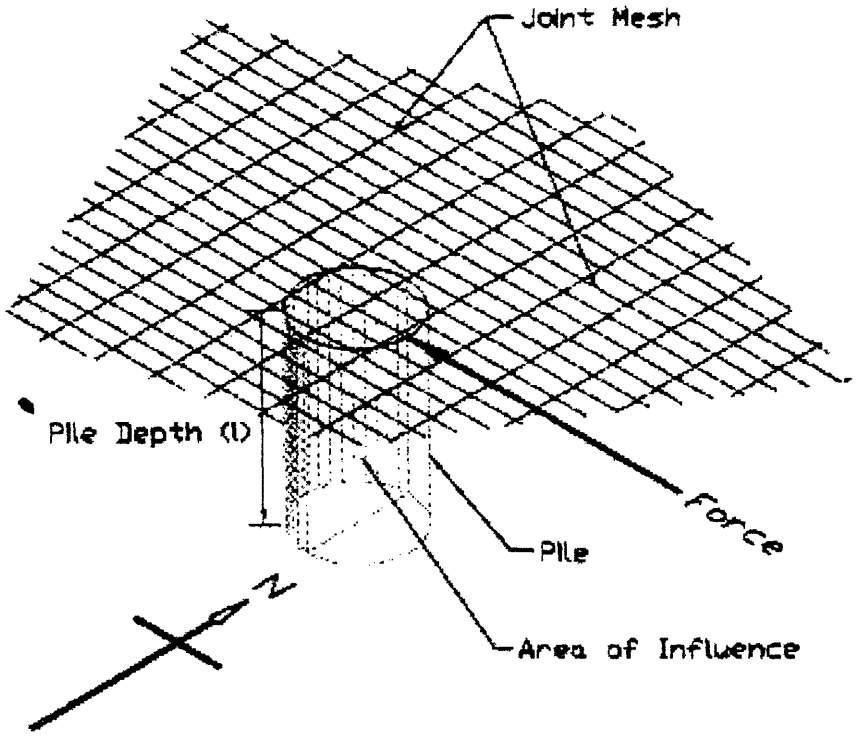

Figure 2.24 Area of Influence

2.7 SELECTION OF A REMOVABLE COMBINATION OF BLOCKS IN A 2-JOINT-SET SYSTEM

Assuming that joints in a joint set are assumed to be parallel to each other and have the same spacing, the removability of each individual block can be determined efficiently. Figures 2.25a-e show six basic types of blocks in a two-joint-set system used in the preceding example in Chapter 2.5. Figure 2.26 shows the grids of these blocks on the joint map. According to the removability theorem of a block, a block is removable if it satisfies BP = ∅ and JP ≠ ∅. As mentioned before, removability can be proved graphically or algebraically. However, if a block satisfies BP = ∅ and JP ≠ ∅, conceptually it is a finite block that can be displaced out of its original place into open space (i.e. above ground surface) without any interference. This concept will be followed in determining the removability of different types of blocks below.

A Type I block is defined as a block that dips toward the pile from the surface and intersects the pile entirely. For example, block 34NO(R) is a Type I block as shown in Figure 2.25a. On the joint map in Figure 2.26, grid 34NO(R) is bounded by four joints and has four vertices, and thus block 34NO(R) intersects the pile entirely. It is removable because (1) it is a finite block since it intersects the pile entirely and (2) the two adjacent joints from each joint set are parallel and the top face of the block is open to open space so that the block can be displaced without any interference.

A Type II block is defined as a block that intersects the pile partially. It can intersect the pile partially with two to four joints. As shown in Figure 2.25b, block 45MN is a Type II block that intersects the pile partially. Notice that the intersection between the block and pile is bounded by two joints. Thus, as shown in Figure 2.26, its grid is bounded by two joints. The block is not removable because (1) the block does not have finite length and (2) the block cannot be displaced without interference since the pile is blocking the block movement at part of the intersection as indicated in Figure 2.25b. However, assuming that a Type II block breaks apart right above the interference area when the pile is acted on by a force, the top part of the block becomes removable. The top part of the block satisfies the removability theorem because (1) it has finite length since it breaks apart from the original block; (2) the pile is no longer blocking its

way out: (3) the two adjacent joints from each joint set are parallel and the top face of the block is open to open space so that it can be displaced without any interference.

A Type III block is defined as a block that intersects the pile entirely but beings dipping from the intersection with the pile. For example. block 34NO(N) in Figure 2.25a is a Type III block since it intersects the pile entirely but begins dipping away from the intersection with the pile. Its grid is bounded by four joints and has four vertices as shown in Figure 2.26. A Type III block is not removable because (1) it does not have finite length and (2) no face of the block is open to open space.

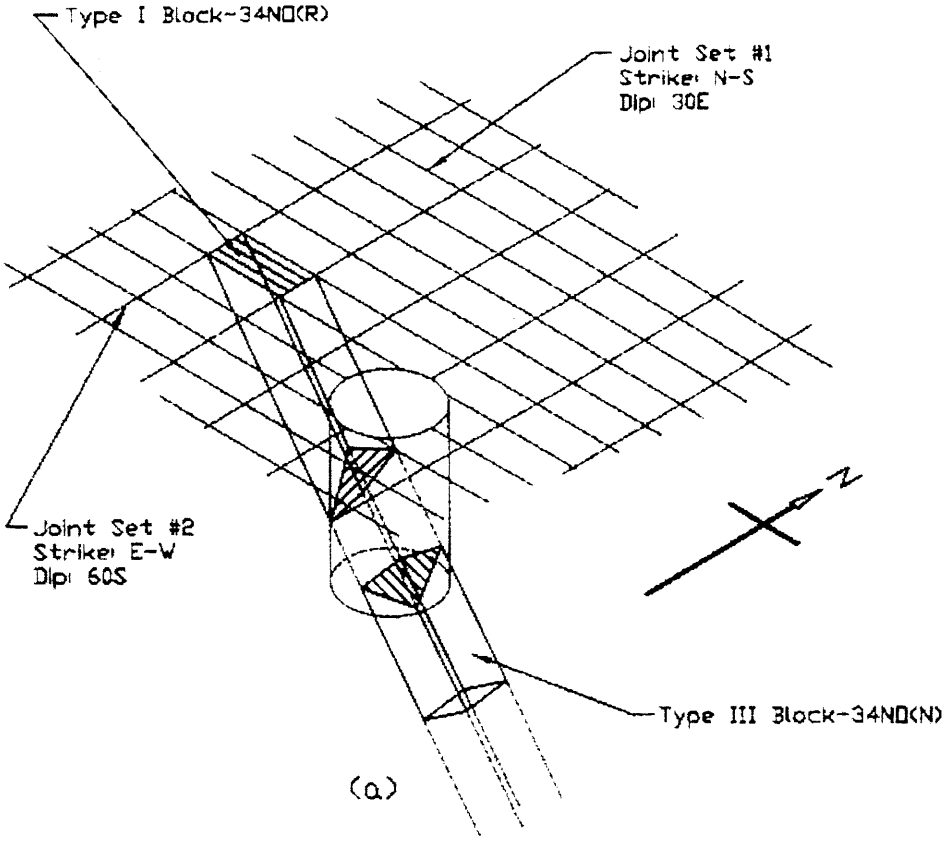

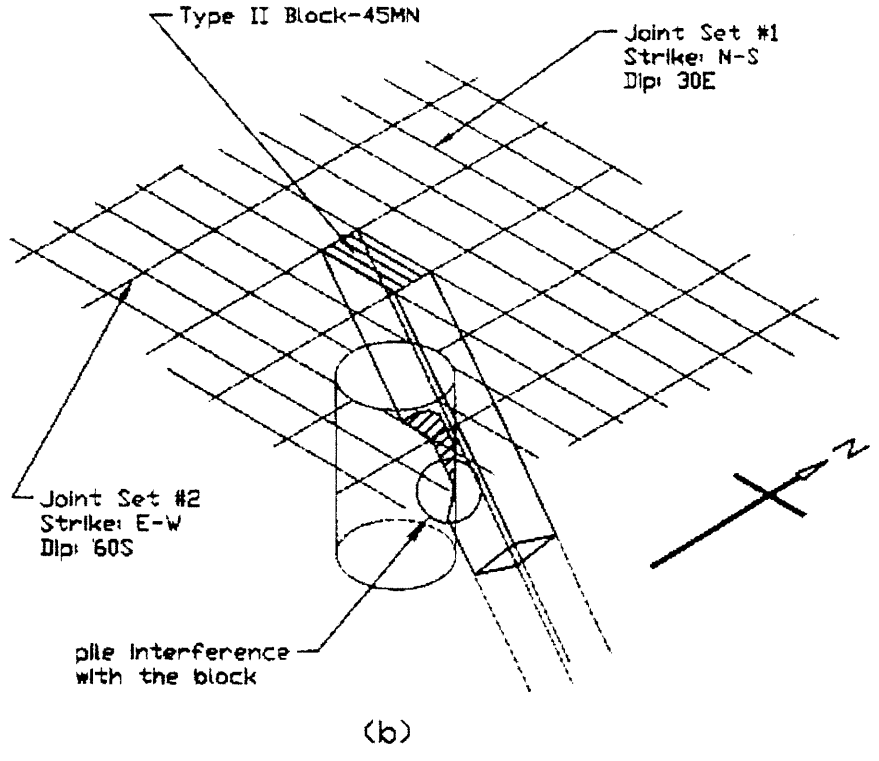

Figure 2.25 Basic Types of Blocks

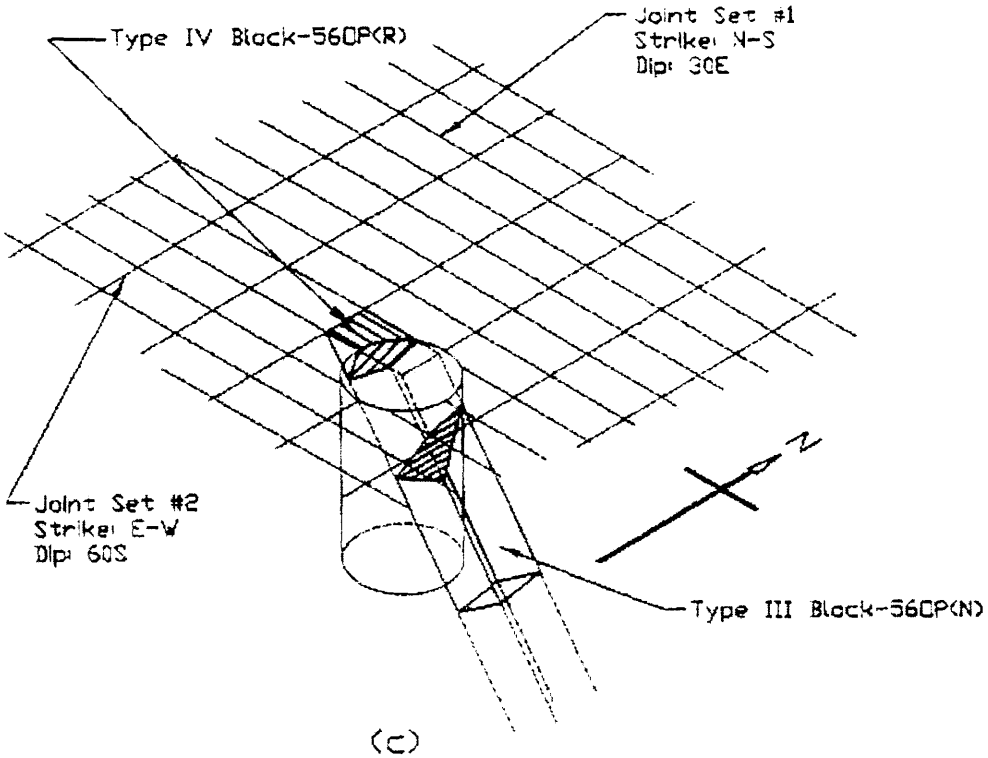

(c)

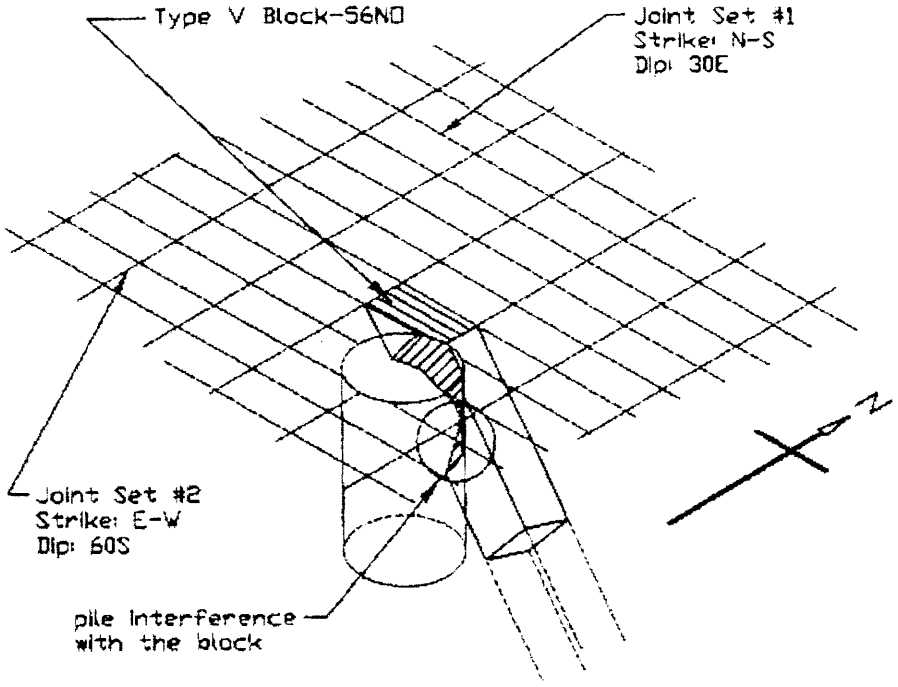

(d)

Figure 2.25 Basic Types of Blocks

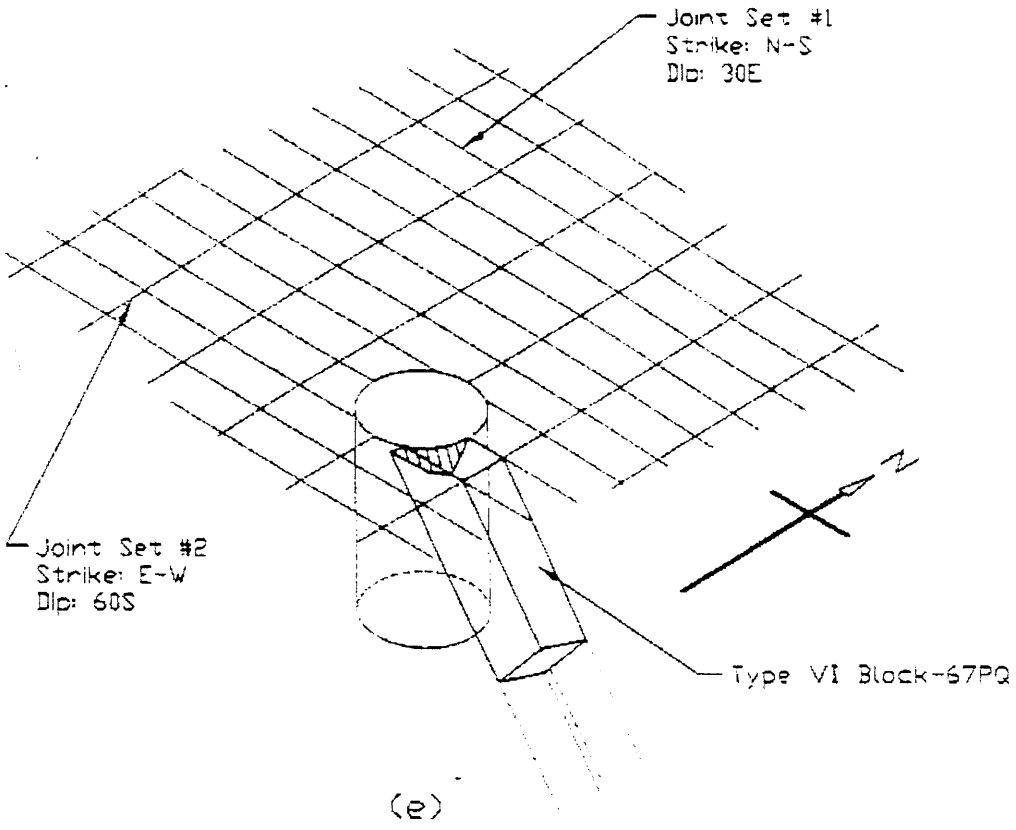

Figure 2.25 Basic Types of Blocks

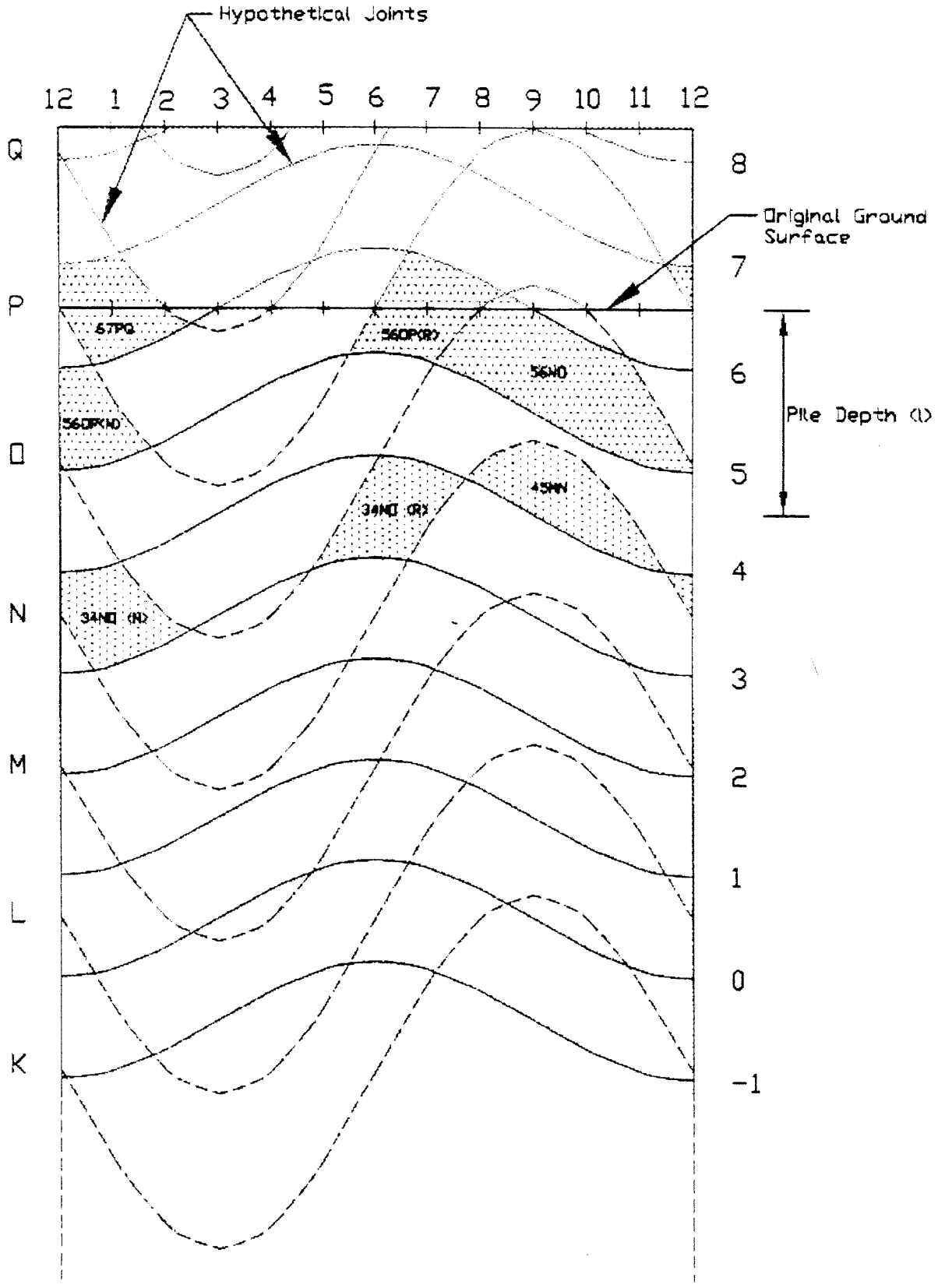

Figure 2.26 Joint Map on a Pile

The removability of the blocks that intersects the pile on the surface is tricky to determine because the grids of these blocks are also bounded by the ground surface line in addition to the joints. According to the removability theorem, the removability of a block does not change as long as the orientation of the bounding joints and ground surface do not change even if the location of them changes. Therefore, the way to determine the removability of these blocks is to use hypothetical joints above the ground surface on the joint map. These hypothetical joints are obvious when the ground surface is raised as shown on the joint map in Figure 2.26. The procedure is identical for determining the removability of Type I, II, and III b locks as discussed before.

A Type IV block, similar to a Type I block, is defined as a block that intersects the pile entirely on the surface and dips toward the pile from the surface. For example, block 56OP(R) is a Type IV block as shown in Figure 2.25c. Notice that 56OP(N) in the same figure was part of the original 56OP block and is now a Type III block that is not removable. On the joint map in Figure 2.26, its hypothetical grid is bounded by four joints and has four vertices, and thus block 56OP(R) intersects the pile entirely. It is removable because (1) it has finite length since it intersects the pile entirely and (2) the two adjacent joints from each joint set are parallel and the top face of the block is open to open space so that the block can be displaced without any interference.

A Type V block, similar to a Type II block, is defined as a block that intersects the pile partially with two to four joints on the surface. For example, block 56NO in Figure 2.25d is a Type II block that intersects the pile with three joints. Notice that its hypothetical grid is bounded by three joints as shown in Figure 2.26. The block is not removable because (1) the block does not have finite length and (2) the block cannot be displaced without interference since the pile is blocking the block movement at part of the intersection as indicated in Figure 2.25d. However, assuming that a Type V block breaks apart right above the interference area when the pile is acted on by a force, the top part of the block becomes removable. The top part of the block satisfies the removability theorem because (1) it has finite length since it breaks apart from the original block; (2) the pile is no longer blocking its way out; (3) the two adjacent joints from each joint set are parallel and the top face of the block is open to open space so that it can be displaced without any interference.

A Type VI block, similar to a Type III block, is defined as a block that intersects the pile entirely on the surface but dips away from the intersection with the pile. As shown in Figure 2.25e, block 67PQ is a Type VI block because it intersects the pile entirely but dips away from the intersection with the pile. Notice that its hypothetical grid is bounded by four joints and has four vertices as shown in Figure 2.26. A Type VI block is not removable because (1) it does not have finite length and (2) no face of the block is open to open space.

A summary of the types of blocks are shown in the table below:

Table 2.1 Type of Blocks

Type of Block	Characteristics	Removability
I	Block dips toward the pile from the surface and intersects the pile entirely.	Removable
II	Block intersects the pile partially.	Removable Under Certain Assumptions
III	Block intersects the pile entirely but dips away from the intersection with the pile.	Non-removable
IV	Block intersects the pile entirely on the surface and dips toward the pile from the surface.	Removable
V	Block intersects the pile partially on the surface.	Removable Under Certain Assumptions
VI	Block is intersects the pile entirely on the surface but dips away from the intersection with the pile.	Non-removable

2.8 A COMPLETE EXAMPLE ON SELECTION OF A REMOVABLE COMBINATION OF BLOCKS

The following is the complete step-by-step demonstration of construction of joint mesh and joint map and identification of different types of blocks. The pile has a diameter (D) of 5ft and a depth (l) of 5ft. The orientation of the first joint set is N-S, 30°E and its horizontal spacing (s) is 0.866D. The orientation of the second joint set is E-W, 60°S and its horizontal spacing (s) is 0.433D. A 3D view of the pile and the ground surface is shown in Figure 2.27. The procedures are as follow

1. First the surface joint mesh shall be constructed. Recall that equation (2.12), $y=\tan\beta \cdot x+n \cdot s/\cos\beta$, is used to construct each joint on the joint mesh. β and s are substituted directly into the equation and are identical for each joint of the same joint set. n is an integer and is different for each joint. When n=0, the joint passes through the origin (0,0) or the center of the pile. By setting $n=\pm1, \pm2$, and so on, different joints are generated immediately above and below joint n=0. For a particular n, two different x values are selected and are substituted into equation (2.12) to obtain two y values and thus two points in the x,y coordinates. By connecting these two points together, a joint on the joint mesh is obtained. Thus, the selection of the x values is based on the size of the joint mesh one needs. However, in the case when a joint is a vertical line on the joint mesh, two different y values, instead of two different x values, are selected to obtain two points to construct the joint because the x value does not change for any points on a vertical line. This is the case for the first joint set. From the information given above, $\beta=90^\circ$ for the first joint set. Since $\tan 90^\circ$ and $n \cdot s/\cos 90^\circ$ go to infinity in the equation, the equation should be rewritten by multiplying both sides by $\cos\beta$ so that it becomes $y \cdot \cos\beta=\sin\beta \cdot x+n \cdot s$. Substituting 90° for β, this equation becomes $x=-n \cdot s$, which is the equation for a vertical line. With $s=0.866D=0.866 \cdot 5ft=4.33ft$, and thus $x=-4.33n$ (ft). The spreadsheet is set up for the first joint set in Table 2.2. In the first column in Table 2.2, y=-30ft and y=30ft are selected for the end points of each joint. To the right of the first column, n varies from –5 to 5. Under each n, each x corresponds to the y on the same row and is calculated by $x=-4.33n$. For instance, for n=-1 and y=-30, $x=-4.33 \bullet -1=4.33$, which

is the first number under n=-1. And for the same n and y=30, x=-4.33•-1=4.33, which is the second number under n=-1. By connecting points (4.33, -30) and (4.33, 30) with a line, joint n=-1 is completed on the joint mesh. The joints of the first joint set are plotted in Figure 2.28, and the x and y axes are both in feet. Each joint is denoted by a number followed by its n value. The number notation for each joint is solely for identification purpose to avoid confusion when distinguishing two joints from different joint sets having the same n values.

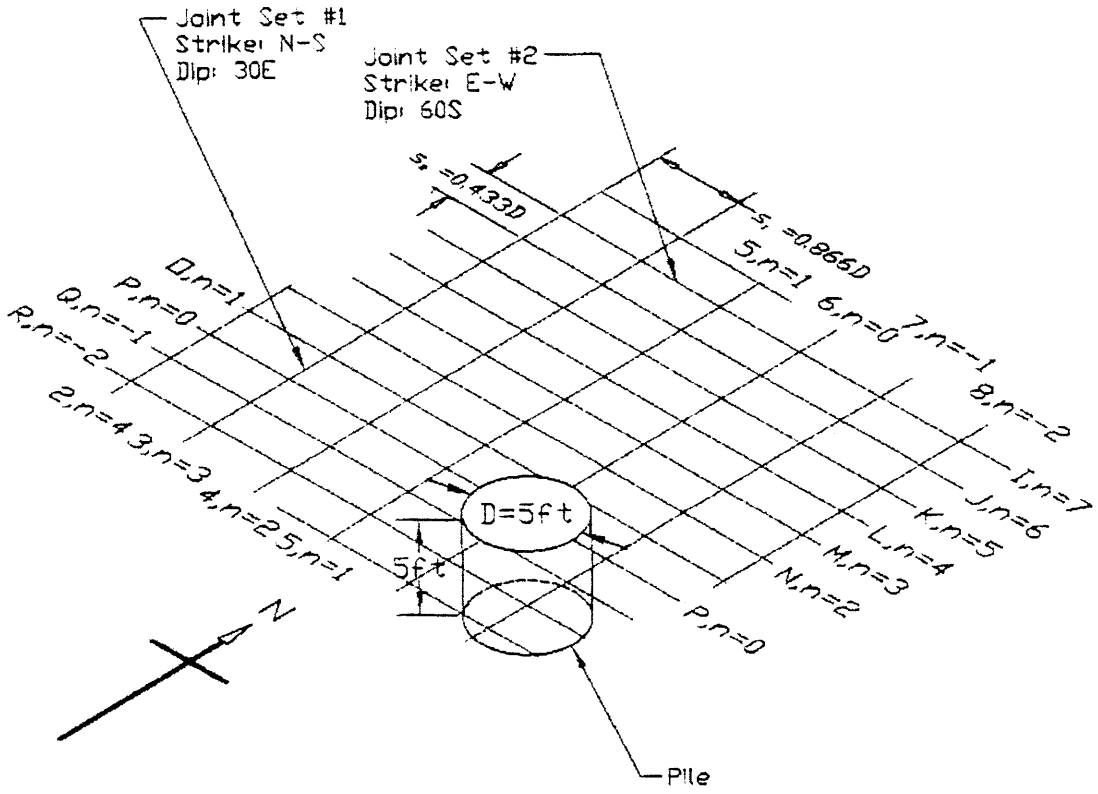

Figure 2.27 A 3D View of the Pile and Ground Surface

Table 2.2 Spreadsheet Setup for Joint N-S, 30°E on a Surface Joint Mesh

N-S,30E	s=0.866*D=0.866*5=4.33											
Y	x											
	n=	-5	-4	-3	-2	-1	0	1	2	3	4	5
-30		21.65	17.32	12.99	8.66	4.33	0	-4.33	-8.66	-12.99	-17.32	-21.65
30		21.65	17.32	12.99	8.66	4.33	0	-4.33	-8.66	-12.99	-17.32	-21.65

Table 2.3 Spreadsheet Setup for Joint E-W, 60°S on a Surface Joint Mesh

E-W,60S	s=0.433*D=0.433*5=2.165											
x	y											
	n=	-8	-7	-6	-5	-4	-3	-2	-1	0		
-20		-17.32	-15.155	-12.99	-10.825	-8.66	-6.495	-4.33	-2.165	0		
20		-17.32	-15.155	-12.99	-10.825	-8.66	-6.495	-4.33	-2.165	0		
x	y											
	n=				1	2	3	4	5	6	7	8
-20					2.165	4.33	6.495	8.66	10.825	12.99	15.155	17.32
20					2.165	4.33	6.495	8.66	10.825	12.99	15.155	17.32

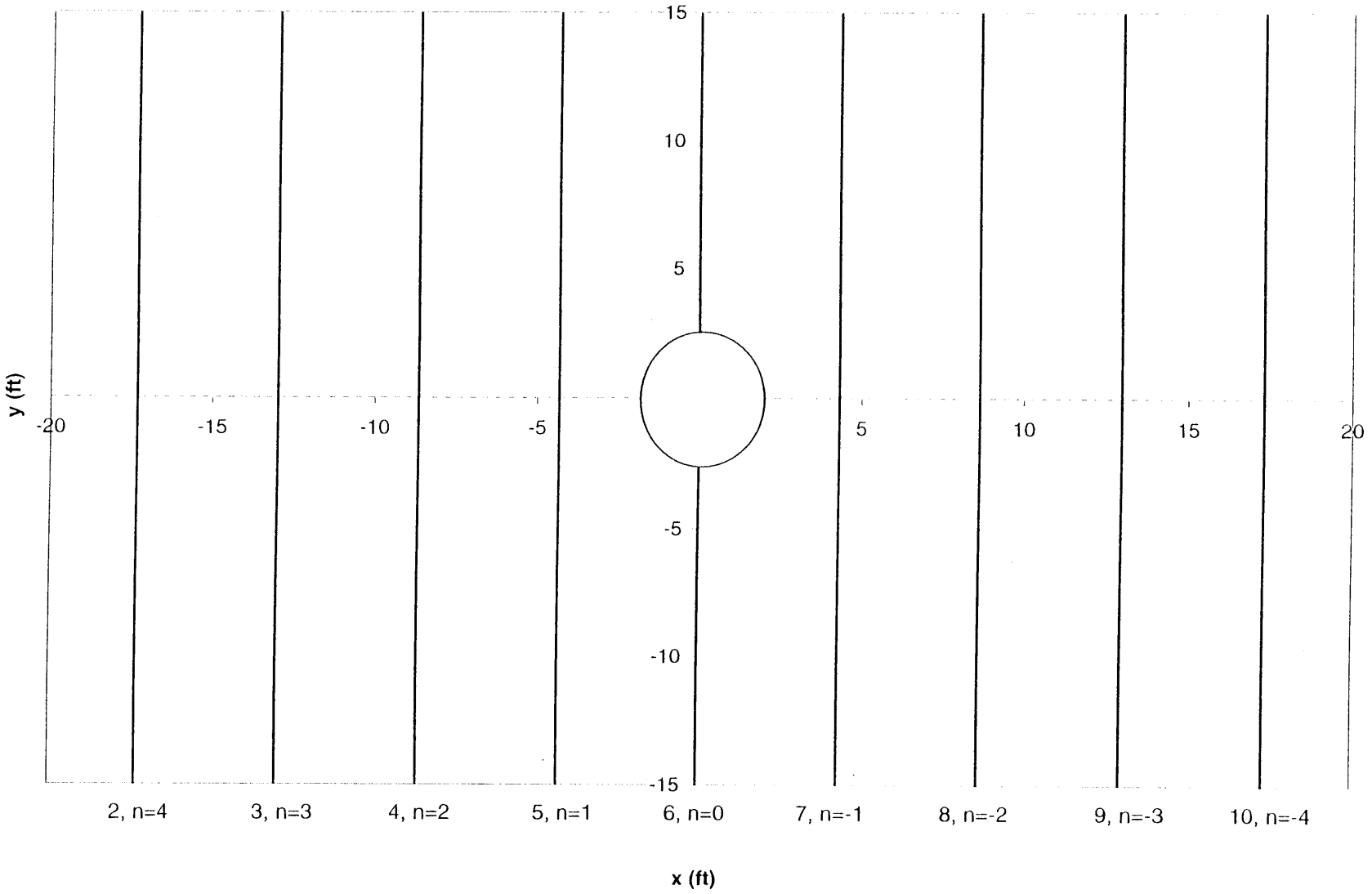

Figure 2.28 Construction of Joint Mesh of Joint Set N-S, 30°E by Spreadsheet

2. From the information given above, $\beta=0^{o}$ for the second joint set. $\tan\beta=0$ and $\cos\beta=1$, and thus substituting these values into $y=\tan\beta \cdot x+n \cdot s/\cos\beta$, $y=n \cdot s$. $s=0.433D=0.433 \cdot 5ft=2.165ft$, and thus $y=2.165n$. The spreadsheet is set up for the second joint set in Table 2.3. In the first column in Table 2.3, x=-20ft and y=20ft are selected for the end points of each joint. To the right of the first column, n varies from –8 to 8. Under each n, each y corresponds to the x on the same row and is calculated by $y=2.165n$. For instance, for n=3 and x=-20, $x=2.165 \bullet 3=6.495$, which is the first number under n=3. And for the same n and x=20, $x=2.165 \bullet 3=6.495$, which is the second number under n=3. By connecting points (-20, 6.495) and (20, 6.495) with a line, joint n=3 is completed on the joint mesh. The joints of the second joint set are plotted in Figure 2.29, and the x and y axes are in feet. Each joint is denoted by a letter followed by its n value. The letter notation for each joint is solely for identification purpose to avoid confusion when distinguishing two. The whole joint mesh is completed by combining Figure 2.28 and Figure 2.29 as shown in Figure 2.30. Notice that joint 5 and joint O both have n=1, and thus the purpose of using a different notation is served.

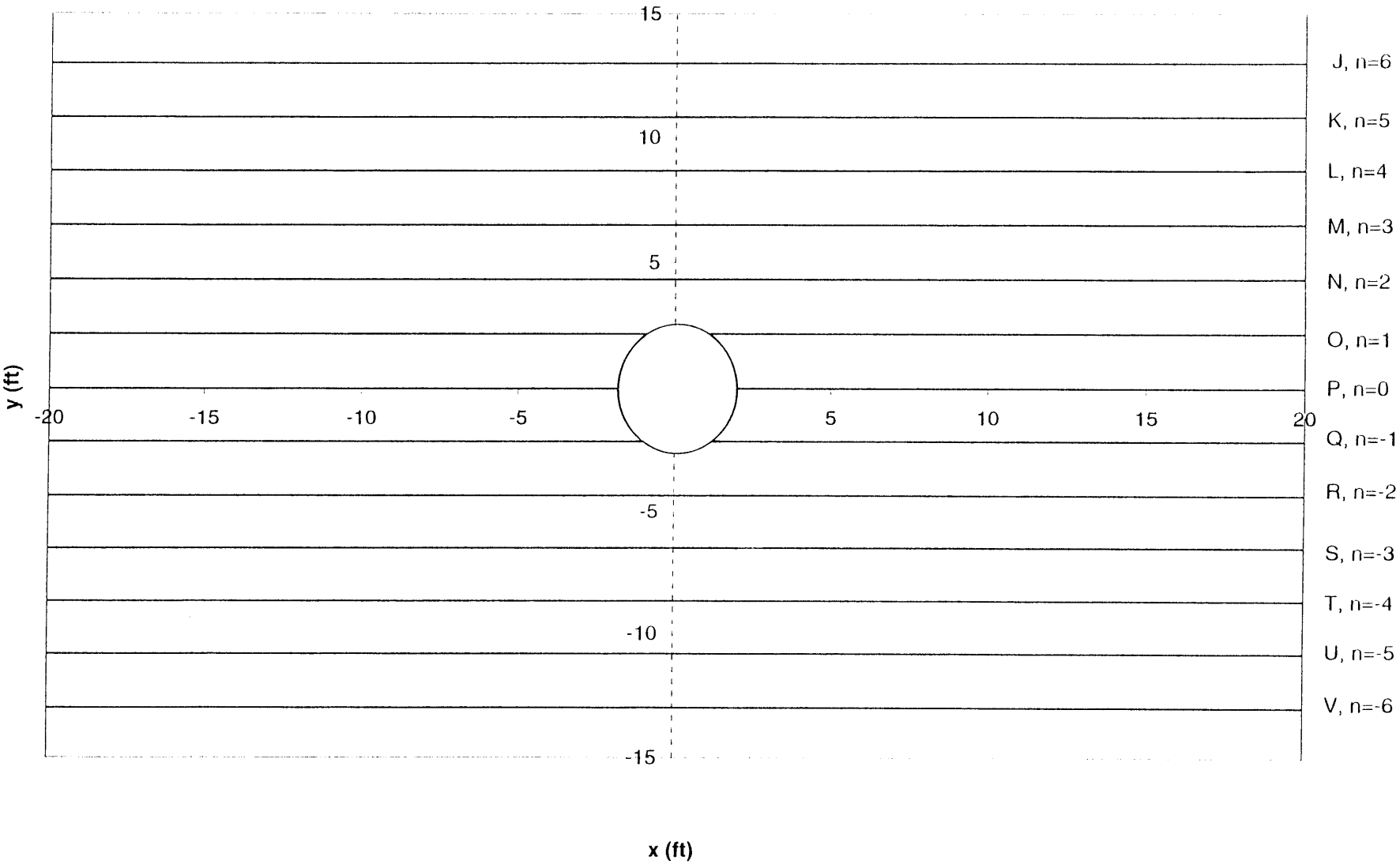

Figure 2.29 Construction of a Joint Mesh of Joint Set E-W, 60°S by Spreadsheet

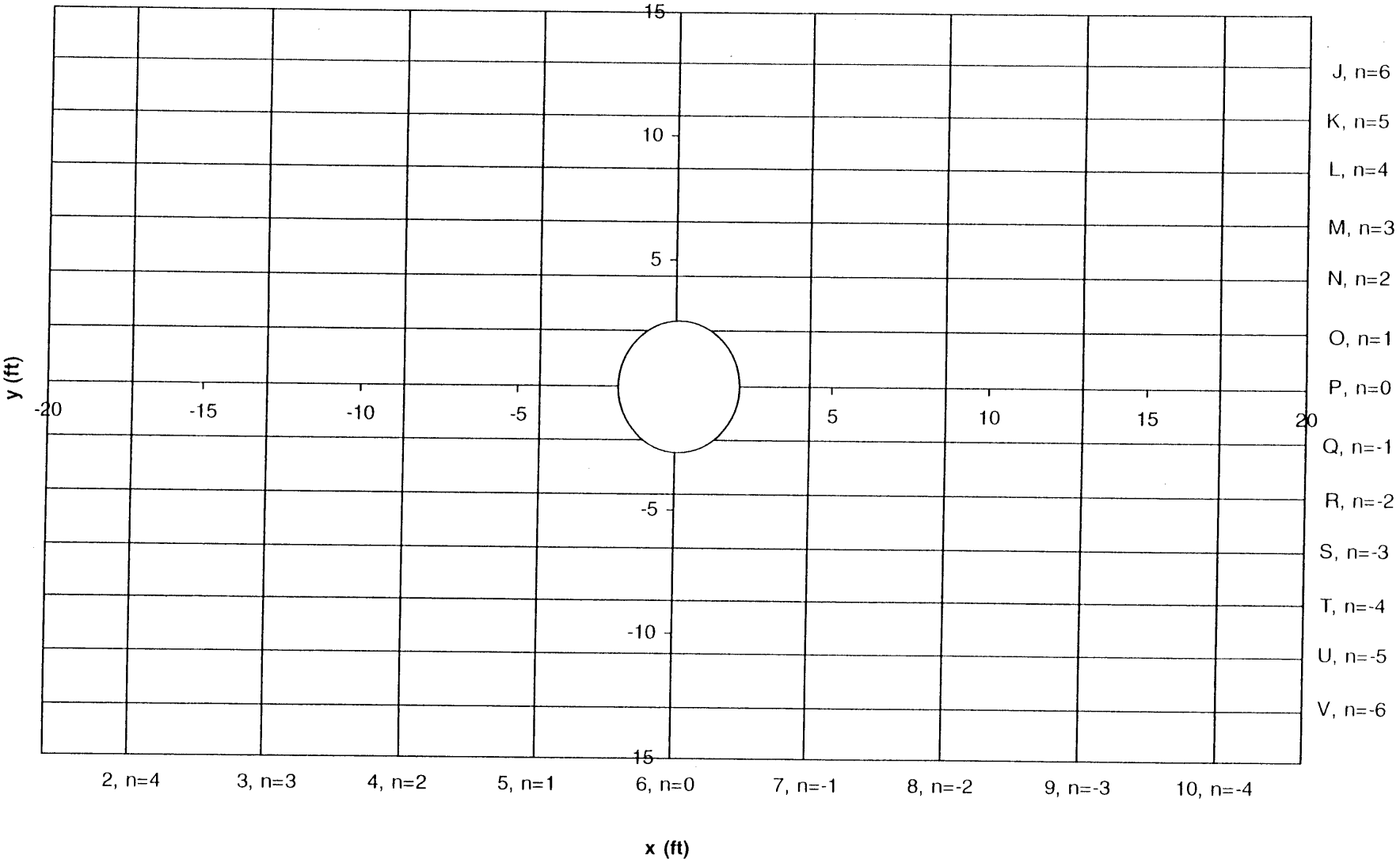

Figure 2.30 Construction of a Joint Mesh of a 2-Joint-Set System by Spreadsheet

3. A joint map is obtained by unfolding the surface of the pile into a plane and mapping all the intersecting joints onto it. The unfolding of a joint intersection on the pile is a sinusoidal function and is described by equation (2.13) as $z=0.5 \cdot D \tan\gamma \cdot \cos(\theta+\beta-270^{o})-n \cdot s \cdot \tan\gamma$. D, γ, β, and s are substituted directly into the equation and are identical for each joint of the same joint set. The n in equation (2.13) corresponds to the same n of a joint from the same joint set on the joint mesh. n is an integer and is different for each joint. The selection of the number of n values to be used in the equation is based on the number of joints on the joint map one needs. Typically, the n values selected in the construction of the joint mesh are used in the construction of the joint map on the pile. θ is the azimuth angle (0^{o}-360^{o}) beginning from the East in a clockwise direction in plan view. Thus, for each joint n, different θ values between 0^{o} and 360^{o} are substituted into equation (2.13) to obtain z. Points are plotted in the θ-z plane and are connected together to obtain joint n on the joint map. Thus, the more θ values are used to obtain z and thus more points, the more accurate the curve is. According to the author's experience, it is adequate to vary θ from 0^{o} to 360^{o} with an increment of 30^{o} and substitute these θ values into the equation. For the first joint set, substituting $\beta=90^{o}$, $\gamma=30^{o}$, D=5ft, and s=4.33ft, $z=0.5 \cdot 5 \cdot \tan 30^{o} \cdot \cos(\theta+90^{o}-270^{o})-n \cdot 4.33 \cdot \tan 30^{o}=1.4434\cos(\theta-180^{o})-2.5n$. The spreadsheet setup for the first joint set is shown in top half of Table 2.4. In the first column, θ varies from 0^{o} to 360^{o} with an increment of 30^{o}. To the right of the first column, n varies from –2 to 5 for the first joint set. Below each n, each z corresponds to the θ on the same row and is calculated by $z=1.4434\cos(\theta-180^{o})-2.5n$. For instance, for n=0 and $\theta=0^{o}$, $z=1.4434\cos(0^{o}-180^{o})-2.5 \cdot 0=-1.44$, which is the first number below n=0. And for n=0 and $\theta=150^{o}$, $z=1.4434\cos(150^{o}-180^{o})-2.5 \cdot 0=1.25$, which is the sixth number below n=0. By plotting all the θ, z points for n=0 and connecting them together, joint n=0 on the joint map is completed. The joints of the first joint set are plotted in Figure 2.31. The horizontal axis is the azimuth angle (θ) in degrees and the vertical axis is the z-axis in feet. Notice that the joints above the ground surface (z=0) are hypothetical joints, which will be used to identify grids later. Each joint is denoted by a number followed by its n value on the right side of Figure 2.31. The number

notation of a joint on the joint map corresponds to the same number notation of a joint on the joint mesh. For example, joint 5 (n=1) on the joint map in Figure 2.31 is the same joint 5 (n=1) on the joint mesh in Figure 2.30.

Table 2.4 Spreadsheet Setup for Joints on a Joint Map on a Pile

N-S,30E θ	z								
	n=	-2	-1	0	1	2	3	4	5
0		3.56	1.06	-1.44	-3.94	-6.44	-8.94	-11.44	-13.94
30		3.75	1.25	-1.25	-3.75	-6.25	-8.75	-11.25	-13.75
60		4.28	1.78	-0.72	-3.22	-5.72	-8.22	-10.72	-13.22
90		5.00	2.50	0.00	-2.50	-5.00	-7.50	-10.00	-12.50
120		5.72	3.22	0.72	-1.78	-4.28	-6.78	-9.28	-11.78
150		6.25	3.75	1.25	-1.25	-3.75	-6.25	-8.75	-11.25
180		6.44	3.94	1.44	-1.06	-3.56	-6.06	-8.56	-11.06
210		6.25	3.75	1.25	-1.25	-3.75	-6.25	-8.75	-11.25
240		5.72	3.22	0.72	-1.78	-4.28	-6.78	-9.28	-11.78
270		5.00	2.50	0.00	-2.50	-5.00	-7.50	-10.00	-12.50
300		4.28	1.78	-0.72	-3.22	-5.72	-8.22	-10.72	-13.22
330		3.75	1.25	-1.25	-3.75	-6.25	-8.75	-11.25	-13.75
360		3.56	1.06	-1.44	-3.94	-6.44	-8.94	-11.44	-13.94
E-W, 60S θ	z								
	n=	-3	-2	-1	0	1	2	3	4	5
0		11.25	7.50	3.75	0.00	-3.75	-7.50	-11.25	-15.00	-18.75
30		9.08	5.33	1.58	-2.17	-5.91	-9.66	-13.41	-17.16	-20.91
60		7.50	3.75	0.00	-3.75	-7.50	-11.25	-15.00	-18.75	-22.50
90		6.92	3.17	-0.58	-4.33	-8.08	-11.83	-15.58	-19.33	-23.08
120		7.50	3.75	0.00	-3.75	-7.50	-11.25	-15.00	-18.75	-22.50
150		9.08	5.33	1.58	-2.17	-5.91	-9.66	-13.41	-17.16	-20.91
180		11.25	7.50	3.75	0.00	-3.75	-7.50	-11.25	-15.00	-18.75
210		13.41	9.66	5.91	2.17	-1.58	-5.33	-9.08	-12.83	-16.58
240		15.00	11.25	7.50	3.75	0.00	-3.75	-7.50	-11.25	-15.00
270		15.58	11.83	8.08	4.33	0.58	-3.17	-6.92	-10.67	-14.42
300		15.00	11.25	7.50	3.75	0.00	-3.75	-7.50	-11.25	-15.00
330		13.41	9.66	5.91	2.17	-1.58	-5.33	-9.08	-12.83	-16.58
360		11.25	7.50	3.75	0.00	-3.75	-7.50	-11.25	-15.00	-18.75

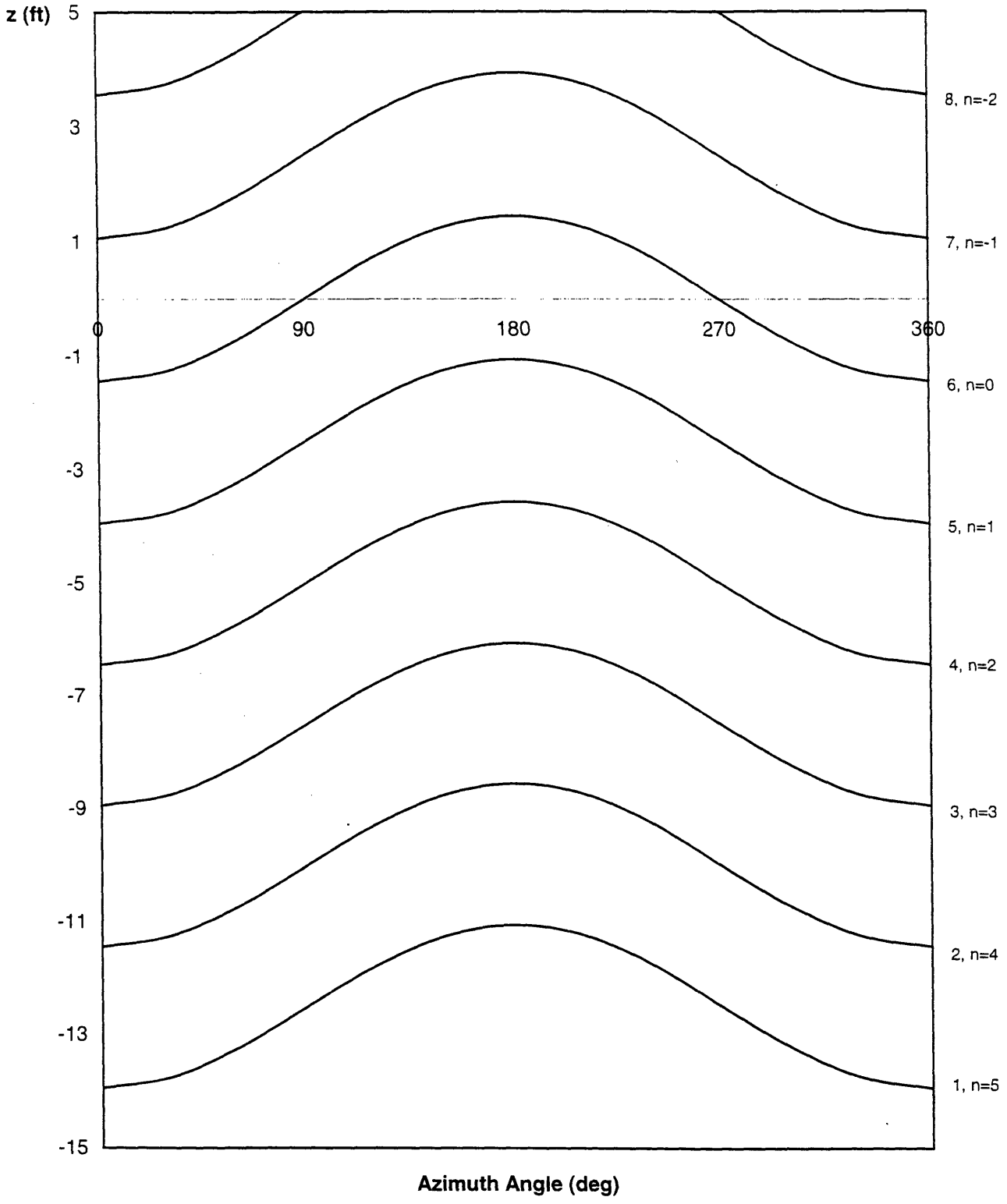

Figure 2.31 Construction of a Joint Map on a Pile of Joint Set N-S, 30°E by Spreadsheet

4. The same procedure for generating a joint on the joint map follows for the second joint set as for the first. For the second joint set, substituting $\beta=0^{o}$, $\gamma=60^{o}$, D=5, and s=2.165ft, $z=0.5\bullet5\bullet\tan60^{o}\bullet\cos(\theta+0^{o}-270^{o})-n\bullet2.165\bullet\tan60^{o}=4.330\cos(\theta-270^{o})-3.75n$. The spreadsheet setup for the second joint set is shown in the bottom half of Table 2.4. In the first column, θ varies from 0^{o} to 360^{o} with an increment of 30^{o}. To the right of the first column, n varies from –3 to 5 for the second joint set. Below each n, each z corresponds to the θ on the same row and is calculated by $z=4.330\cos(\theta-270^{o})-3.75n$. For instance, for n=1 and $\theta=0^{o}$, $z=4.330\cos(0^{o}-270^{o})-3.75\bullet1=-3.75$, which is the first number below n=1. And for n=1 and $\theta=150^{o}$, $z=4.330\cos(150^{o}-270^{o})-3.75\bullet1=-5.91$, which is the sixth number below n=1. By plotting all the θ, z points for n=1 and connecting them together, joint n=1 on the joint map is completed. The joints of the second joint set are plotted in Figure 2.32. The horizontal axis is the azimuth angle (θ) in degrees and the vertical axis is the z-axis in feet. Notice that the joints above the ground surface (z=0) are hypothetical joints, which will be used to identify grids later. Each joint is denoted by a letter followed by its n value on the left side of Figure 2.32. The letter notation of a joint on the joint map corresponds to the same letter notation of a joint on the joint mesh. For example, joint O (n=1) on the joint map in Figure 2.32 is the same joint O (n=1) on the joint mesh in Figure 2.30. Combining Figure 2.31 and Figure 2.32, the complete joint map for the two joint sets is formed as shown in Figure 2.33.

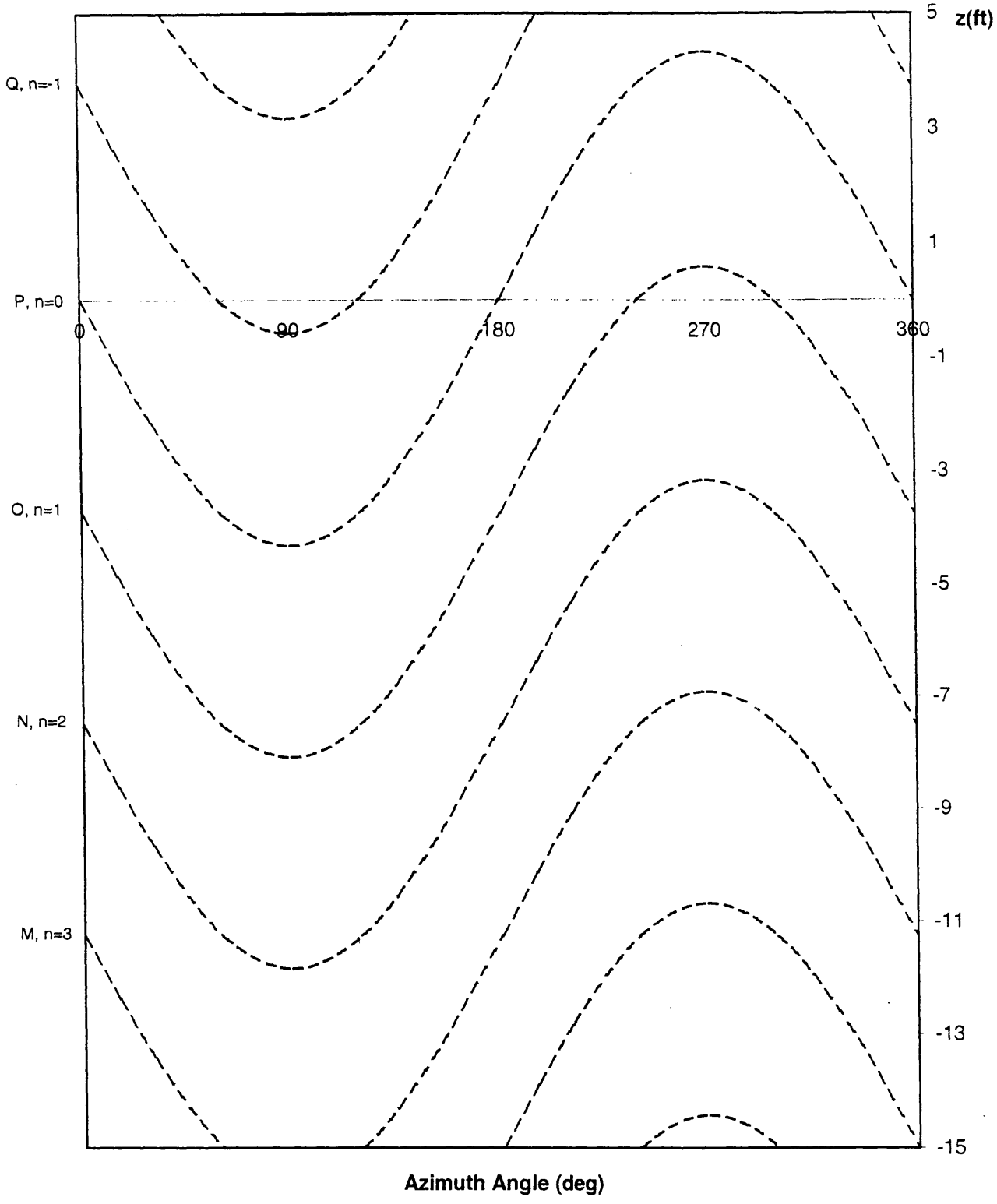

Figure 2.32 Construction of a Joint Map on a Pile of Joint Set E-W, 60°S by Spreadsheet

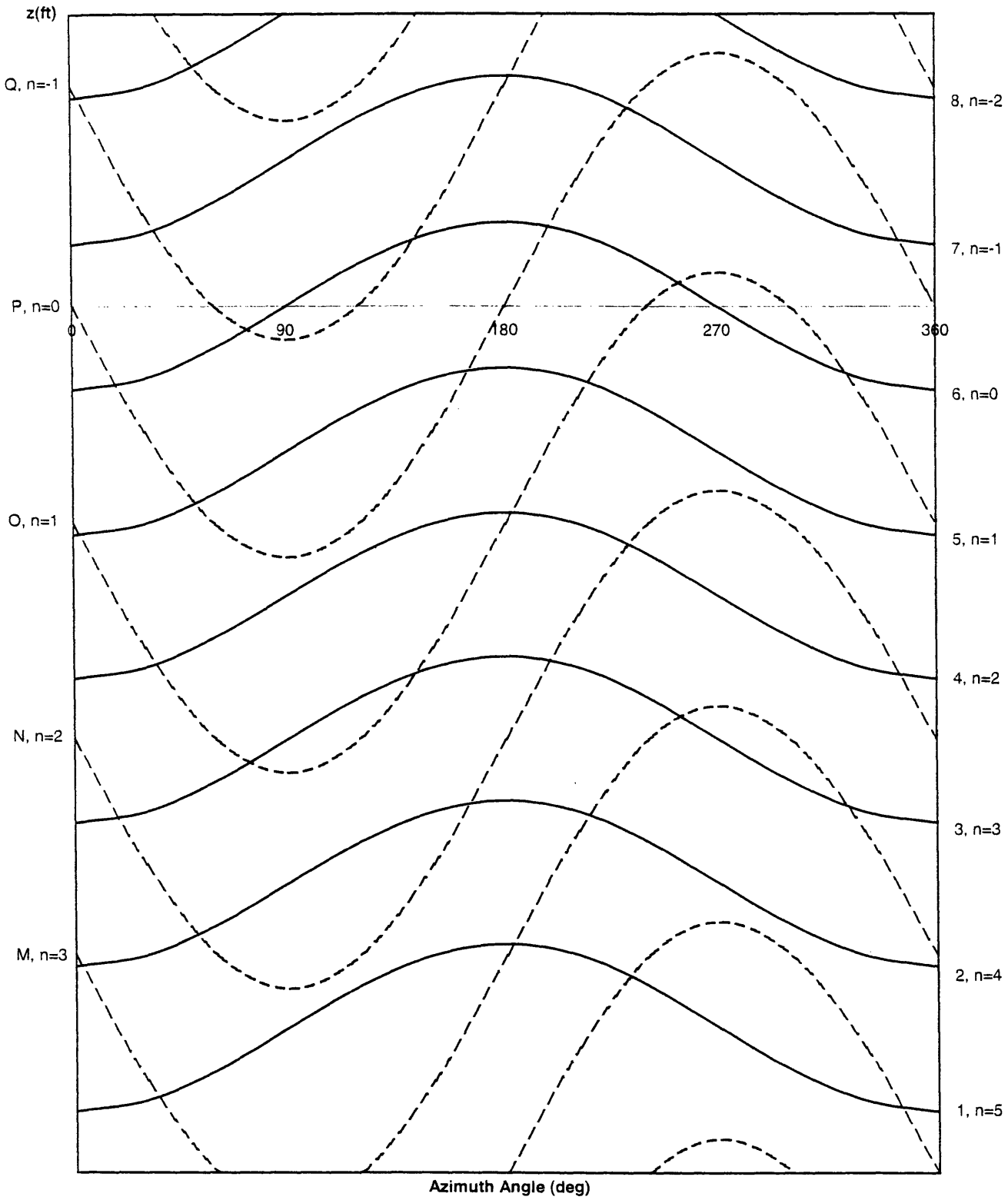

Figure 2.33 Construction of a Joint Map on a Pile of a 2-Joint-Set System by Spreadsheet

5. Each grid on the joint map is then denoted by combining the four codes of its bounding joints. Only the grids from the surface to the pile depth need to be denoted. The hypothetical joints above the ground surface (z=0) are used to identify grids. The procedures are described in detail in Chapter 2.5. A simple way to begin denoting the grids is to focus on two adjacent joints from the same joint set. For example, in Figure 2.34, the space between adjacent joints 4 and 5 is shown dotted. Any grid that lies in this dotted band consists of codes 45 and two other codes from the other joint set. Next, the space between adjacent joints O and P is chosen arbitrarily to be considered as shown dotted in Figure 2.35. Notice that the grid already coded 45 also intersects the OP dotted band, and thus this grid is coded 45OP. The same process can be followed to code the grids for other adjacent joints. The codes of all the relevant grids are shown on the joint map in Figure 2.36.

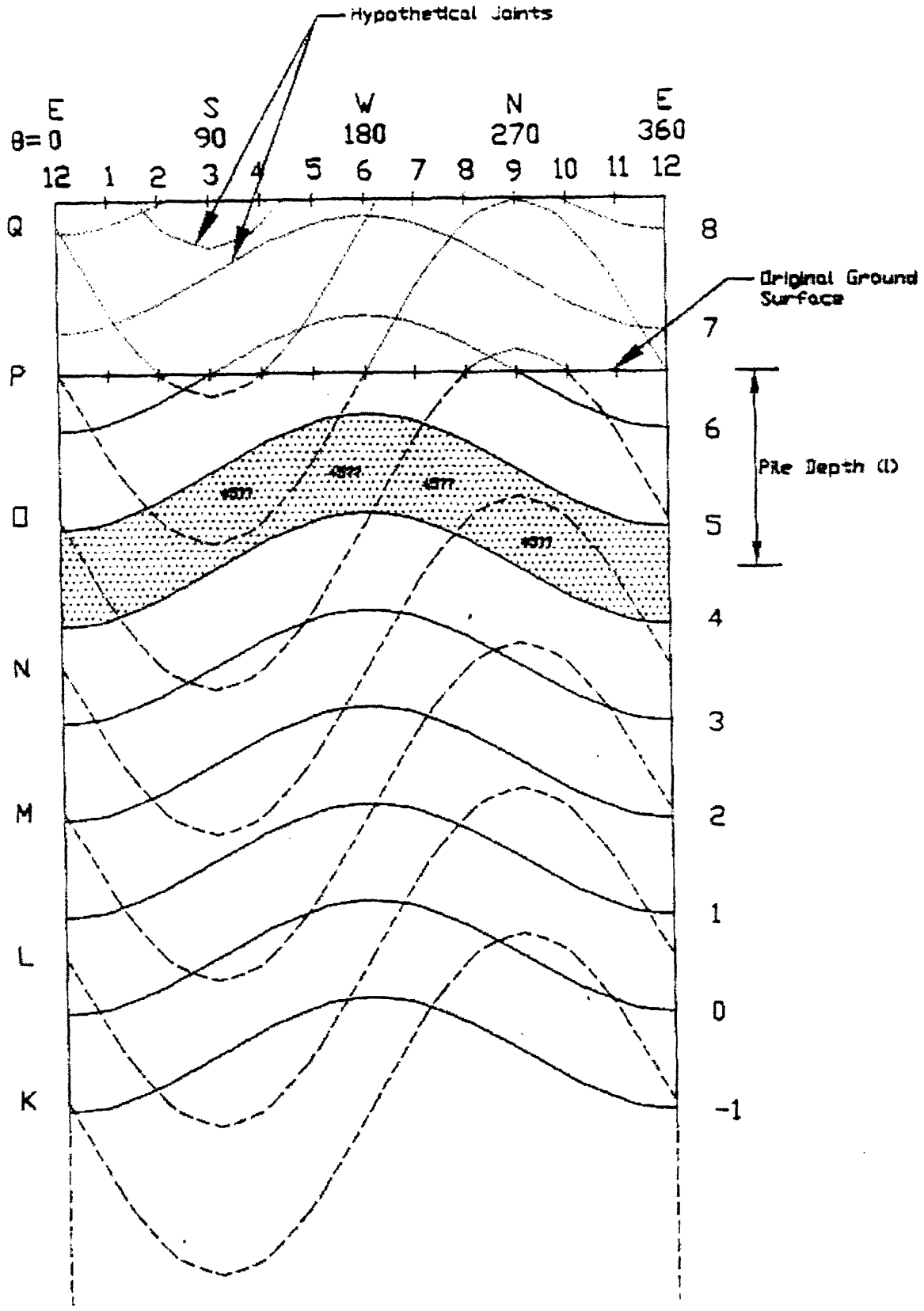

Figure 2.34 Identifying Blocks on a Joint Map on a Pile

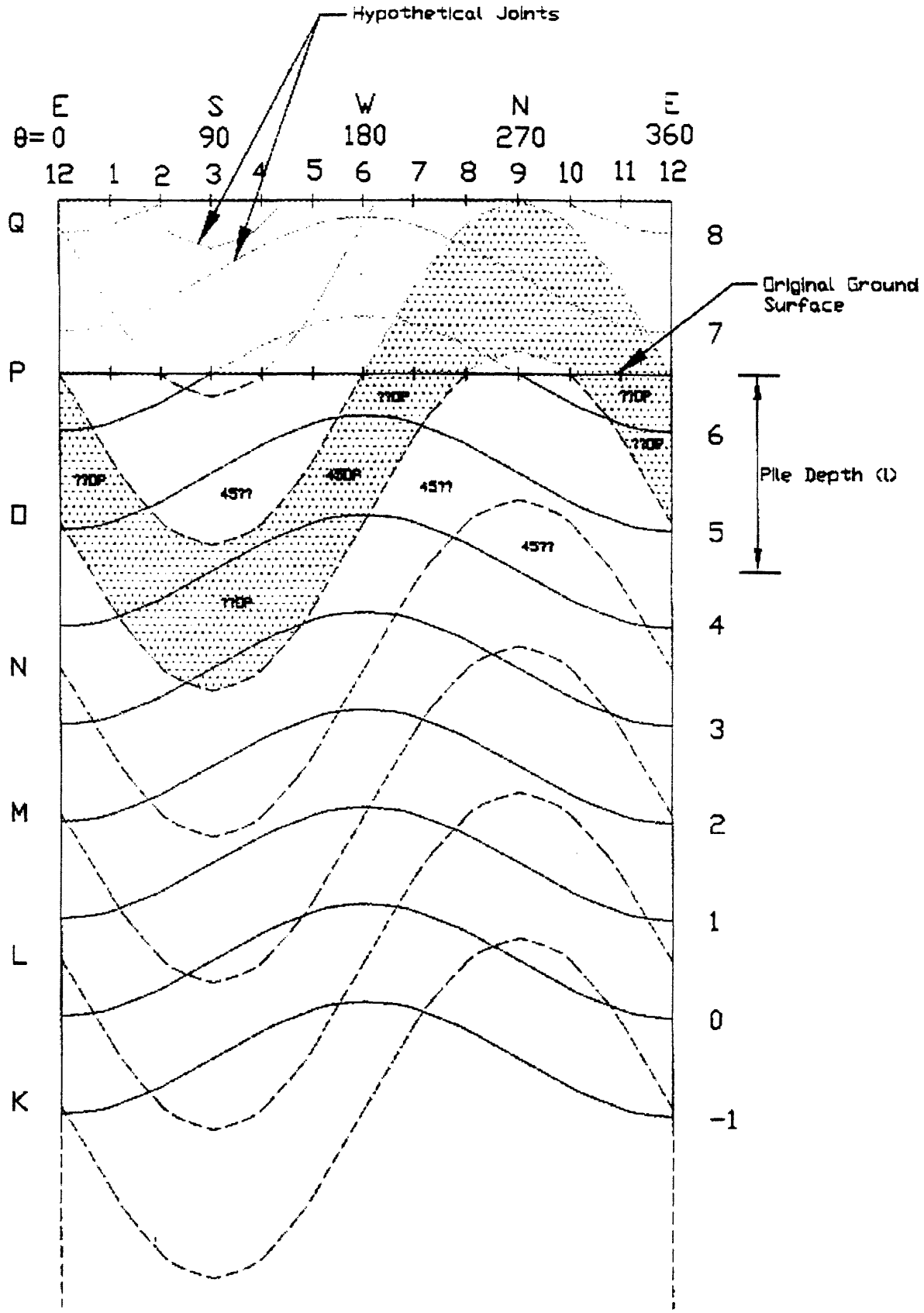

Figure 2.35 Identifying Blocks on a Joint Map on a Pile

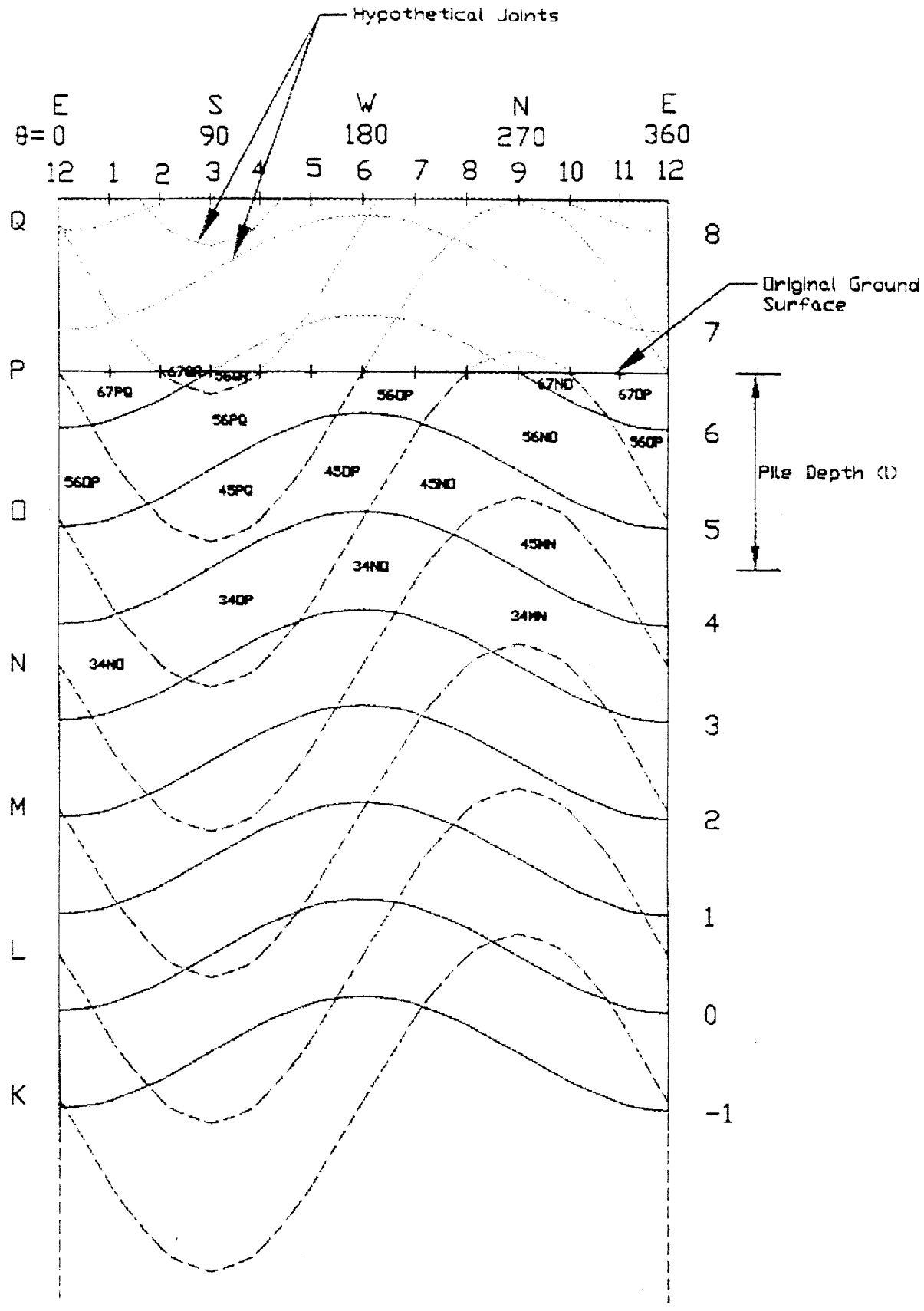

Figure 2.36 Identifying Blocks on a Joint Map on a Pile

6. To identify different types of blocks, one must understand the dipping direction of the blocks. In this particular example, since the first joint set dips eastward and the second dips southward as shown on the joint mesh in Figure 2.37, the general dipping direction must be southeastward. With this in mind, Type I, III, IV, and VI blocks are identified first. Recall that Type I and IV blocks have joints dipping toward the pile and have grids that have four vertices and two pairs of adjacent joints. Type III and VI blocks have joints dipping away from the pile and have grids that have four vertices and two pair of adjacent joints. One thing in common in Type I, III, IV, and VI blocks is that their grids all have four vertices and are bounded by two pairs of adjacent joints on the joint map. The only way to distinguish them on these 2D drawings is to interpret from the general dipping direction of the blocks. As shown dotted on the joint map in Figure 2.38, there are two 34NO grids, two 56OP grids, and a 67PQ grid, each grid having four vertices and being bounded by two pairs of adjacent joints. Now, grids 34NO, 56OP, and 67PQ are traced back to the joint mesh in Figure 2.37. Since the dipping direction of each block is southeastward, by examining Figure 2.37, block 34NO dips from the surface southeastward and intersects the pile somewhere between $\theta=90^{\circ}$ to $\theta=360^{\circ}$. Going back to the joint map in Figure 2.38, the grid that lies between $\theta=90^{\circ}$ to $\theta=360^{\circ}$ is the Type I block, and thus is labeled 34NO(R). Consequently, the other 34NO grid belongs to a Type III block and thus is labeled 34NO(N). Examining the joint mesh in Figure 2.37, block 56OP dips toward the pile and intersects the pile on the surface between $\theta=180^{\circ}$ to $\theta=240^{\circ}$, and thus is a Type IV block. Therefore, the grid that lies between $\theta=180^{\circ}$ to $\theta=240^{\circ}$ on the joint map in Figure 2.38 is labeled 56OP(R). Consequently, the other 56OP grid belongs to a Type III block, and thus is labeled 56OP(N). Examining the joint mesh in Figure 2.37, the entire block 67PQ intersects the pile on the surface, but dips away from the pile because all the blocks dip southeastward. Thus, it is a Type VI block, and its grid on the joint map is labeled 67PQ(N). Next, Type II and V blocks are identified. Recall that Type II and V blocks are partially intersecting blocks. Type II and V block have grids that do not have four vertices and are not bounded by two pairs of adjacent joints. Basically, all the blocks that do not belong

to Type I, III, IV, and VI blocks are Type II and V blocks. As shown in Figure 2.39, Type I and IV blocks are shown shaded with slanted lines, Type II and V blocks are shown dotted, and Type III and VI blocks are shown shaded with zigzag lines.

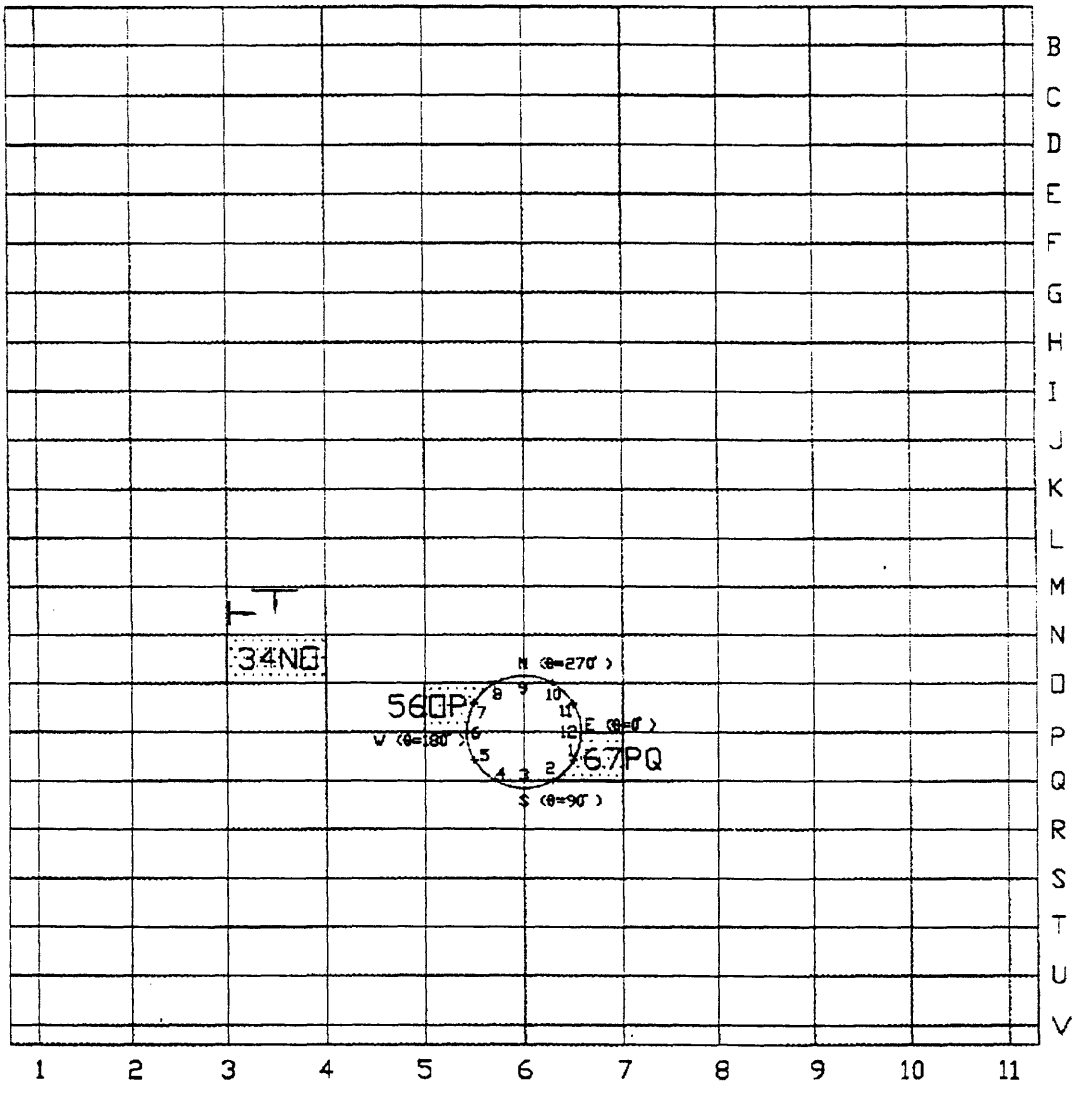

Figure 2.37 Identifying Blocks on a Surface Joint Mesh

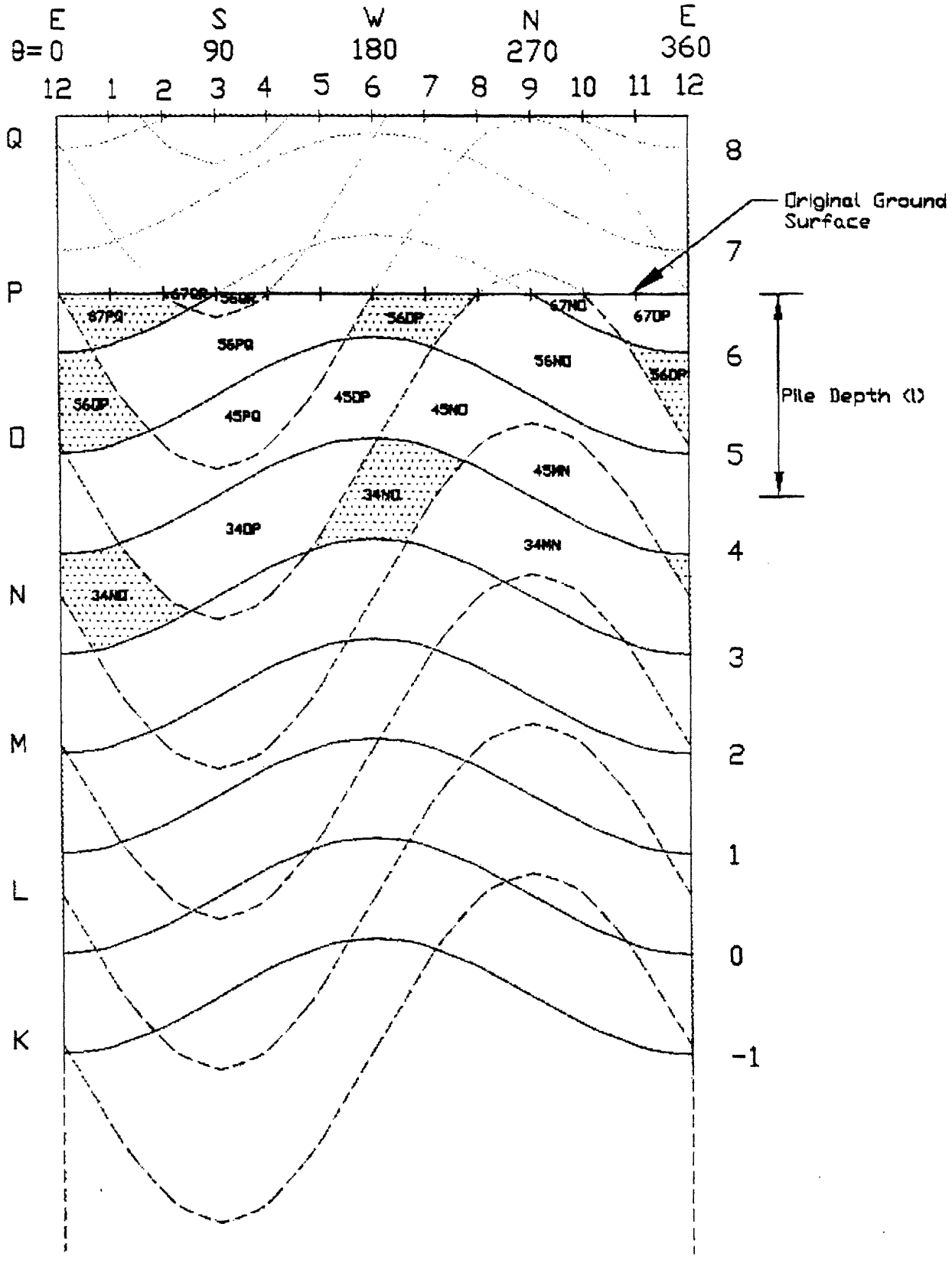

Figure 2.38 Identifying Blocks on a Joint Map on a Pile

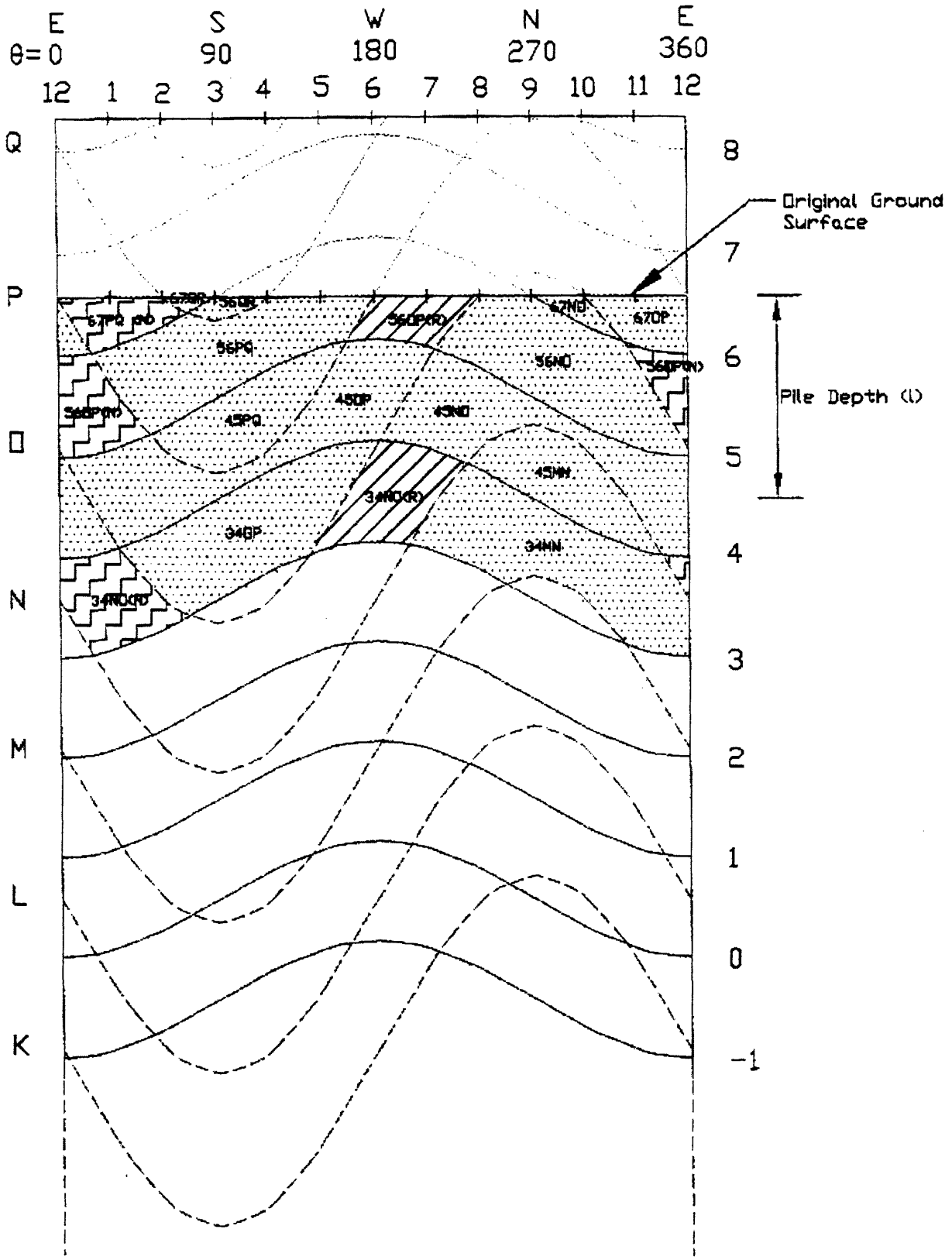

Figure 2.39 Identifying Blocks on a Joint Map on a Pile

7. Since only Type I, II, IV, and V blocks are removable and Type III and VI blocks are not removable, there is a removable zone within which combinations of removable blocks can be found. In other words, this removable zone consists of only removable blocks and is bounded by the extremes of the non-removable blocks. In this case, the removable zone is between $\theta=75^{\circ}$ to 324° on top of the joint map in Figure 2.40. Notice that on the left extreme, the removable zone is bounded by non-removable block 34NO(N). On the right extreme, the removable zone is bounded by non-removable block 56OP(N). Recall that the area of influence encompasses half of the pile or 180°. Therefore, this 180° of the area of influence can shift between $\theta=75^{\circ}$ to 324° to obtain a combination of removable blocks. When the area of influence is at the left extreme of the removable zone, it is between $\theta=75^{\circ}$ and $\theta=255^{\circ}$ ($75^{\circ}+180^{\circ}$) as shown in Figure 2.41. For this area of influence, the force acts in $\theta=165^{\circ}$ ($75^{\circ}+90^{\circ}$) as shown in the lower right hand corner in Figure 2.41. When the area of influence is at the right extreme of the removable zone, it is between $\theta=324^{\circ}$ and $\theta=144^{\circ}$ ($324^{\circ}-180^{\circ}$) as shown in Figure 2.42. For this area of influence, the force acts in $\theta=234^{\circ}$ ($324^{\circ}-90^{\circ}$) as shown in the lower right hand corner in Figure 2.42. The range between the extreme force directions is called the possible removable range as shown in Figure 2.43.

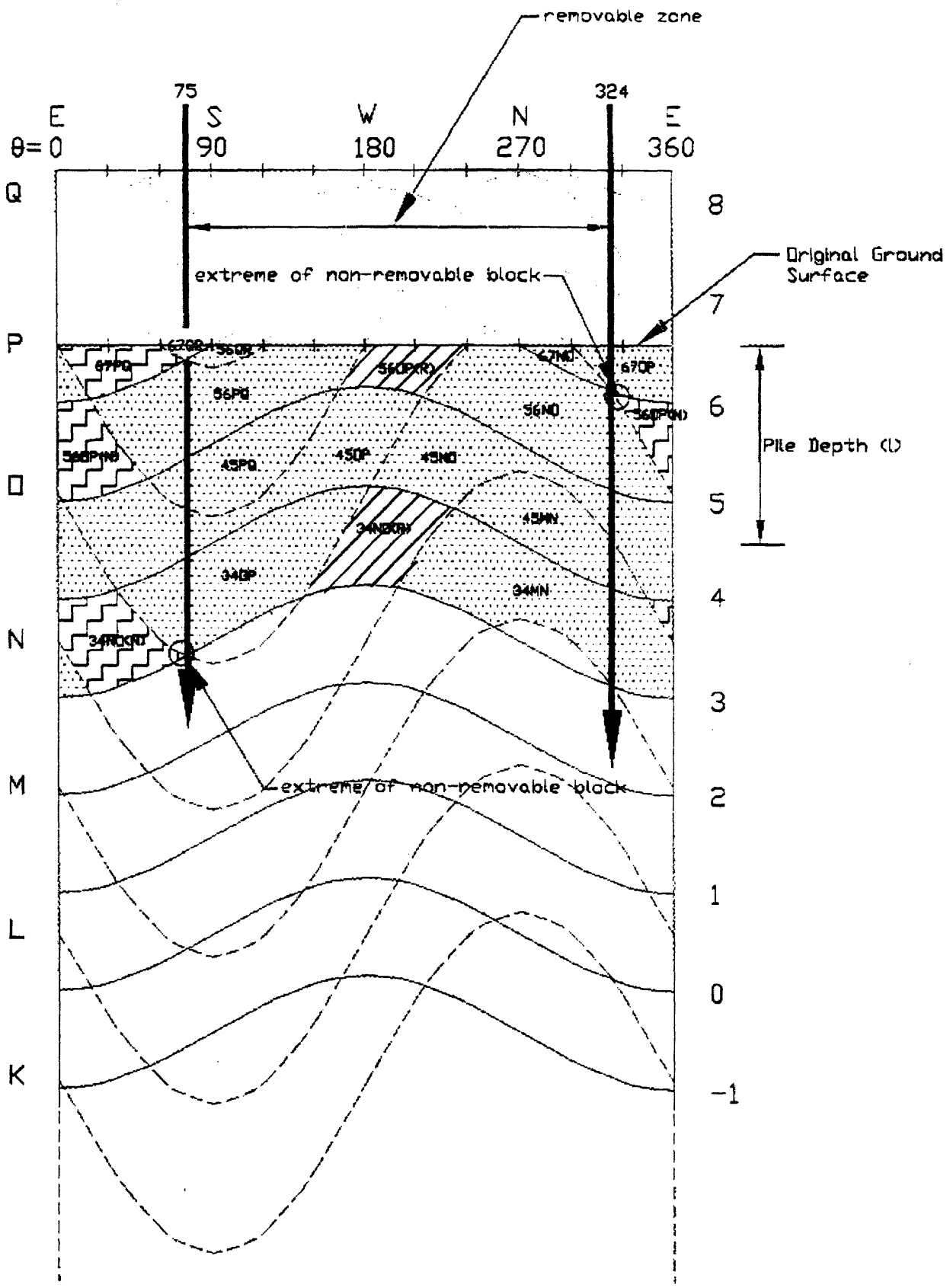

Figure 2.40 Removable Zone on a Joint Map on a Pile

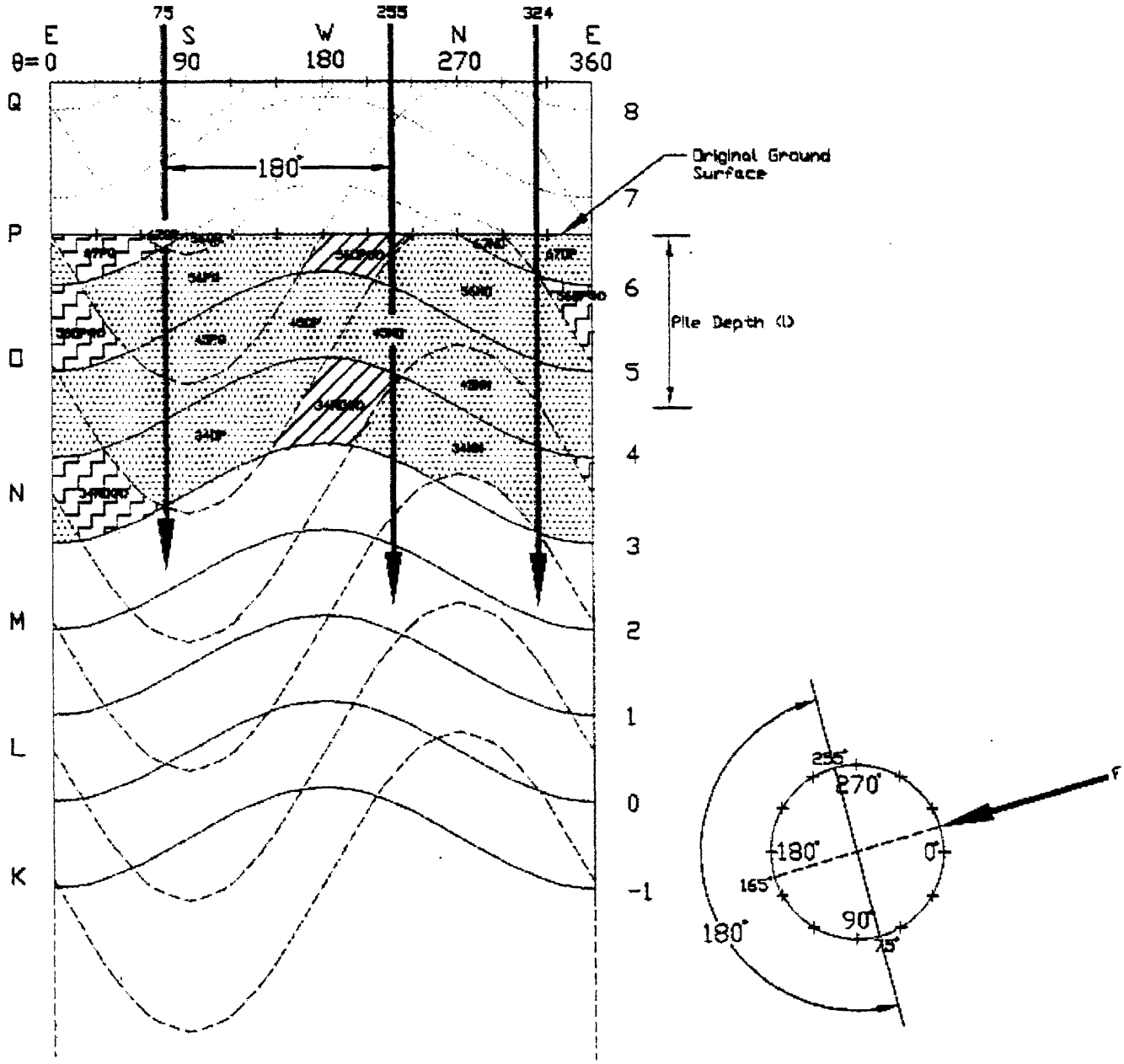

Figure 2.41 Area of Influence on the Left Extreme on a Joint Map on a Pile

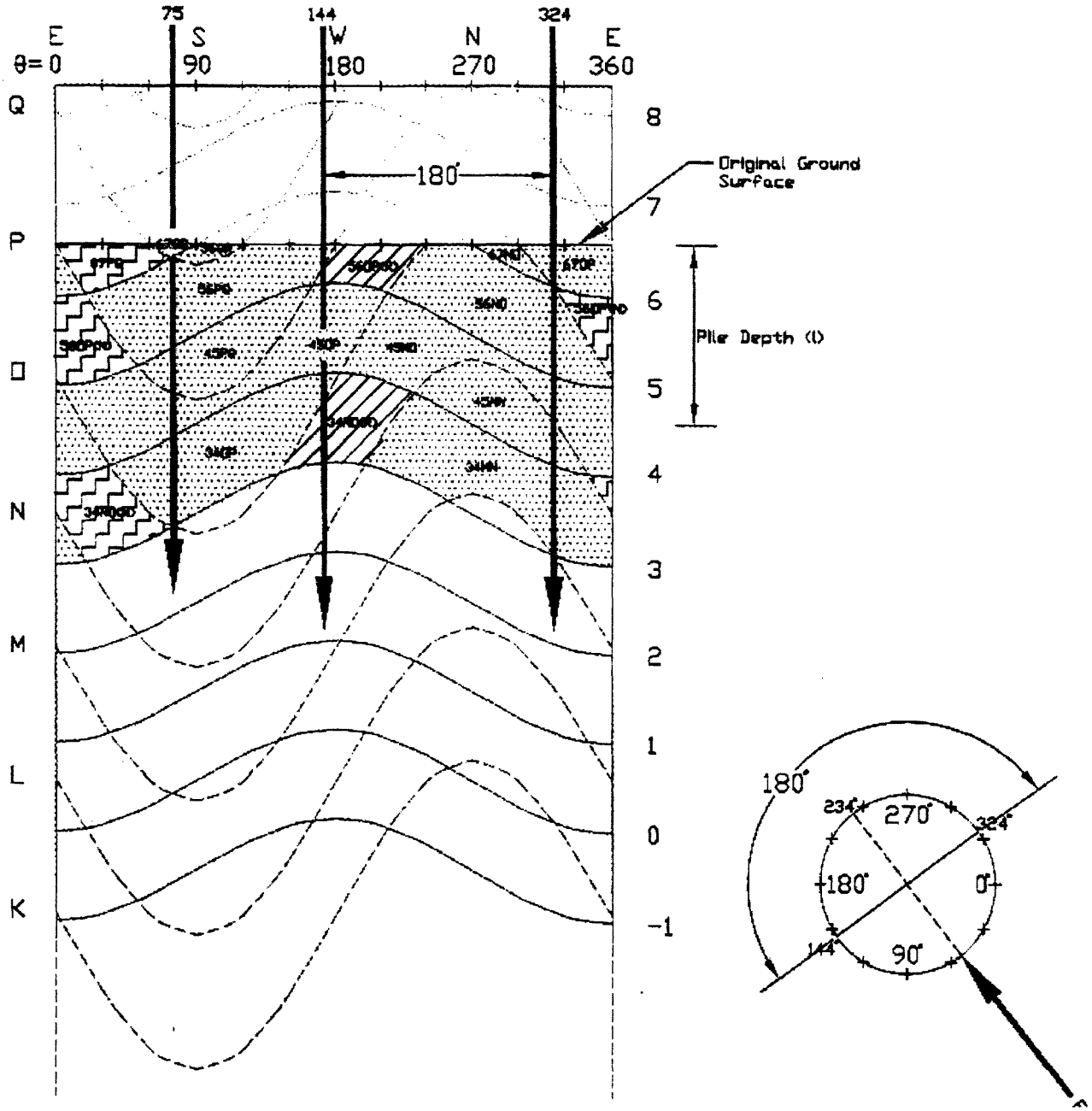

Figure 2.42 Area of Influence on the Right Extreme on a Joint Map on a Pile

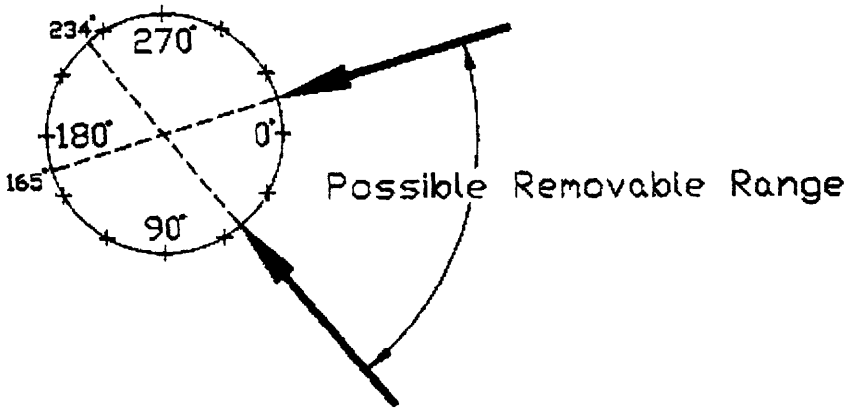

Figure 2.43 Possible Removable Range of Force Direction

8. If a force acts westward on the pile, a combination of removable blocks will be displaced because the area of influence is within the removable zone as shown on the joint map in Figure 2.44. In Figure 2.45, only the codes of the blocks that will be removed are shown. Here, blocks 56OP(R) and 34NO(R) are directly removable, but blocks 56QR, 56PQ, 56NO, 45PQ, 45OP, 45NO, 45MN, 34OP, and 34MN are made removable under the previous assumption that each block breaks apart right above the interference area when the pile is acted on by a force. Then, the codes of these blocks are then traced back to the joint mesh as shown in Figure 2.46. The whole wedge is displaced together with the pile as shown in Figure 2.47. An assumption is made here that a vertical cutting plane, which is perpendicular to the force direction and crosses the center of the pile, breaks the partially intersecting blocks (Type II and V blocks) apart. These blocks are shown dotted on the vertical cutting plane in Figure 2.44. This is a conservative assumption for ease of kinetic analysis, and more details will be added to this assumption in Chapter 3.

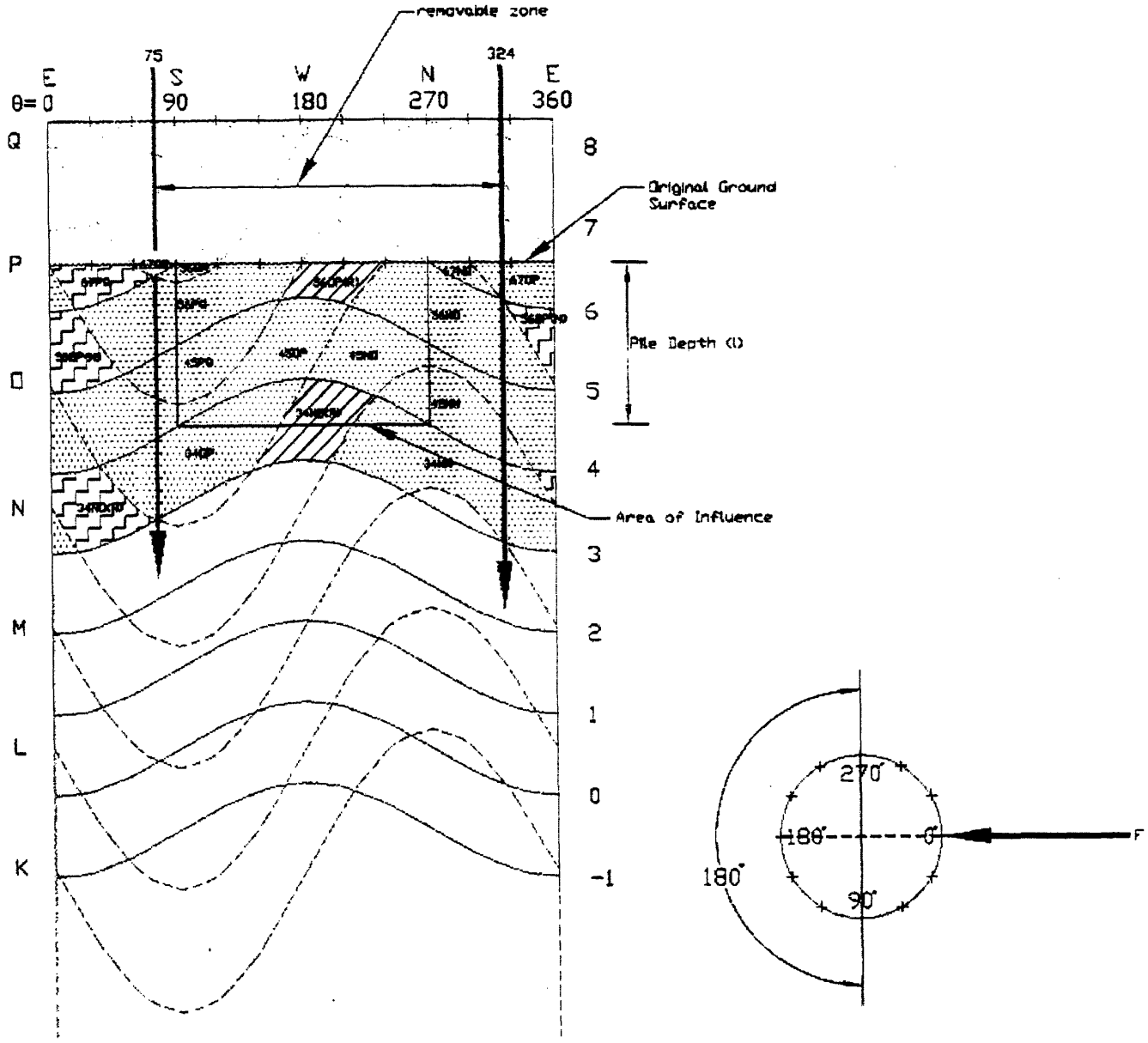

Figure 2.44 Identifying a Removable Combination of Blocks on a Joint Map on a Pile

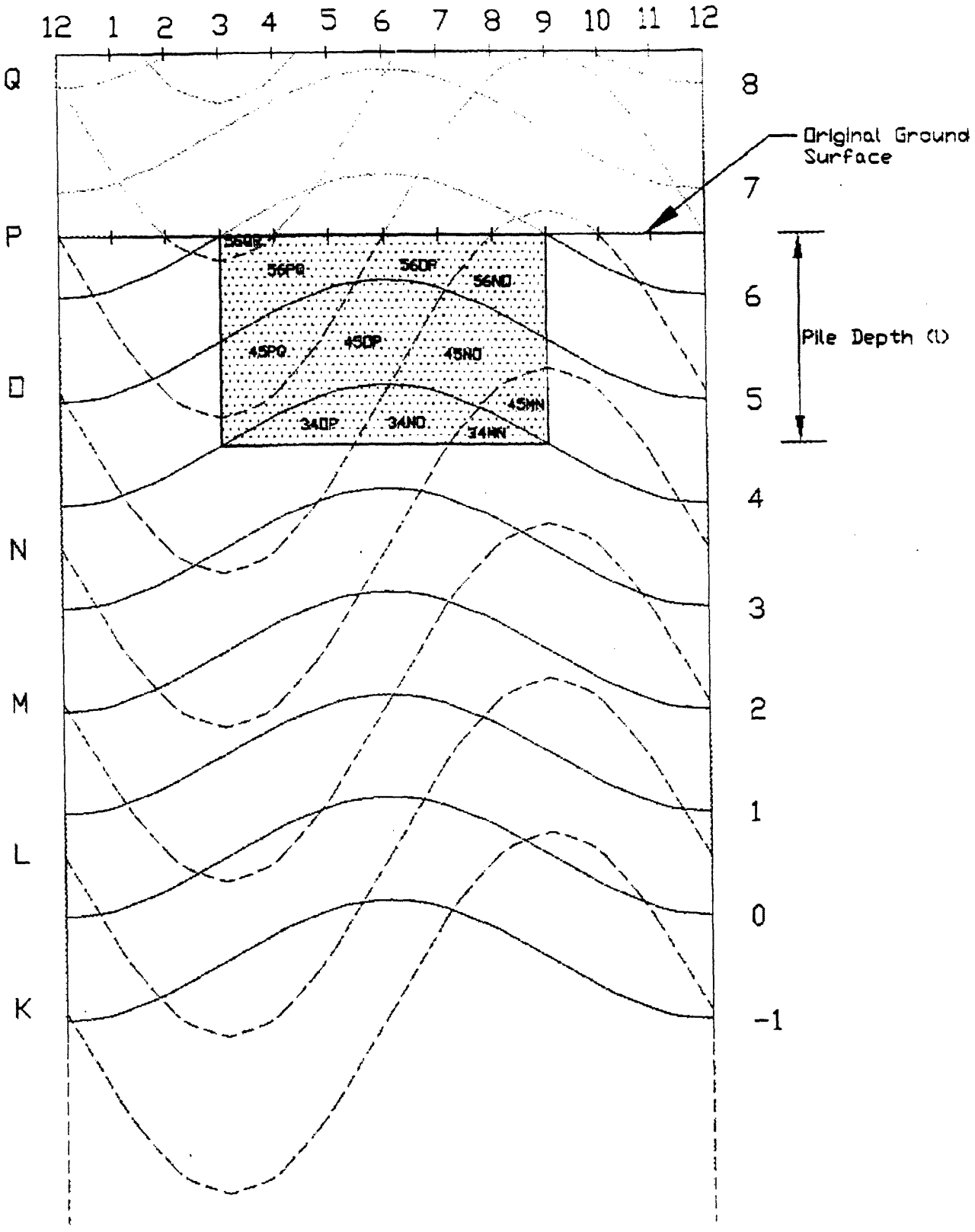

Figure 2.45 A Removable Combination of Blocks on a Joint Map on a Pile

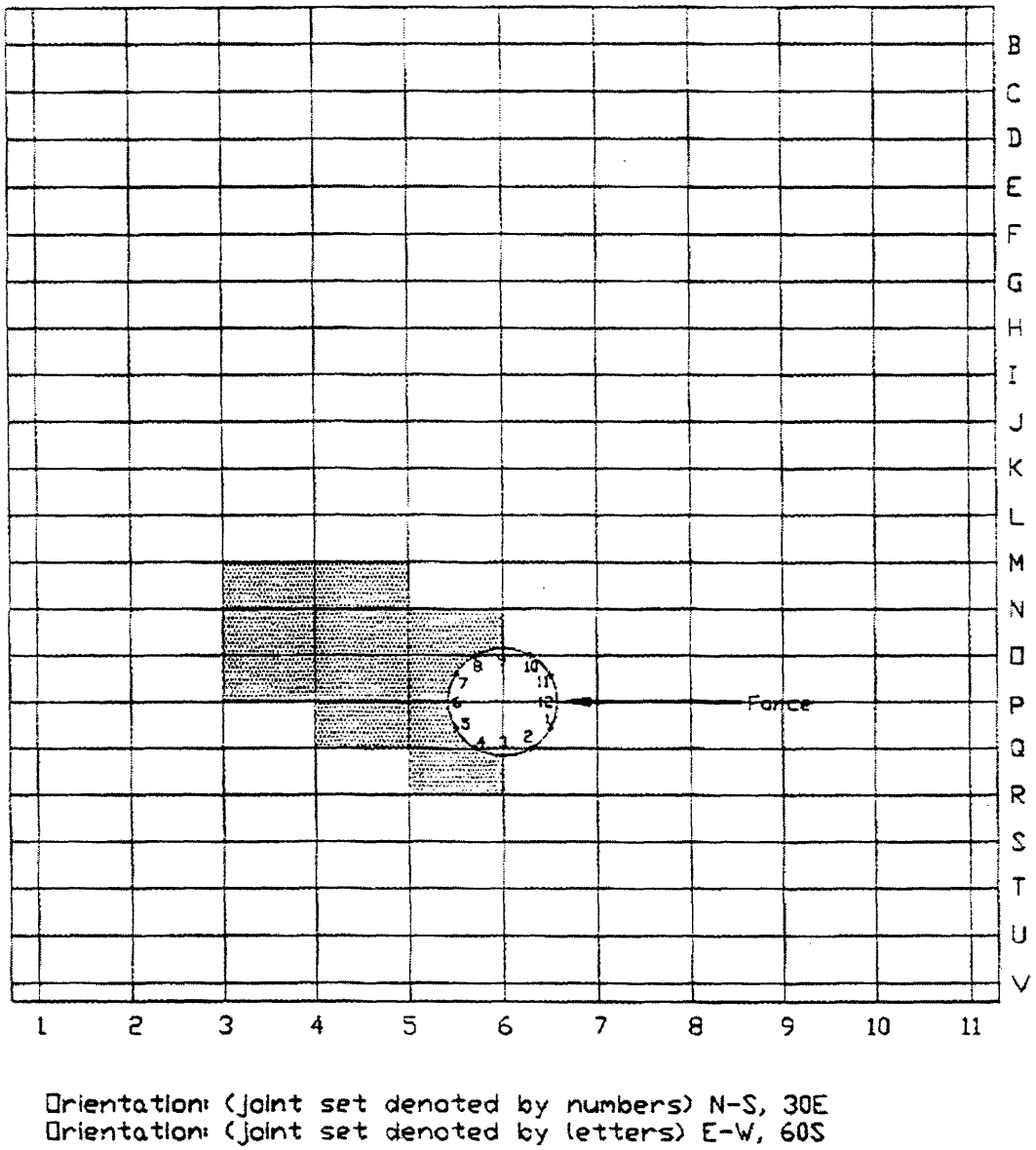

Figure 2.46 A Removable Combination of Blocks on the Surface Joint Mesh

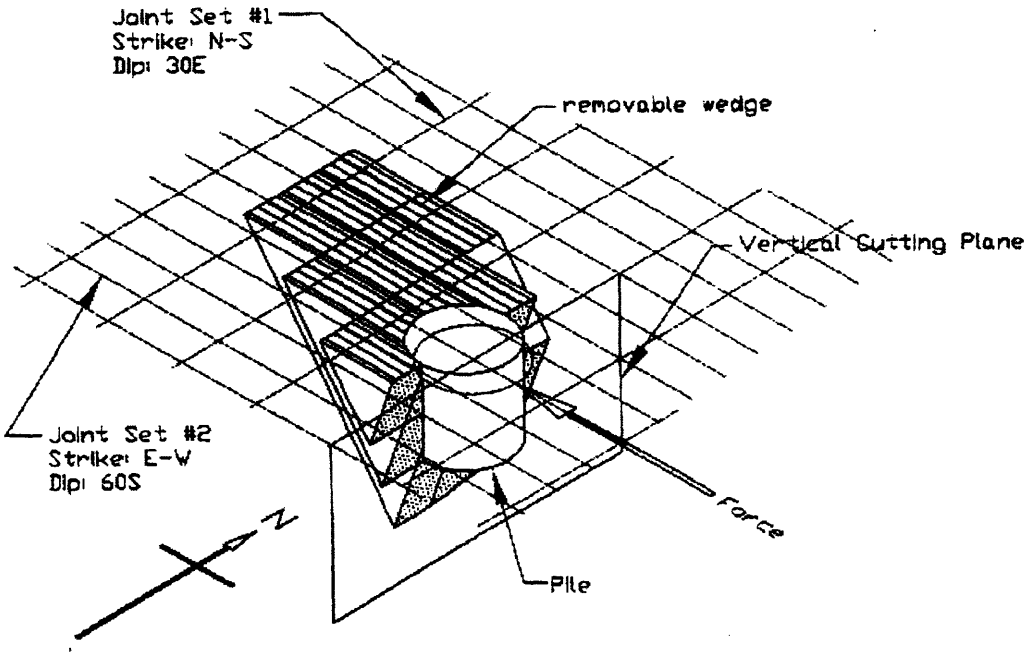

Figure 2.47 A Removable Wedge Moving Together With the Pile

2.9 SELECTION OF A REMOVABLE COMBINATION OF BLOCKS IN A 3-JOINT-SET SYSTEM

In a three-joint set system, many removable combinations of blocks may be identified for a single force since the degree of freedom is much greater in a three-joint set system than in a two-joint set system. The goal of selecting potential removable combinations here is to limit the number of them based on joint characteristics as will be discussed below. The 2D graphical methods discussed in Chapter 2.5 are used in the selection.

One more joint set is added to the previous example of a 2-joint set system in Chapter 2.7 to make it a 3-joint set system. Thus, the orientations of the joint sets are N-S, 30°E (1st joint set); E-W, 60°S (2nd joint set); and N45°E, 45°NW (3rd joint set) respectively. The joint mesh is shown in Figure 2.48 and the joint map on the pile is shown in Figure 2.49. Notice that joint set N-S, 30°E is denoted with numbers; joint set E-W, 60°S is denoted with capital letters; and joint set N45°E, 45°NW is denoted with small letters.

A 3D view of block 45NO, a Type II block, is shown in Figure 2.50. Notice that joints of the third joint set N45°E, 45°NW cut across block 45NO at equal intervals. When a force acts on the pile such that block 45NO lies in the area of influence, the block may be displaced off a joint near the interference area between the pile and the block as shown in Figure 2.51. This displacement off a joint is similar to the assumption made earlier in a 2-joint set system that a Type II or Type V block breaks apart somewhere in the interference area. The previous assumption can still be used in a 3-joint set system when no joint cuts across a block right above the interference area so that the block can be made removable.

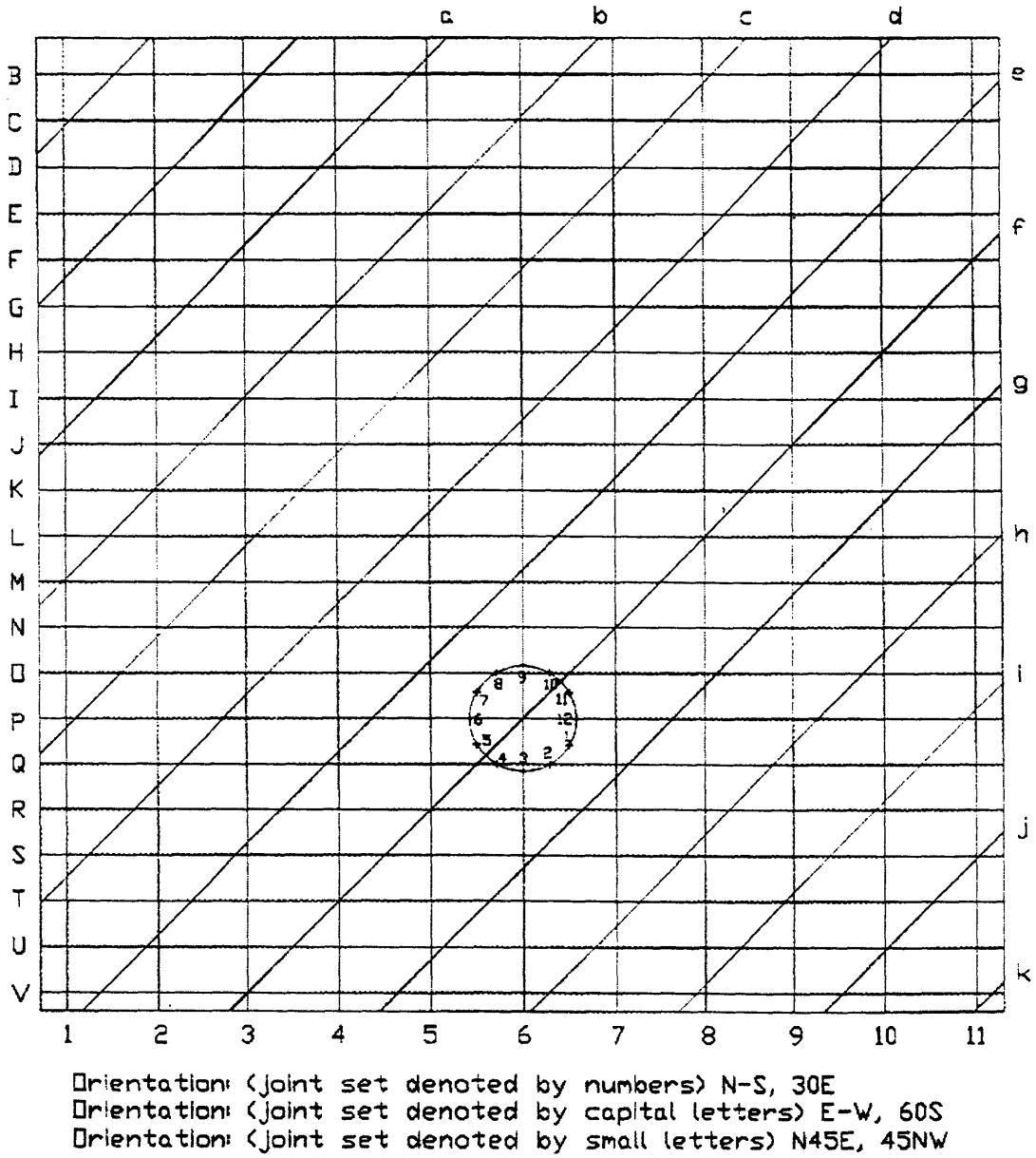

Figure 2.48 Joint Mesh of a Three-Joint-Set System

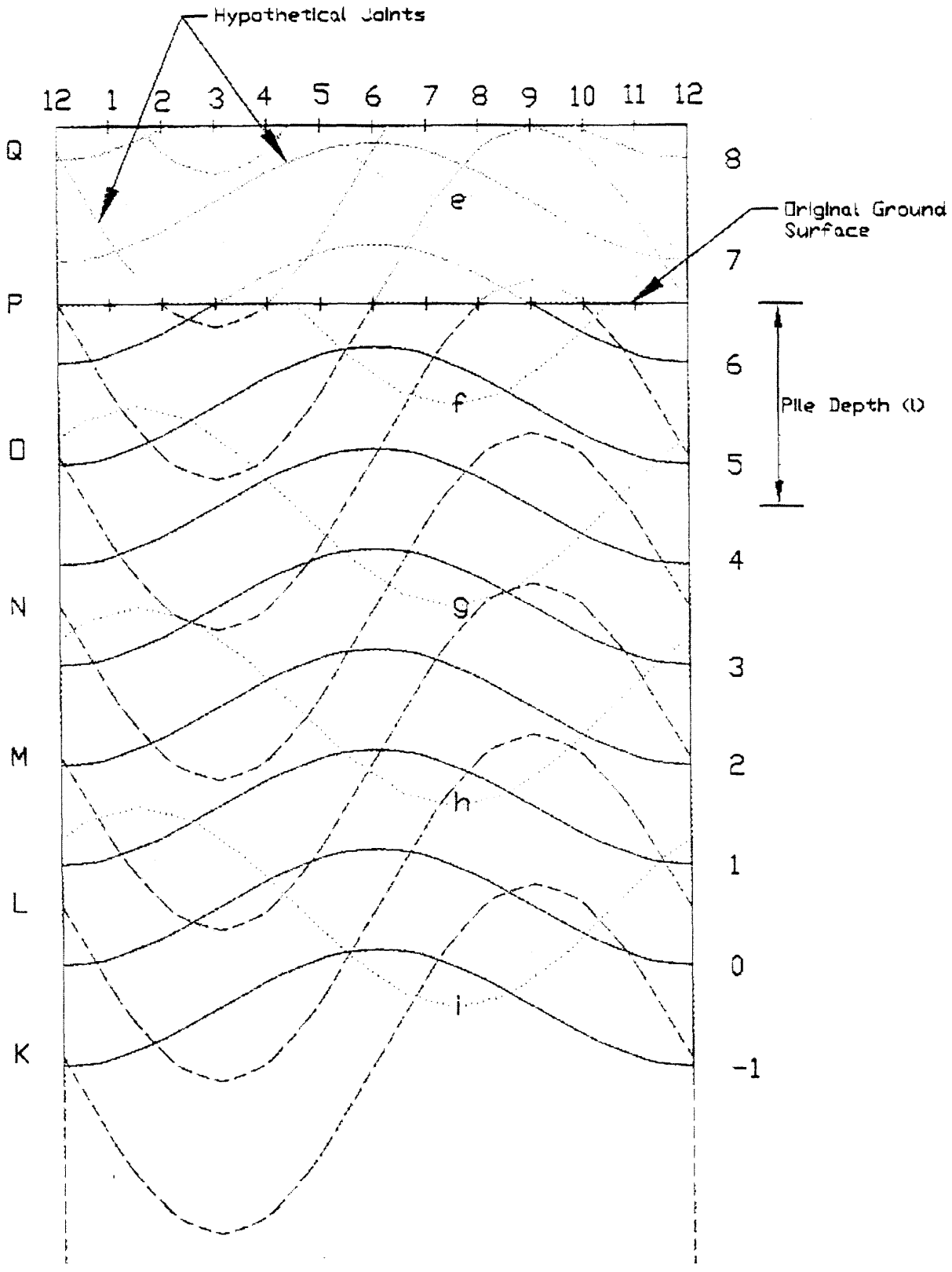

Figure 2.49 Joint Map of a Three-Joint-Set System

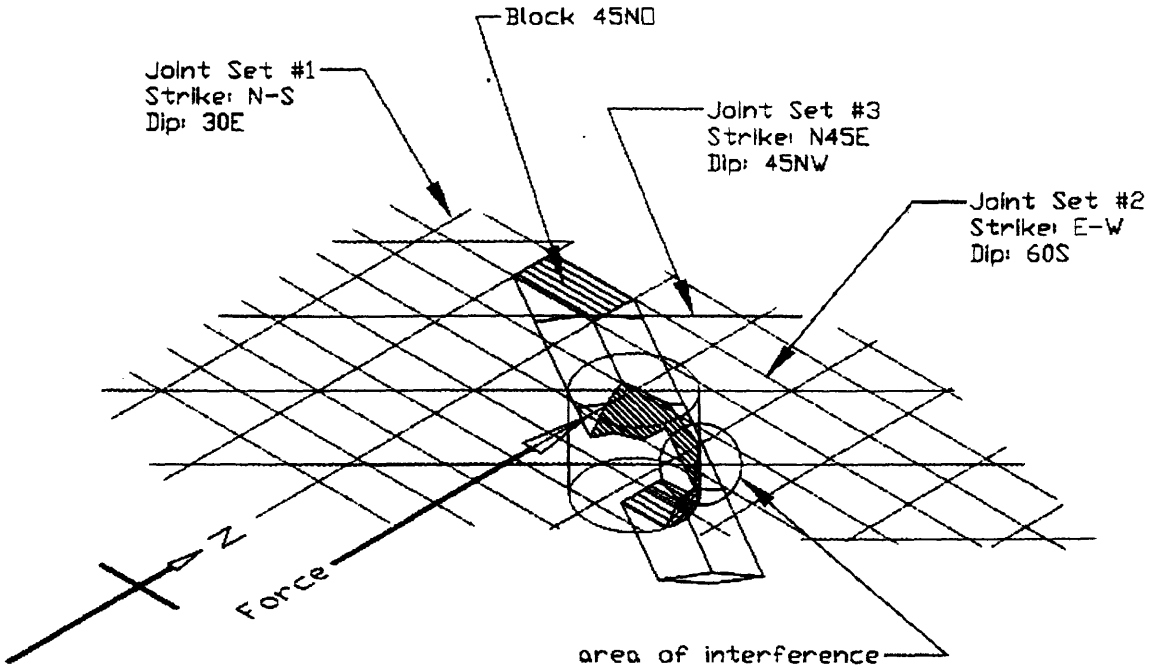

Figure 2.50 Block 45NO in 3D View

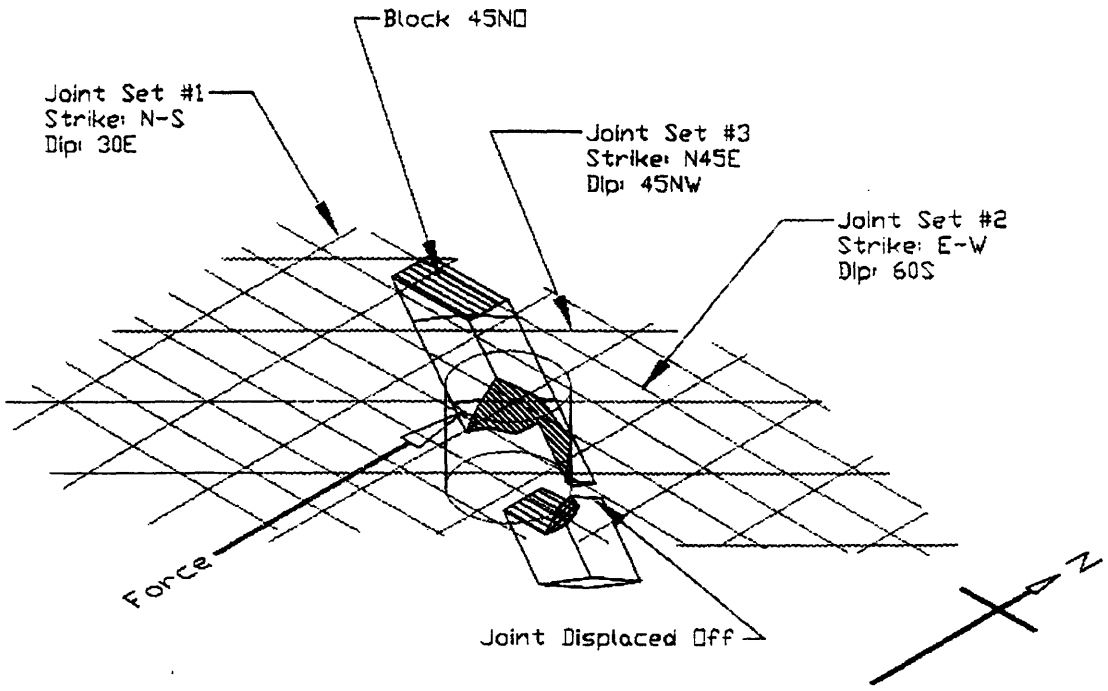

Figure 2.51 Displacement of Block 45NO

Now, the kinematics of blocks sharing a common intersection with the pile is examined. Figures 2.52 and 2.53 shows block fgNO and block 45fg respectively, which are Type II blocks. Block 45NO, block fgNO, and block 45fg share a common intersection as shown in Figure 2.54 since each block has a pair of adjacent joints in common with another block. The grids of these blocks are shown on the joint mesh in Figure 2.55 and on the joint map on the pile Figure 2.56, where the common intersection can also be seen.

Assuming that a force acts on the pile northward, since the grids of these three blocks intersect the area of influence on the joint map as shown in Figure 2.56, displacement of blocks may result. The removal direction of each block is indicated by its arrow direction in Figure 2.55. Although block fgNO lies within the area of influence, its removal direction is almost opposite to the force direction, and thus by intuition, block fgNO cannot be displaced by this particular force. This can actually be proved by kinetic analysis, and the force will turn out to be negative, meaning that the block is stable. Block 45fg and block 45NO have no such problem since their removal directions have components that lie in the force direction. Sometimes it may not be obvious whether a removable block (Type I, II, IV, or V block) can be displaced by a particular force, and thus such block should be considered for kinetic analysis as well.

Two ways that block 45NO and block fgNO can be displaced are shown in Figures 2.57 and 2.58. Block 45NO and block fgNO have a volume of common intersection that also intersects the pile. When the force acts on the pile northward, the pile pushes on this volume of common intersection. This volume of common intersection then displaces either block 45NO or fgNO because this volume can move in only one direction, namely the removal direction of block 45NO or that of block fgNO. In Figure 2.57, the pile pushes the common intersection to displace block fgNO. When the pile is moving in the removal direction of block fgNO, block 45NO is also displaced because block 45NO also intersects the pile elsewhere in addition to the common intersection as indicated on the joint map in Figure 2.59. In Figure 2.58, the pile pushes the common intersection to displace block 45NO. Similar to block 45NO in Figure 2.57, block fgNO is displaced only because it also intersects the pile elsewhere in addition to the common intersection as indicated on the joint map in Figure 2.59.

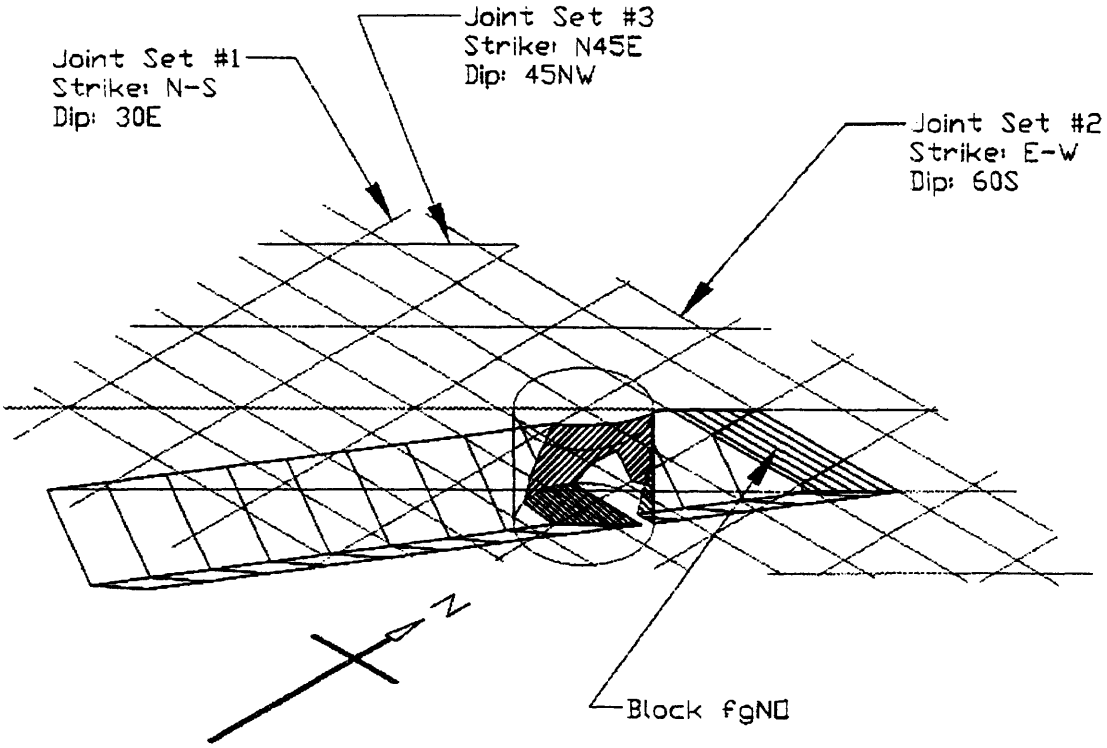

Figure 2.52 Block Nofg in 3D View

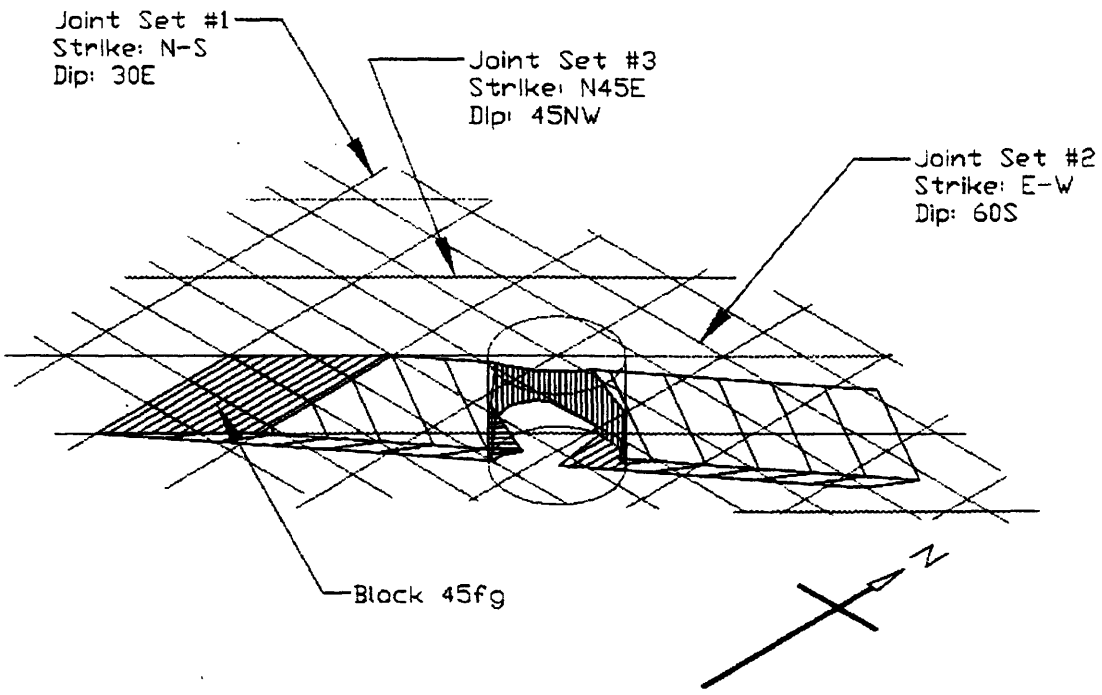

Figure 2.53 Block 45fg in 3D View

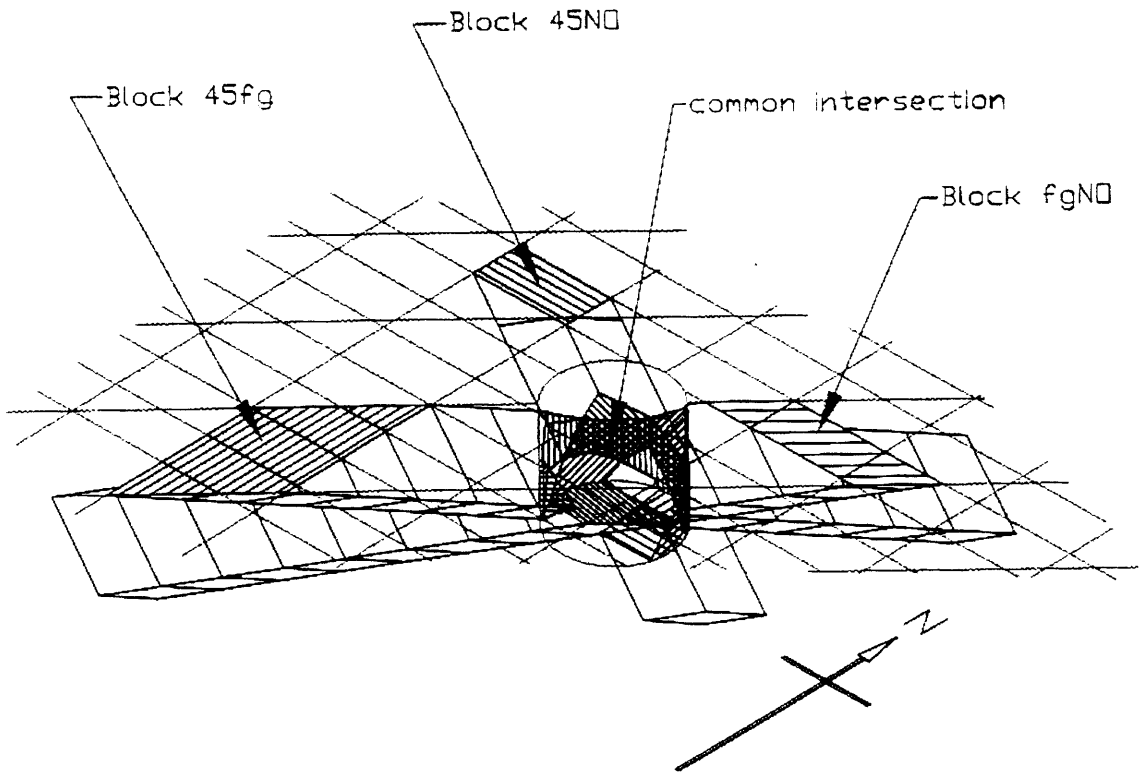

Figure 2.54 Three Blocks Sharing a Common Intersection

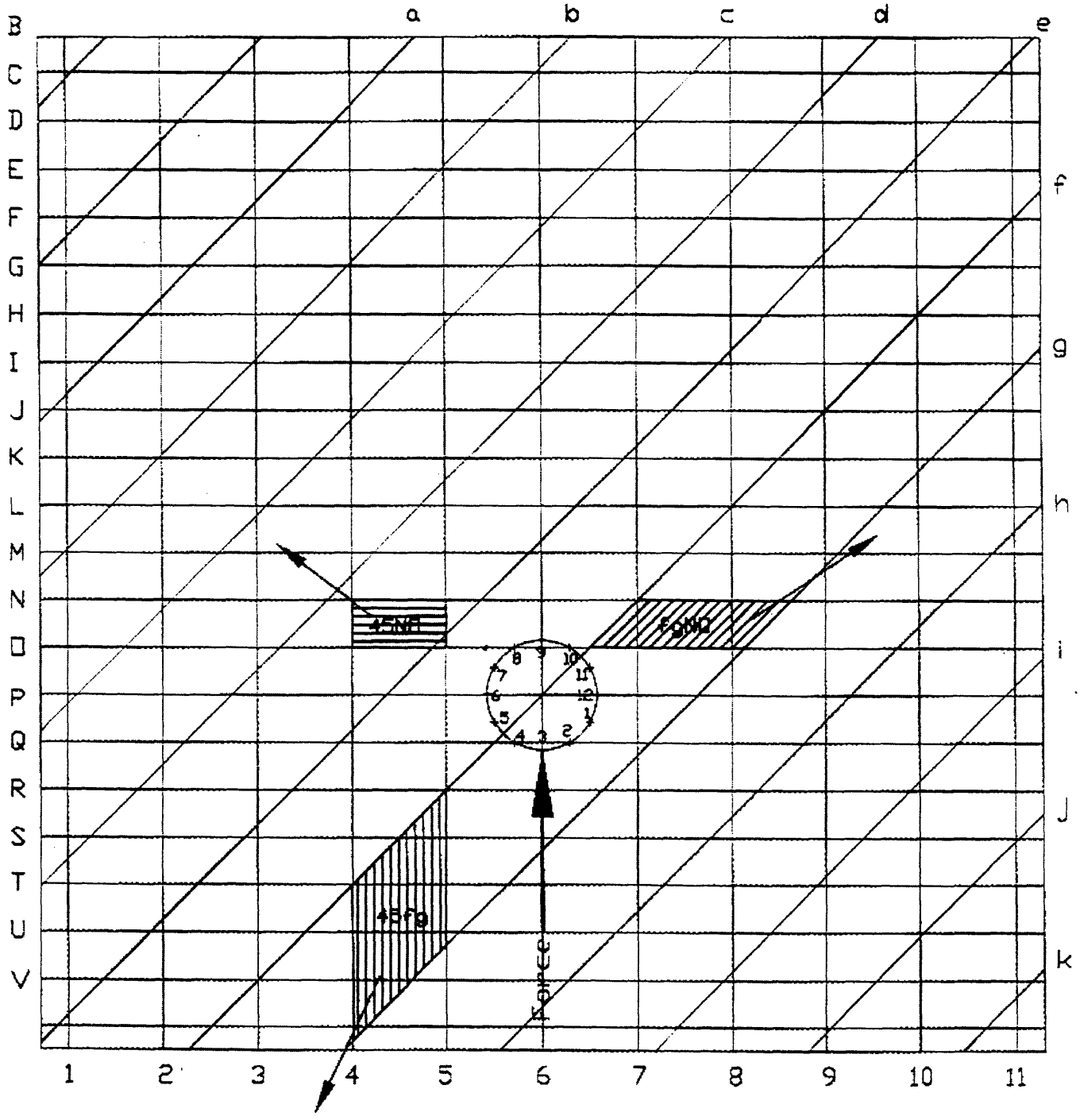

Figure 2.55 Removal Direction of Blocks in Plan View

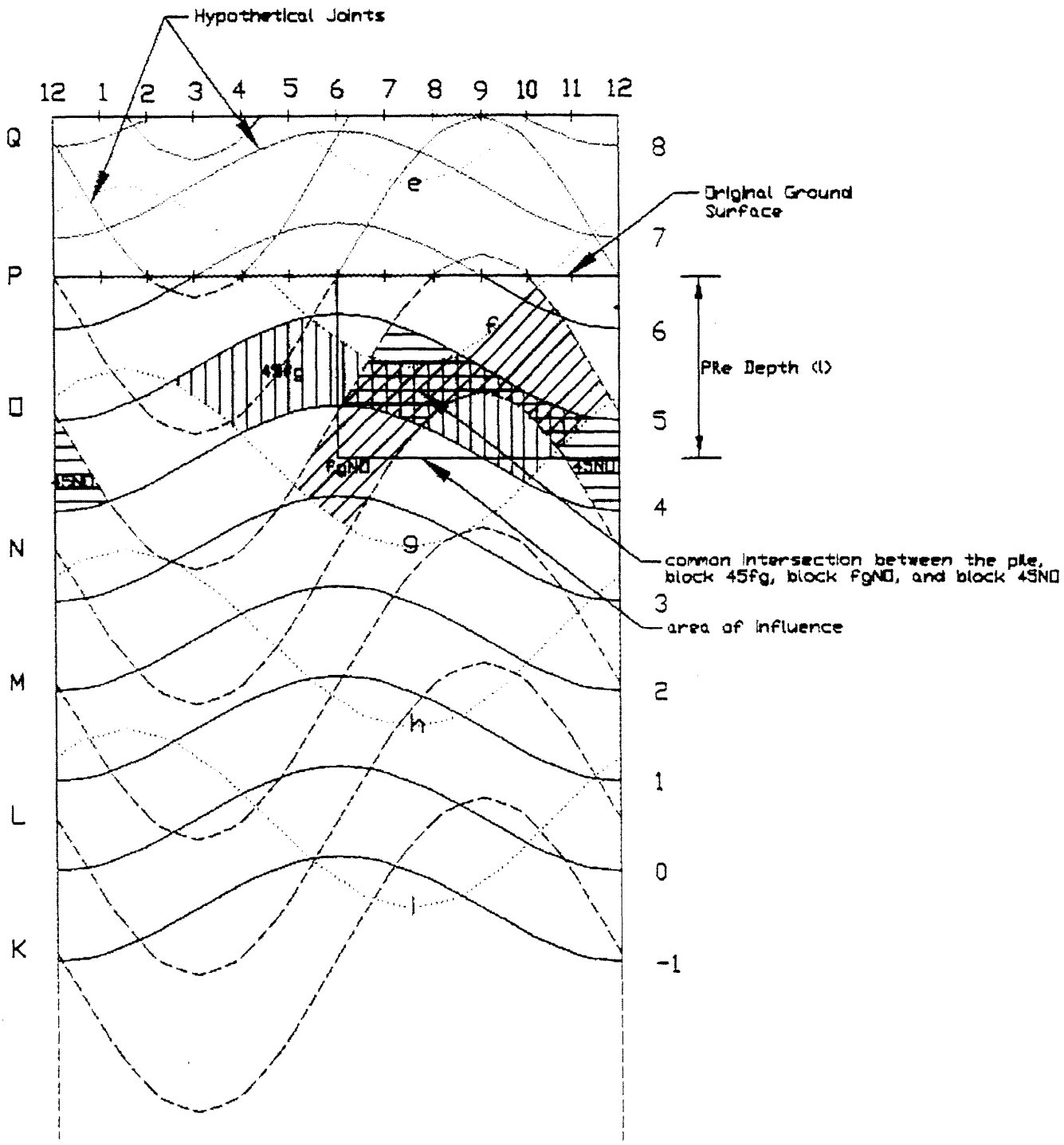

Figure 2.56 Common Intersection of Three Different Blocks and the Pile

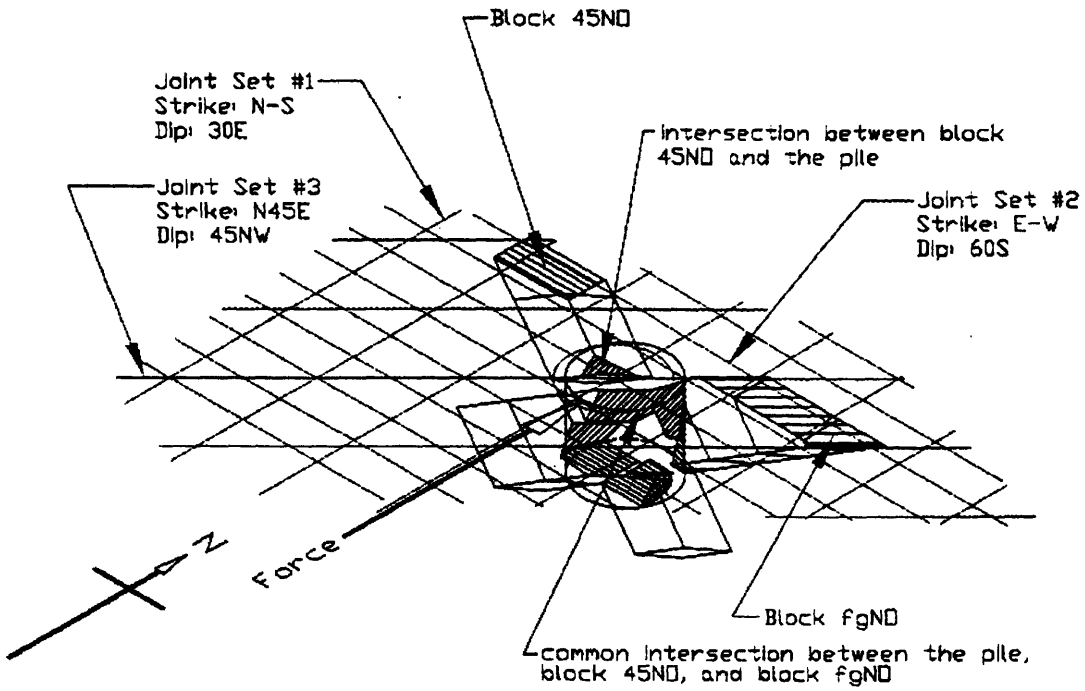

Figure 2.57 Displacement of Block fgNO and 45NO

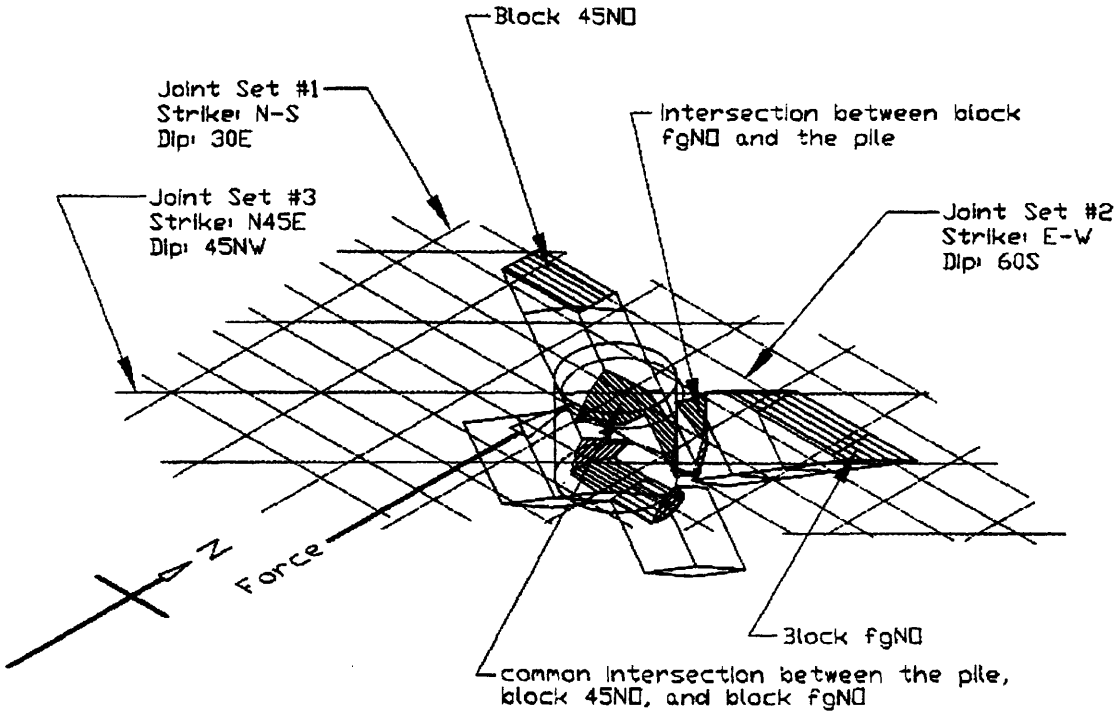

Figure 2.58 Displacement of Block 45NO and fgNO

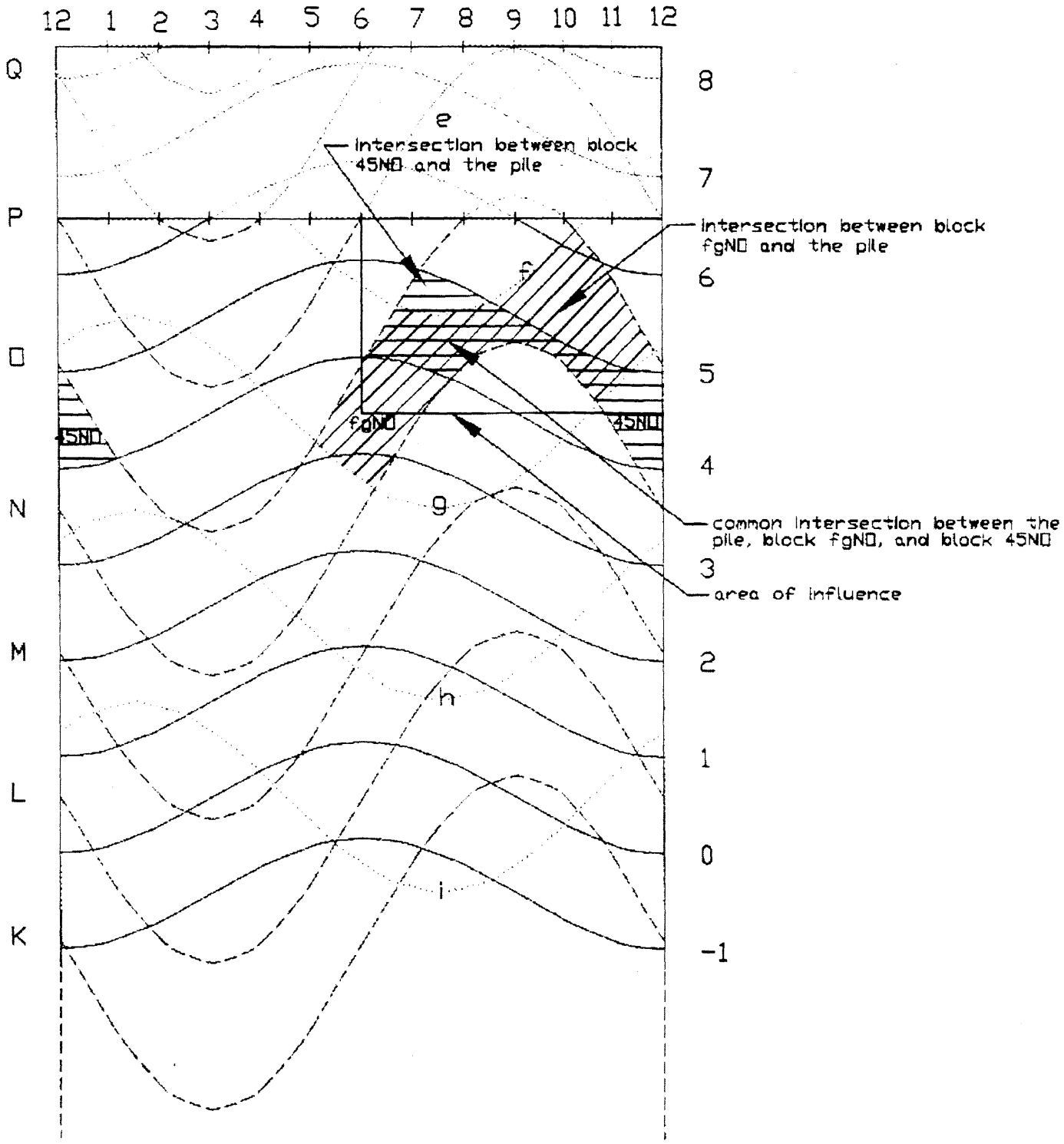

Figure 2.59 Common Intersections Among Block fgNO, Block 45NO, and the Pile

Now all the removable blocks intersecting the pile shall be examined to see the big picture, and the 2D graphical methods are used to accomplish this task. Three joint maps on the pile, each composed of two different joint sets, are shown in Figures 2.60, 2.61, and 2.62. On these joint maps, Type I and IV blocks are shaded and Type II and V blocks are dotted, and the removable range is bounded by the vertical arrows. Notice that in Figure 2.62, since all the blocks are Type II partially intersecting blocks, the area from the surface to just below the bottom of the pile is dotted. These Type I, II, IV, and V blocks on the joint maps in Figures 2.60, 2.61, and 2.62 are traced to the joint mesh in Figure 2.63 and are hatched based on their bounding joints. In the same figure, the removal directions of blocks bounded by different pairs of joint sets are shown with arrows.

If a force acts on the pile northward, some blocks bounded by joints of the 1^{st} and 2^{nd} joint sets and some blocks bounded by joints of the 2^{nd} and 3^{rd} joint sets will be displaced based on the force direction and removal direction of blocks. Before kinetic analysis, it is not known whether more blocks bounded by joints of the 1^{st} and 2^{nd} joint sets will be displaced or more blocks bounded by joints of the 2^{nd} and 3^{rd} joint sets will be displaced. Thus, one should select as many removable blocks bounded by joints of one pair of joint sets as possible first. This pair of joint sets is called the primary pair of joint sets. Then, blocks bounded by joints of the other pair of joint sets are selected. This second pair of joint sets is called the secondary pair. In this particular example, when the force pushes northward, there are two combinations of removable blocks, one having the 1^{st} and 2^{nd} joint sets as the primary pair and the second having the 2^{nd} and 3^{rd} joint sets as the primary pair. In general, there can be as many as six possible combinations in a 3-joint-set system when selecting combinations in such way for a particular force as shown in Table 2.5. But in this case, since the 1^{st} and 3^{rd} joint sets cannot be a possible pair, the number of possible combinations is reduced to two.

Table 2.5 Possible Removable Combinations

Primary Pair	Secondary Pair
1st and 2nd	1st and 3rd
1st and 2nd	2nd and 3rd
1st and 3rd	1st and 2nd
1st and 3rd	2nd and 3rd
2nd and 3rd	1st and 2nd
2nd and 3rd	1st and 3rd

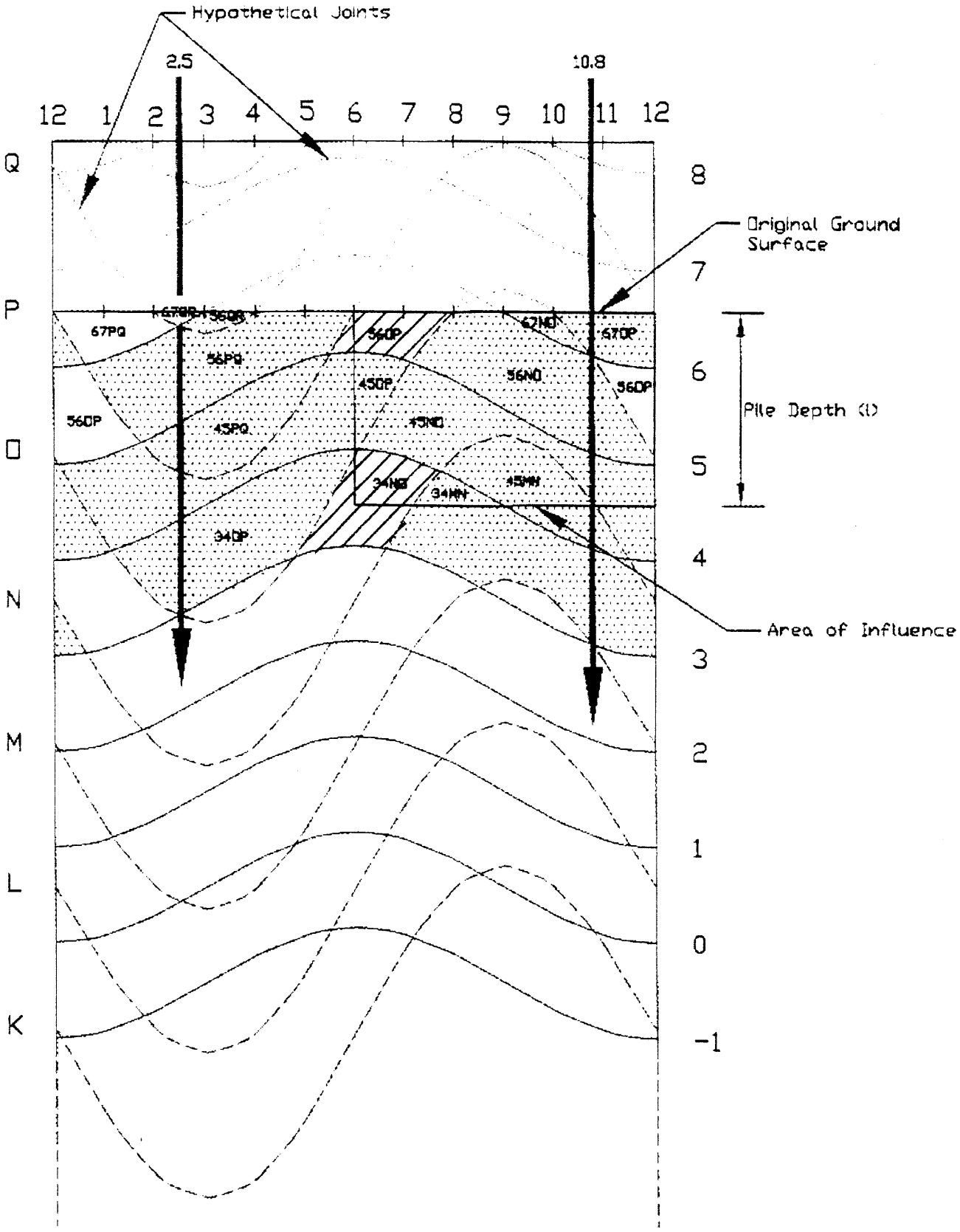

Figure 2.60 Joint Map on a Pile for the 1st and 2nd Joint Sets

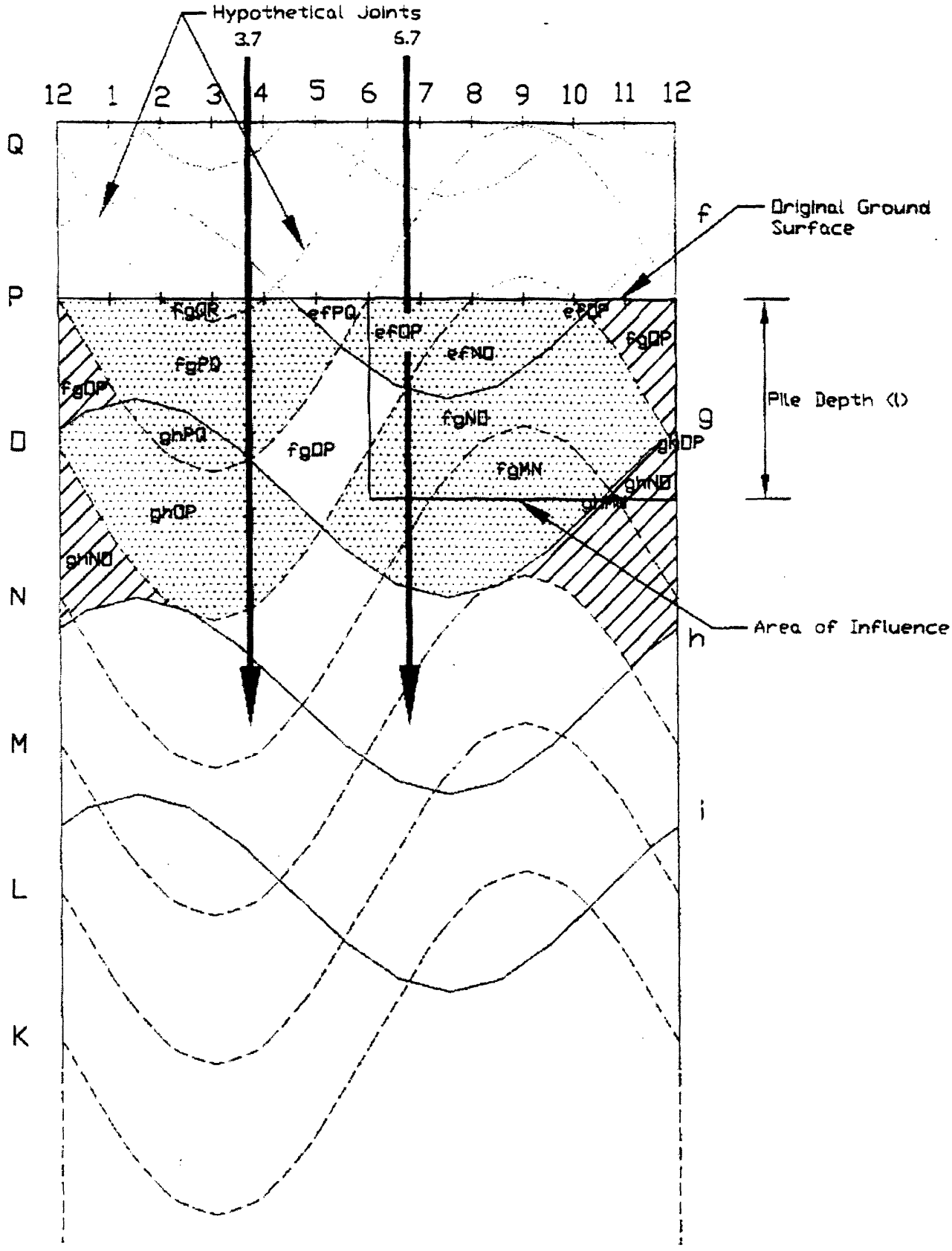

Figure 2.61 Joint Map on a Pile for the 2nd and 3rd Joint Sets

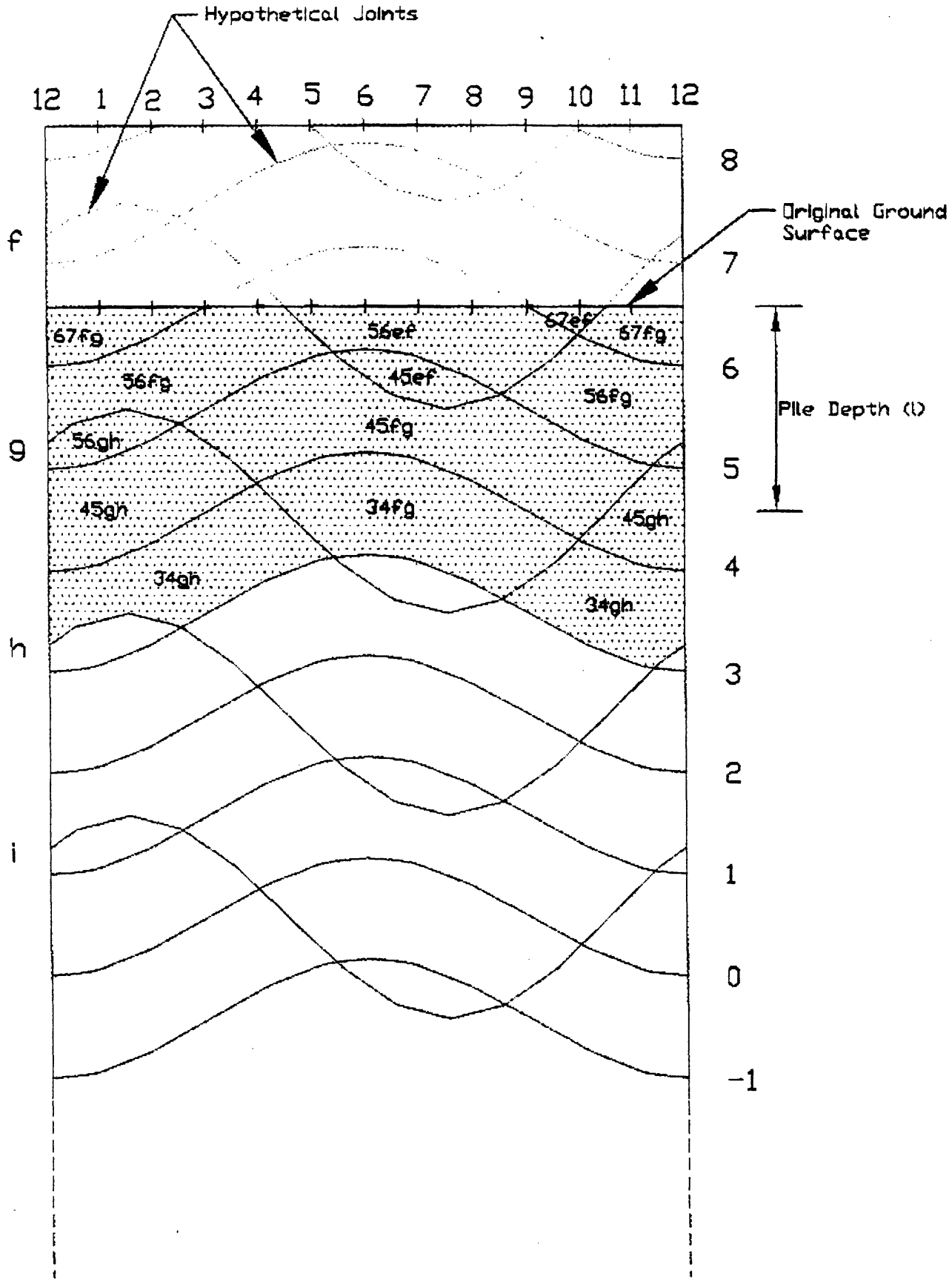

Figure 2.62 Joint Map on a Pile for the 1st and 3rd Joint Sets

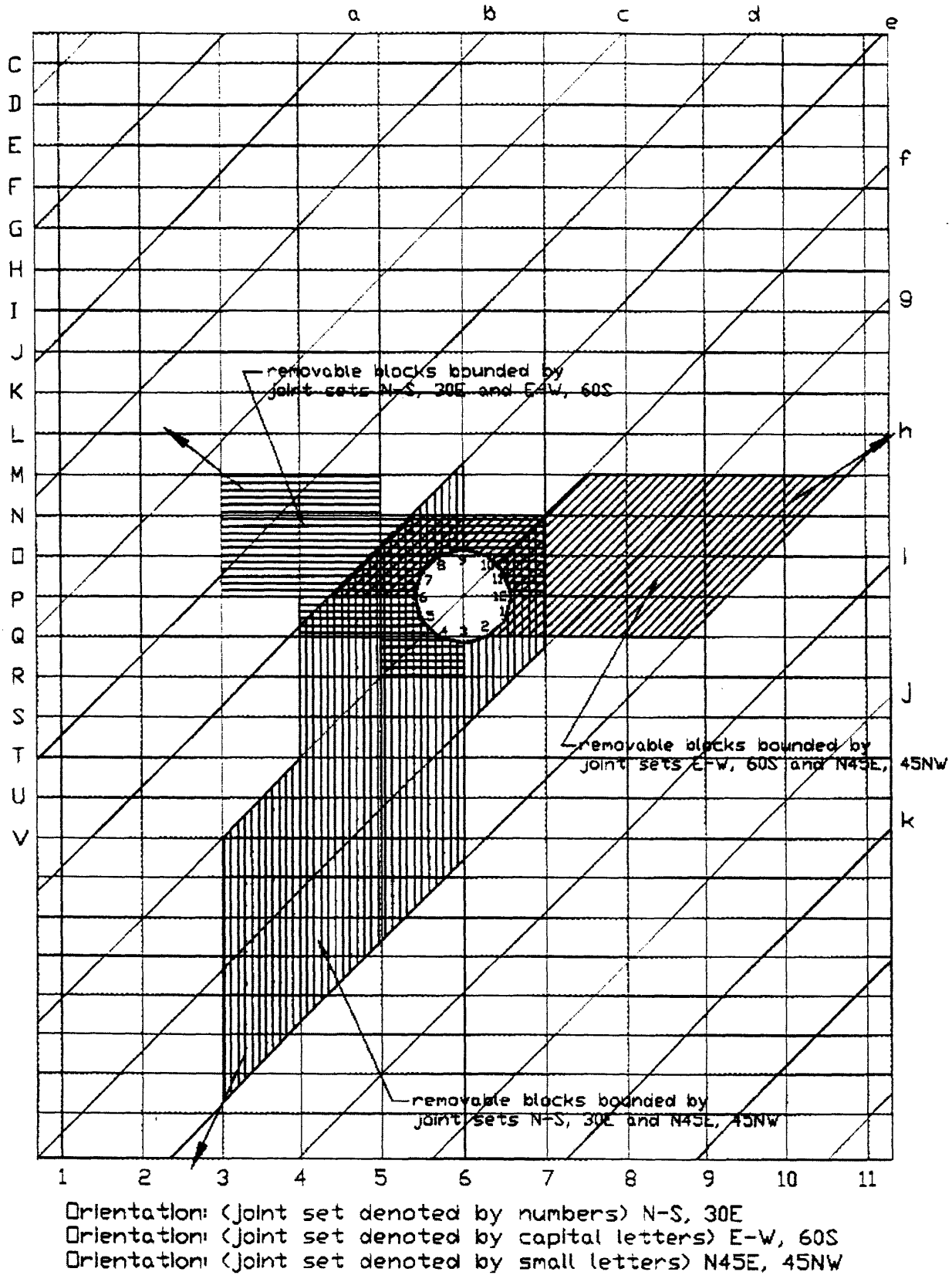

Figure 2.63 Removable Blocks for Each Pair of Joint Sets

The area of influence is shown on the joint map of the 1st and 2nd joint sets in Figure 2.64 and that of the 2nd and 3rd joint sets in Figure 2.65. For the first combination, the 1st and 2nd joint sets are treated as the primary pair. The removable blocks that intersect the area of influence are selected first by using Figure 2.64, and the blocks selected are shown shaded with vertical lines on the joint mesh in Figure 2.66. Since block 56OP(N) is a non-removable block in Figure 2.64, some removable block(s) bounded by joints of the secondary pair of joint sets must be selected to cover grid 56OP(N) in the area of influence. Thus, block fgOP(R) is selected from Figure 2.65 to be part of the removable combination since its grid covers the whole grid 56OP(N). Block fgOP(R) is traced to the joint mesh in Figure 2.66 and is shown shaded with slanted lines. The 3D views of all the selected blocks bounded by joints from the 1st and 2nd joint sets, block fgOP(R), and the whole combination of removable blocks are shown in Figures 2.67, 2.68, and 2.69 respectively. Similar to a 2-joint-set system, it is assumed that a vertical cutting plane, which is perpendicular to the force direction, breaks the partially intersecting blocks apart. These blocks are shown dotted on the vertical cutting plane in Figure 2.67, 2.68, and 2.69. Again, this is a conservative assumption for ease of kinetic analysis, and more details will be added to this assumption later in Chapter 3. The displacement process is shown in Figure 2.70. The blocks composed of the primary pair are displaced together with the pile in the northwestern direction. Block fgOP(R), however, is displaced in the northeastern direction.

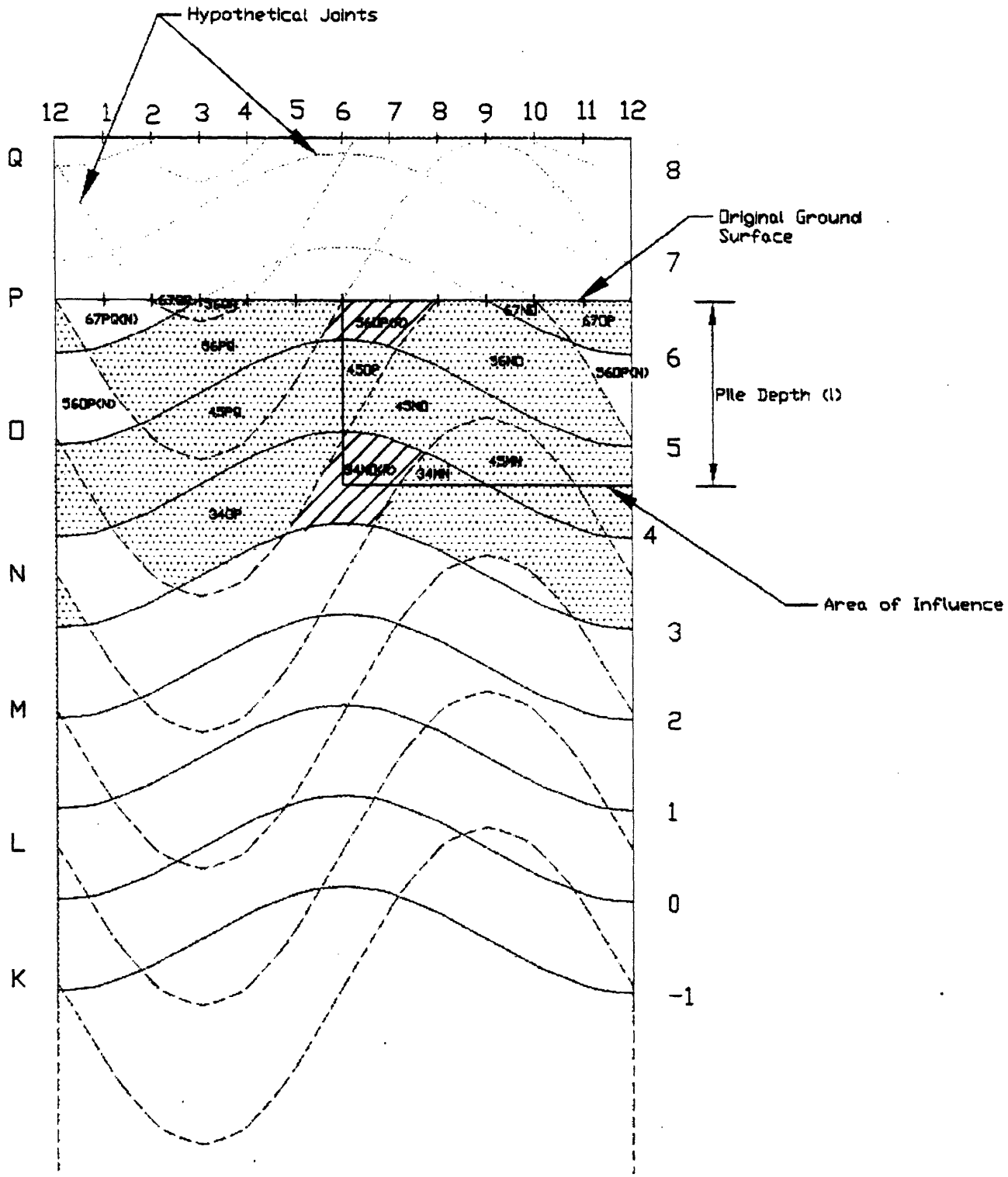

Figure 2.64 Joint Map on a Pile for the 1st and 2nd Joint Sets

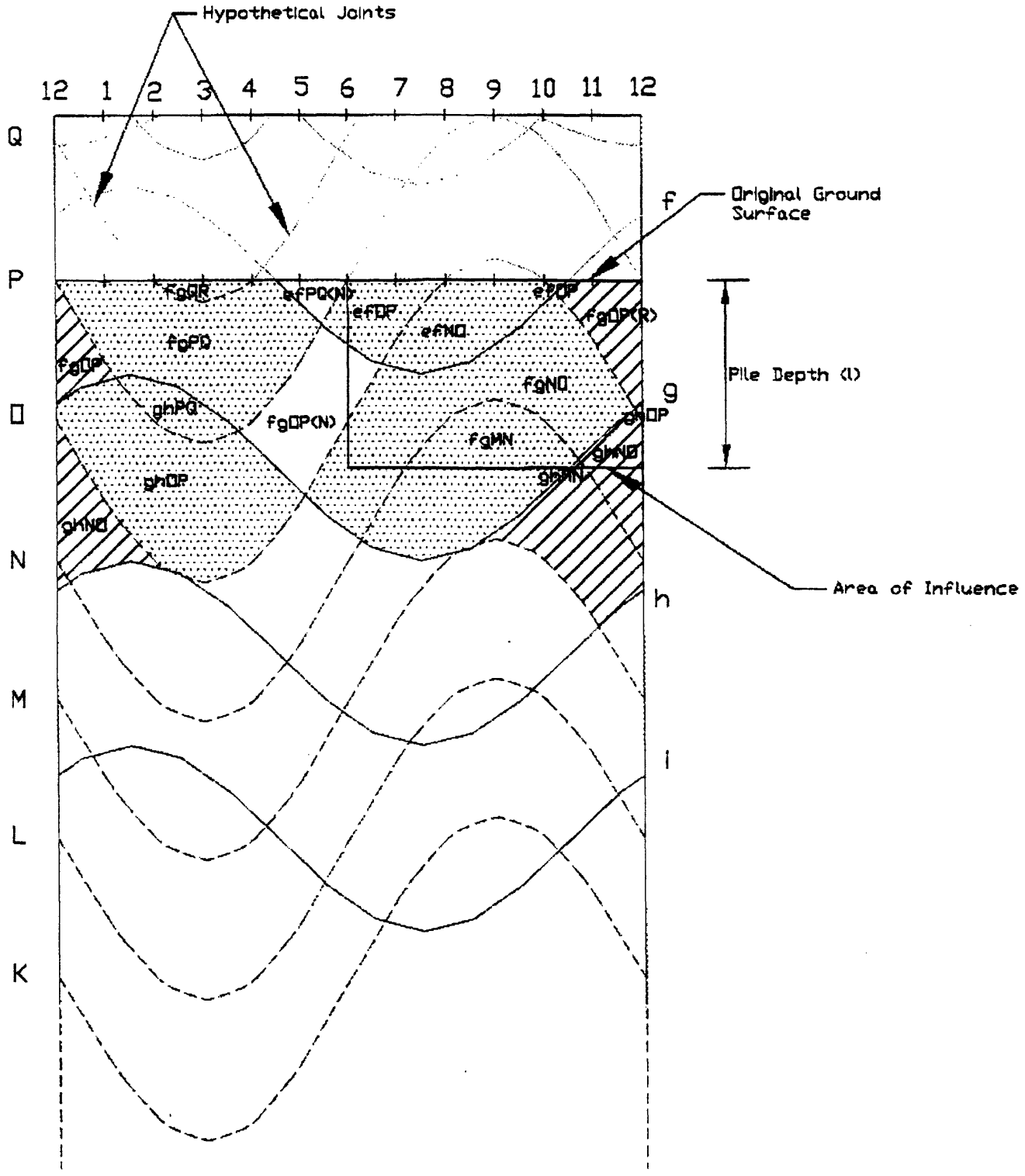

Figure 2.65 Joint Map on a Pile for the 2nd and 3rd Joint Sets

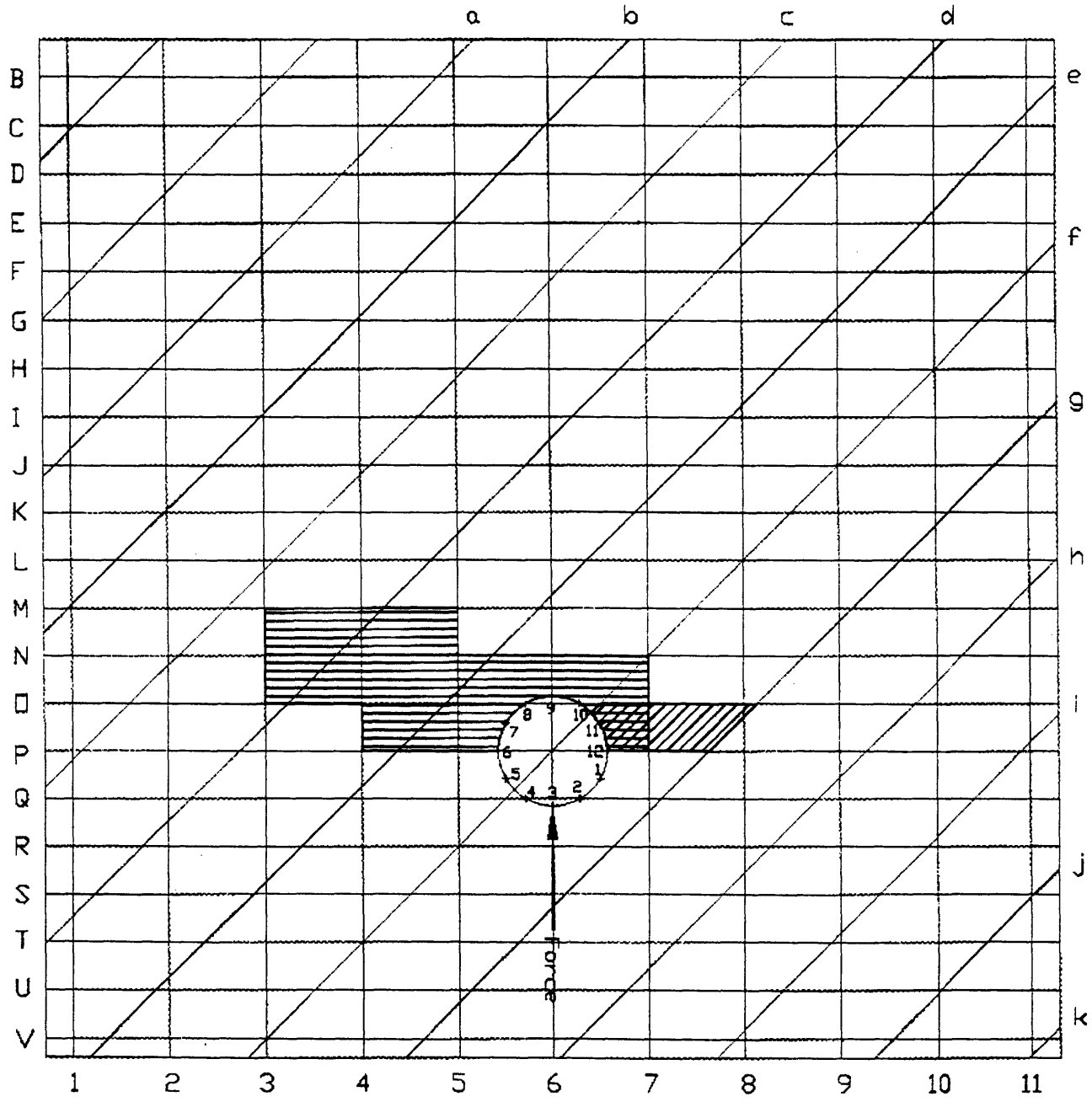

Figure 2.66 A Combination of Removable Blocks

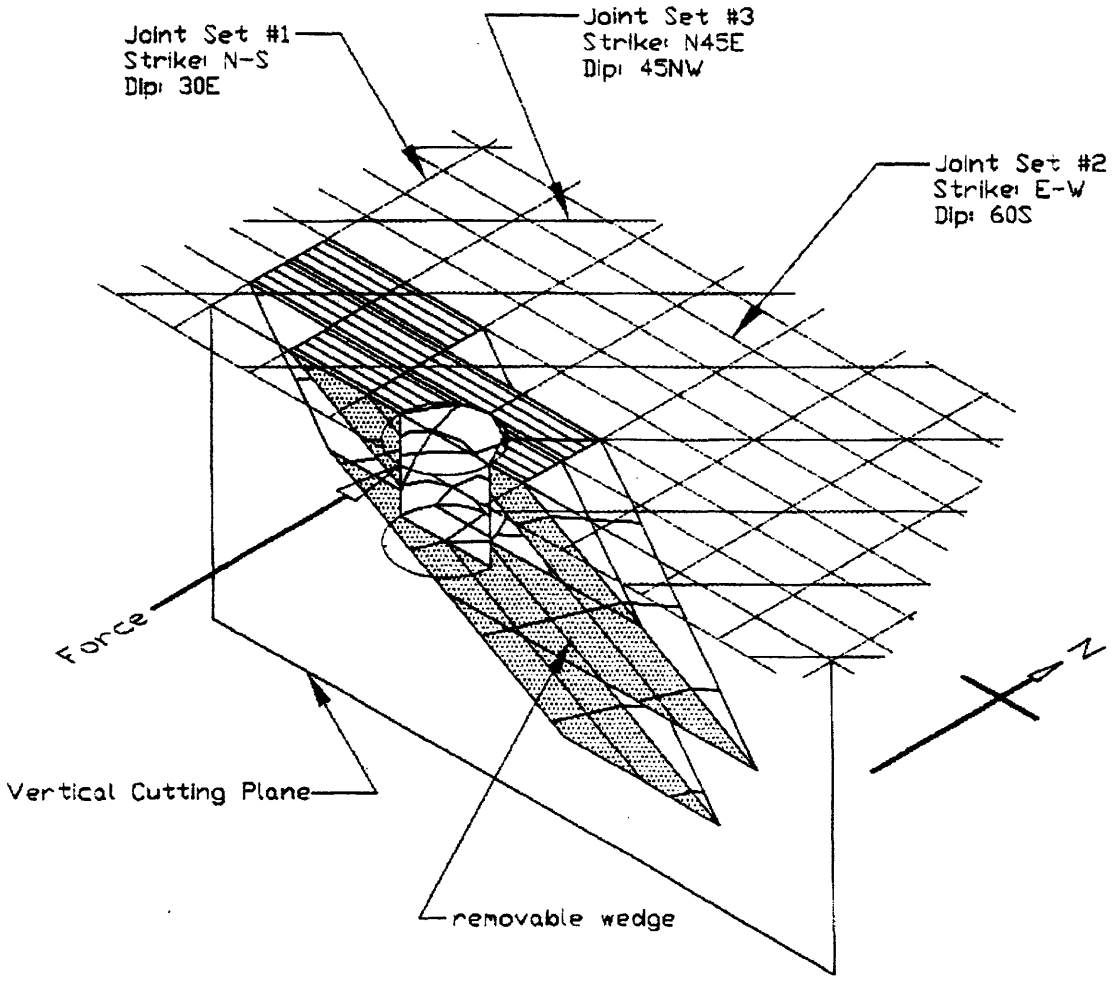

Figure 2.67 Blocks Bounded by the 1st and 2nd Joint Sets in a Removable Combination

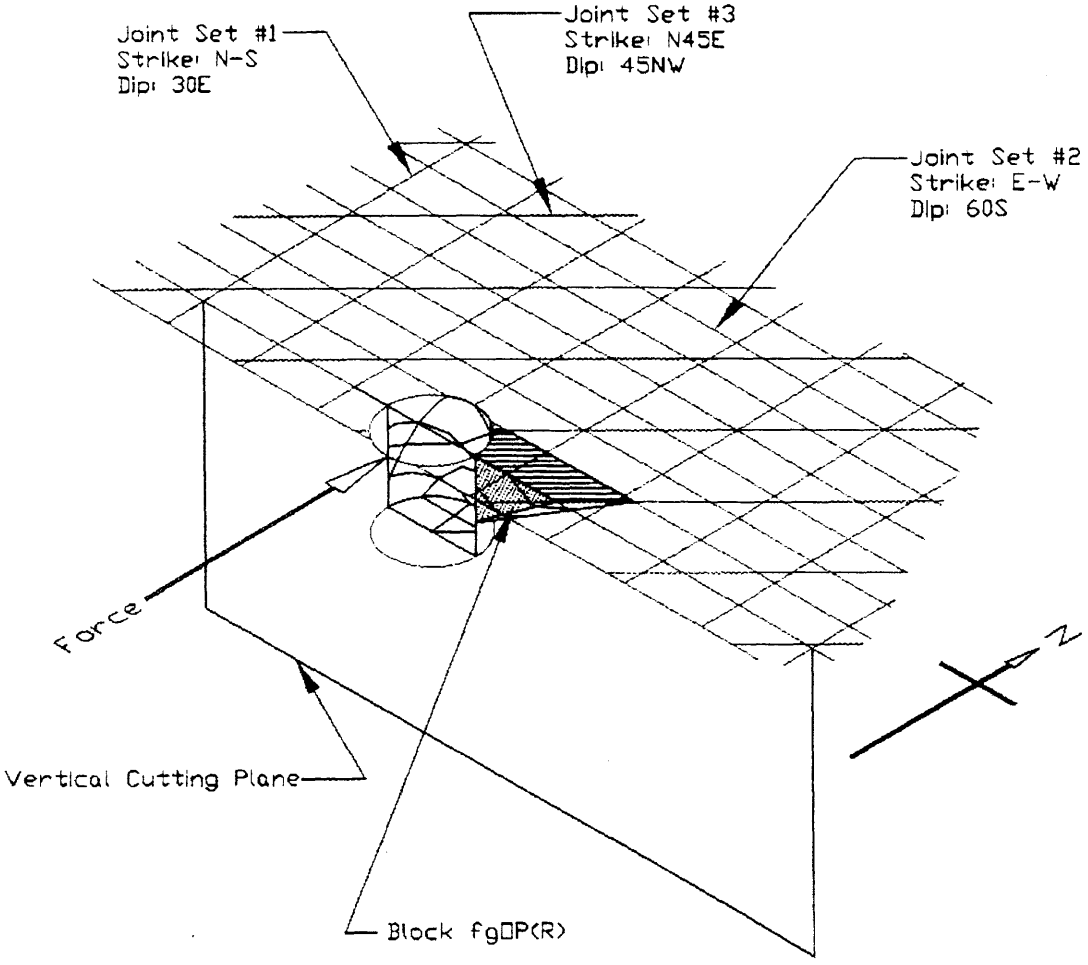

Figure 2.68 A Block Bounded by the 2nd and 3rd Joint Sets in a Removable Combination

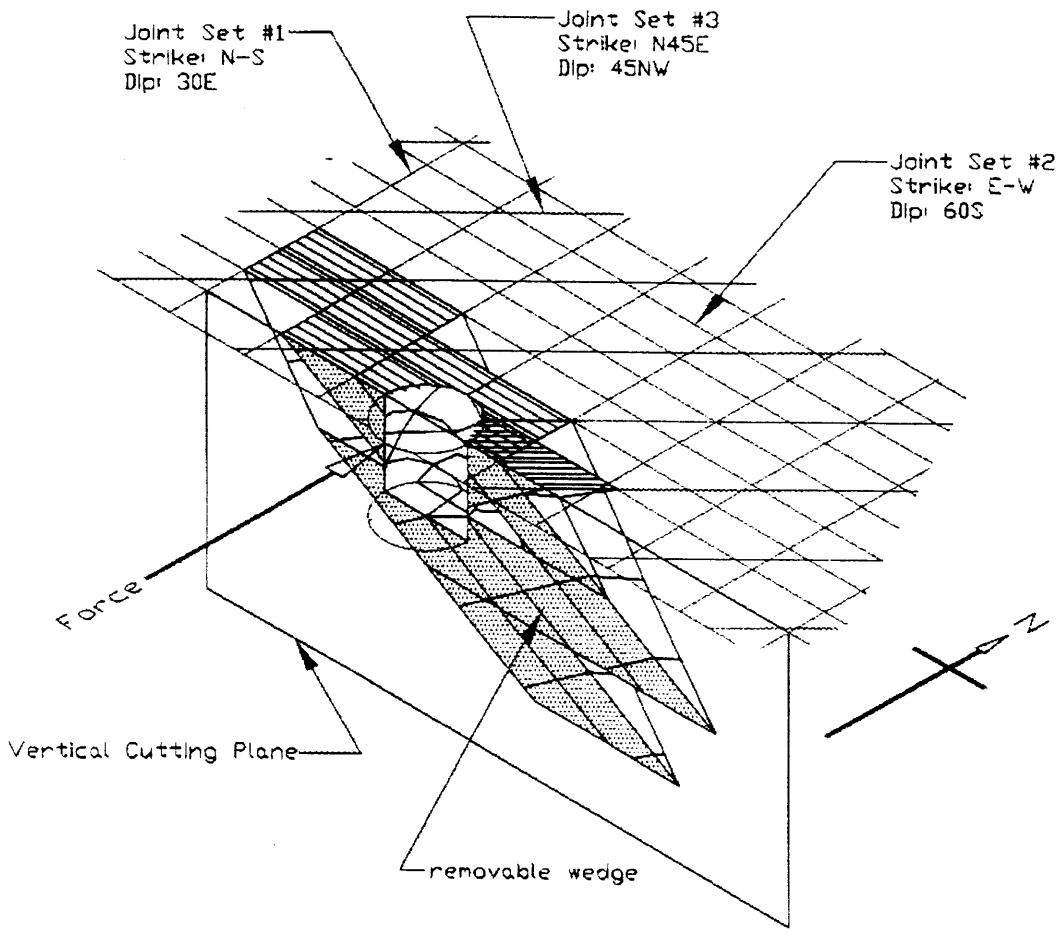

Figure 2.69 A Removable Combination of Blocks in 3D View

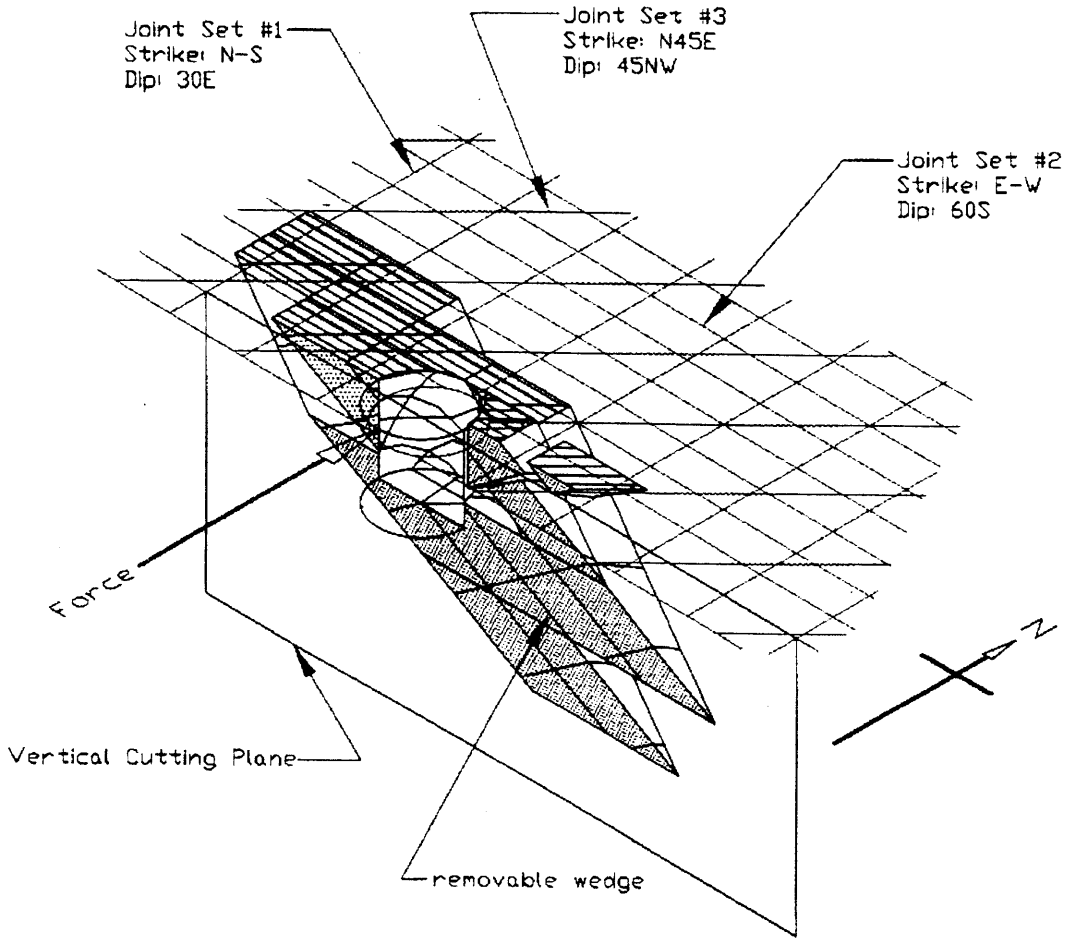

Figure 2.70 Removal of a Removable Combination

For the second combination, the 2nd and 3rd joint sets are treated as the primary pair. The removable blocks that intersect the area of influence are selected first by the using Figure 2.65, and the blocks selected are shown shaded in Figure 2.71. Since block fgOP(N) is a non-removable block in Figure 2.65, some removable block(s) bounded by joints of the secondary pair of joint sets must be selected to cover grid fgOP(N) in the area of influence. Thus, block 45OP is selected from Figure 2.64 to be part of the removable combination since its grid covers the whole grid fgOP(N). Block fgOP(R) is traced to the joint mesh in Figure 2.70 and is shown shaded with vertical lines. The 3D views of all the selected blocks bounded by joints from the 2nd and 3rd joint sets, block 45OP, and the whole combination of removable blocks are shown in Figures 2.72, 2.73, and 2.74 respectively. The displacement process is shown in Figure 2.75. The blocks composed of the primary pair are displaced together with the pile in the northeastern direction. Block 45OP, however, is displaced in the northwestern direction.

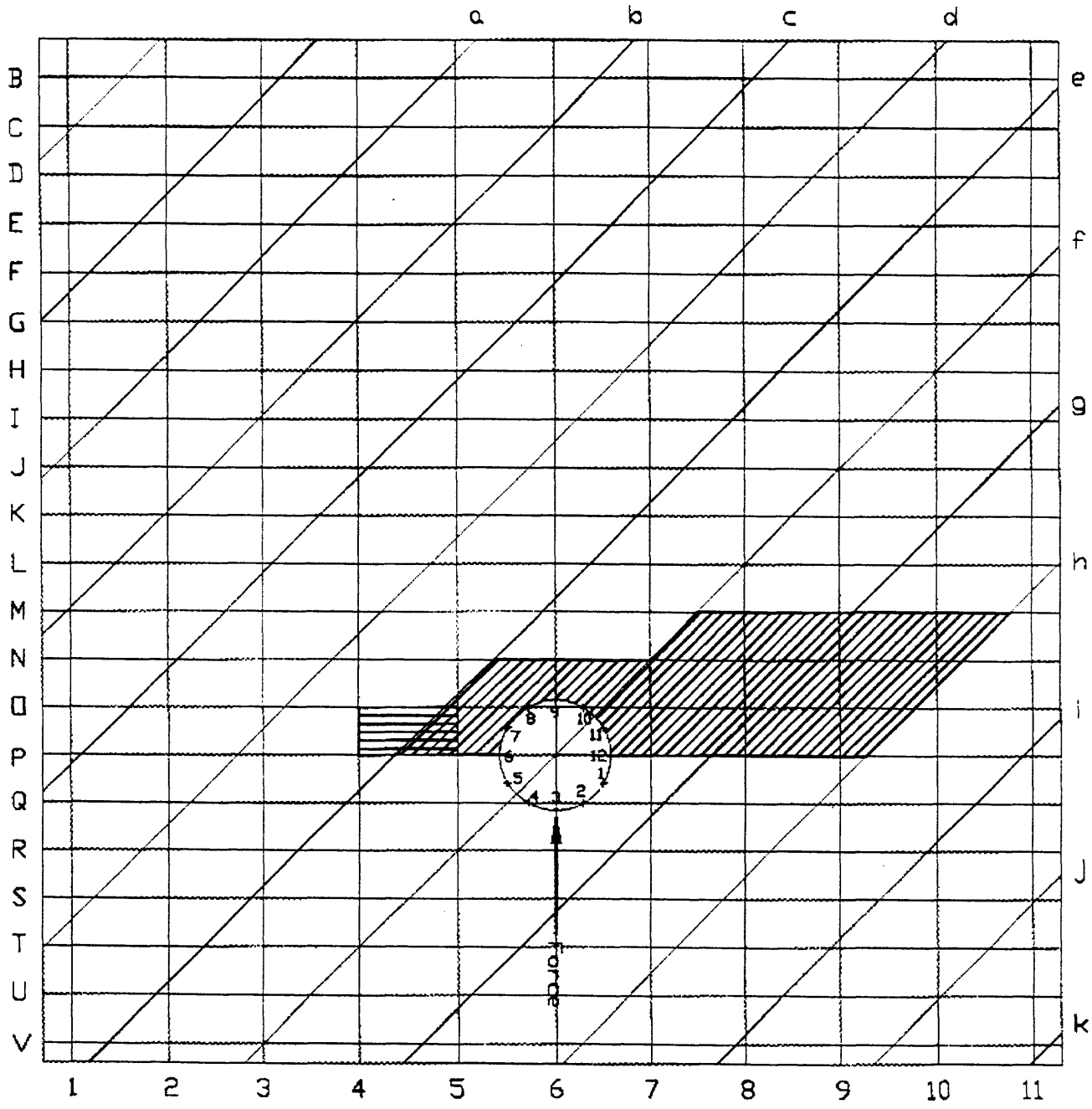

Figure 2.71 A Combination of Removable Blocks

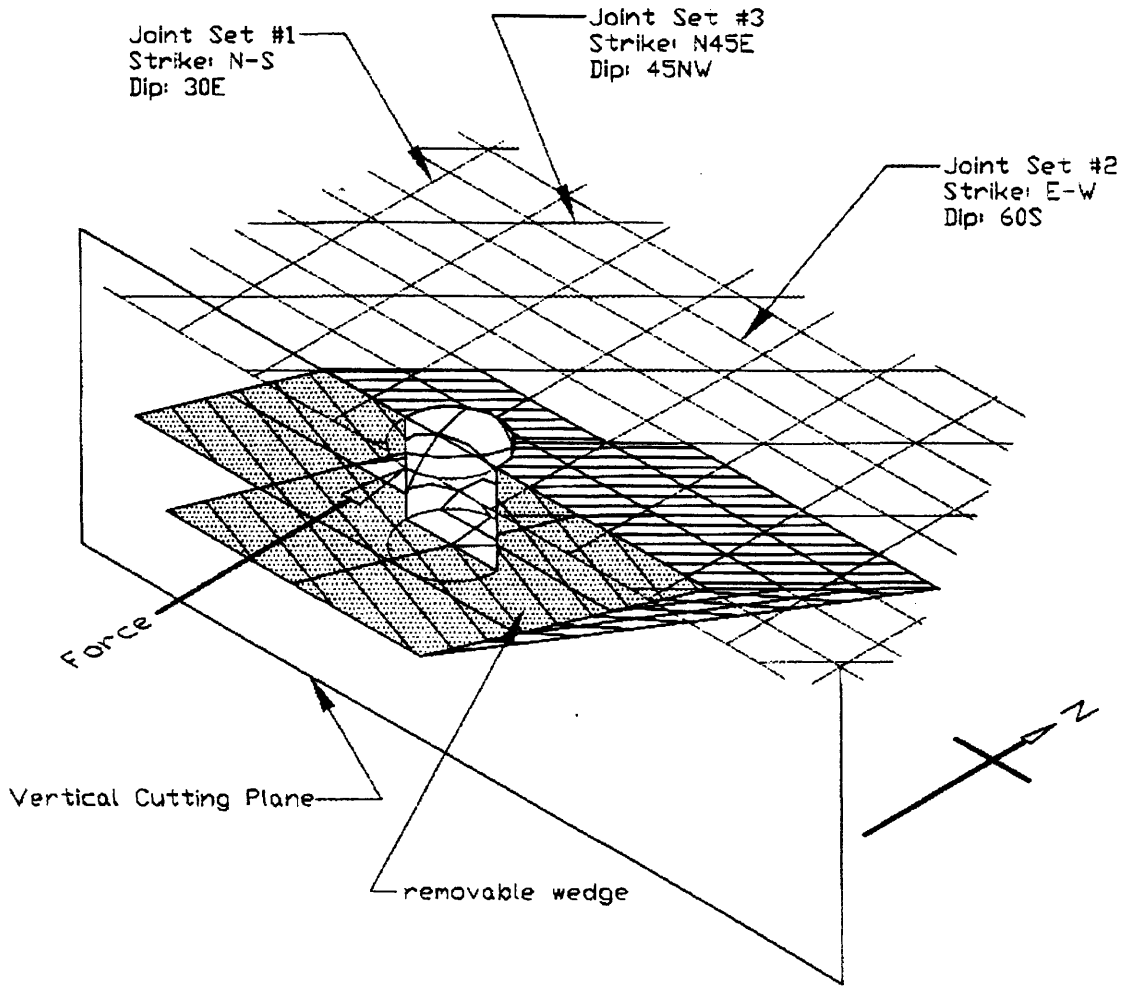

Figure 2.72 Blocks Bounded by the 2nd and 3rd Joint Sets in a Removable Combination

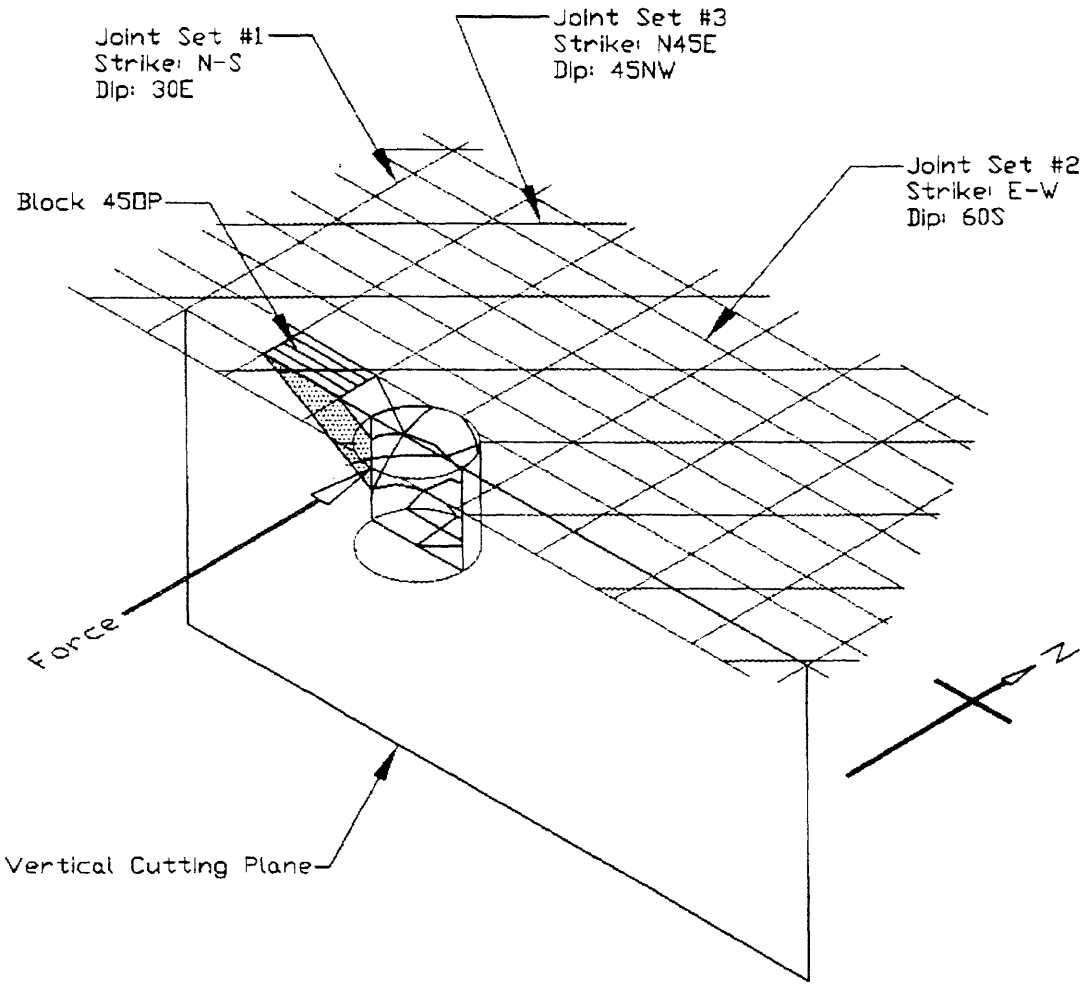

Figure 2.73 A Block Bounded by the 1st and 2nd Joint Sets in a Removable Combination

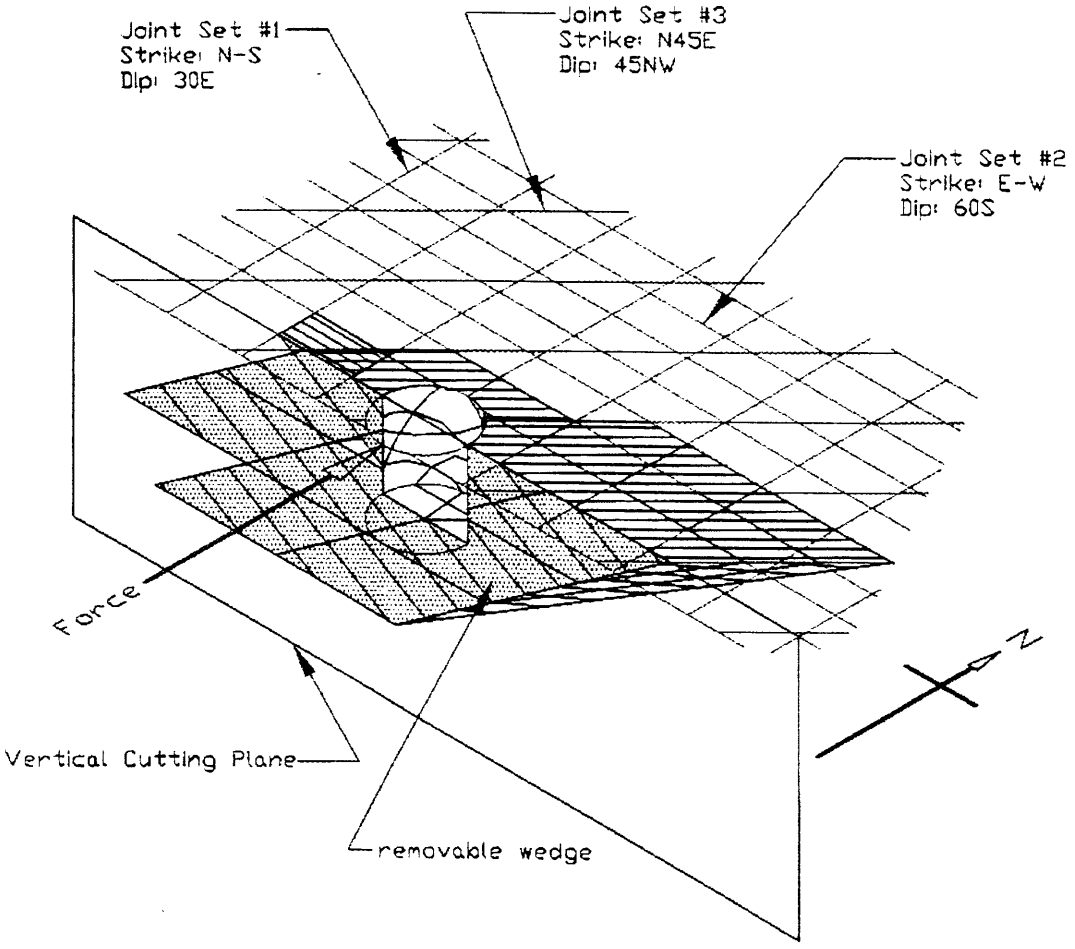

Figure 2.74 A Removable Combination of Blocks in 3D View

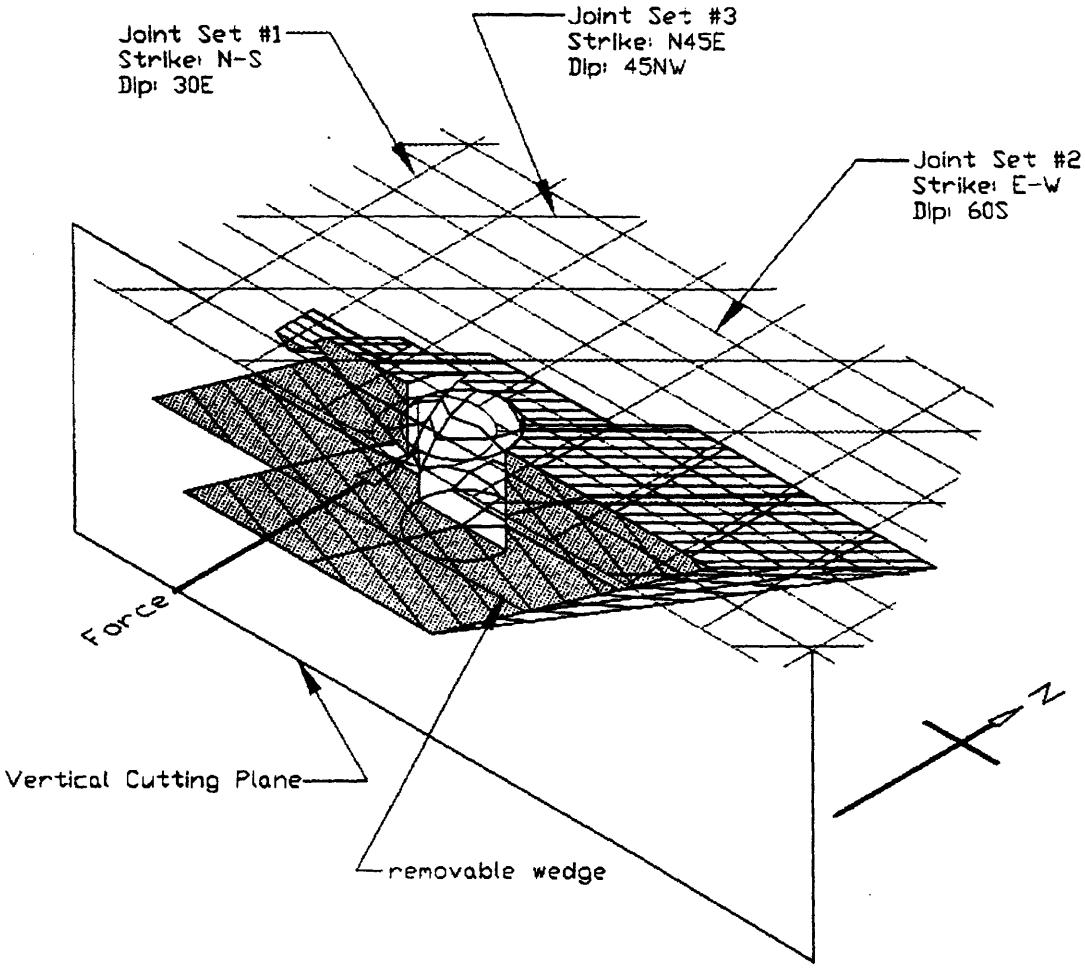

Figure 2.75 Removal of a Removable Combination

CHAPTER 3
KINETICS

3.1 INTRODUCTION

The stability of a removable combination of blocks is analyzed by the limit equilibrium approach. Although this analysis is similar to the slope stability analysis, it is made more complicated by the addition of a lateral force by the pile and the dead load exerted on the blocks.

3.2 KINETICS OF A TWO-JOINT SET SYSTEM

The previous example of a two-joint set system in Chapter 2.7 is used here again for kinetics analysis. In Figure 3.1, a wedge is displaced by a force acting westward in a rock mass with two joint sets. The orientations of the joint sets are N-S, 30E and E-W, 60S respectively. The top of the wedge is shown dotted on the surface joint mesh in Figure 3.2, and the intersection between the pile and the blocks is shown dotted on the joint map in Figure 3.3. A previous assumption made in the kinematics section is that each Type II and Type V block being affected by the pile breaks apart right above the interference area when the pile is acted on by a force, and the top part of the block becomes removable. However, for ease of kinetic analysis, it is assumed here that each Type II and Type V block breaks away from a vertical cutting plane that is perpendicular to the force direction and lies across the center of the pile. This is a valid assumption because the breaking location is close to the breaking location assumed in the kinematics section as shown in Figure 3.4. The intersection between the blocks in the combination and the cutting plane is shown dotted in Figure 3.1.

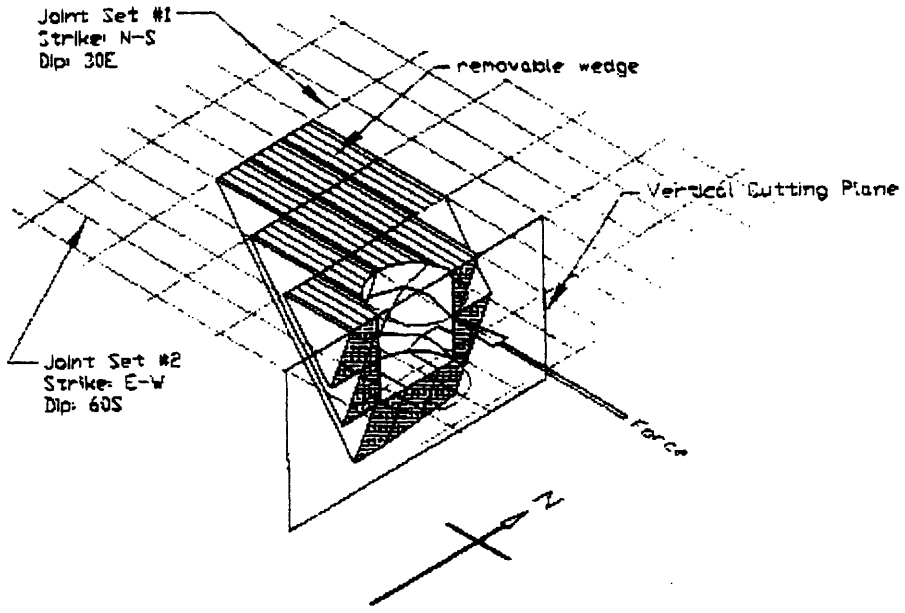

Figure 3.1 Removable Wedge Consisting of a Number of Joint Blocks with Force Acting As Shown

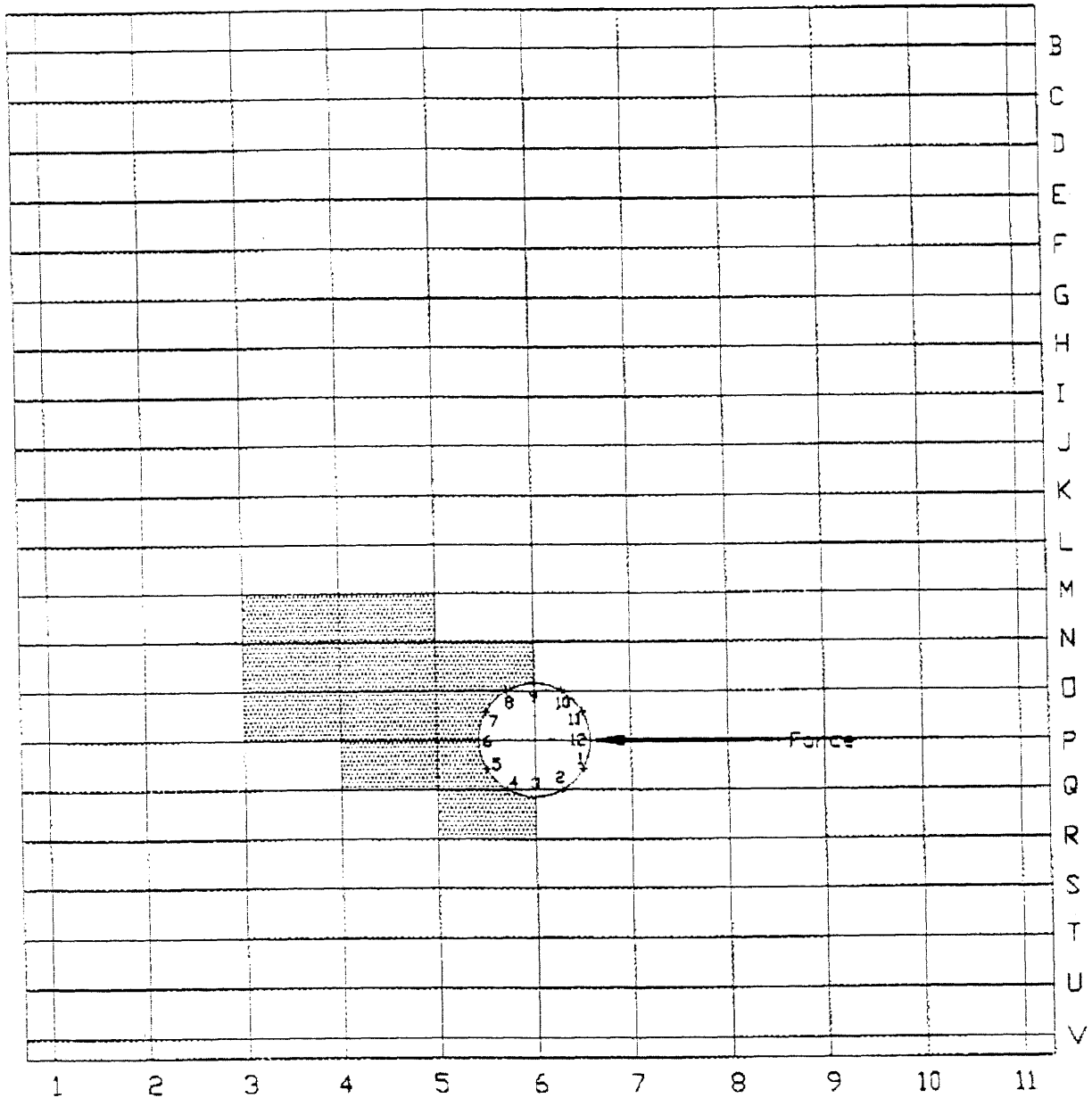

Figure 3.2 Removable Wedge as Shown on the Joint Mesh

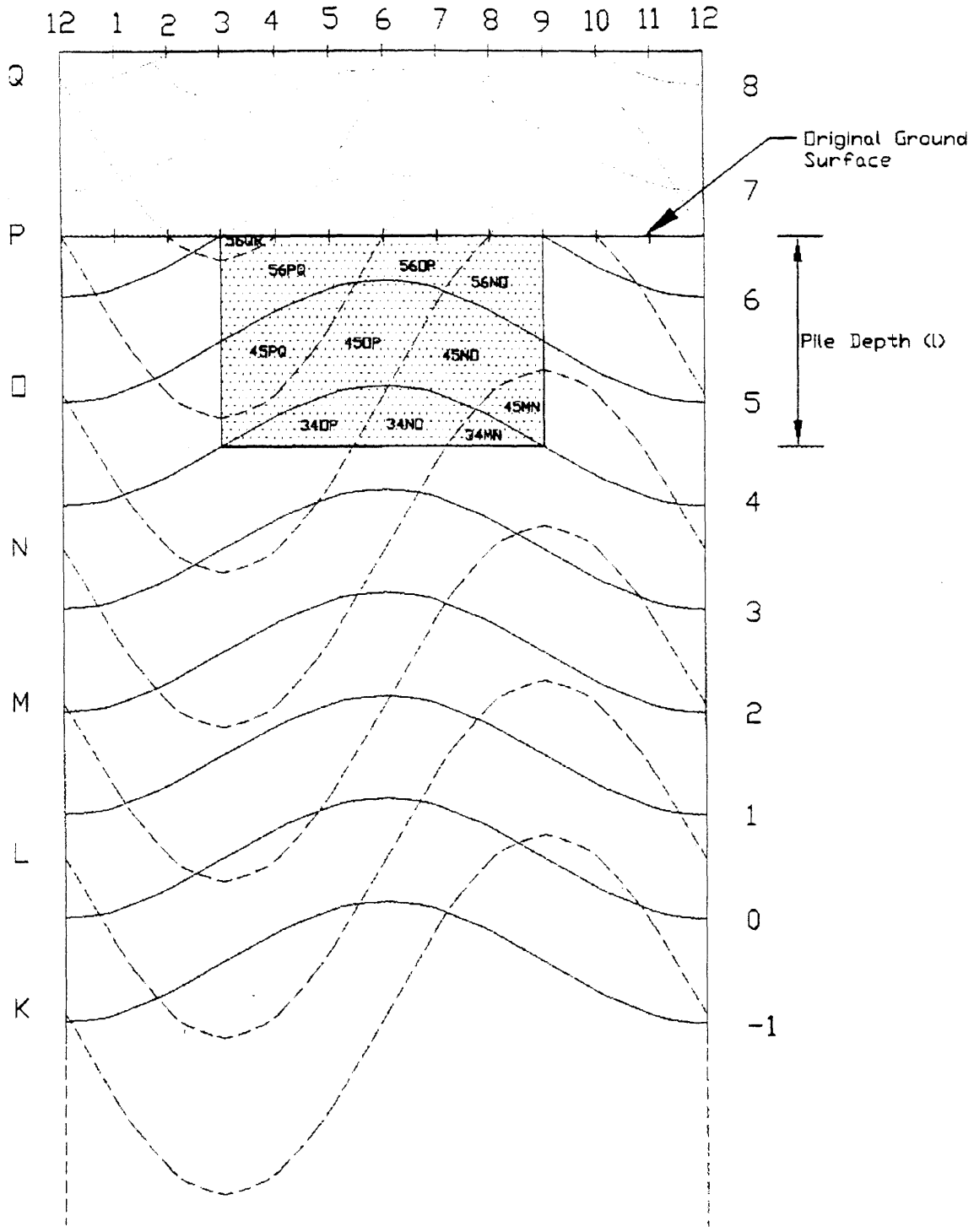

Figure 3.3 Removable Wedge as Shown on the Joint Map on a Pile

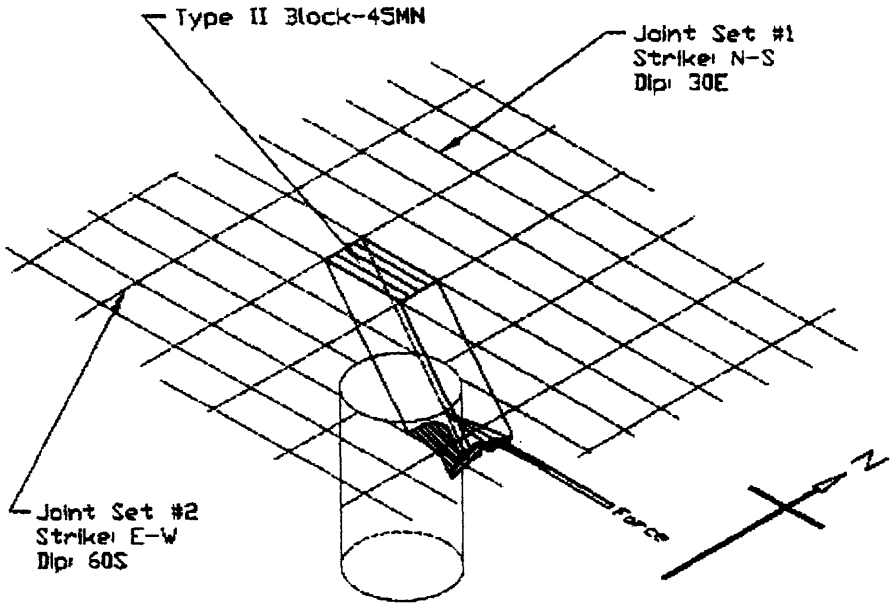

(a)

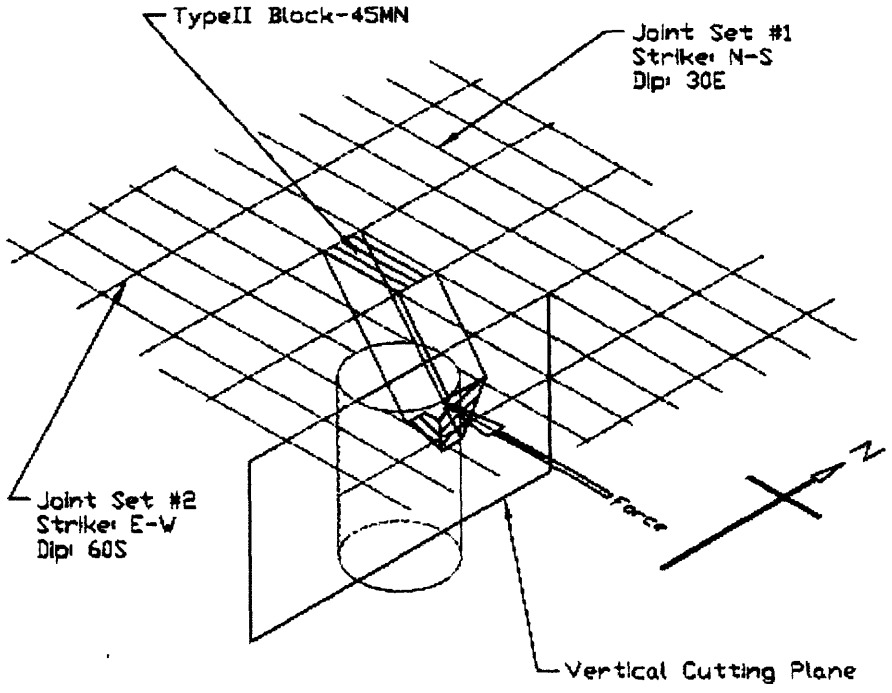

(b)

Figure 3.4 (a) Block After Breaking Up Due to Force; (b) Block Cut by Assumed Vertical Plane

3.2.1 LATERAL DRIVING FORCE

Figure 3.5 shows the typical forces acting on the wedge, and for clarity of presentation, the normal forces (N) and tangential forces (R) are drawn for each set separately, but all these forces actually occur together.

θ is defined as shown in Figure 3.5a and β and γ as shown in Figure 3.5b. The lateral driving force vector is expressed as follows

$$\vec{F} = F\cos\theta\,\hat{i} + F\sin\theta\,\hat{j} \tag{3.1}$$

where F is the lateral driving force.

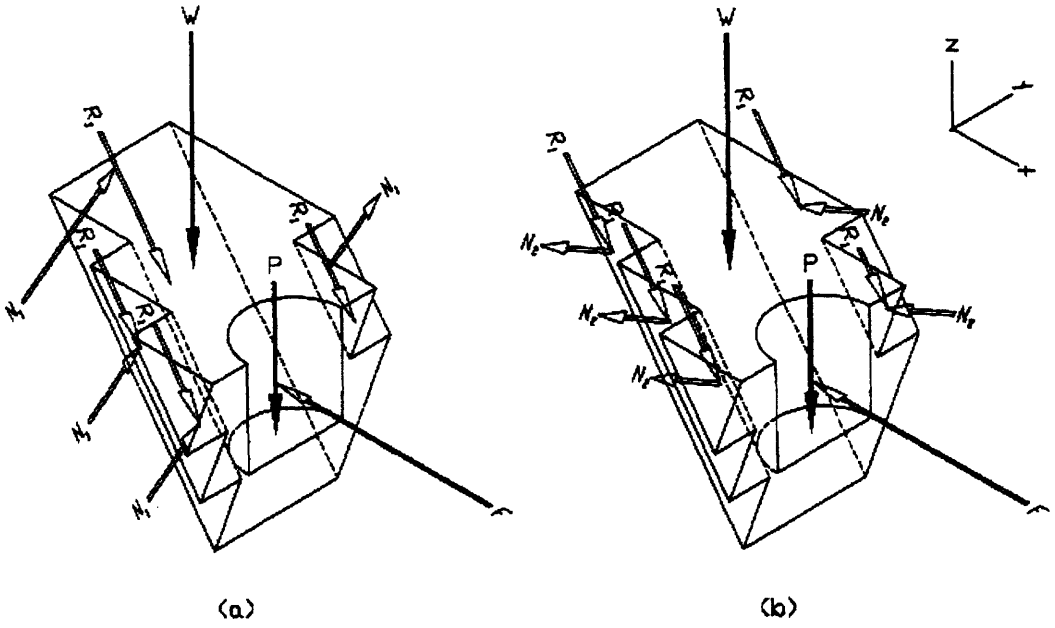

Figure 3.5 Typical Forces on the Wedge for (a) Joint Set N-S, 30°E and (b) Joint Set E-W, 60°S

R_1=tangential force on joint set 1
N_1=normal force on joint set 1
R_2=tangential force on joint set 2
N_2=normal force on joint set 2

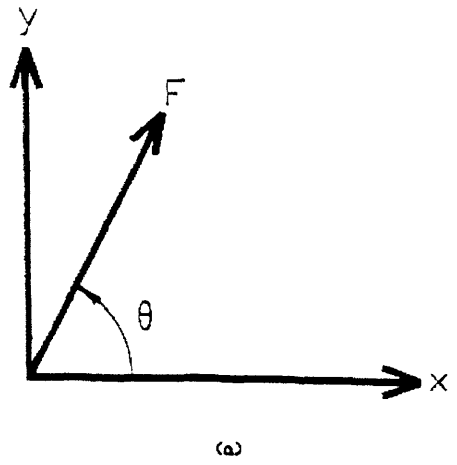

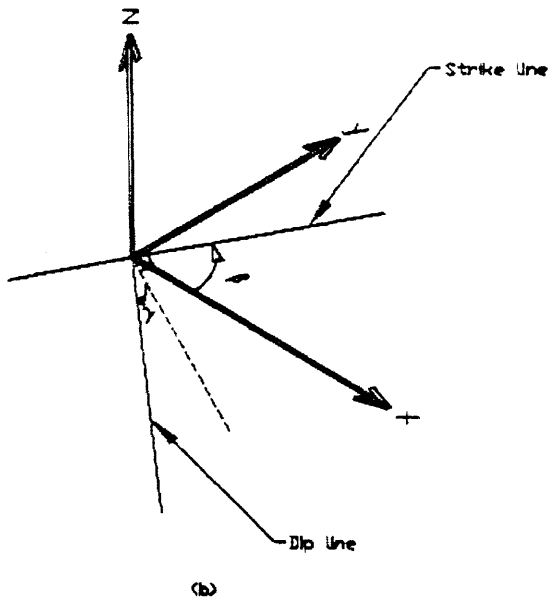

Figure 3.6 (a) Typical Force Vector; (b) Dip and Strike Lines

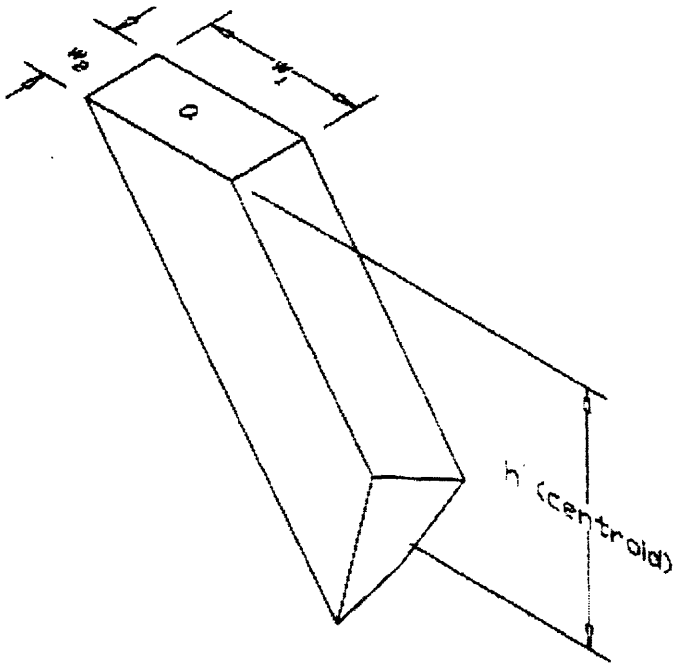

Figure 3.7 A Typical Block That Intercepts the Pile as a Whole

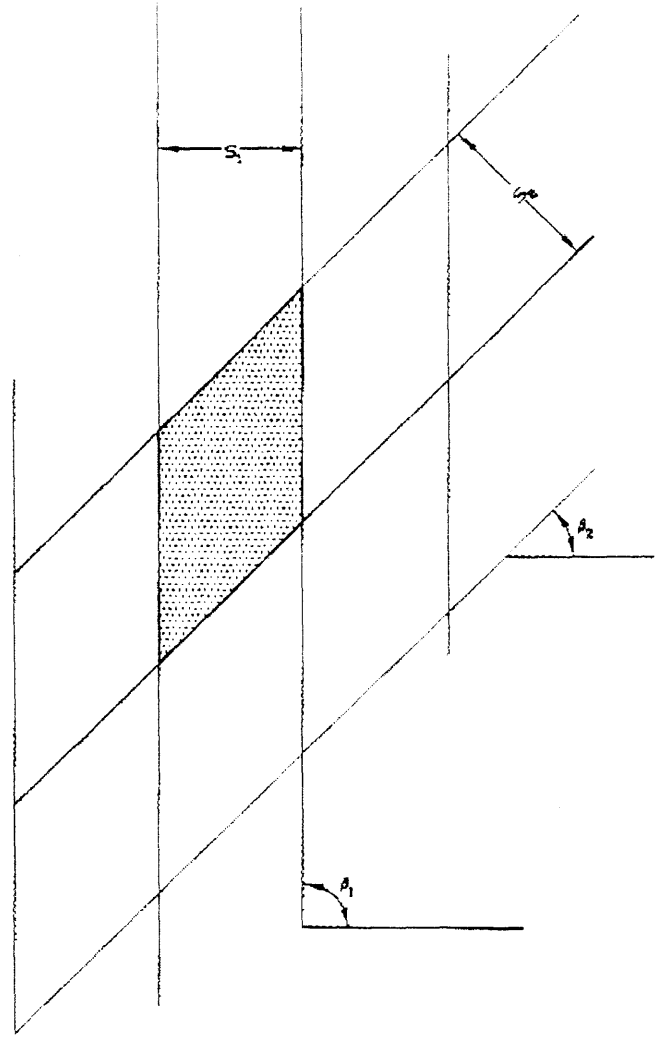

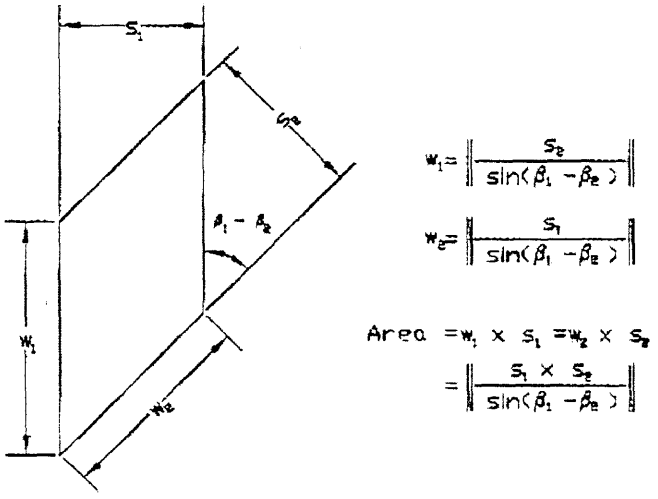

Figure 3.8 Area of a Block on the Surface

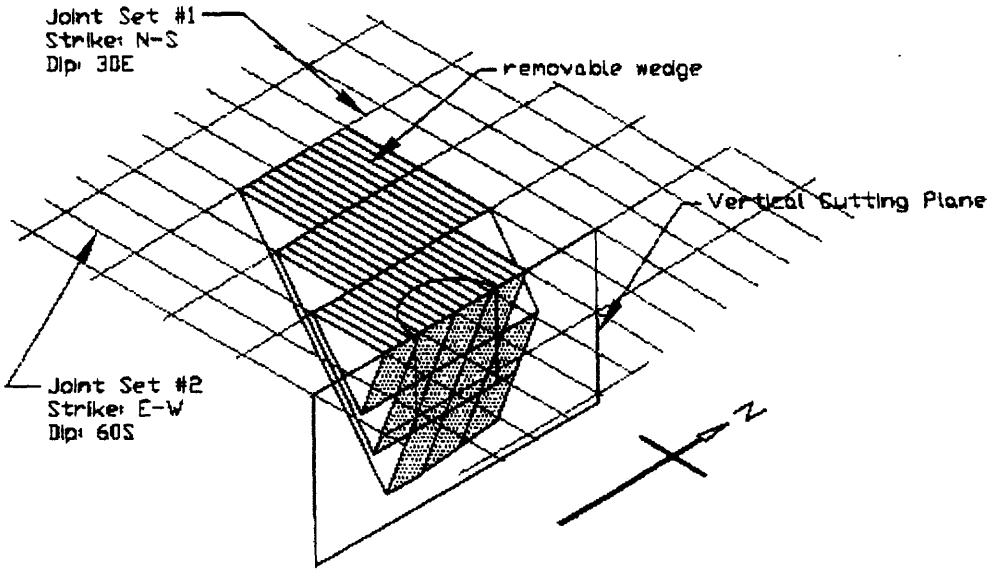

Figure 3.9 Imaginary Blocks Extending to the Cutting Plane

3.2.2 WEIGHT OF WEDGE

The weight vector is expressed as follows

$$\vec{W} = -\gamma_r V \hat{k} \tag{3.2}$$

where γ_r is the unit weight of the rock mass and V is the volume of the wedge.

A typical block that intersects the pile as a whole is shown in Figure 3.7. The volume of each block is approximately

$$V_{block} \approx h_{centroid} \bullet a = h_{centroid} \bullet \| (s_1 \bullet s_2)/sin(\beta_1 - \beta_2) \| \tag{3.3}$$

where $h_{centroid}$ is the distance from the surface to the centroid of the area of intersection between the block and the pile, a is the area of the block on the surface, s_i is the horizontal spacing of joint set i, and β_i is defined for joint set i as shown in Figure 3.6b. $\| (s_1 \bullet s_2)/sin(\beta_1 - \beta_2) \|$ is the equation for the area of a parallelogram as shown in Figure 3.8. The rectangular shape of the area on top of the block in Figure 3.7 is just a special case, and the area is simplified to $s_1 \bullet s_2$.

$h_{centroid}$ of a entirely intersecting block can be obtained from the joint map in Figure 3.3, but that of a partially intersecting block cannot. A more effective way to estimate the volume of a block is to assume that the pile does not exist and that the blocks extend to the cutting plane creating imaginary blocks as shown in Figure 3.9. By totaling the volume of each imaginary block and then subtracting half of the volume of the pile, the volume of the removable wedge is obtained. In this process, it is very useful to have a figure of joint intersections on the cutting plane. The method of constructing such a figure is as follows

1. On the joint map on the pile, connect two points of intersections where a specific joint in a joint set meets the line of intersection between the pile and the cutting plane. An example is shown in Figure 3.10a for joint 5 and joint N, both shown with dotted lines.
2. Replicate and extend the lines produced in (1) based on the spacing of that particular joint set as shown in Figure 3.10b for joint N.
3. Repeat (1) and (2) for a joint in the other joint set as shown in Figure 3.10c.

4. Label the newly constructed joint lines accordingly and erase the original joint intersection lines on the pile as shown in Figure 3.10d. The removable combination of blocks is shown dotted.

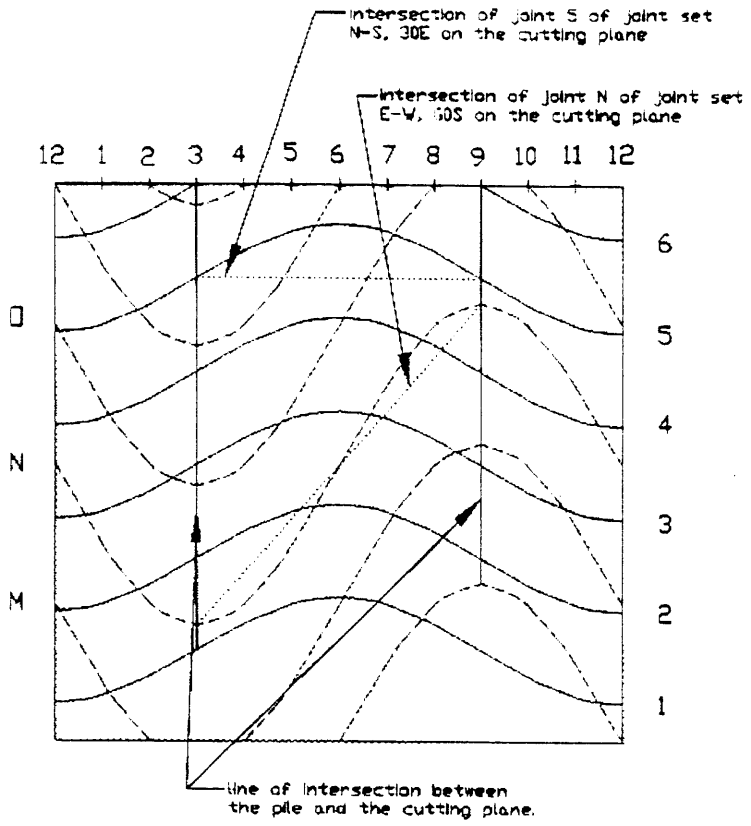

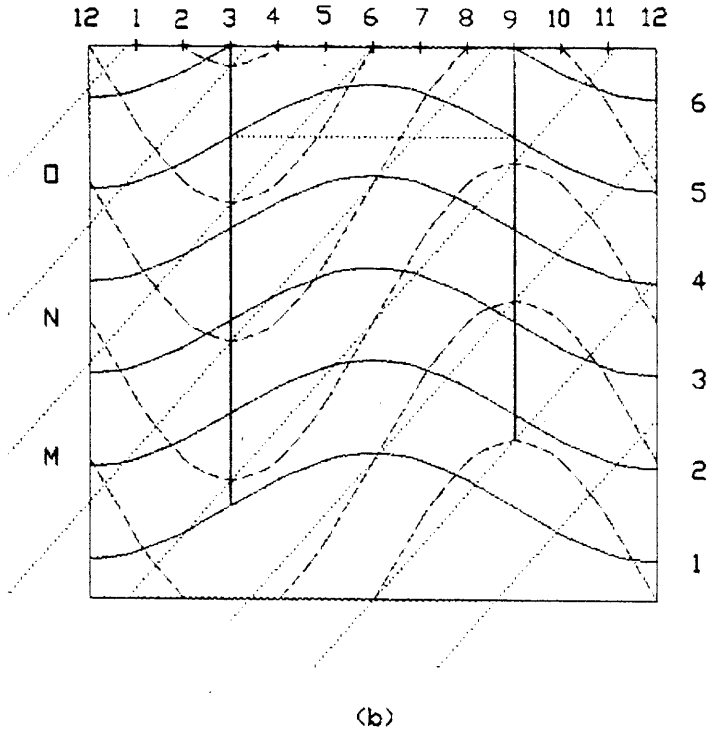

Figure 3.10 Construction of a Joint Map on a Vertical Cutting Plane

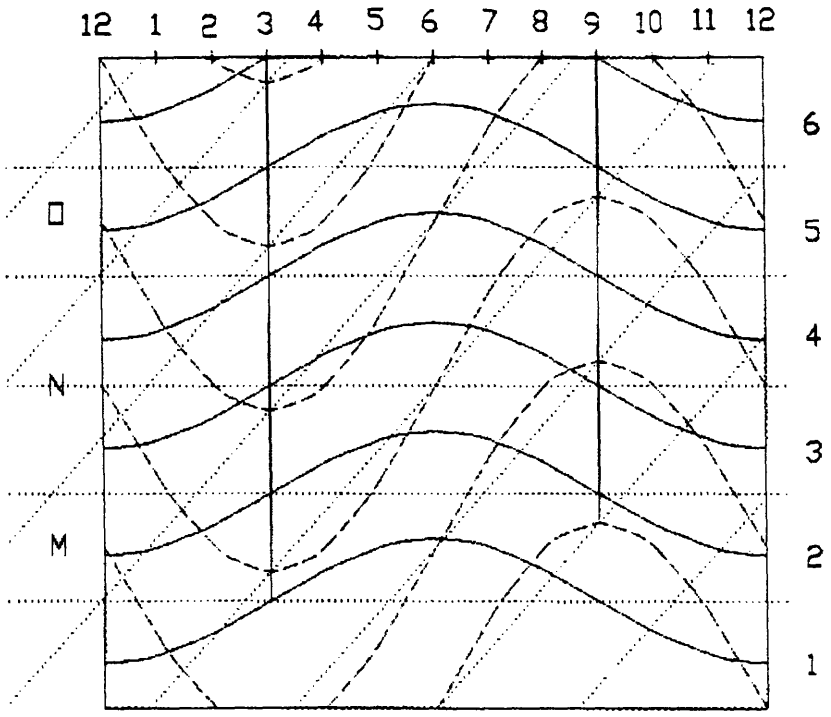

(c)

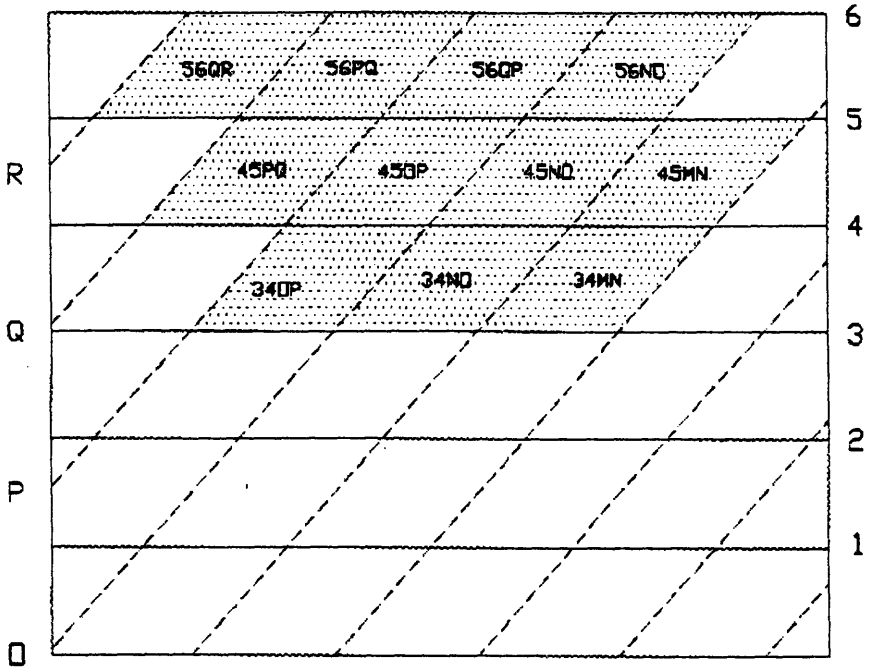

(d)

Figure 3.10 Construction of a Joint Map on a Vertical Cutting Plane

$h_{centroid}$ can be obtained from the joint map on the cutting plane and typical $h_{centroid}$'s are shown in Figure 3.12. h_1 is the $h_{centroid}$ for Block 56PQ, h_2 is that for Block 45OP, and h_3 is that for Block 34MN.

The volume of the wedge is expressed as follows

$$V = \sum_{i=1}^{n} a_i h_{i\,(centroid)} - \frac{\pi D^2}{8} l \tag{3.4}$$

where n is the total number of blocks and a_i is the area of block i on the surface. D is the diameter of the pile and l is the pile depth as shown in Figure 3.11. The volume (V) of the wedge is the total volume of all the blocks minus half of the volume of the pile. However, this technique is too time consuming to apply when the removable wedge has too many blocks. A simplified way to estimate the volume of the removable wedge is given as follows:

$$\begin{aligned} V &= n \bullet a \bullet AVG(h_1, h_2, \ldots, h_n) - (\pi D^2 l)/8 \\ &\approx n \bullet a \bullet 0.5 \bullet b - (\pi D^2 l)/8 \end{aligned} \tag{3.5}$$

where b is the distance from the surface to the bottom of the wedge as indicated in Figure 3.13. a_i in equation (3.4) becomes a in equation (3.5) since it is assumed that the surface area of each block in the wedge is the same. The basic assumption of equation (3.5) is that the blocks in a wedge are fairly evenly distributed in each layer. In this example, four blocks form the top layer, four blocks form the middle layer, and three blocks form the bottom layer. As shown in the calculations later in this chapter, the simplified method overestimates the volume by 7.44% for this example. However, if the wedge is composed of many blocks, the error would be small.

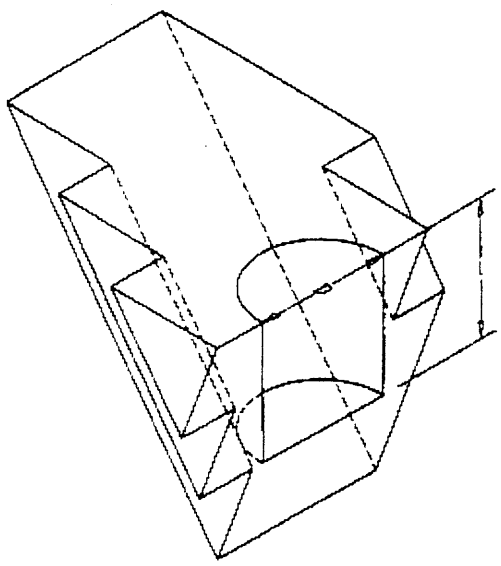

Figure 3.11 A Removable Wedge

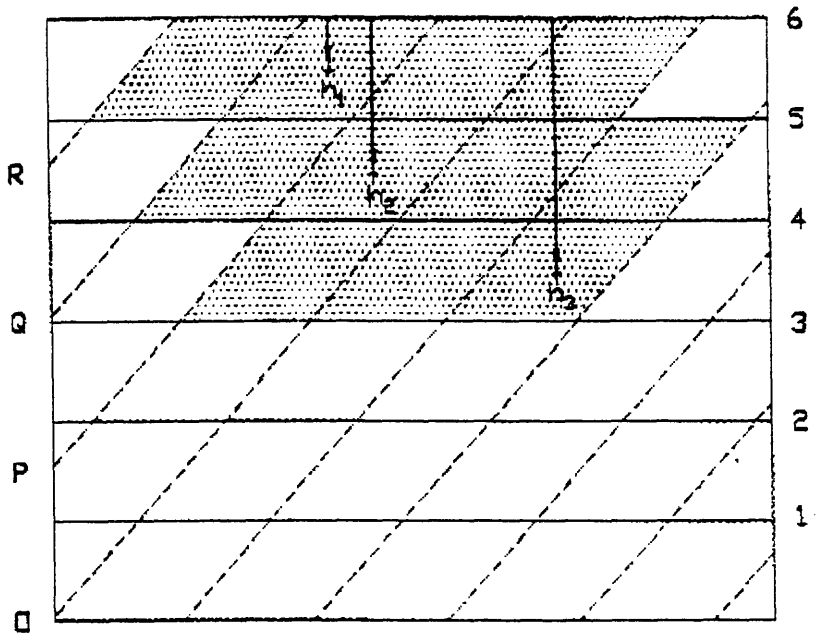

Figure 3.12 Typical h(centroid)'s for Various Blocks

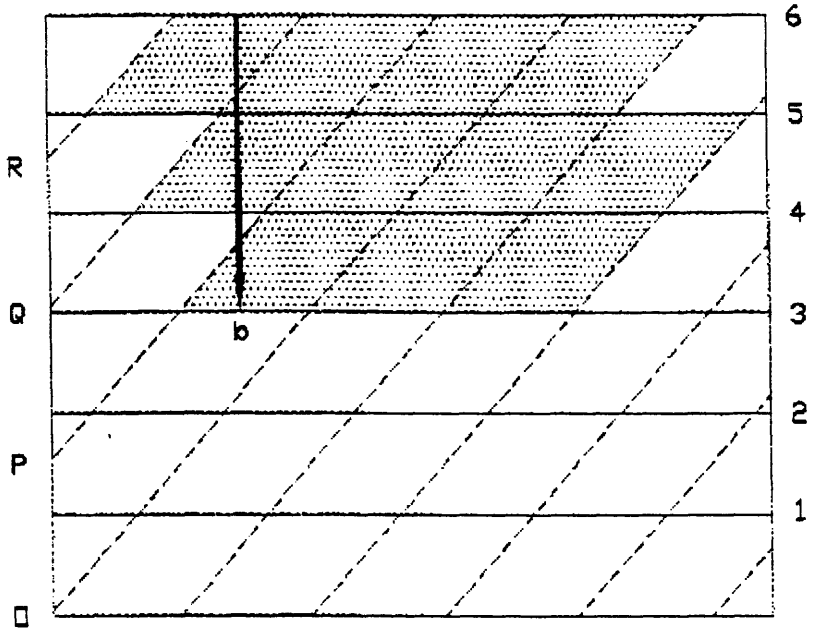

Figure 3.13 b, Height of the Wedge

3.2.3 NORMAL AND TANGENTIAL FORCES

In order to express the normal forces (N) and tangential forces (R) in vector form, the strike vector and dip vector of each joint are needed. The strike vector is expressed as follows

$$\vec{u} = \cos\beta\,\hat{i} + \sin\beta\,\hat{j} \tag{3.6}$$

and the dip vector is

$$\vec{v} = \cos\gamma\sin\beta\,\hat{i} - \cos\gamma\cos\beta\,\hat{j} - \sin\gamma\,\hat{k} \tag{3.7}$$

where β and γ are defined as shown in Figure 3.6b.

The normal vector is the cross product of the dip vector and strike vector:

$$\vec{w} = \vec{v}\,x\,\vec{u} \tag{3.8}$$

$$= \sin\gamma\sin\beta\,\hat{i} - \sin\gamma\cos\beta\,\hat{j} + \cos\gamma\,\hat{k} \tag{3.9}$$

Recalling Figure 3.5, the normal force vector can then be written accordingly:

$$\vec{N} = N(\vec{w}) = N\sin\gamma\sin\beta\,\hat{i} - N\sin\gamma\cos\beta\,\hat{j} + N\cos\gamma\,\hat{k} \tag{3.10}$$

Since the removal direction of a block follows the orientation of the intersection between the two joint sets, the tangential force vector is parallel to the intersection vector. The intersection vector ($\hat{I}$) is the cross product of the normal vectors of the joint sets:

$$\hat{I} = \hat{w}_1 x \hat{w}_2 = (-\sin\gamma_1\cos\beta_1\cos\gamma_2 + \cos\gamma_1\sin\gamma_2\cos\beta_2)\hat{i} +$$

$$(-\sin\gamma_1\sin\beta_1\cos\gamma_2 + \cos\gamma_1\sin\gamma_2\sin\beta_2)\hat{j} + (-\sin\gamma_1\sin\gamma_2\sin(\beta_1 - \beta_2))\hat{k} \tag{3.11}$$

Recalling Figure 3.5, the tangential force vector is written as follows

$$\vec{R} = R(\hat{I}) = R(-\sin\gamma_1\cos\beta_1\cos\gamma_2 + \cos\gamma_1\sin\gamma_2\cos\beta_2)\hat{i} +$$

$$R(-\sin\gamma_1\sin\beta_1\cos\gamma_2 + \cos\gamma_1\sin\gamma_2\sin\beta_2)\hat{j} + R(-\sin\gamma_1\sin\gamma_2\sin(\beta_1 - \beta_2))\hat{k} \tag{3.12}$$

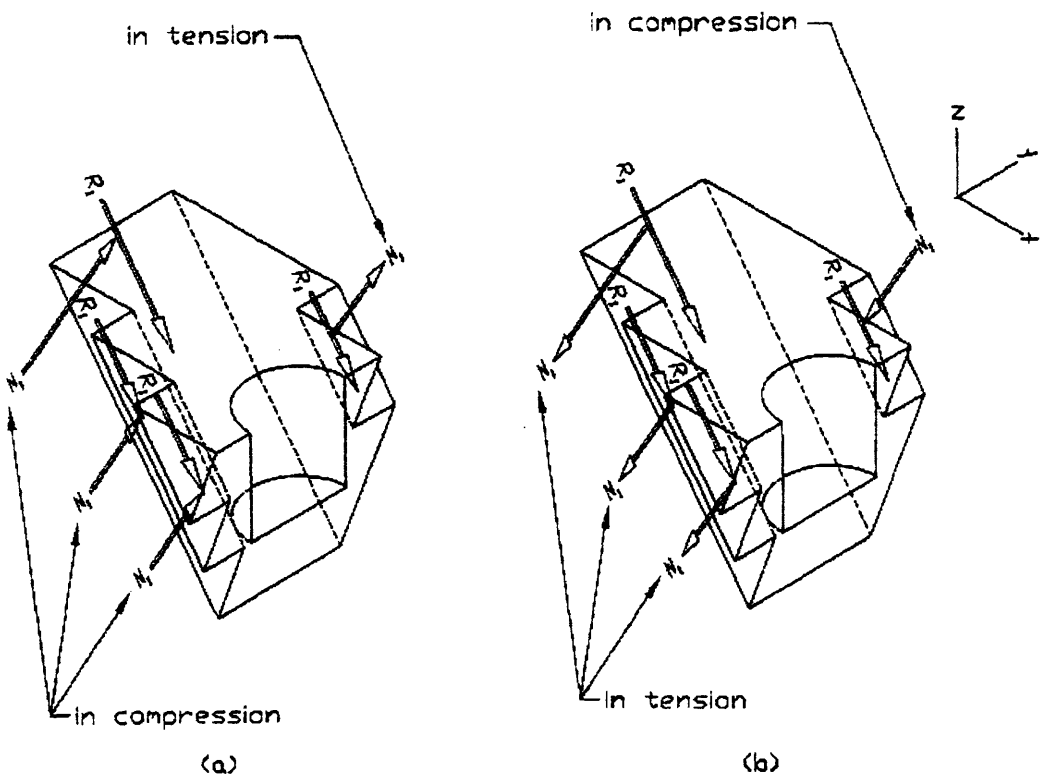

Figure 3.14 Faces in Tension/Compression When Normal Force Acts in Opposite Direction

N and R can be related by the Coulomb failure criterion as follows

$$\tau = c + \sigma \tan\phi \tag{3.13}$$

where τ is shear stress, c is cohesion, σ is the normal stress, and ϕ is the friction angle. When a wedge is being removed, some faces from each joint set are in compression and some faces from each joint set are in tension. Whether a face is in compression or in tension depends on the direction of the normal stress. For example, a face is in compression when the normal stress acts in one direction as shown in Figure 3.14a, but the same face is in tension when the normal stress acts in the opposite direction as shown in Figure 3.14b. Although shear resistance is different for a face in compression and in tension, it is not necessary to distinguish faces in compression from faces in tension as shown in the following equations.

Let A_c be the total area in compression for a joint set and A_t be the total area in tension for the same joint set. For faces in compression from a joint set, replace τ with R_c/A_c and σ with N/A_c, and thus,

$$\frac{R_c}{A_c} = c + \frac{N}{A_c}\tan\phi \tag{3.14}$$

where R_c is the tangential force on faces in compression for a joint set.

For faces in tension from the same joint set, the tensile normal force is negative, and thus it is assumed that shear resistance of the faces in tension is governed by cohesion only. Replace τ with T/A_c, and the equation for faces in tension from the same joint set is then

$$\frac{R_t}{A_t} = c \tag{3.15}$$

where R_t is the tangential force on faces in tension for a joint set.

The total tangential force (R) is the sum of R_c and R_t, and thus

$$\begin{aligned} R = R_c + R_t &= cA_c + N\tan\phi + cA_t \\ &= c(A_c + A_t) + N\tan\phi \\ &= cA + N\tan\phi \end{aligned} \tag{3.16}$$

where A is the total area of the faces from the same joint set on the removable wedge. One can conclude from the above equation that it is not necessary to distinguish faces in tension from faces in compression.

A typical face of a block is shown in Figure 3.15. In many cases, the intersection between a face and a pile is not a straight line, but it is recommended that the face be assumed to be a parallelogram. Thus, its area is expressed as L•w, where L is the height of the parallelogram on the joint plane and s is the horizontal spacing. L is computed by H/sinγ, where H is the height from the surface to the center of the edge that intersects the pile or the cutting plane. $w=\| s/\sin(\beta_1-\beta_2) \|$ is the length of the edge on the surface as shown in Figure 3.8.

H for each face is obtained by the following procedures: (1) when blocks have a face that intersects the pile as a whole, the joint map on the pile should be used to locate H; (2) when blocks have a face that intersects partially, the joint map on the cutting plane should be used instead. In this particular example, no faces of the wedge intersect the pile as shown in Figure 3.16, and thus the joint map on the cutting plane must be used to find H. Each H for each face of joint set N-S, 30°E is shown in Figure 3.17, and each H for each face of joint set E-W, 60°W is shown in Figure 3.18.

The total A for each joint set is then

$$A = \sum_{i=1}^{n} \frac{H_i w_i}{\sin\gamma} = \sum_{i=1}^{n} \left[\frac{H_i}{\sin\gamma} \bullet \left\| \frac{s_i}{\sin(\beta_1 - \beta_2)} \right\| \right] \tag{3.17}$$

The total A for joint N-S. 30°E is $A_1+\ldots+A_4$ and the total A for joint E-W, 60°W is $A_5+\ldots+A_{10}$ as shown in Figure 3.16.

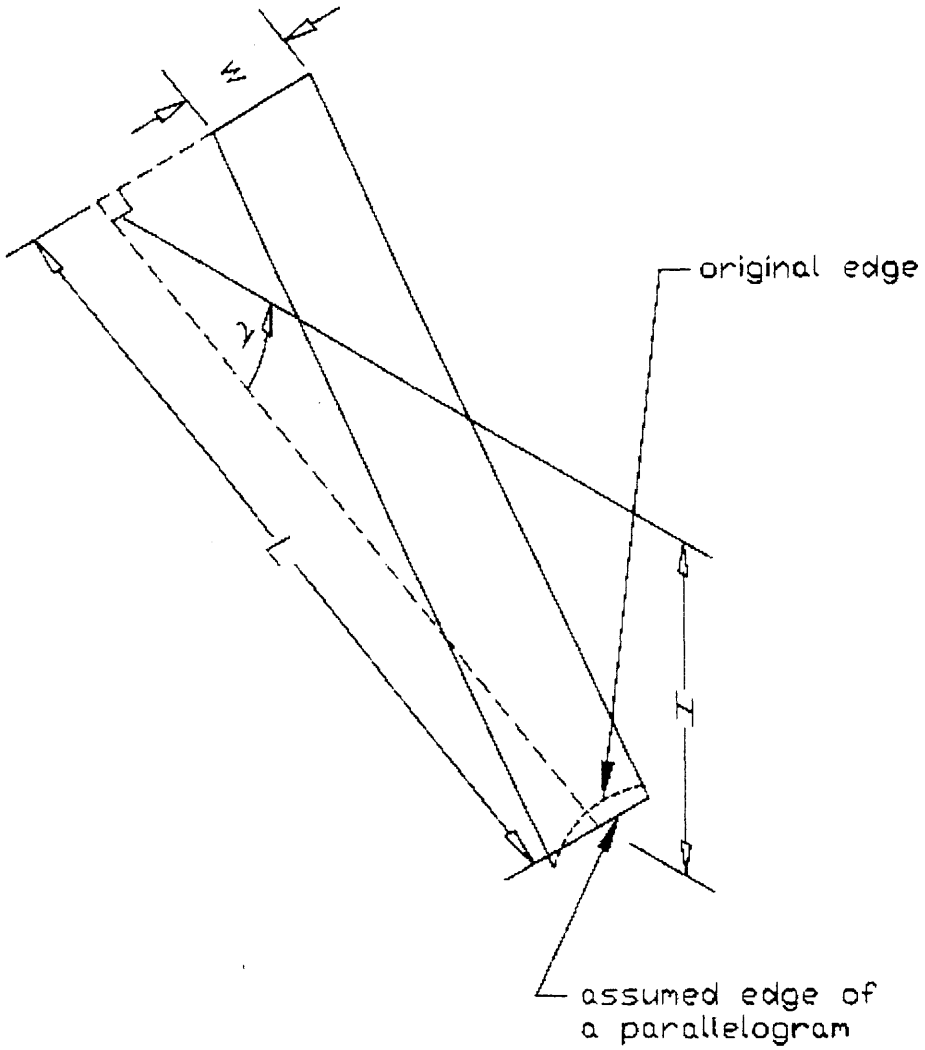

Figure 3.15 A Typical Face of a Block

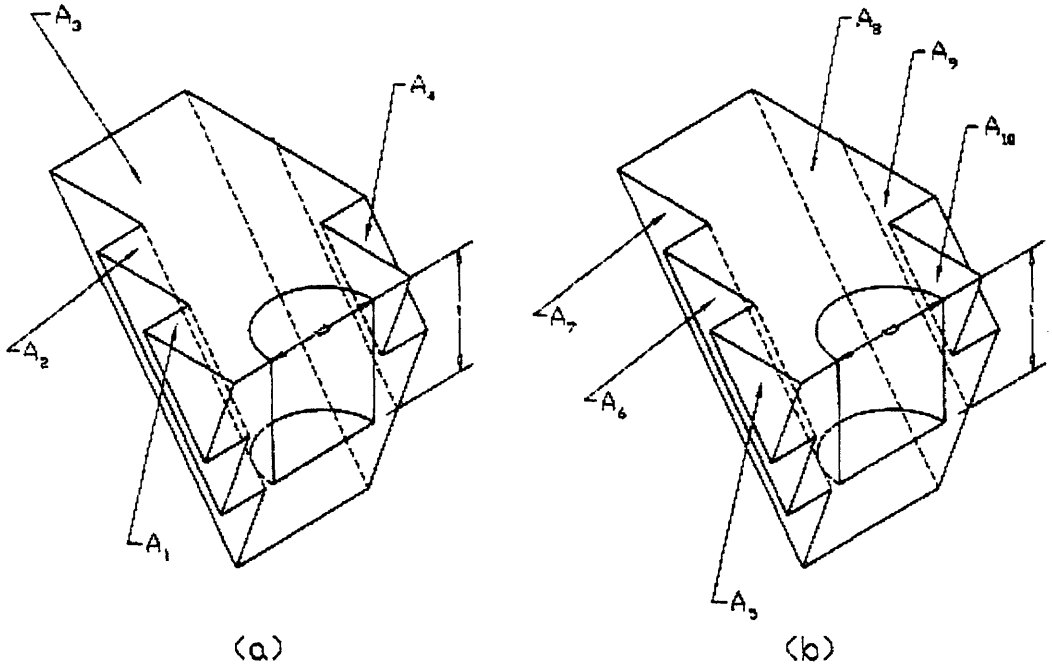

Figure 3.16 Faces of Joint Set (a) N-S, 30°E and (b) E-W, 60°S on the Wedge

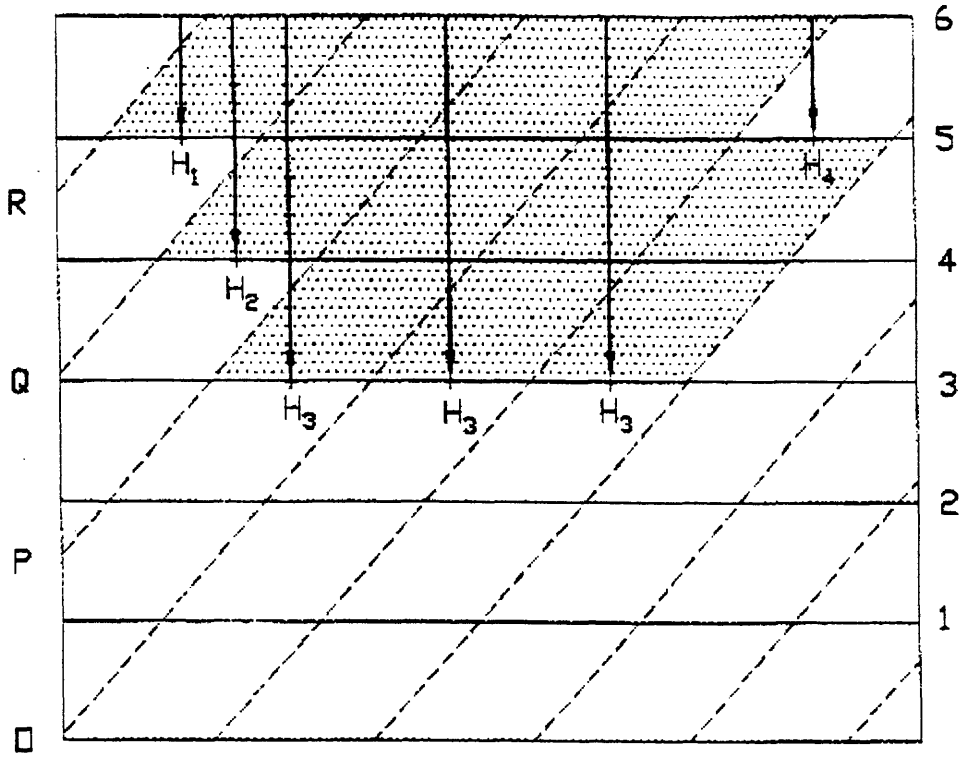

Figure 3.17 H's for Faces of Joint Set N-S, 30°E

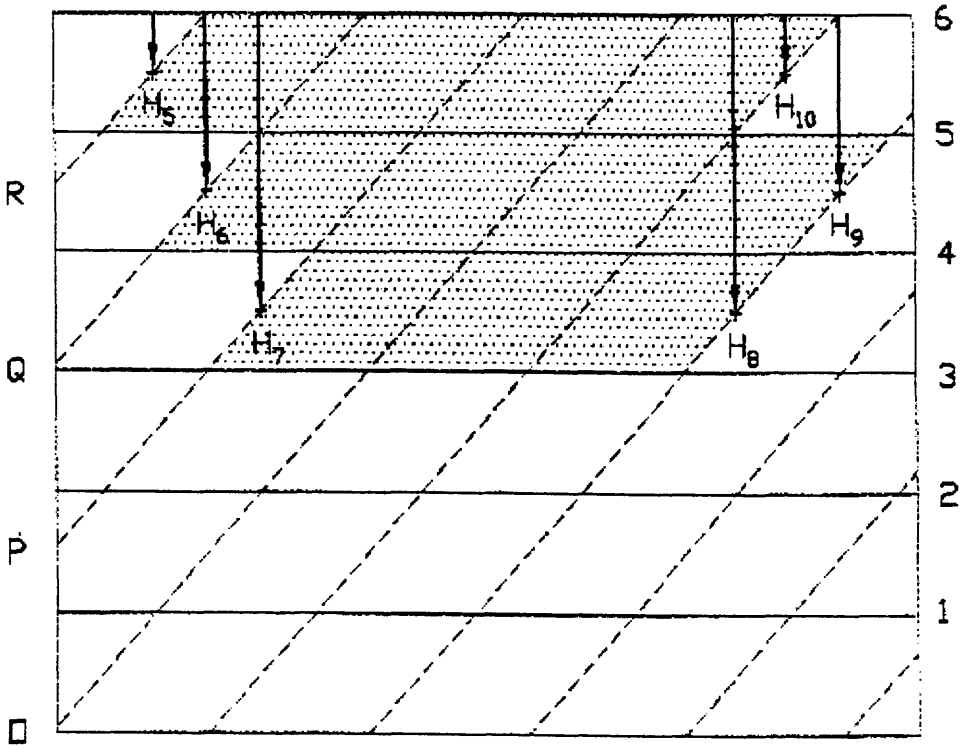

Figure 3.18 H's for Faces of Joint Set E-W, 60°S

3.2.4 DEAD LOAD OF THE PILE

Finally, the expression for the Dead Load (P) of the pile on the wedge is:

$$\vec{P} = -P\hat{k} \tag{3.18}$$

The forces in each direction (x, y, and z) are summarized in the table below:

3.2.5 SUMMARY OF FORCES

A summary of forces in each direction is presented in Table 3.1 below:

Table 3.1 Summary of Forces in Each Direction

	X	Y	Z
Lateral Force	$F\cos\theta$	$F\sin\theta$	
Weight of Wedge			$-W$
Tangential Force of Joint Set #1	$R_1(-\sin\gamma_1\cos\beta_1\cos\gamma_2 + \cos\gamma_1\sin\gamma_2\cos\beta_2)$	$R_1(-\sin\gamma_1\sin\beta_1\cos\gamma_2 + \cos\gamma_1\sin\gamma_2\sin\beta_2)$	$R_1(-\sin\gamma_1\sin\gamma_2 \sin(\beta_1-\beta_2))$
Normal Force of Joint Set #1	$N_1\sin\gamma_1\sin\beta_1$	$-N_1\sin\gamma_1\cos\beta_1$	$N_1\cos\gamma_1$
Tangential Force of Joint Set #2	$R_2(-\sin\gamma_1\cos\beta_1\cos\gamma_2 + \cos\gamma_1\sin\gamma_2\cos\beta_2)$	$-R_2(-\sin\gamma_1\sin\beta_1\cos\gamma_2 + \cos\gamma_1\sin\gamma_2\sin\beta_2)$	$R_2(-\sin\gamma_1\sin\gamma_2 \sin(\beta_1-\beta_2))$
Normal Force of Joint Set #2	$N_2\sin\gamma_2\sin\beta_2$	$-N_2\sin\gamma_2\cos\beta_2$	$N_2\cos\gamma_2$
Dead Load of the Pile			$-P$

3.2.6 CALCULATING THE LATERAL LOAD CAPACITY

Substitute R with $cA + N\tan\phi$, the equation in x-direction becomes

$$F\cos\theta+c_1A_1(-\sin\gamma_1\cos\beta_1\cos\gamma_2+\cos\gamma_1\sin\gamma_2\cos\beta_2)+N_1\tan\phi_1(-\sin\gamma_1\cos\beta_1\cos\gamma_2+\cos\gamma_1\sin\gamma_2\cos\beta_2)+N_1\sin\gamma_1\sin\beta_1+c_2A_2(-\sin\gamma_1\cos\beta_1\cos\gamma_2+\cos\gamma_1\sin\gamma_2\cos\beta_2)+N_2\tan\phi_2(-\sin\gamma_1\cos\beta_1\cos\gamma_2+\cos\gamma_1\sin\gamma_2\cos\beta_2)+N_2\sin\gamma_2\sin\beta_2=0 \tag{3.19}$$

Rearrange terms:

$$(\sin\gamma_1\sin\beta_1-\tan\phi_1\sin\gamma_1\cos\beta_1\cos\gamma_2+\tan\phi_1\cos\gamma_1\sin\gamma_2\cos\beta_2)N_1+(\sin\gamma_2\sin\beta_2-\tan\phi_2\sin\gamma_1\cos\beta_1\cos\gamma_2+\tan\phi_2\cos\gamma_1\sin\gamma_2\cos\beta_2)N_2+(\cos\theta)F=c_1A_1\sin\gamma_1\cos\beta_1\cos\gamma_2-c_1A_1\cos\gamma_1\sin\gamma_2\cos\beta_2+c_2A_2\sin\gamma_1\cos\beta_1\cos\gamma_2-c_2A_2\cos\gamma_1\sin\gamma_2\cos\beta_2 \tag{3.20}$$

For the equation in y-direction:

$$F\sin\theta+c_1A_1(-\sin\gamma_1\sin\beta_1\cos\gamma_2+\cos\gamma_1\sin\gamma_2\sin\beta_2)+N_1\tan\phi_1(-\sin\gamma_1\sin\beta_1\cos\gamma_2+\cos\gamma_1\sin\gamma_2\sin\beta_2)-N_1\sin\gamma_1\cos\beta_1+c_2A_2(-\sin\gamma_1\sin\beta_1\cos\gamma_2+\cos\gamma_1\sin\gamma_2\sin\beta_2)+N_2\tan\phi_2(-\sin\gamma_1\sin\beta_1\cos\gamma_2+\cos\gamma_1\sin\gamma_2\sin\beta_2)-N_2\sin\gamma_2\cos\beta_2=0 \quad (3.21)$$

Rearrange terms:

$$(-\sin\gamma_1\cos\beta_1-\tan\phi_1\sin\gamma_1\sin\beta_1\cos\gamma_2+\tan\phi_1\cos\gamma_1\sin\gamma_2\sin\beta_2)N_1+(-\sin\gamma_2\cos\beta_2-\tan\phi_2\sin\gamma_1\sin\beta_1\cos\gamma_2+\tan\phi_2\cos\gamma_1\sin\gamma_2\sin\beta_2)N_2+(\sin\theta)F=c_1A_1\sin\gamma_1\sin\beta_1\cos\gamma_2-c_1A_1\cos\gamma_1\sin\gamma_2\sin\beta_2+c_2A_2\sin\gamma_1\sin\beta_1\cos\gamma_2-c_2A_2\cos\gamma_1\sin\gamma_2\sin\beta_2 \quad (3.22)$$

For the equation in z-direction:

$$-W-c_1A_1\sin\gamma_1\sin\gamma_2\sin(\beta_1-\beta_2)-N_1\tan\phi_1\sin\gamma_1\sin\gamma_2\sin(\beta_1-\beta_2)+N_1\cos\gamma_1-c_2A_2\sin\gamma_1\sin\gamma_2\sin(\beta_1-\beta_2)-N_2\tan\phi_2\sin\gamma_1\sin\gamma_2\sin(\beta_1-\beta_2)+N_2\cos\gamma_1-P=0 \quad (3.23)$$

Rearrange terms:

$$(\cos\gamma_1-\tan\phi_1\sin\gamma_1\sin\gamma_2\sin(\beta_1-\beta_2))N_1+(\cos\gamma_2-\tan\phi_2\sin\gamma_1\sin\gamma_2\sin(\beta_1-\beta_2))N_2+(0)F=W+P+c_1A_1\sin\gamma_1\sin\gamma_2\sin(\beta_1+\beta_2)+c_2A_2\sin\gamma_1\sin\gamma_2\sin(\beta_1-\beta_2) \quad (3.24)$$

N_1, N_2, and F can be computed by solving these three equations. These three equations can be put into matrix form and then can be easily solved with math programs such as Matlab. The matrix can be set up as follows:

$$\begin{bmatrix} A_{11} & A_{12} & A_{13} \\ A_{21} & A_{22} & A_{23} \\ A_{31} & A_{32} & A_{33} \end{bmatrix} \begin{bmatrix} N_1 \\ N_2 \\ F \end{bmatrix} = \begin{bmatrix} B_{11} \\ B_{21} \\ B_{31} \end{bmatrix} \quad (3.25)$$

$$Af=B \quad (3.26)$$

where

$A_{11}=\sin\gamma_1\sin\beta_1-\tan\phi_1\sin\gamma_1\cos\beta_1\cos\gamma_2+\tan\phi_1\cos\gamma_1\sin\gamma_2\cos\beta_2$

$A_{12}=\sin\gamma_2\sin\beta_2-\tan\phi_2\sin\gamma_1\cos\beta_1\cos\gamma_2+\tan\phi_2\cos\gamma_1\sin\gamma_2\cos\beta_2$

$A_{13}=\cos\theta$

$B_{11}=c_1A_1\sin\gamma_1\cos\beta_1\cos\gamma_2-c_1A_1\cos\gamma_1\sin\gamma_2\cos\beta_2+c_2A_2\sin\gamma_1\cos\beta_1\cos\gamma_2-c_2A_2\cos\gamma_1\sin\gamma_2\cos\beta_2$

$A_{21}=-\sin\gamma_1\cos\beta_1-\tan\phi_1\sin\gamma_1\sin\beta_1\cos\gamma_2+\tan\phi_1\cos\gamma_1\sin\gamma_2\sin\beta_2$

$A_{22}=-\sin\gamma_2\cos\beta_2-\tan\phi_2\sin\gamma_1\sin\beta_1\cos\gamma_2+\tan\phi_2\cos\gamma_1\sin\gamma_2\sin\beta_2$

$A_{23}=\sin\theta$

$B_{21}=c_1A_1\sin\gamma_1\sin\beta_1\cos\gamma_2-c_1A_1\cos\gamma_1\sin\gamma_2\sin\beta_2+c_2A_2\sin\gamma_1\sin\beta_1\cos\gamma_2-c_2A_2\cos\gamma_1\sin\gamma_2\sin\beta_2$

$A_{31}=\cos\gamma_1-\tan\phi_1\sin\gamma_1\sin\gamma_2\sin(\beta_1-\beta_2)$

$A_{32}=\cos\gamma_2-\tan\phi_2\sin\gamma_1\sin\gamma_2\sin(\beta_1-\beta_2)$

$A_{33}=0$

$B_{31}=W+P+c_1A_1\sin\gamma_1\sin\gamma_2\sin(\beta_1-\beta_2)+c_2A_2\sin\gamma_1\sin\gamma_2\sin(\beta_1-\beta_2)$

3.2.7 AN EXAMPLE ON CALCULATING THE LATERAL LOAD CAPACITY IN A 2-JOINT-SET SYSTEM

1st Joint Set N-S, 30°E:
$\phi_1=22.5^o$ ($\pi/8$)
$c_1=2$ psi
$\beta_1=90^o$ ($\pi/2$)
$\gamma_1=30^o$ ($\pi/6$)
$s_1=0.866 \cdot D$

2nd Joint Set E-W, 60°S:
$\phi_2=30^o$ ($\pi/6$)
$c_2=3$ psi
$\beta_2=0^o$
$\gamma_2=60^o$ ($\pi/3$)
$s_2=0.433 \cdot D$

Force Direction:
$\theta=180^o$

Pile:
l=D

Rock Unit Weight:
$\gamma_r=2.75 \cdot 62.4$ lb/ft^3 = 171.6 lb/ft^3

Pile Diameter:
D=5ft

Dead Load of Pile:
P=1400k

Volume of Wedge:

Complete Method:
Use equation (3.4) to calculate the volume of the wedge.

$$V = \sum_{i=1}^{n} a_i h_{i\,(centroid)} - \frac{\pi D^2}{8} l$$

where
a=area of a block on the surface
$h_{centroid}$=height from the surface to the centroid of the area of intersection between the block and the vertical cutting plane
D=diameter of the pile

$a_i = \| (s_1 \bullet s_2)/\sin(\beta_1 - \beta_2) \| = \| (0.866D \bullet 0.433D)/\sin(90^o - 0^o) \| = 0.375D^2$

As shown in Figure 3.19, $h_1=0.25D$, $h_2=0.75D$, and $h_3=1.25D$

$V=0.375D^2 \bullet (4 \bullet h_1+4 \bullet h_2+3 \bullet h_3) - \pi D^2 \bullet D/8$

$=0.375D^2 \bullet (4 \bullet 0.25D+4 \bullet 0.75D+3 \bullet 1.25D) - \pi D^3/8$

$=2.906D^3 - \pi D^3/8$

$=2.514D^3 = 314.25 \text{ ft}^3$

Simplified Way:

Use equation (3.5) to quickly estimate the volume of the wedge.

$V=n \bullet a \bullet 0.5 \bullet b - \pi D^2 \bullet l/8$

where b is the height from the surface to the bottom of the wedge, and as shown in Figure 3.20, b=1.5D.

$V=11 \bullet 0.375D^2 \bullet 0.5 \bullet 1.5D - \pi D^2 \bullet D/8$

$=2.701D^3$

% Difference: $(2.701-2.514)/2.514 \bullet 100\% = 7.44\%$

$V=2.514D^3 = 314.25 \text{ ft}^3$

$W=\gamma_r \bullet V = 171.6 \text{ lb/ft}^3 \bullet 314.25 \text{ ft}^3 = 53925.3 \text{ lb}$

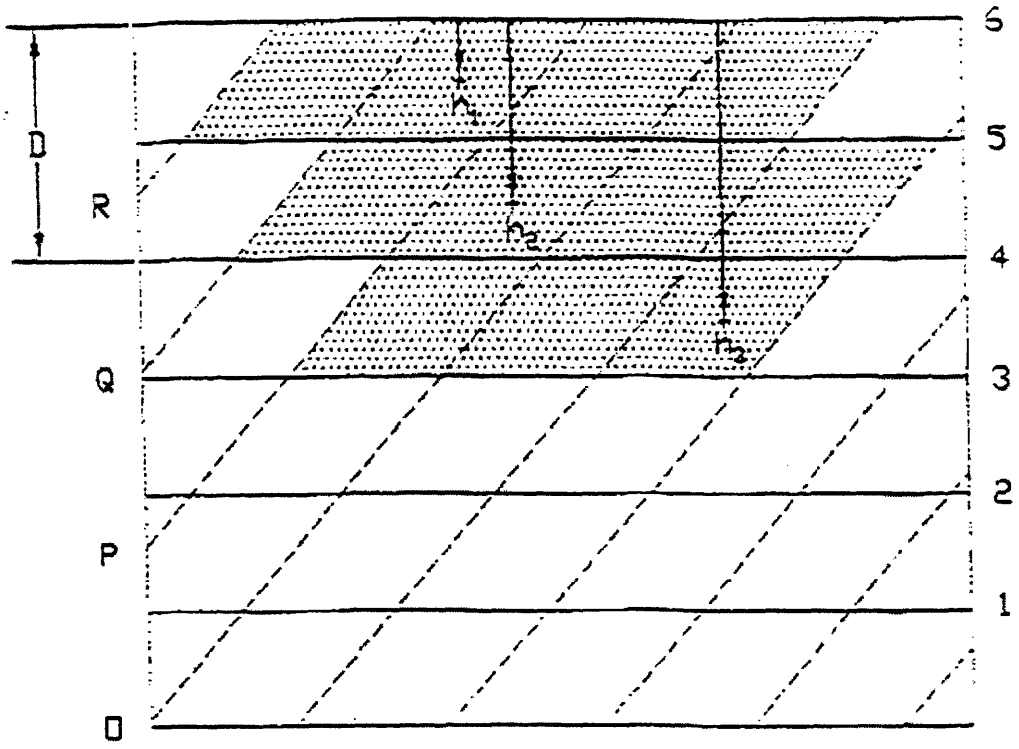

Figure 3.19 h's of Various Blocks

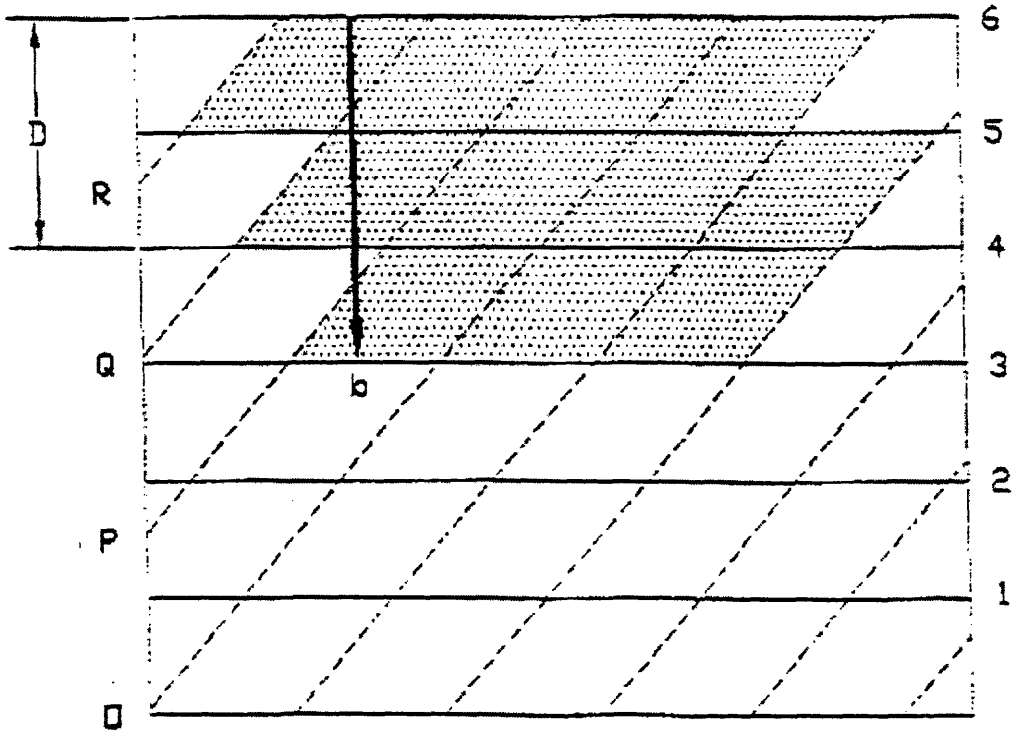

Figure 3.20 b, Height of the Wedge

Area of Faces:

Use equation (3.17) to calculate the area of the faces for each joint set:

$$A = \sum_{i=1}^{n} \left[\frac{H_i}{\sin\gamma} \bullet \left\| \frac{s_i}{\sin(\beta_1 - \beta_2)} \right\| \right]$$

where

H=height from the surface to the center of the edge that intersects the pile or the cutting plane

γ=dip angle of the respective joint set

β=angle measured counterclockwise from the x-axis to the strike line of the respective joint set

s=the horizontal spacing of the other joint set

Since s and γ are the same for the faces of the same joint set and $\sin(\beta_1-\beta_2)=\sin(90-0)=1$, and thus

$$A = \frac{s}{\sin\gamma} \sum_{i=1}^{n} H_i$$

For A_1 (joint set N-S, 30°E):

γ=30° for joint set N-S, 30°E

s=0.433D for joint set E-W, 60°S

As shown in Figure 3.21, H_1=0.5D, H_2=D, H_3=1.5D, and H_4=0.5D:

$$\sum_{i=1}^{n} H_i = (H_1 + H_2 + 3H_3 + H_4)$$

$$= \sum_{i=1}^{n} H_i = (0.5D + D + 3 \cdot 1.5D + 0.5D) = 6.5D = 32.5\,ft$$

$$A_1 = \frac{s}{\sin\gamma} \sum_{i=1}^{n} H_i = \frac{0.433D}{\sin 30°} \cdot 32.5\,ft = 140.725\,ft^2 = 20264.4\,in^2$$

For A_2 (joint set E-W, 60°S):
γ=60° for joint set E-W, 60°S
s=0.866D for joint set N-S, 30°E

As shown in Figure 3.22, H_5=0.25D, H_6=0.75D, H_7=1.25D, H_8=1.25D, H_9=0.75D, and H_{10}=0.25D:

$$\sum_{i=1}^{n} H_i = (H_5 + H_6 + H_7 + H_8 + H_9 + H_{10})$$

$$= \sum_{i=1}^{n} H_i = (0.25D + 0.75D + 1.25D + 1.25D + 0.75D + 0.25D) = 4.5D = 22.5\,ft$$

$$A_2 = \frac{s}{\sin\gamma} \sum_{i=1}^{n} H_i = \frac{0.866D}{\sin 60°} \cdot 22.5\,ft = 112.5\,ft^2 = 16199.5\,in^2$$

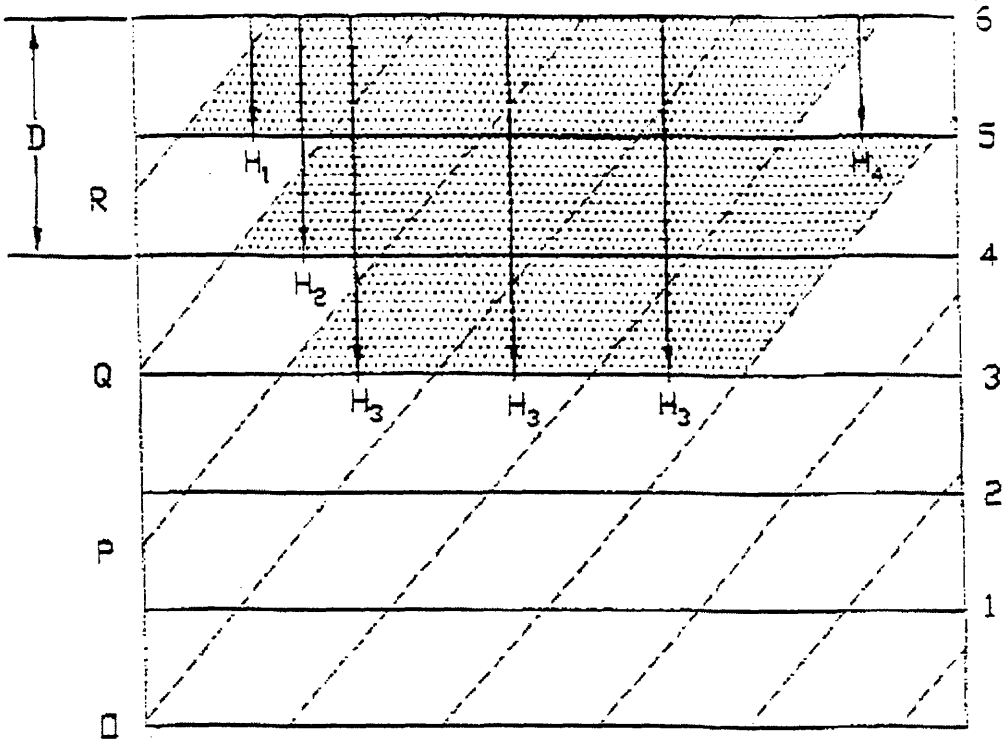

Figure 3.21 H's for Faces of Joint Set N-S. 30°E

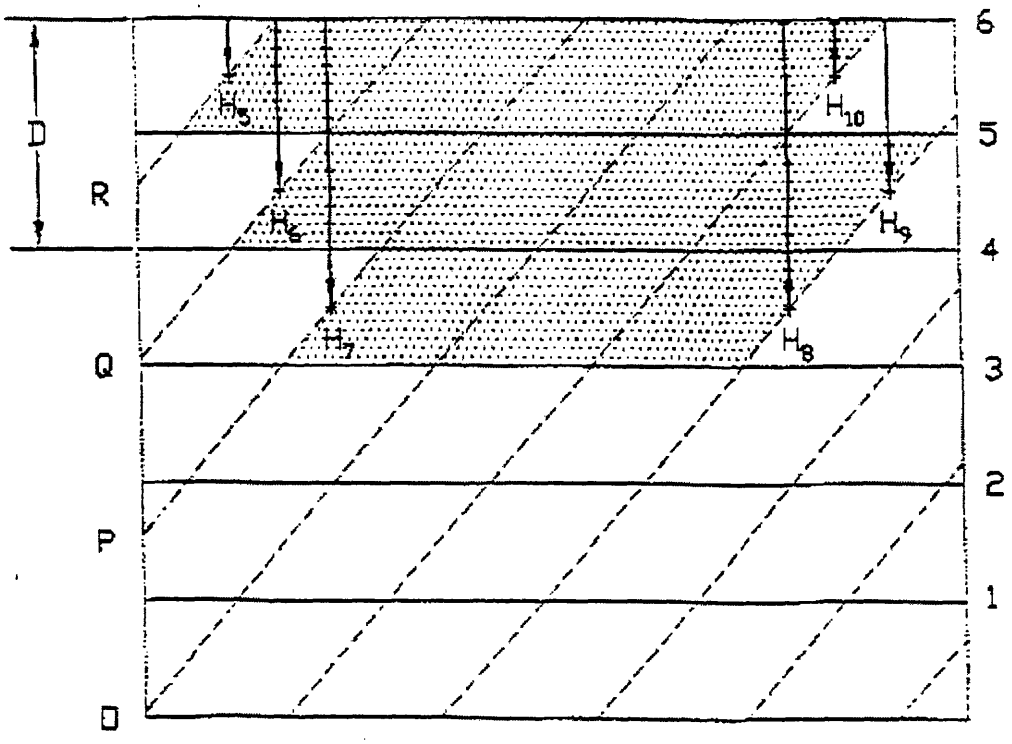

Figure 3.22 H's for Faces of Joint Set E-W, 60°S

Limit Equilibrium:

In the x-direction:

$(\sin\gamma_1\sin\beta_1-\tan\phi_1\sin\gamma_1\cos\beta_1\cos\gamma_2+\tan\phi_1\cos\gamma_1\sin\gamma_2\cos\beta_2)N_1+(\sin\gamma_2\sin\beta_2-\tan\phi_2\sin\gamma_1\cos\beta_1\cos\gamma_2+\tan\phi_2\cos\gamma_1\sin\gamma_2\cos\beta_2)N_2+(\cos\theta)F=c_1A_1\sin\gamma_1\cos\beta_1\cos\gamma_2-c_1A_1\cos\gamma_1\sin\gamma_2\cos\beta_2+c_2A_2\sin\gamma_1\cos\beta_1\cos\gamma_2-c_2A_2\cos\gamma_1\sin\gamma_2\cos\beta_2$

$(\sin30^o\sin90^o-\tan22.5^o\sin30^o\cos90^o\cos0^o+\tan22.5^o\cos30^o\sin60^o\cos0^o)N_1+(\sin60^o\sin0^o-\tan30^o\sin30^o\cos90^o\cos0^o+\tan30^o\cos30^o\sin60^o\cos0^o)N_2+(\cos180^o)F=2\cdot20264.4\cdot\sin30^o\cos90^o\cos0^o-2\cdot20264.4\cdot\cos30^o\sin60^o\cos0^o+3\cdot16199.5\cdot\sin30^o\cos90^o\cos0^o-3\cdot16199.5\cdot\cos30^o\sin60^o\cos0^o$

$0.811)N_1+(0.433)N_2+(-1)F=-66,845.475$ [lb]

In the y-direction:

$(-\sin\gamma_1\cos\beta_1-\tan\phi_1\sin\gamma_1\sin\beta_1\cos\gamma_2+\tan\phi_1\cos\gamma_1\sin\gamma_2\sin\beta_2)N_1+(-\sin\gamma_2\cos\beta_2-\tan\phi_2\sin\gamma_1\sin\beta_1\cos\gamma_2+\tan\phi_2\cos\gamma_1\sin\gamma_2\sin\beta_2)N_2+(\sin\theta)F=c_1A_1\sin\gamma_1\sin\beta_1\cos\gamma_2-c_1A_1\cos\gamma_1\sin\gamma_2\sin\beta_2+c_2A_2\sin\gamma_1\sin\beta_1\cos\gamma_2-c_2A_2\cos\gamma_1\sin\gamma_2\sin\beta_2$

$(-\sin30^o\cos90^o-\tan22.5^o\sin30^o\sin90^o\cos60^o+\tan22.5^o\cos30^o\sin60^o\sin0^o)N_1+(-\sin60^o\cos0^o-\tan30^o\sin30^o\sin90^o\cos60^o+\tan30^o\cos30^o\sin60^o\sin0^o)N_2+(\sin180^o)F=2\cdot20264.4\cdot\sin30^o\sin90^o\cos60^o-2\cdot20264.4\cdot\cos30^o\sin60^o\sin0^o+3\cdot16199.5\cdot\sin30^o\sin90^o\cos60^o-3\cdot16199.5\cdot\cos30^o\sin60^o\sin0^o$

$(-0.104)N_1+(-1.010)N_2+(0)F=22,281.83$ [lb]

In the z-direction:

$(\cos\gamma_1-\tan\phi_1\sin\gamma_1\sin\gamma_2\sin(\beta_1-\beta_2))N_1+(\cos\gamma_2-\tan\phi_2\sin\gamma_1\sin\gamma_2\sin(\beta_1-\beta_2))N_2+(0)F=W+P+c_1A_1\sin\gamma_1\sin\gamma_2\sin(\beta_1-\beta_2)+c_2A_2\sin\gamma_1\sin\gamma_2\sin(\beta_1-\beta_2)$

$(\cos30^o-\tan22.5^o\sin30^o\sin60^o\sin(90^o-0^o))N_1+(\cos60^o-\tan30^o\sin30^o\sin60^o\sin(90^o-0^o)N_2+(0)F=53925.3+1,400.000+2\cdot20264.4\cdot\sin30^o\sin60^o\sin(90^o-0^o)+3\cdot16199.5\cdot\sin30^o\sin60^o\sin(90^o-0^o)$

$(0.687)N_1+(0.250)N_2+(0)F=1,492,518.55$ [lb]

Solve these three equations and obtain the results:

$N_1=2266.2k$
$N_2=-254.3k$
F=1794 k

As mentioned previously, a normal force acting on a joint set can act in one of two possible directions. The direction is initially unknown until after the kinetic analysis. A negative value in N_1, N_2, and/or F indicates that the initial assumed direction is in the opposite direction. In the example above, N_2 is initially defined to point upward as shown in Figure 3.14a. However, since N_2 is negative, it should then be in the opposite direction as shown in Figure 3.14b. Also, the magnitude of the values N_1, N_2, and F does not change as a result of N_2 being negative.

In any case when F is negative, the system is stable and thus is not removable. F may be negative when the shear resistance in the joints is very high and/or the orientation of the joint sets prevents the wedge from displacing and/or the vertical load on the pile is very high.

As mentioned before, a math program can be used to solve the equations and to manipulate inputs and outputs easily. Matlab is run to solve the problem above, and the program for solving the matrix, inputs, and outputs are attached in the Appendix.

3.3 KINETICS OF A THREE-JOINT SET SYSTEM

The kinetics of a three-joint-set system, identical to that of a two-joint-set system, is based on the limit equilibrium approach. However, the analysis is more complicated for the three-joint-set system since a combination of removable blocks may involve all three joint sets. Also, since more than one combination of blocks often exists, each combination is analyzed independently and the combination having the lowest capacity is the critical combination. The complete kinetic analysis for a three-joint-set system is presented below.

The previous example of a three-joint set system in Chapter 2.9 is used here again for kinetics analysis. The orientations of the joint sets are N-S, 30°E (1st joint set); E-W, 60°S (2nd joint set); and N45°E, 45°NW (3rd joint set) respectively. As determined in Chapter 2.9, when a force acts northward on the pile, two combinations of removable blocks were identified for kinetic analysis and are shown again in Figure 3.23 and Figure 3.24, respectively. A previous assumption made in the kinematics chapter is that each Type II and Type V block being affected by the pile breaks apart right above the interference area when the pile is acted on by a force, and the top part of the block becomes removable. Recalling from Chapter 3.2 that for ease of kinetic analysis, it is assumed here that each Type II and Type V block breaks away from a vertical cutting plane that is perpendicular to the force direction and lies across the center of the pile. The intersection between the blocks in the combination and the cutting plane is shown dotted for each combination in Figure 3.23 and Figure 3.24 respectively.

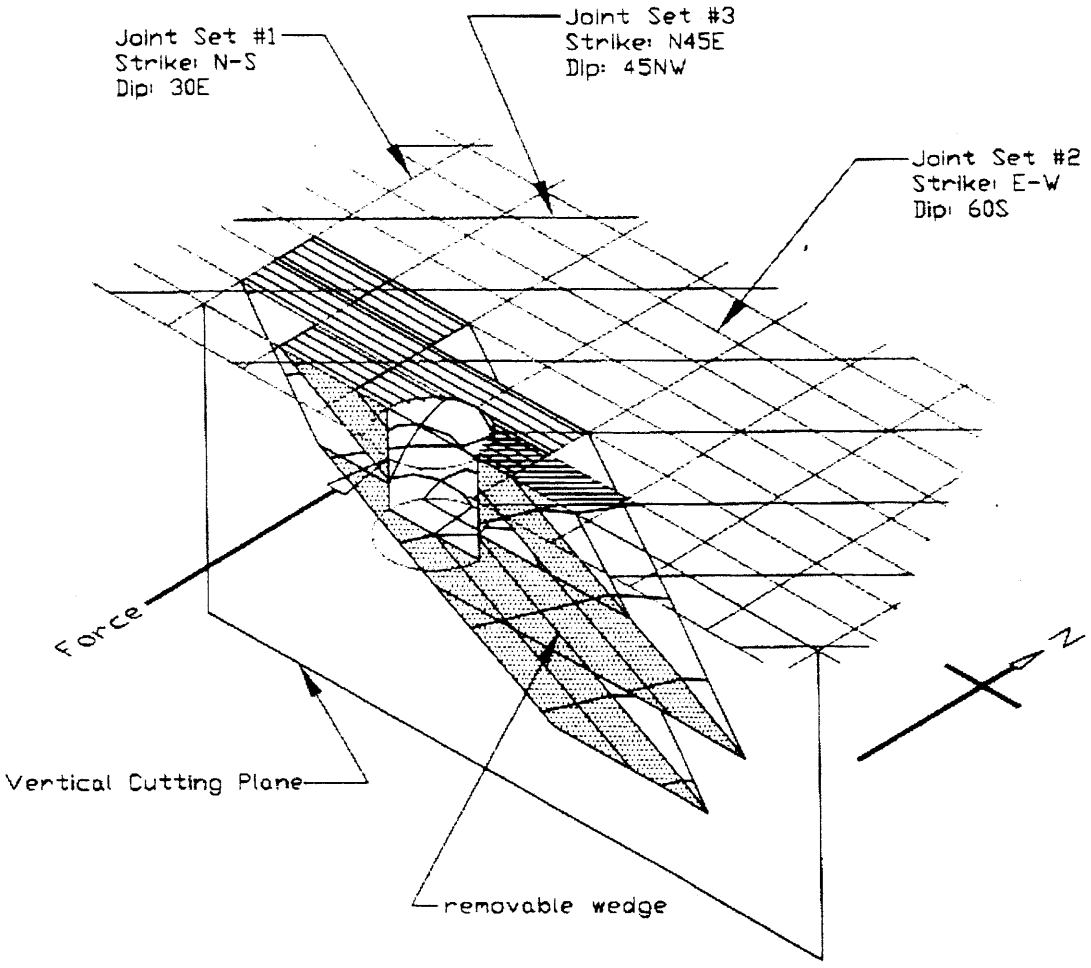

Figure 3.23 A Removable Combination of Blocks in 3D View

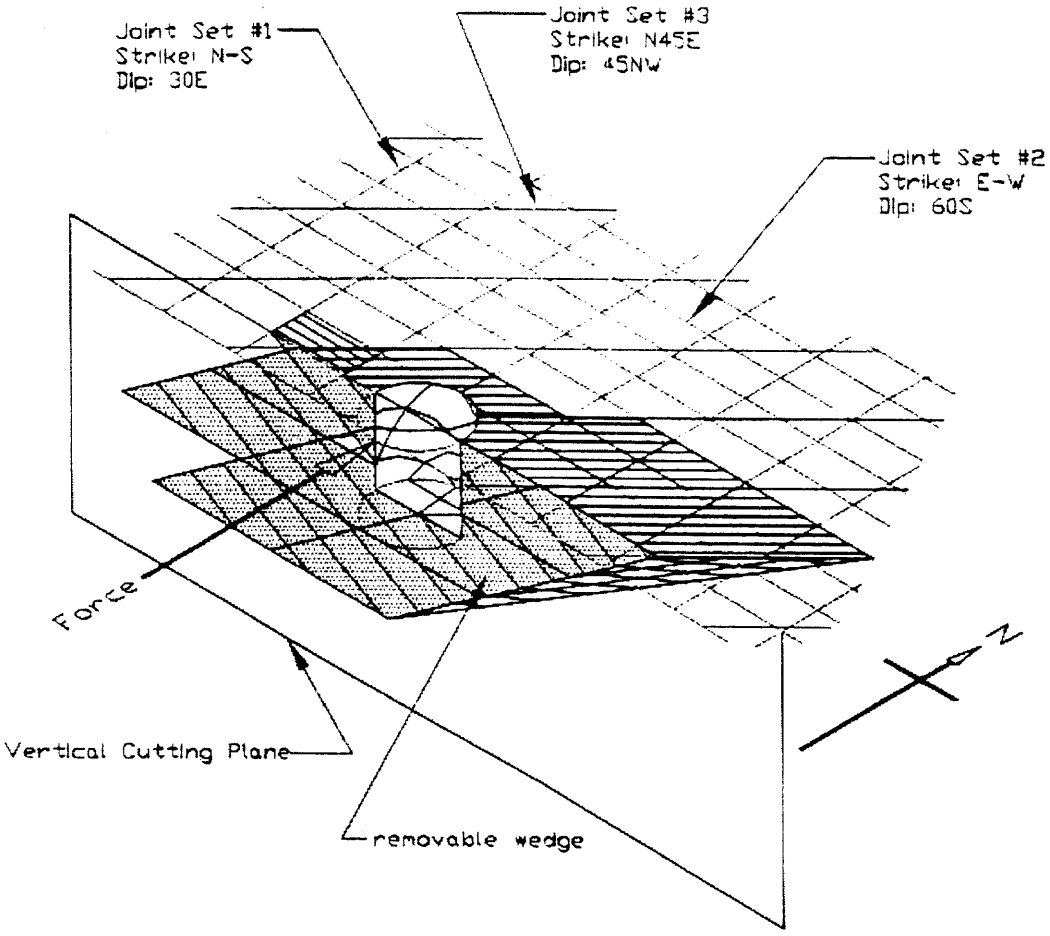

Figure 3.24 A Removable Combination of Blocks in 3D View

The combination of removable blocks in Figure 3.23 is analyzed first. The whole combination is separated into two wedges for kinetic analysis. The primary wedge is composed of the primary pair of joint sets as shown in Figure 3.25 and the secondary wedge is composed of the secondary pair of joint sets as shown in Figure 3.26. Since there are three joint sets in the system and only two joint sets are analyzed for each wedge, confusion may arise when using the equations containing subscripts 1 and 2. From now on, the subscripts 1 and 2 in any of the following equations represent the two joint sets that a wedge being analyzed is composed of.

With modifications, which will be discussed later, to the kinetic analysis used in the 2-joint-set system, the lateral driving force (F) of each wedge is determined. Then the lateral driving forces (F) for the primary wedge and the secondary wedge are summed up to determine the ultimate lateral capacity (F_u) that is required to displace the whole combination. The typical forces acting on each wedge are shown in its respective figure. In Figure 3.24, for clarity of presentation, the normal forces (N) and tangential forces (R) are drawn for each joint set separately, but all these forces actually occur together.

3.3.1 LATERAL DRIVING FORCE

Define θ as shown in Figure 3.27a and β and γ as shown in Figure 3.27b. The lateral driving force vector is expressed as follows

$$\vec{F} = F\cos\theta\,\hat{i} + F\sin\theta\,\hat{j} \tag{3.27}$$

where F is the lateral driving force for a wedge. The ultimate lateral capacity (F_u) is thus the sum of the F for the primary wedge and the F for the secondary wedge.

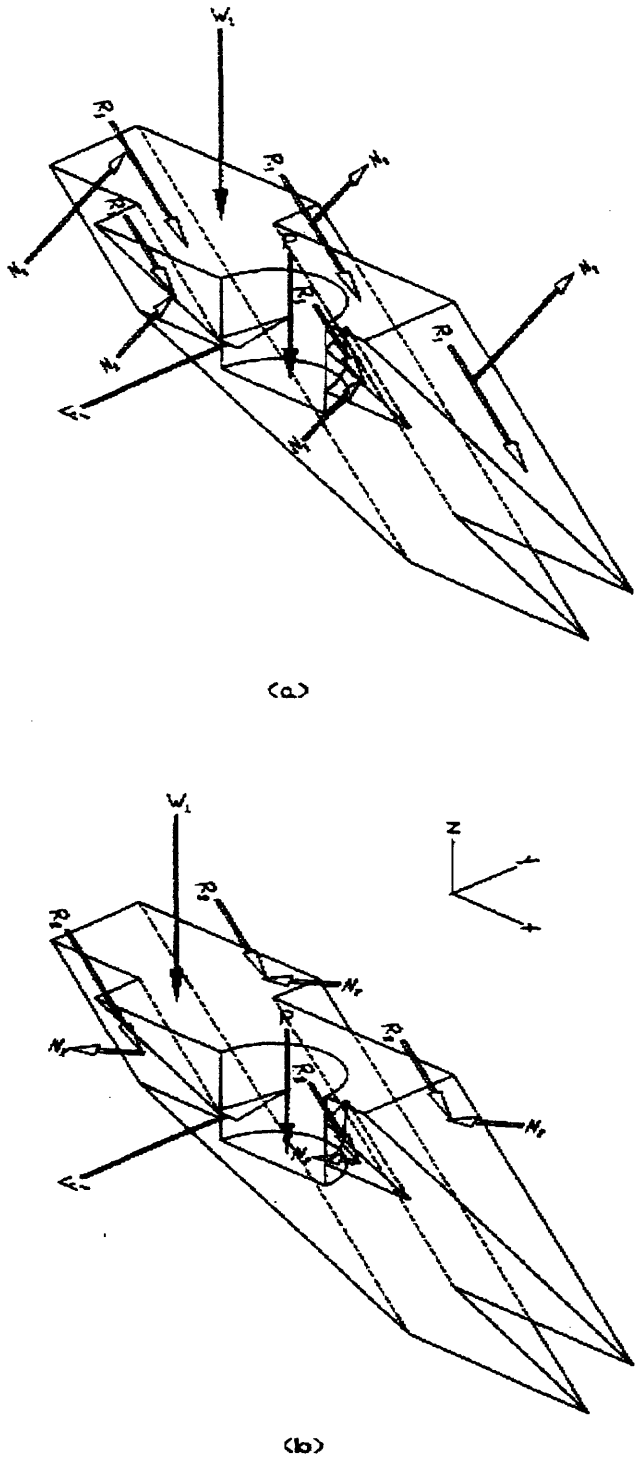

Figure 3.25 Typical Forces on Faces of the Wedge for (a) Joint Set N-S, 30°E and (b) Joint Set E-W, 60°S

F_1=lateral driving force for the primary wedge
W_1=weight of the primary wedge
R_1=tangential force on joint set 1
N_1=normal force on joint set 1
R_2=tangential force on joint set 2
N_2=normal force on joint set 2

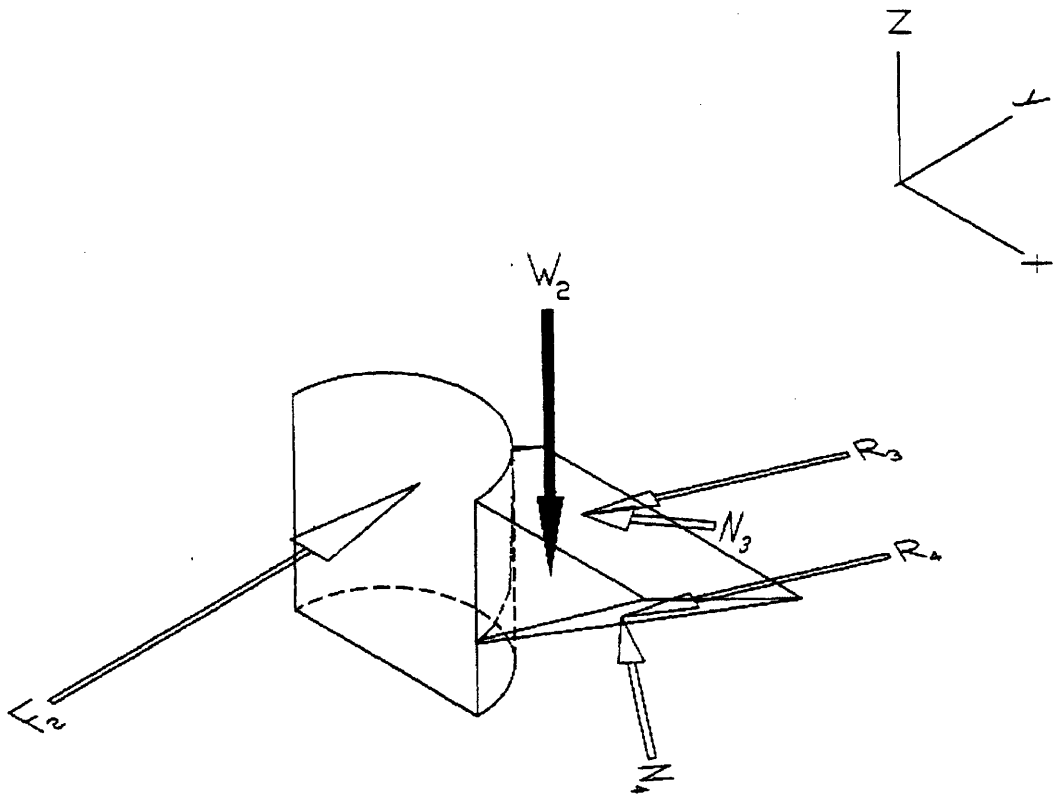

Figure 3.26 Typical Forces on Faces of the Wedge for Joint Set E-W, 60°S and Joint Set N45°E, 45°NW

F_2=lateral driving force for the secondary wedge
W_2=weight of the secondary wedge
R_3=tangential force on joint set 1
N_3=normal force on joint set 1
R_4=tangential force on joint set 2
N_4=normal force on joint set 2

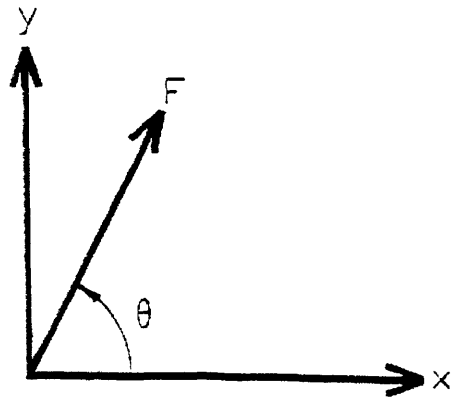

(a)

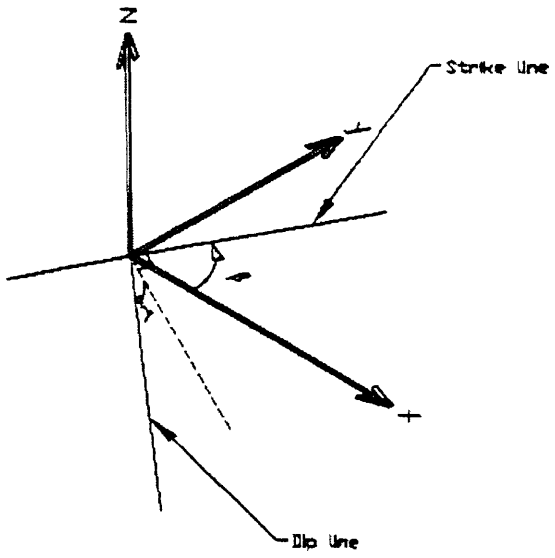

(b)

Figure 3.27 (a) Typical Force Vector; (b) Dip and Strike Lines

3.3.2 WEIGHT OF WEDGE

The weight vector is expressed as follows

$$\vec{W} = -\gamma_r V \hat{k} \tag{3.28}$$

where γ_r is the unit weight of the rock mass and V is the volume of the wedge.

A Type I block is shown in Figure 3.28. The volume of each block is approximately

$$V_{block} \approx h_{centroid} \bullet a = h_{centroid} \bullet \| (s_1 \bullet s_2)/sin(\beta_1 - \beta_2) \| \tag{3.29}$$

where $h_{centroid}$ is the distance from the surface to the centroid of the area of intersection between the block and the pile, a is the area of the block on the surface, s_i is the horizontal spacing of joint set i, and β_i is defined for joint set i as shown in Figure 3.27b. $\| (s_1 \bullet s_2)/sin(\beta_1 - \beta_2) \|$ is the equation for the area of a parallelogram as shown in Figure 3.29. The rectangular shape of the area on top of the block in Figure 3.28 is just a special case, and the area simplifies to $s_1 \bullet s_2$.

$h_{centroid}$ of an entirely intersecting block can be obtained from the joint map on a pile, but that of a partially intersecting block cannot. Also, the volume of a block that intersects the pile and the vertical cutting plane is difficult to estimate. A more effective way to estimate the volume of a block is to assume that the pile does not exist and that the blocks extend to the cutting plane, creating imaginary blocks as shown in Figure 3.30. By totaling the volume of each imaginary block and then subtracting half of the volume of the pile, the volume of the removable wedge is obtained. In this process, it is very useful to have a figure of joint intersections on the cutting plane. The method of constructing such a figure is as follows

1. On a joint map on the pile, connect two points of intersections where a specific joint in a joint set meets the line of intersection between the pile and the cutting plane. An example is shown in Figure 3.31a for joint O and joint h, both shown with dotted lines.
2. Replicate and extend the lines produced in (1) based on the spacing of that particular joint set as shown in Figure 3.31b for joint O.

3. Repeat (1) and (2) for a joint in the other joint set as shown in Figure 3.31c.

4. Label the newly constructed joint lines accordingly and erase the original joint intersection lines on the pile as shown in Figure 3.31d. This is the joint map of the 2nd and 3rd joint sets on the vertical cutting plane.

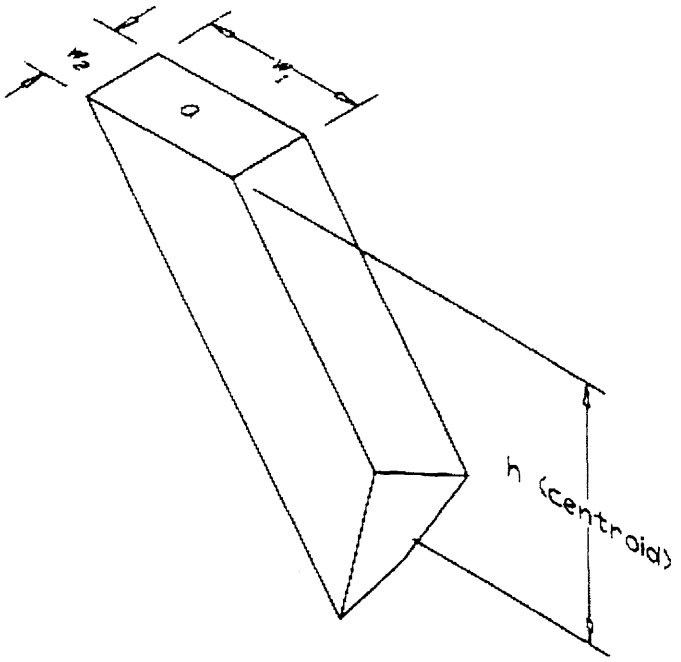

Figure 3.28 A Typical Block That Intercepts the Pile Entirely

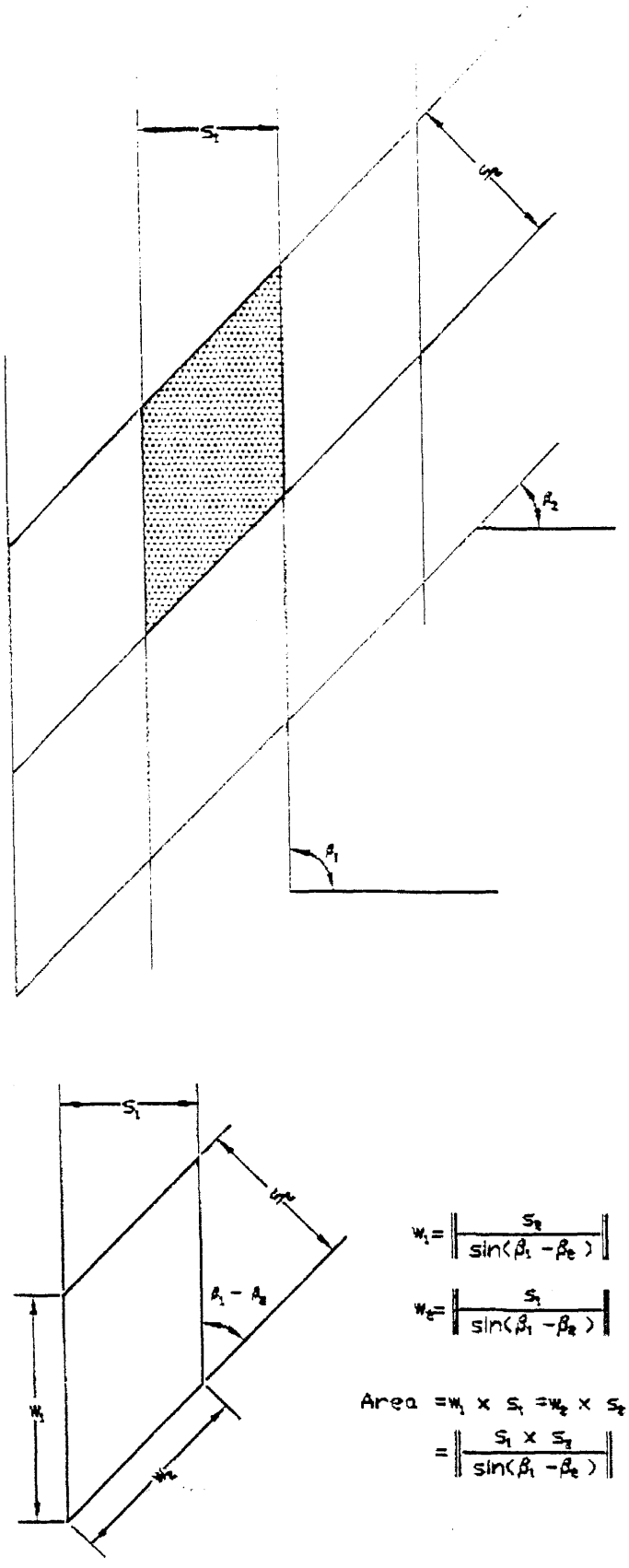

Figure 3.29 Area of a Block on the Surface

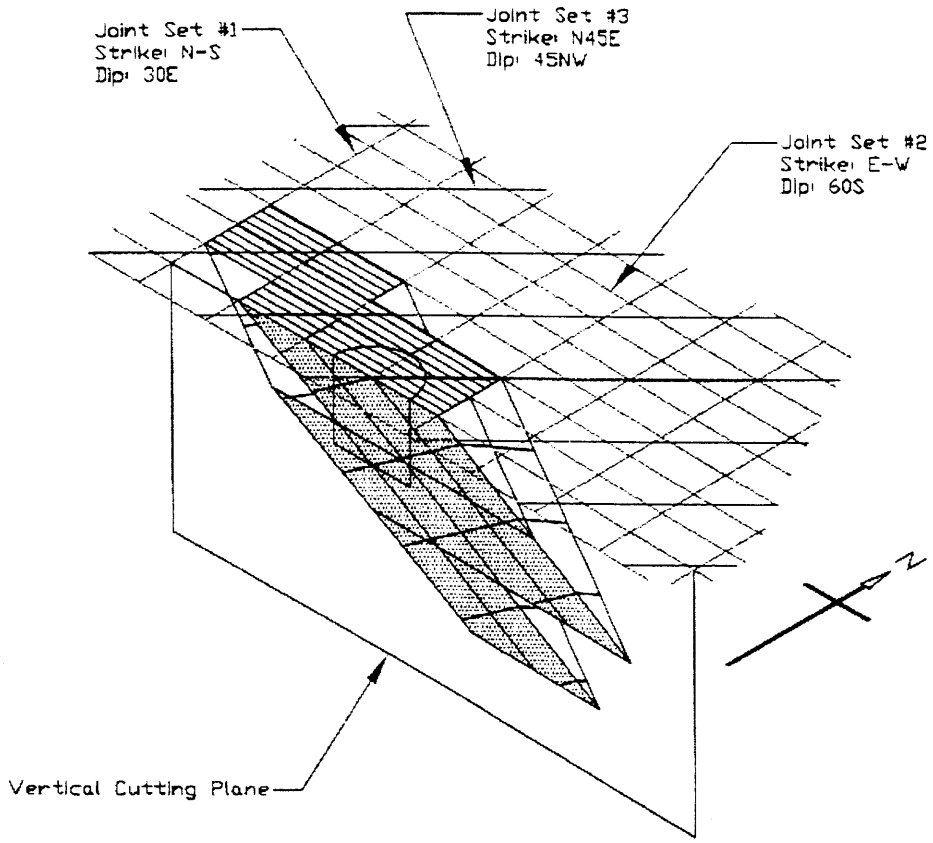

Figure 3.30 Imaginary Blocks of the Primary Wedge Extending to the Cutting Plane

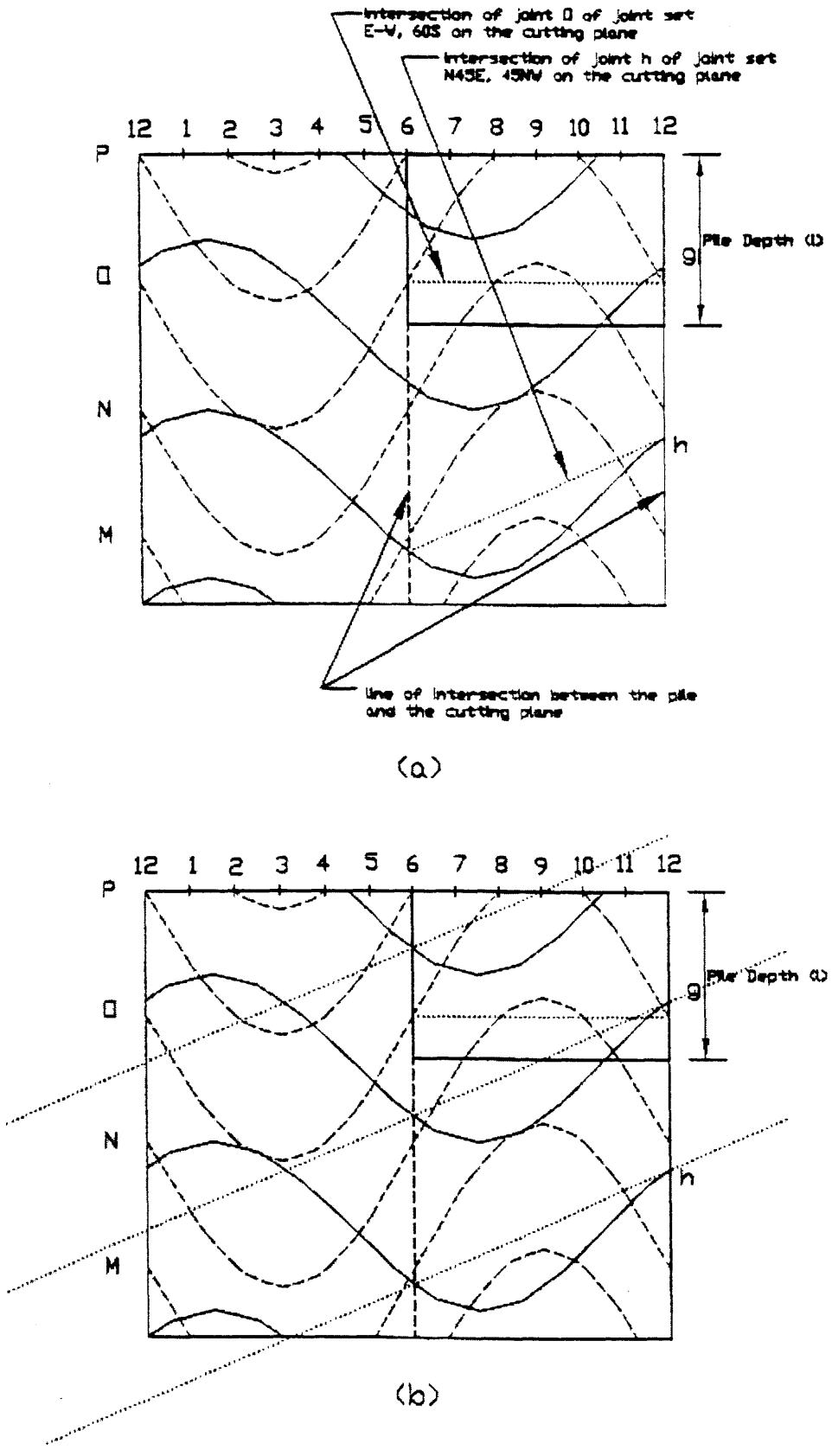

Figure 3.31 Construction of a Joint Map of the 2nd and 3rd Joint Sets on a Cutting Plane

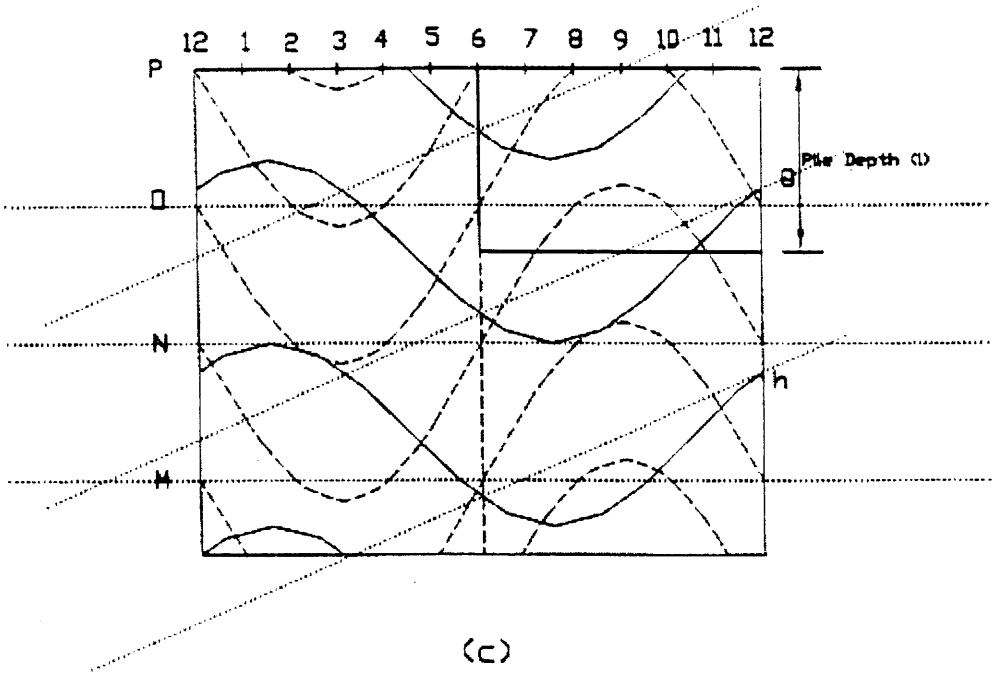

Figure 3. 31 Construction of a Joint Map of the 2nd and 3rd Joint Sets on a Cutting Plane

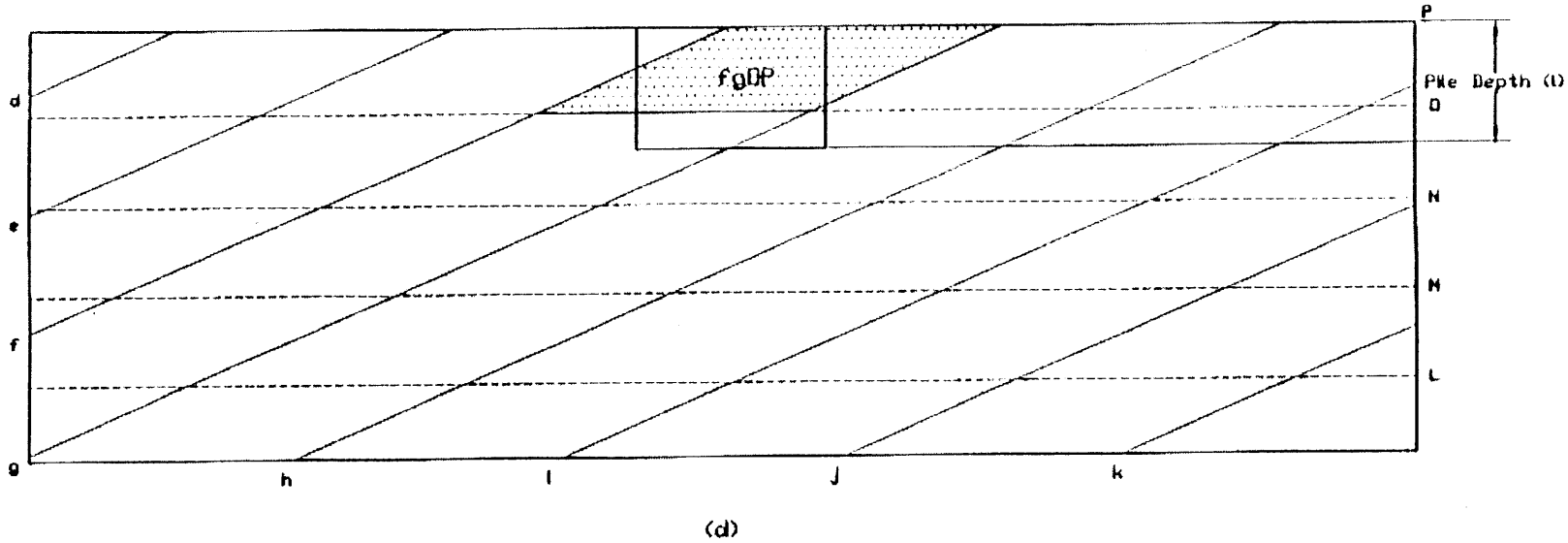

(d)

Figure 3.31 Construction of a Joint Map of the 2nd and 3rd Joint Sets on a Cutting Plane

The joint map of the 1st and 2nd joint sets on the vertical plane is shown in Figure 3.32. and the primary wedge is shown dotted. $h_{centroid}$ can be obtained from the joint map on the cutting plane and typical $h_{centroid}$'s are shown in Figure 3.33. h_1 is the $h_{centroid}$ for Block 56OP, h_2 is that for Block 45MN, and h_3 is that for Block 67NO.

The volume of a primary wedge is expressed as follows

$$V = \sum_{i=1}^{n} a_i h_{i\,(centroid)} - \frac{\pi D^2}{8} l \tag{3.30}$$

where n is the total number of blocks and a_i is the area of block i on the surface. D is the diameter of the pile and l is the pile depth as shown in Figure 3.34. The volume (V) of the wedge is the total volume of all the blocks minus half of the volume of the pile. An assumption made here is that the niche indicated in Figure 3.34 is filled, and the resulting volume of the wedge is larger. The niche exists because block 56OP(R) intersects the pile entirely and does not extend past the pile to intersect the vertical plane. Since the niche is relatively small compared to the volume of the wedge, including it in the wedge volume calculation is acceptable. A second assumption made in this equation is that the primary wedge encompasses half of the pile as shown in Figure 3.25. In most cases, the wedge encompasses most or all of the half pile, and so this assumption is justified.

However, the technique given in equation (3.30) is too time consuming to apply when the removable wedge has too many blocks. A simplified way to estimate the volume of the primary wedge is given as follows:

$$\begin{aligned} V &= n \bullet a \bullet AVG(h_1, h_2, \ldots, h_n) - (\pi D^2 l)/8 \\ &\approx n \bullet a \bullet 0.5 \bullet b - (\pi D^2 l)/8 \end{aligned} \tag{3.31}$$

where b is the distance from the surface to the bottom of the wedge as indicated in Figure 3.35. a_i in equation (3.30) becomes a in equation (3.31) since it is assumed that the surface area of each block in the wedge is the same. The basic assumption of equation (3.31) is that the blocks in a wedge are fairly evenly distributed in each layer. As shown in the Chapter 3.2.2, the error of the simplified method is small.

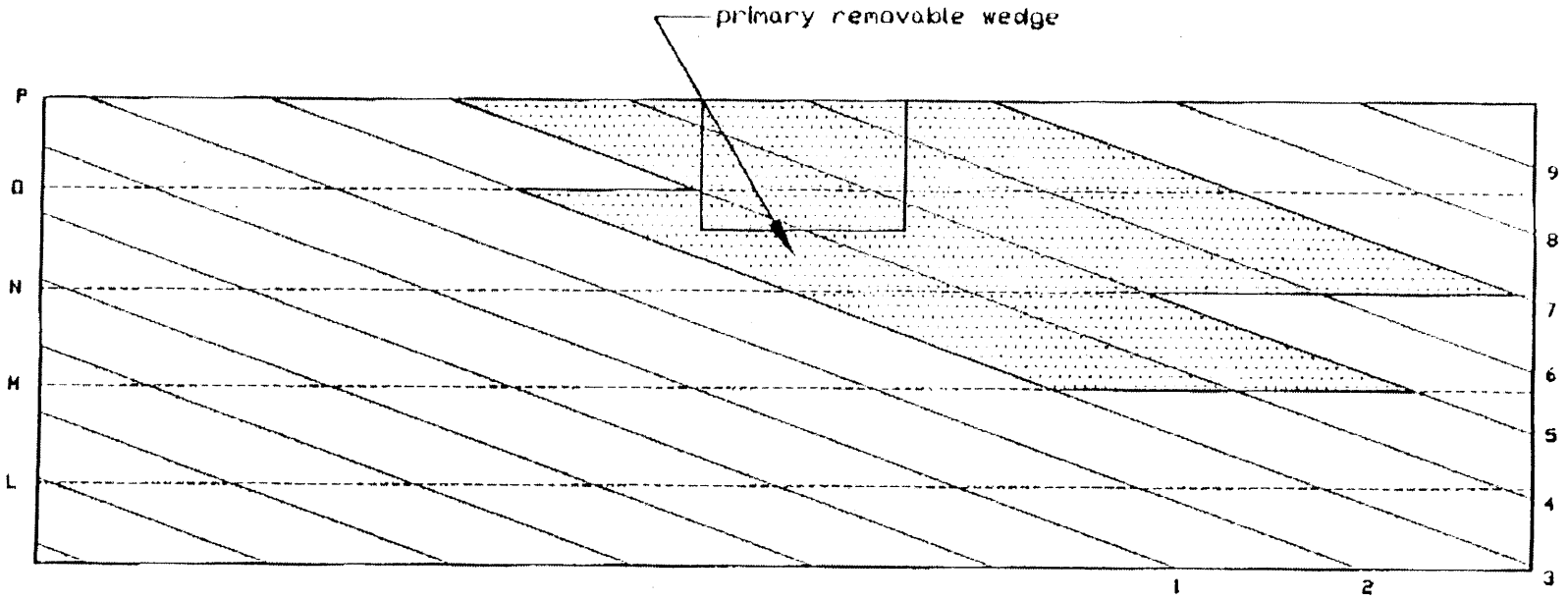

Figure 3.32 Joint Map of the 1st and 2nd Joint Sets on a Cutting Plane

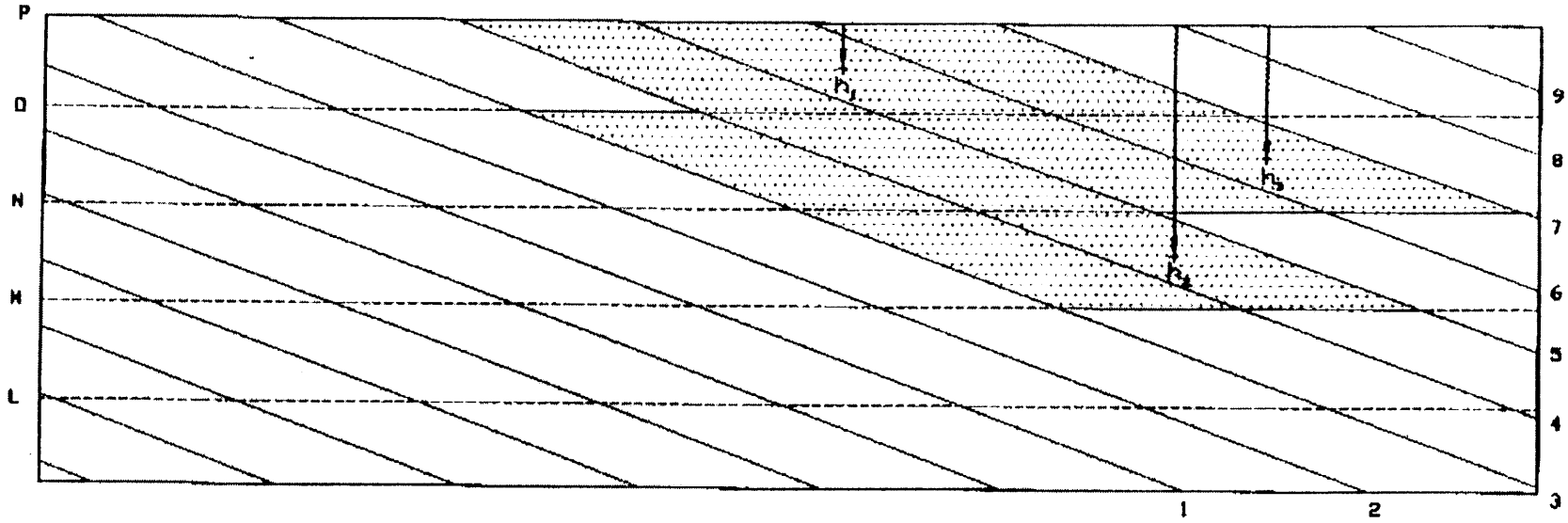

Figure 3.33 Typical h(centroid)'s for Various Blocks of the Primary Wedge

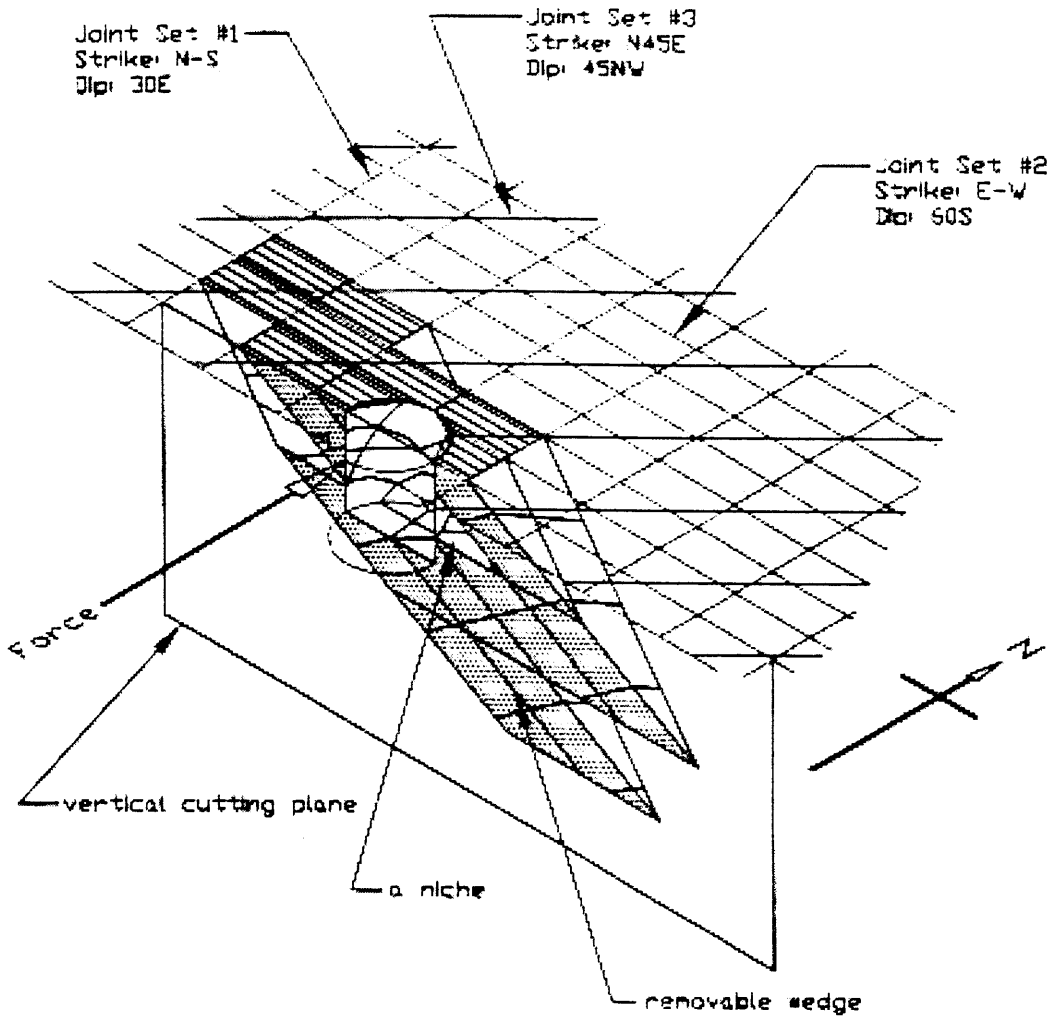

Figure 3.34 Blocks Bounded by the 1st and 2nd Joint Sets in the Primary Wedge

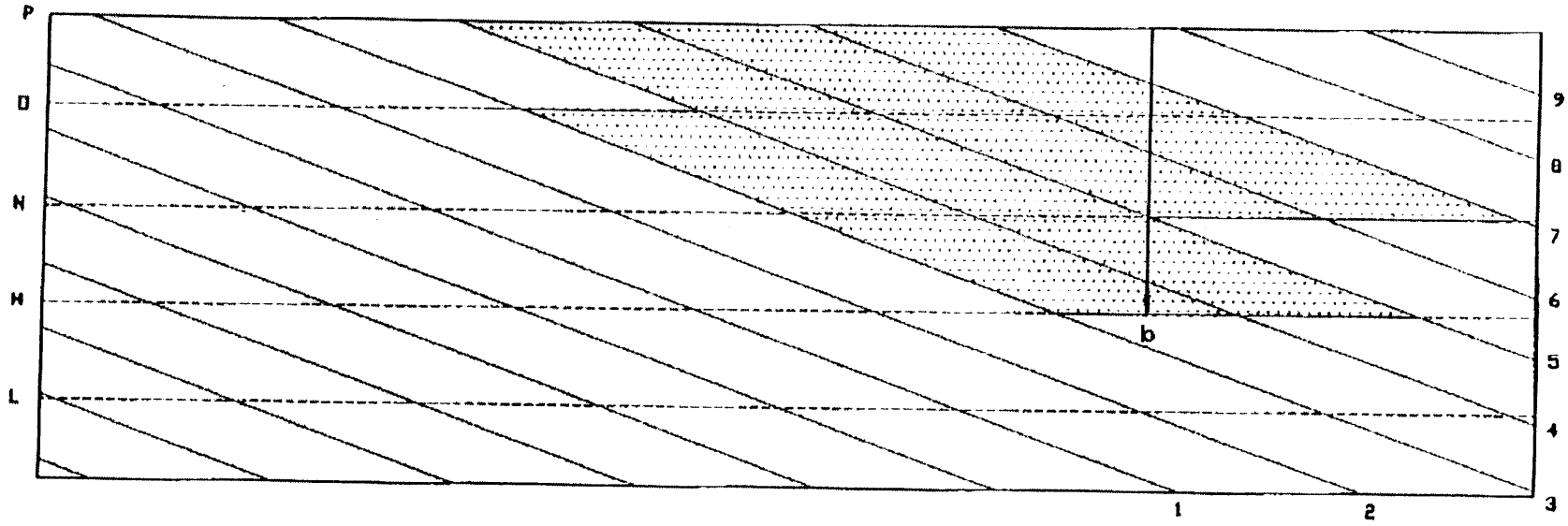

Figure 3.35 b, Height of the Wedge

Figure 3.36 shows the secondary wedge as a single removable block that intersects the pile and the vertical cutting plane. Equation (3.29) cannot be used to estimate its volume because the block intersects both the pile and the vertical cutting plane. Equations (3.30) and (3.31) also cannot be used since the wedge does not encompass most or all of the half pile. Since the geometry of the block is complicated to analyze, it is simplified to become an irregular pyramid as shown in Figure 3.37. And its volume is given by

$$V_{block} \approx V_{pyramid} = a \bullet d/3 \tag{3.32}$$

where a is the area of the block on the surface and can be obtained from the surface joint mesh. d is the height of the wedge and can be obtained from the joint map on the vertical cutting plane. In Figure 3.38, d for the secondary wedge (block fgOP) is shown. Equation (3.32) approximates the volume of the block best when the pile intersects the block on the ground surface such as the block shown in Figure 3.36. Another block that intersects the pile and the vertical plane is shown in Figure 3.39a, but it does not intersect the pile on the surface. As can be seen from the approximation in Figure 3.39b, a certain part of the volume is neglected. However, if the block were to extend and intersect the vertical plane only as shown in Figure 3.40, the volume of such a block can then be calculated by equation (3.29), $V_{block} = a \bullet h_{centroid}$, and $h_{centroid}$ in this case is d/2. Therefore, comparing the volumes given by equation (3.29) and equation (3.32), the percentage difference is

$$\frac{ad/2 - ad/3}{ad/2} x100\% = 33.3\% \tag{3.33}$$

33.3% represents the maximum percentage of underestimation with using equation (3.29). However, equation (3.29) is a conservative assumption and is easy to apply with the 2D figures.

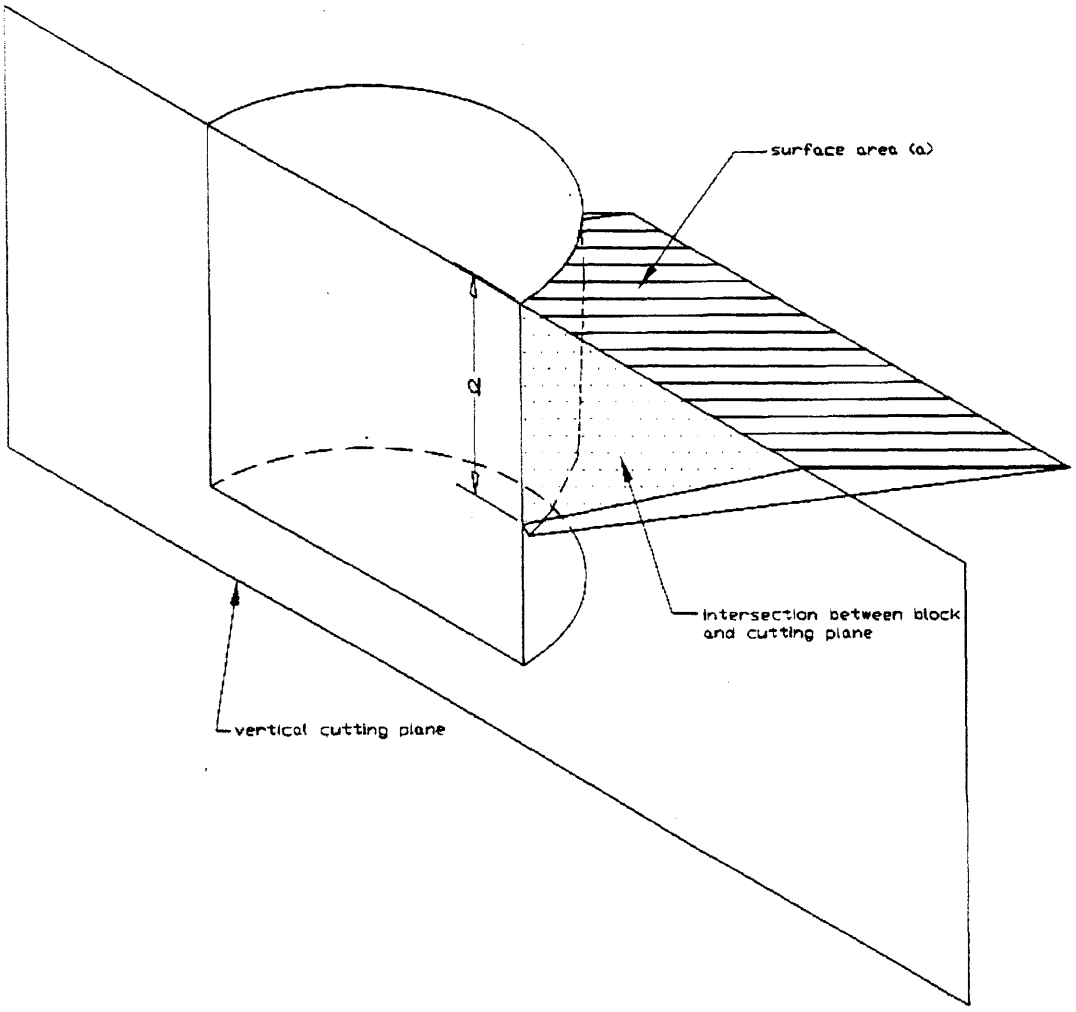

Figure 3.36 Secondary Wedge in 3D View

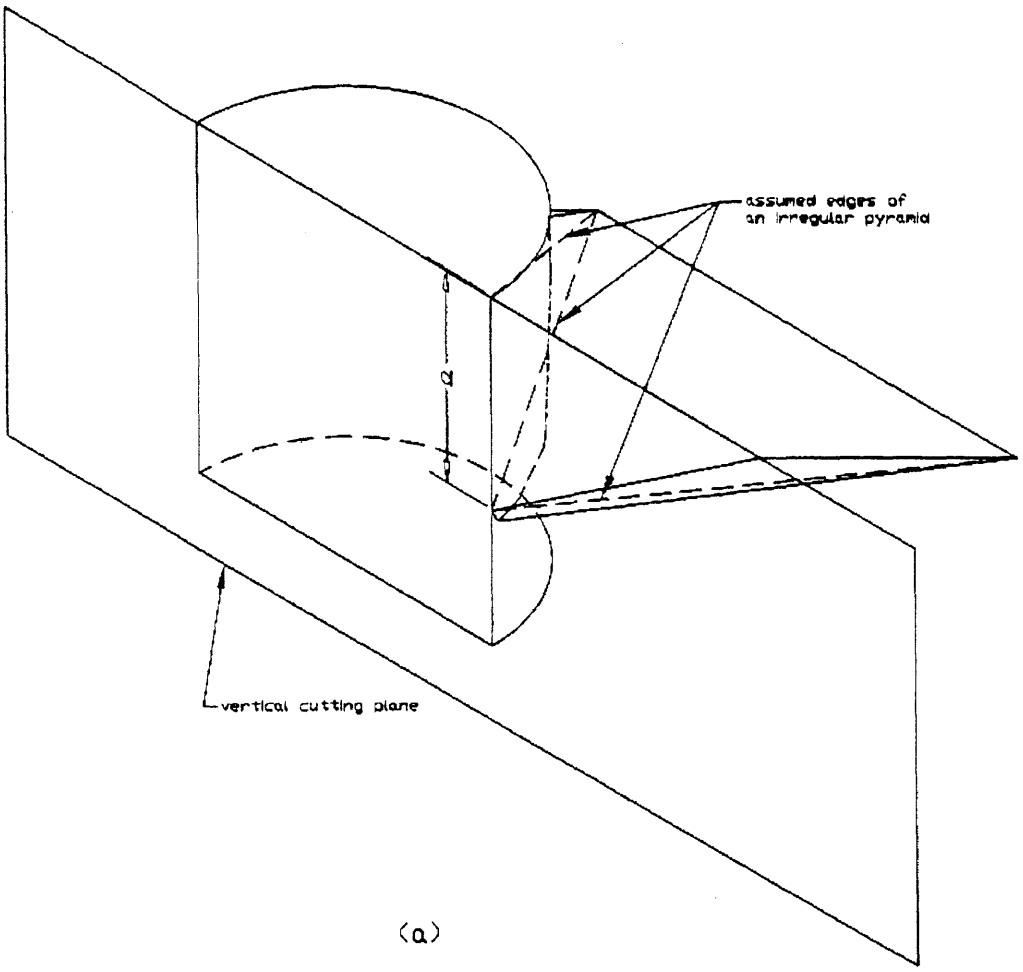

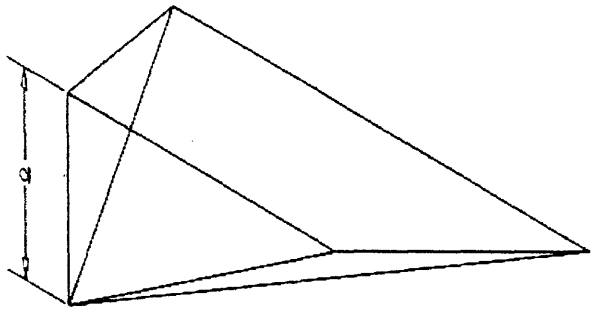

Figure 3.37 An Assumed Irregular Pyramid

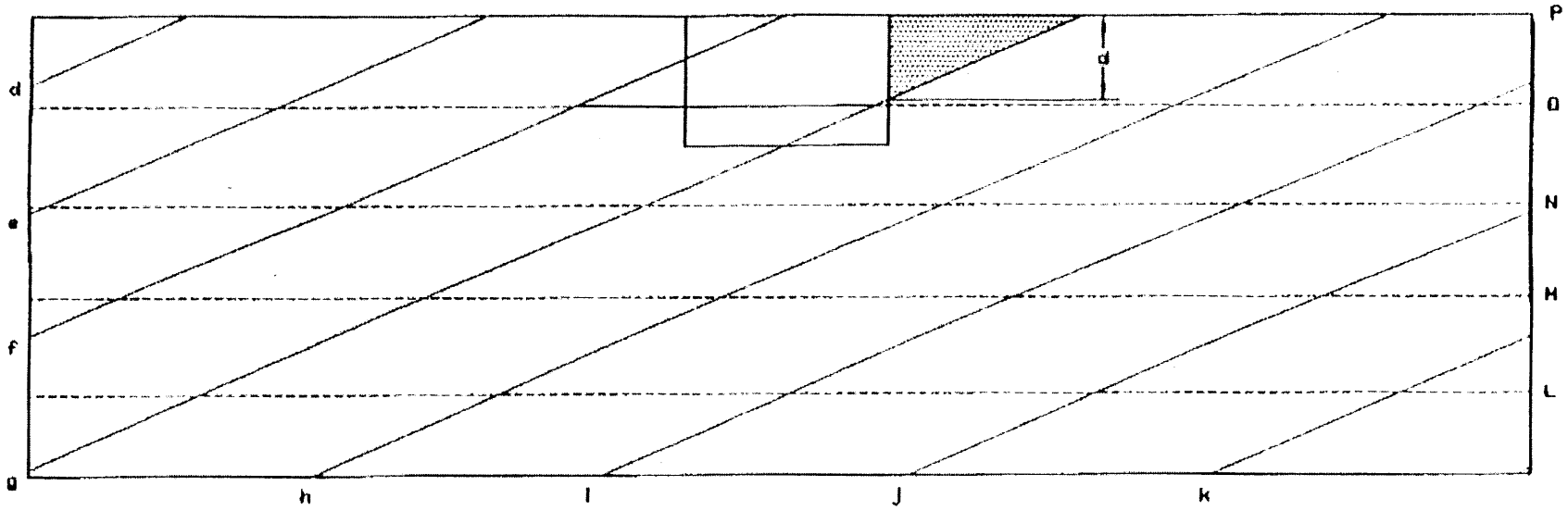

Figure 3.38 d of grid fgOP(R) on a Joint Map on a Cutting Plane

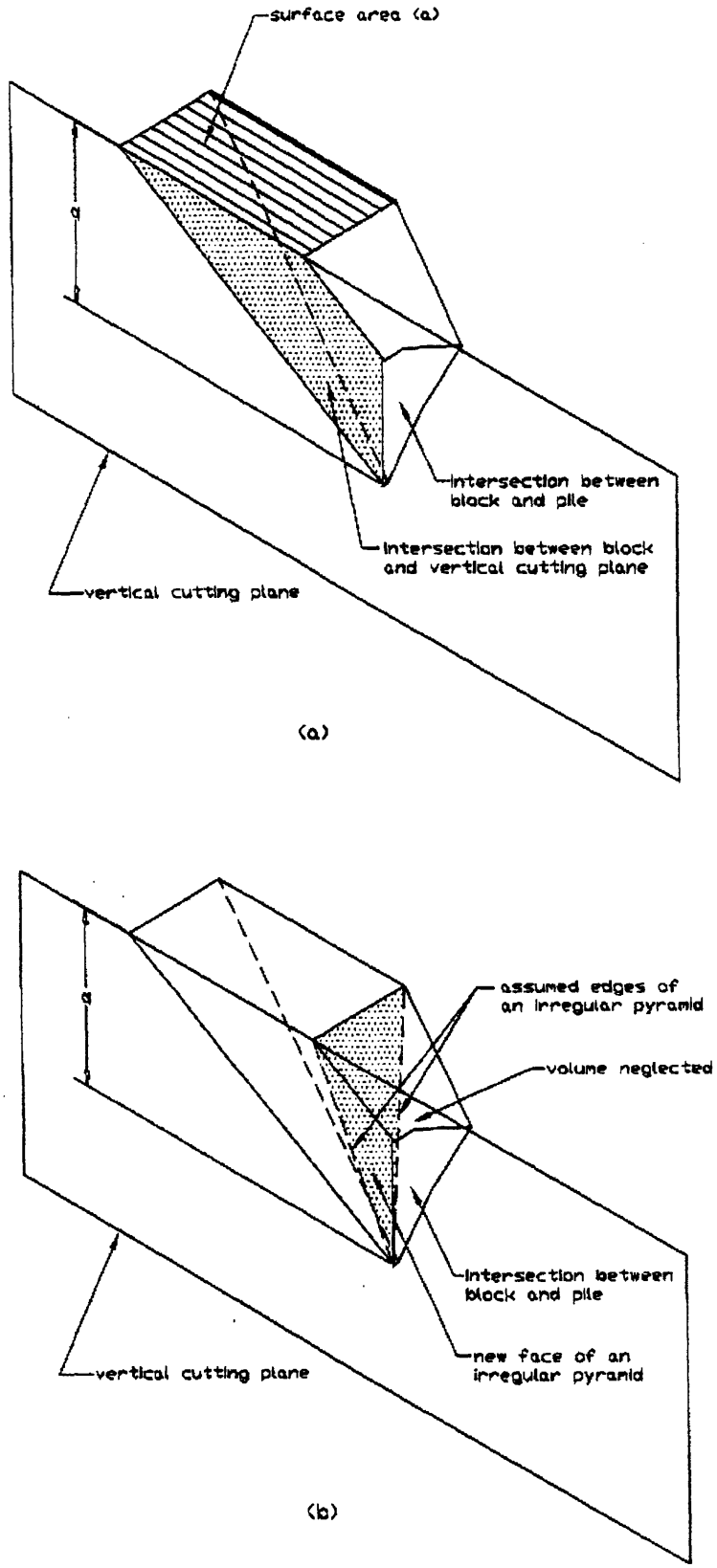

Figure 3.39 A Block that Intersects the Vertical Plane and the Pile, but not on the Surface

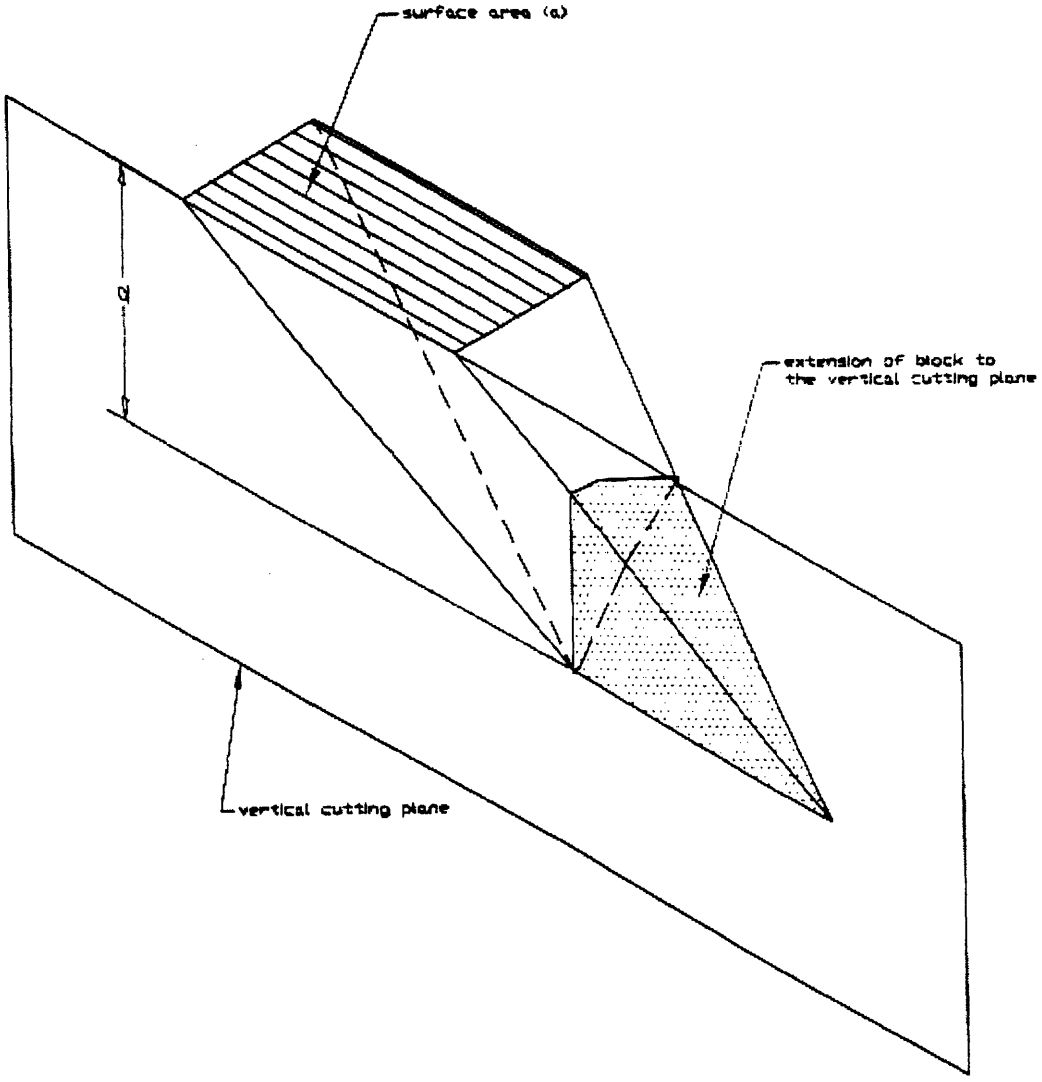

Figure 3.40 Block Extension of the Block in Figure 3.39

3.3.3 NORMAL AND TANGENTIAL FORCES

Equations for expressing the normal forces (N) and tangential forces (R) are identical for a 2-joint-set system and a 3-joint-set system. Thus, only the results will be presented below. One can refer to Chapter 3.2 for details on the derivation of the equations.

The normal force vector for a joint set is expressed as

$$\vec{N} = N\sin\gamma\sin\beta\,\hat{i} - N\sin\gamma\cos\beta\,\hat{j} + N\cos\gamma\,\hat{k} \tag{3.34}$$

where N is the scalar value of the normal force.

The tangential force vector for a joint set is written as follows

$$\vec{R} = R(-\sin\gamma_1\cos\beta_1\cos\gamma_2 + \cos\gamma_1\sin\gamma_2\cos\beta_2)\hat{i} +$$
$$R(-\sin\gamma_1\sin\beta_1\cos\gamma_2 + \cos\gamma_1\sin\gamma_2\sin\beta_2)\hat{j} + R(-\sin\gamma_1\sin\gamma_2\sin(\beta_1 - \beta_2))\hat{k} \tag{3.35}$$

where R is the scalar value of the tangential force. As mentioned before, the subscripts 1 and 2 represent the two joint sets in a wedge, primary or secondary.

The relationship between R and N for a joint set is

$$R = cA + N\tan\phi \tag{3.36}$$

where c is the cohesion of a joint set and A is the total area of the faces from the same joint set on the removable wedge.

There are three types of faces that can exist in a wedge. The first type intersects the pile only as shown in Figure 3.41. The intersection between a face and a pile is not a straight line, and so it is recommended that the face be assumed to be a parallelogram. The second type intersects the vertical cutting plane only as shown in Figure 3.42. Although the ends of the face are not parallel, but the face can still be approximated as a parallelogram. Thus, for these two types of faces, its area is expressed as L•w, where L is the height of the parallelogram on the joint plane and s is the horizontal spacing. L is computed by H/sinγ, where H is the height from the surface to the center of the edge that intersects the pile or the cutting plane. $w=\| s/\sin(\beta_1-\beta_2) \|$ is the length of the edge on the surface as shown in Figure 3.29. Thus, the area of the first two types of faces is H•w/sinγ. H for a face that intersects the pile only can be obtained from the joint map on the pile. H for a face that intersects the vertical cutting plane only can be obtained from the joint map on the cutting plane.

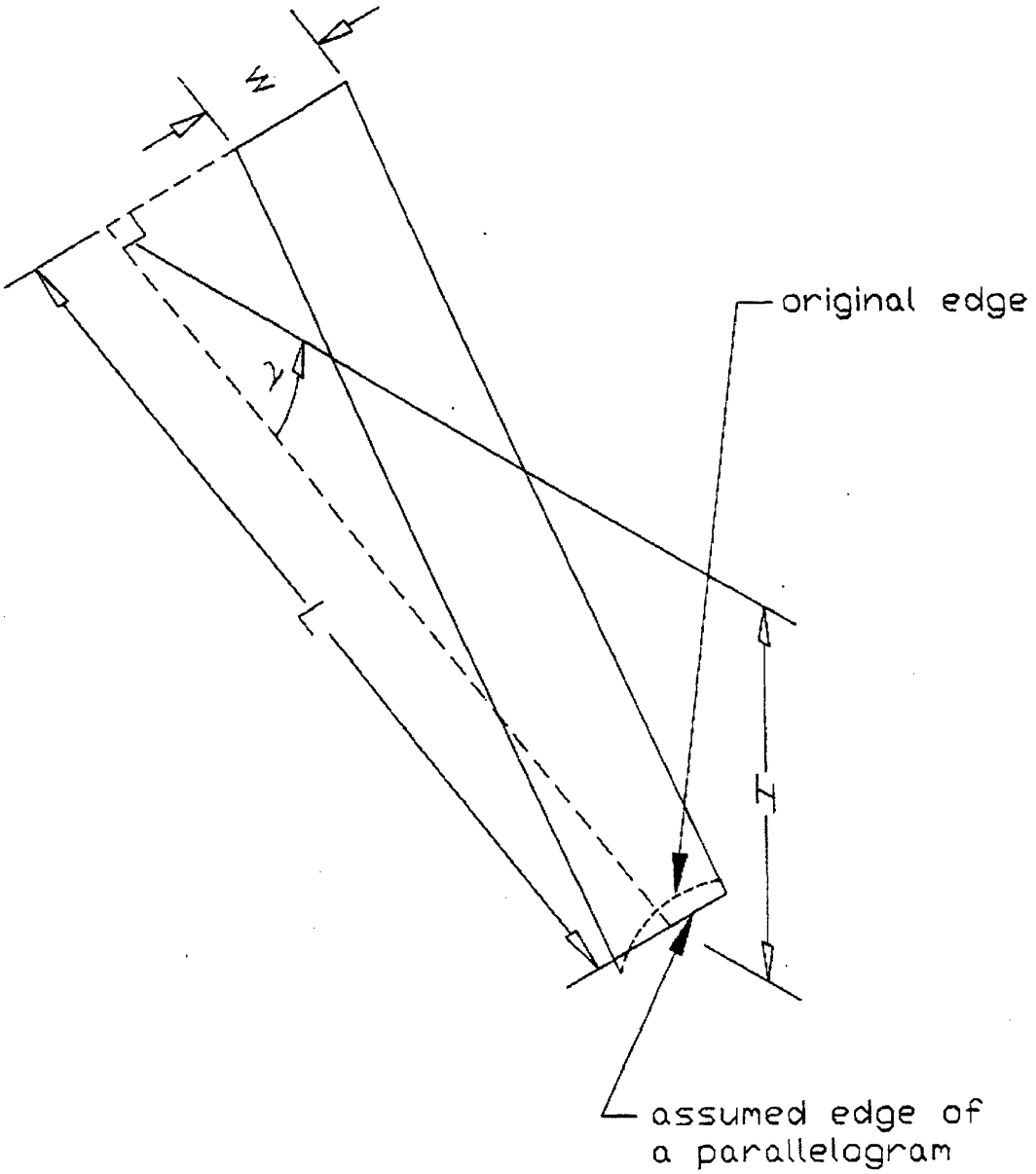

Figure 3.41 A Typical Face That Intersects the Pile Only

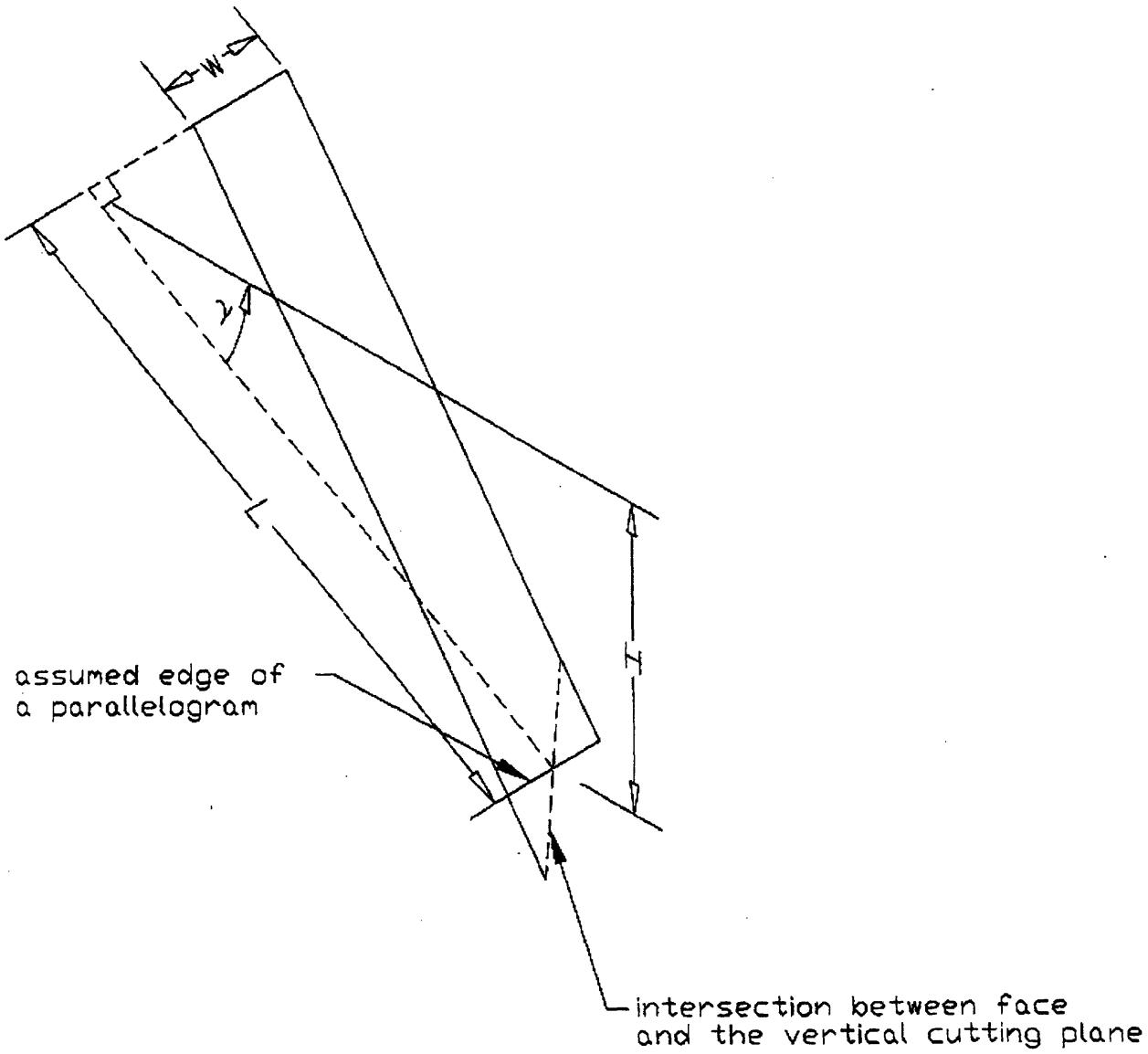

Figure 3.42 A Typical Face That Intersects the Vertical Cutting Plane Only

The third type of face intersects both the pile and the cutting plane. The assumed irregular pyramid for the secondary wedge in Figure 3.37 is used to estimate the area of a face as shown dotted in Figure 3.43. The assumed face is a triangle and is shown in Figure 3.44 from a different perspective. Its area is L•w/2. L is computed by d/sinγ, where d is the height from the surface to bottom of the face. Thus, the area of a face that intersects both the pile and the cutting plane is d•w/2sinγ. d can be obtained from the joint map on the cutting plane. For a face that intersects the vertical cutting plane and the pile from the surface to the bottom. this approximation of area is quite close. However, for a face that intersects the vertical cutting plane and the pile but not from the surface, this area is underestimated if using d•w/2sinγ. An example of such face is shown in Figure 3.45. As can be seen from the approximation in the figure, a certain amount of area is neglected. If the face were to extend and intersect the vertical cutting plane as shown in Figure 3.46, the area can be calculated by H•w/sinγ, where H=d in this case. The percentage difference between the two area calculations is

$$\frac{dw/\sin\gamma - dw/2\sin\gamma}{dw/\sin\gamma} x100\% = 50\% \tag{3.37}$$

50% represents the maximum percentage of underestimation with using d•w/2sinγ to calculate the area of a face. However, this equation is a conservative assumption and is easy to apply with the 2D figures.

The total A for each joint set on the wedge is then

$$A = \sum_{i=1}^{p} \frac{H_i w_i}{\sin\gamma} + \sum_{j=1}^{q} \frac{d_j w_j}{2\sin\gamma} = \sum_{i=1}^{p} \left[\frac{H_i}{\sin\gamma} \bullet \left\| \frac{s_i}{\sin(\beta_1 - \beta_2)} \right\| \right] + \sum_{j=1}^{q} \left[\frac{d_j}{2\sin\gamma} \bullet \left\| \frac{s_j}{\sin(\beta_1 - \beta_2)} \right\| \right] \tag{3.38}$$

where p is the number of faces that intersect the pile only or intersect the vertical cutting plane only and q is the number of faces that intersect both the pile and the vertical cutting plane.

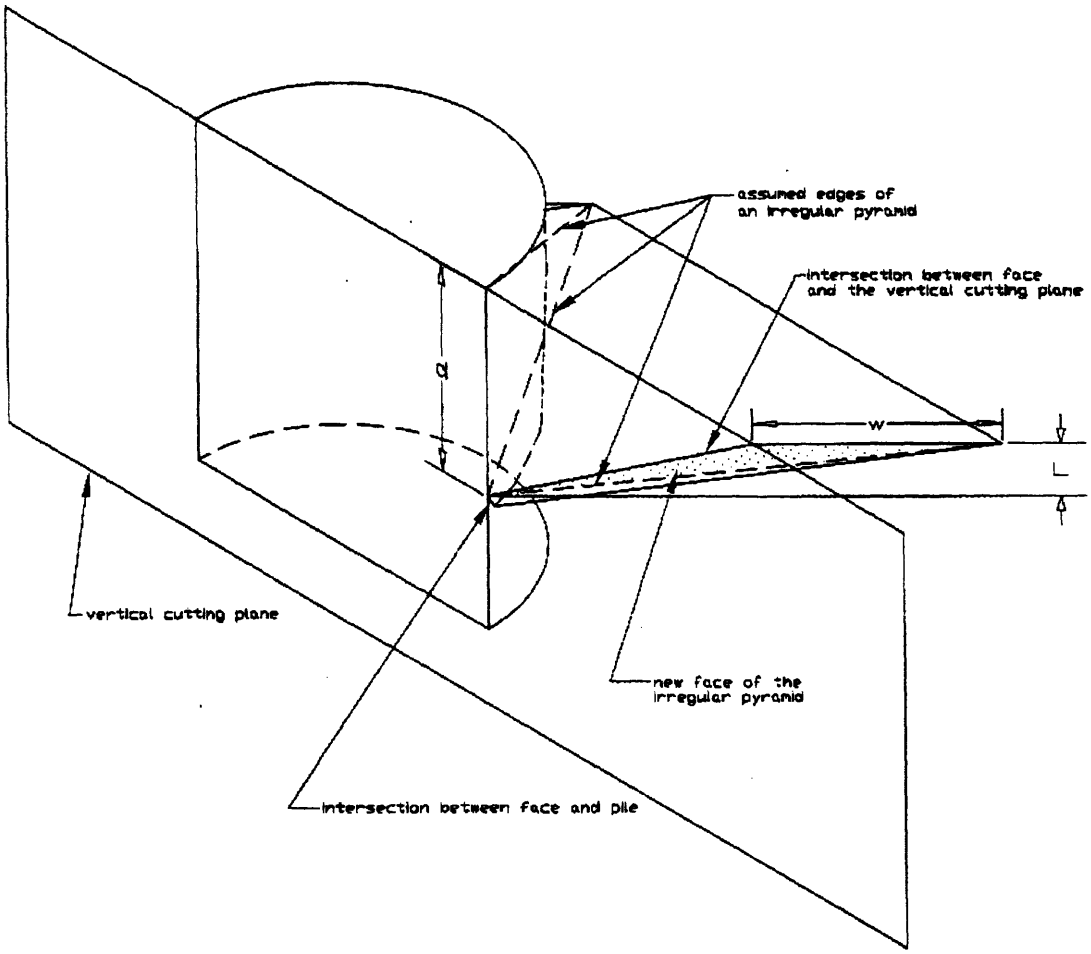

Figure 3.43 A Face That Intersects Both the Pile and the Vertical Cutting Plane

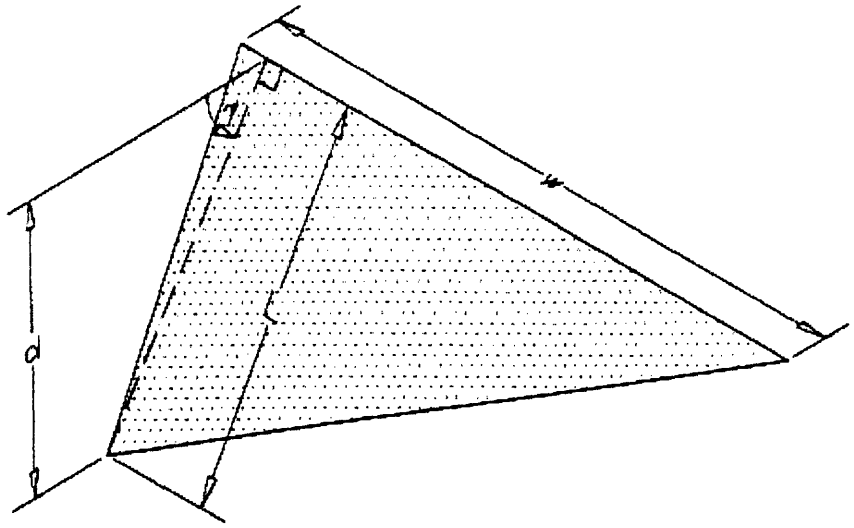

Figure 3.44 An Assumed Triangular Face

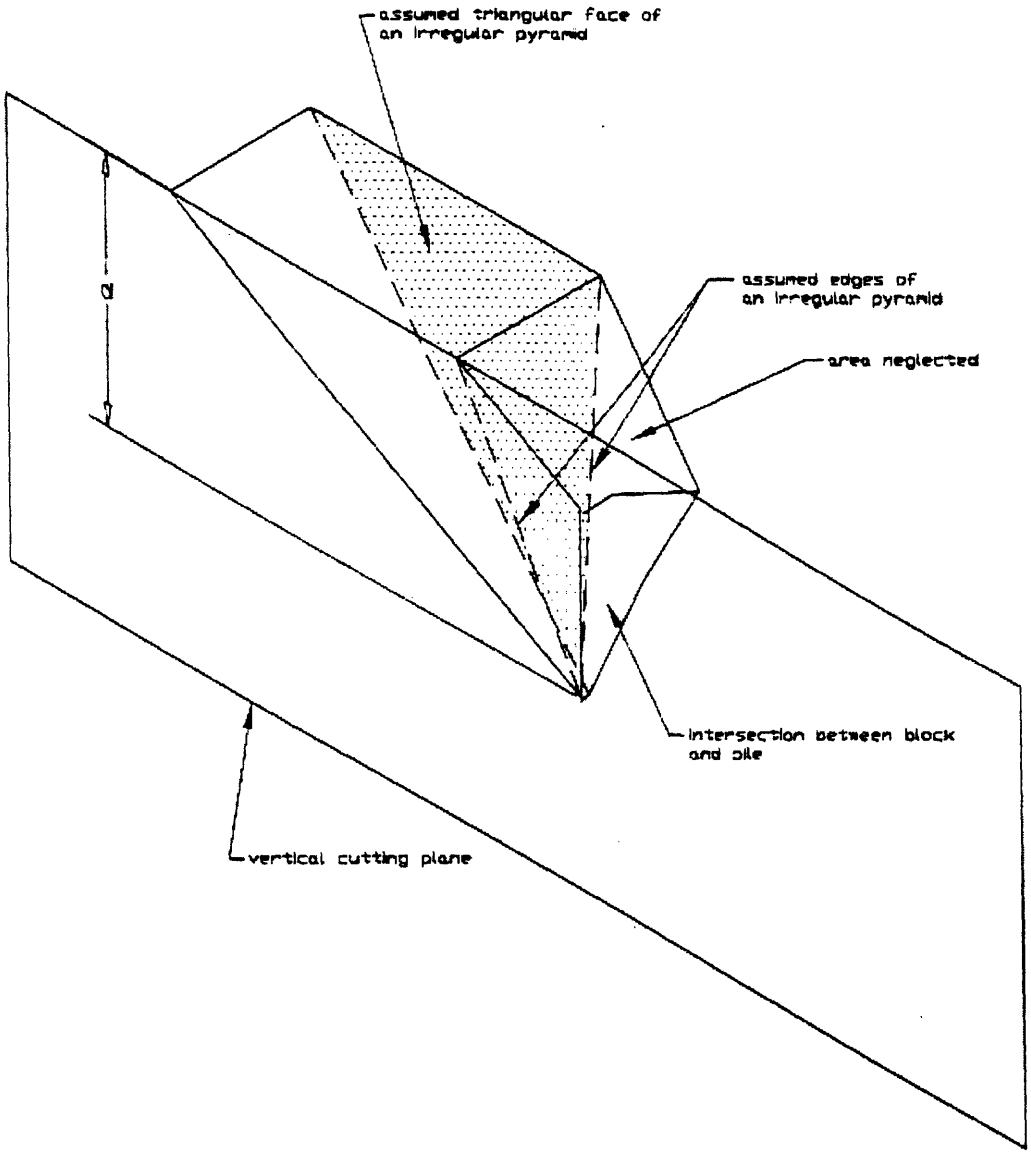

Figure 3.45 An Assumed Triangular Face in a Block That Intersects the Vertical Plane and the Pile, but not on the Surface

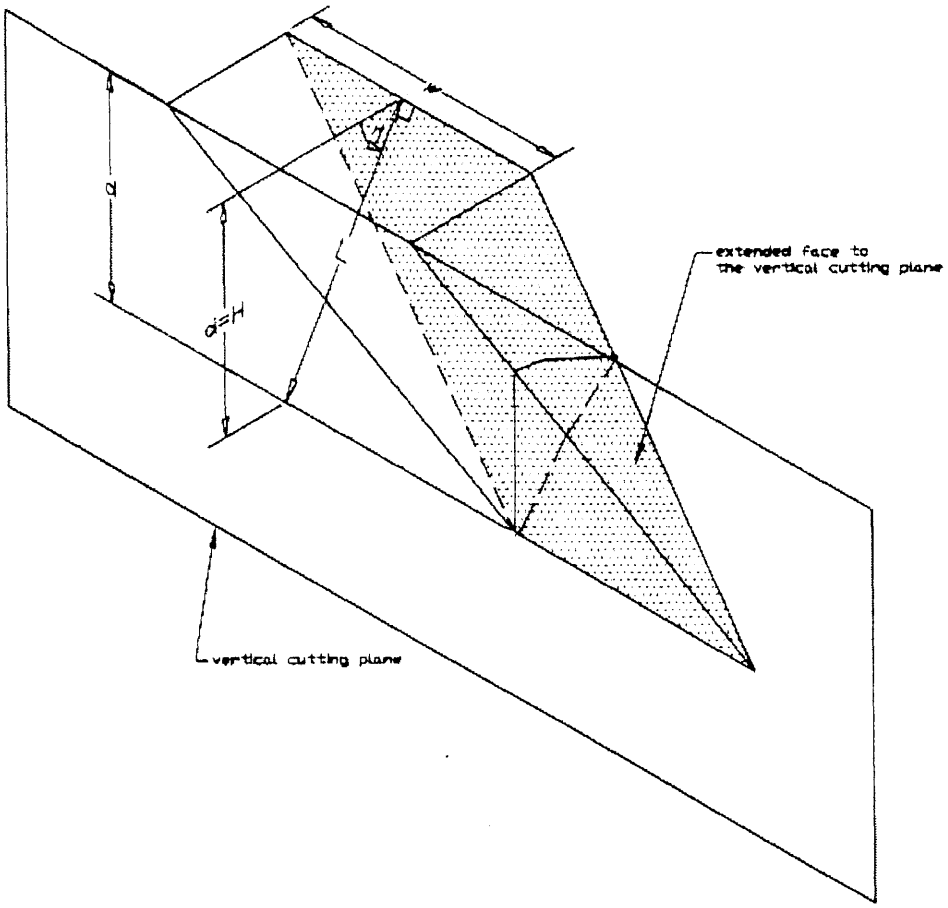

Figure 3.46 Extended Face to the Vertical Cutting Plane

Usually, for a primary wedge, the faces intersect only the vertical cutting plane, and thus only the joint map on the cutting plane is necessary to figure out the total area on a joint set. In this example, no faces of the primary wedge intersect the pile with the previous assumption that the niche is filled as shown in Figure 3.47. As explained previously, the niche is usually small, and thus the assumption is valid. The joint map on the cutting plane must be used to find H. Each H for each face of joint set N-S, 30°E is shown in Figure 3.48, and each H for each face of joint set E-W, 60°W is shown in Figure 3.49.

The total A for each joint set on this primary wedge is calculated by simplifying equation (3.38) to

$$A = \sum_{j=1}^{q} \frac{d_j w_j}{2\sin\gamma} = \sum_{j=1}^{q} \left[\frac{d_j}{2\sin\gamma} \bullet \left\| \frac{s_j}{\sin(\beta_1 - \beta_2)} \right\| \right] \tag{3.39}$$

The total A for joint set N-S, 30°E is A_1+...+A_6 and the total A for joint set E-W, 60°W is A_7+...+A_{11} as shown in Figure 3.47.

On the secondary wedge (block fgOP), the joint O face and joint f face intersect the pile only, but the joint g face intersects both the pile and the vertical plane as shown in Figure 3.50. The joint map on the pile and the joint map on a cutting plane are used to distinguish the three types of faces mentioned before in the kinetic analysis. For example, joint g face on the secondary wedge intersects the pile as shown in Figure 3.51 and also intersects the vertical cutting plane as shown in Figure 3.52. Joint O face and joint f face on the secondary wedge intersect the pile as shown in Figure 3.51, but they do not intersect the vertical cutting plane as shown in Figure 3.52.

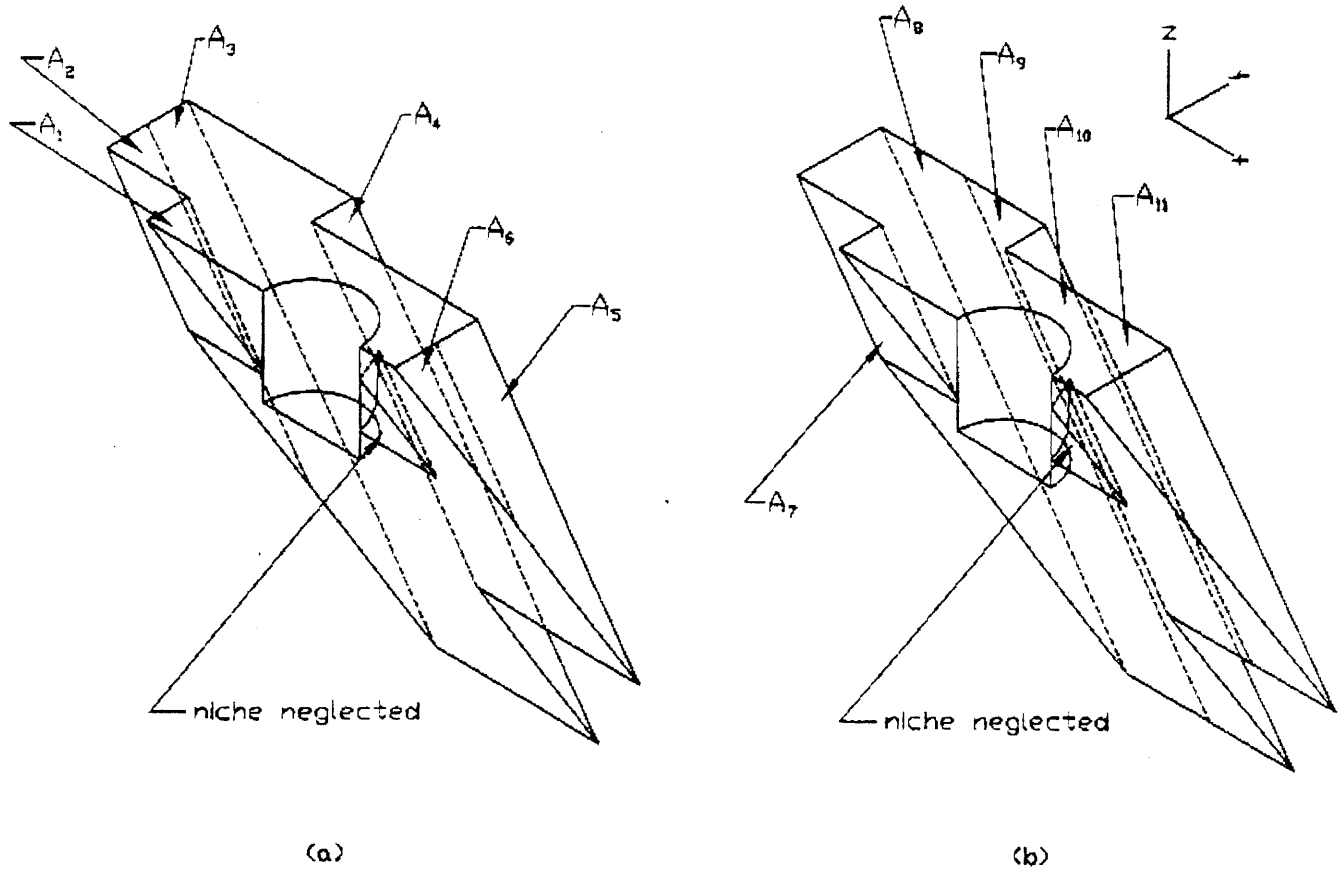

Figure 3.47 Faces of the Primary Wedge for (a) Joint Set N-S, 30°E and (b) Joint Set E-W, 60°S

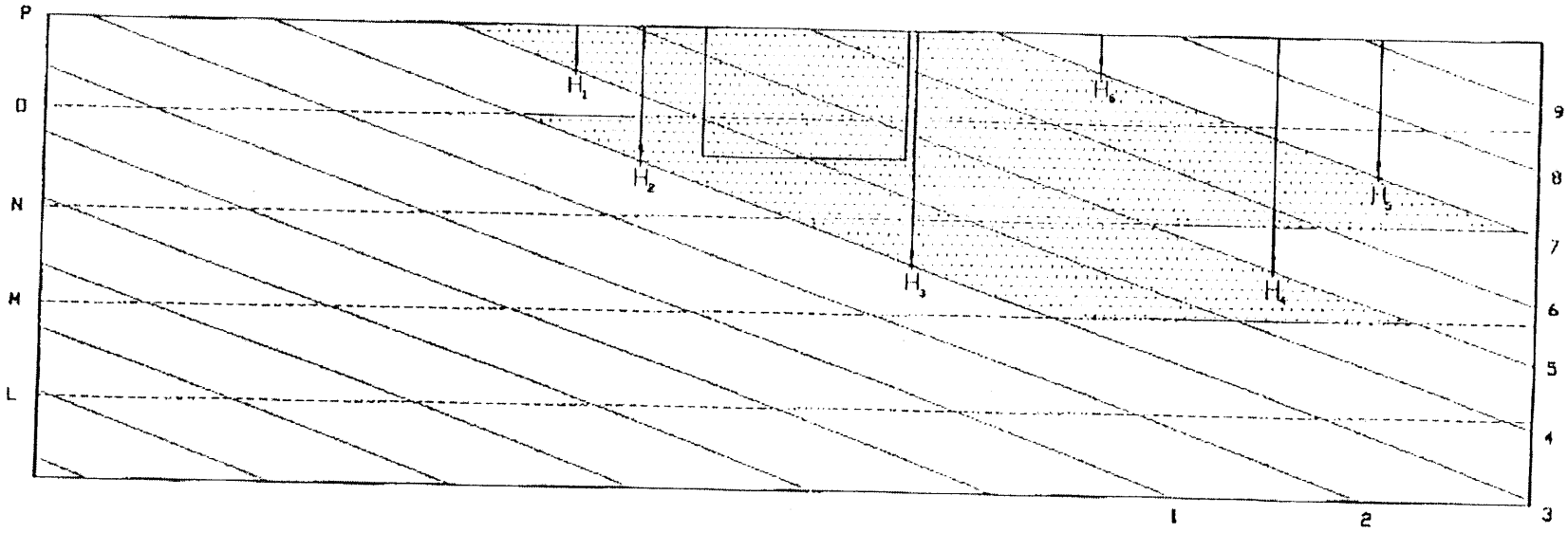

Figure 3.48 H's for faces of Joint Set N-S, 30°E on the Primary Wedge

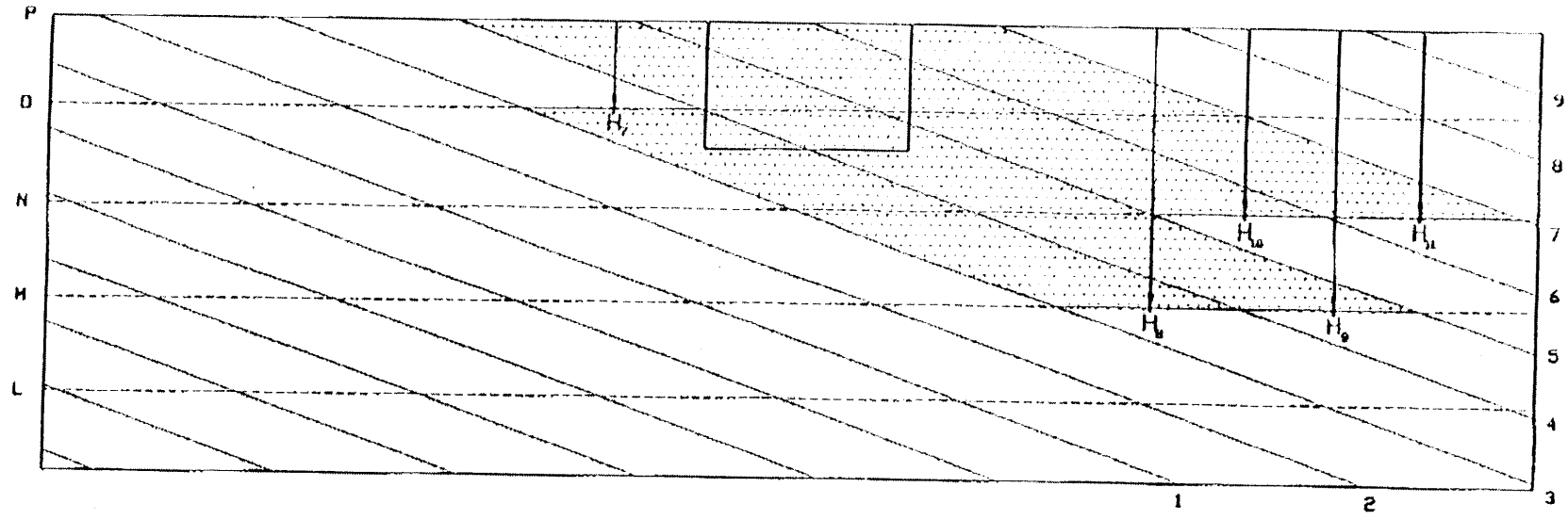

Figure 3.49 H's for Faces of Joint Set E-W, 60°S on the Primary Wedge

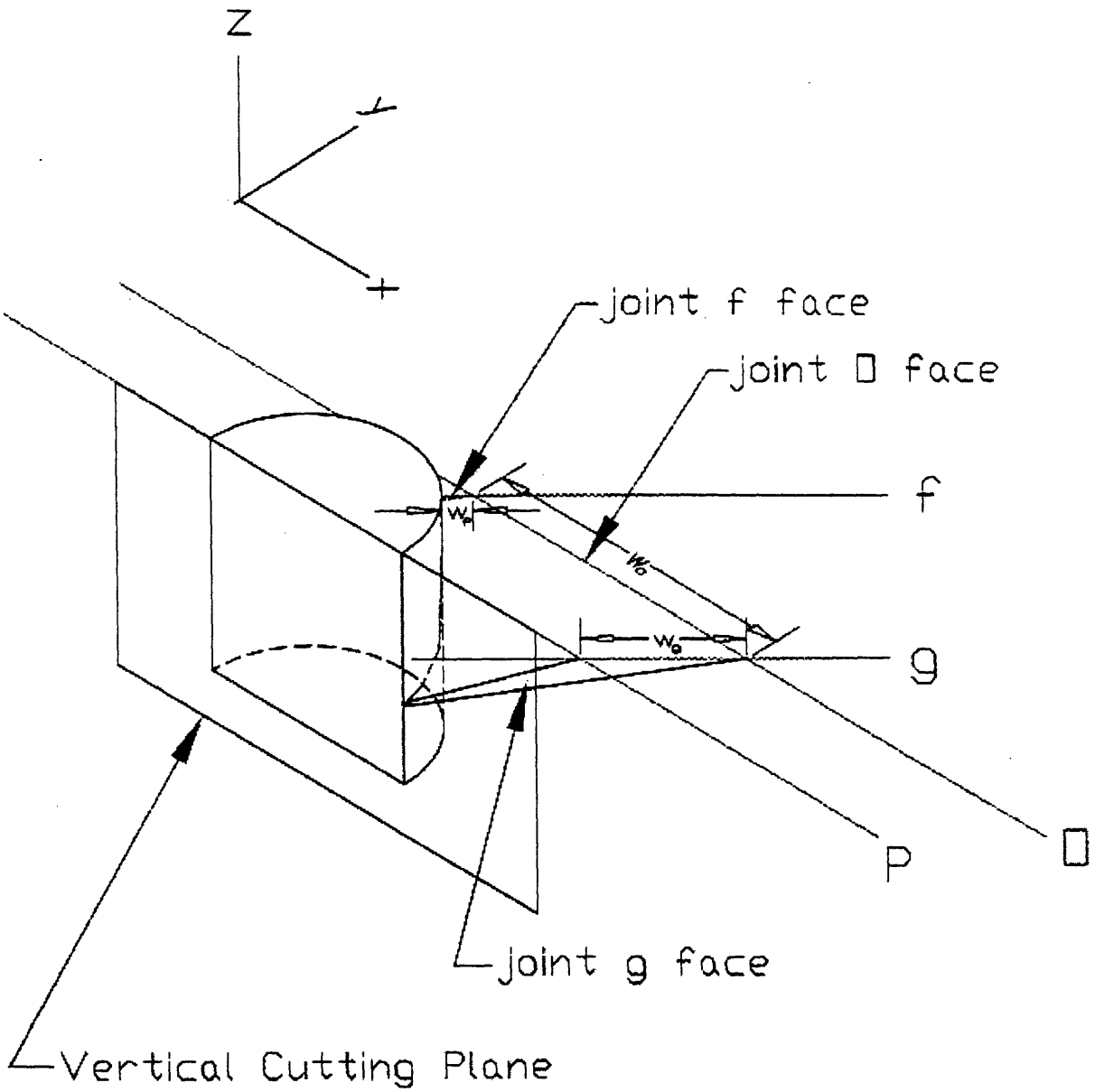

Figure 3.50 Faces of the Secondary Wedge for Joint Set E-W, 60°S and Joint Set N45°E, 45°NW

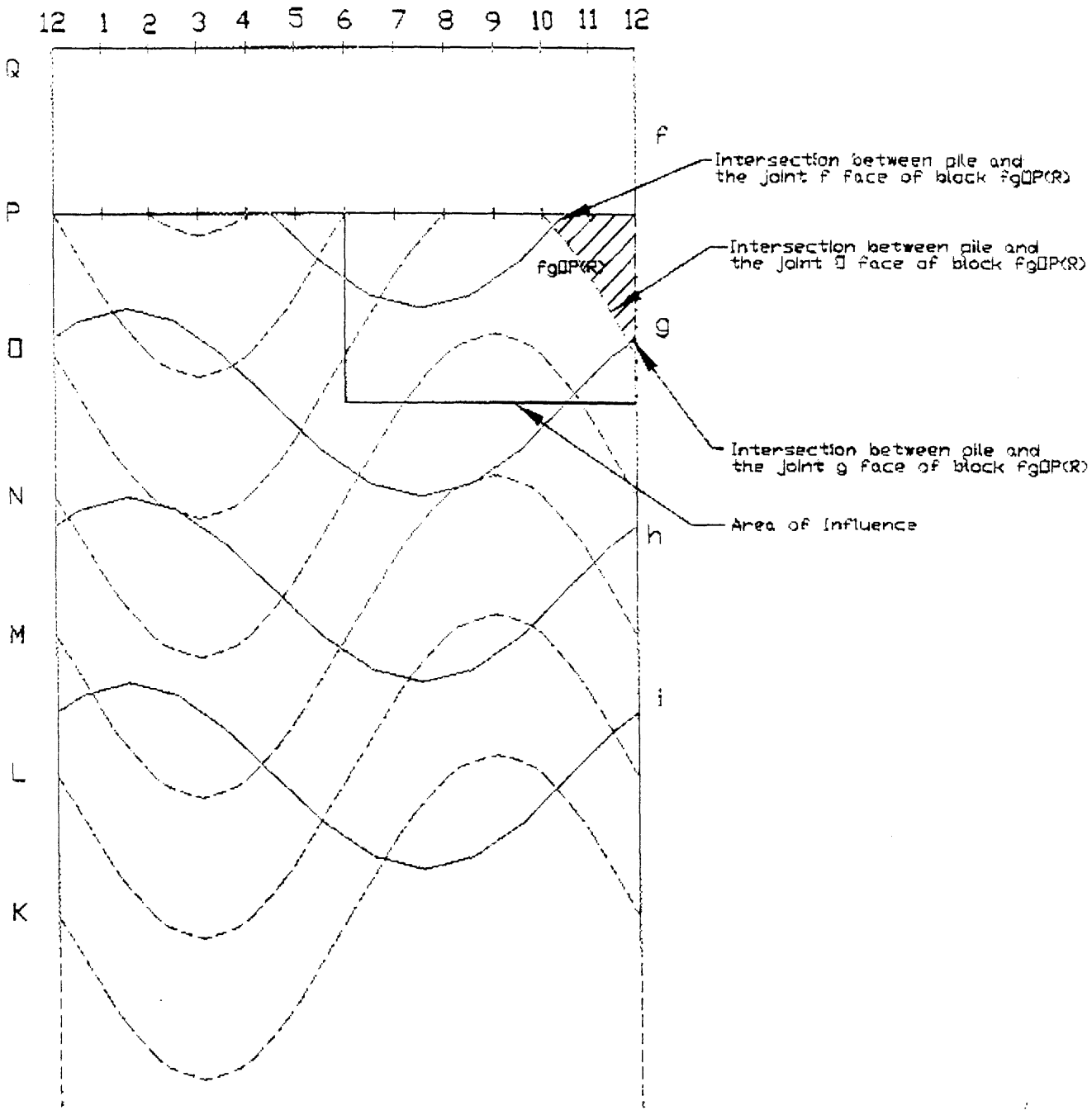

Figure 3.51 Grid fgOP(R) on a Joint Map on a Pile

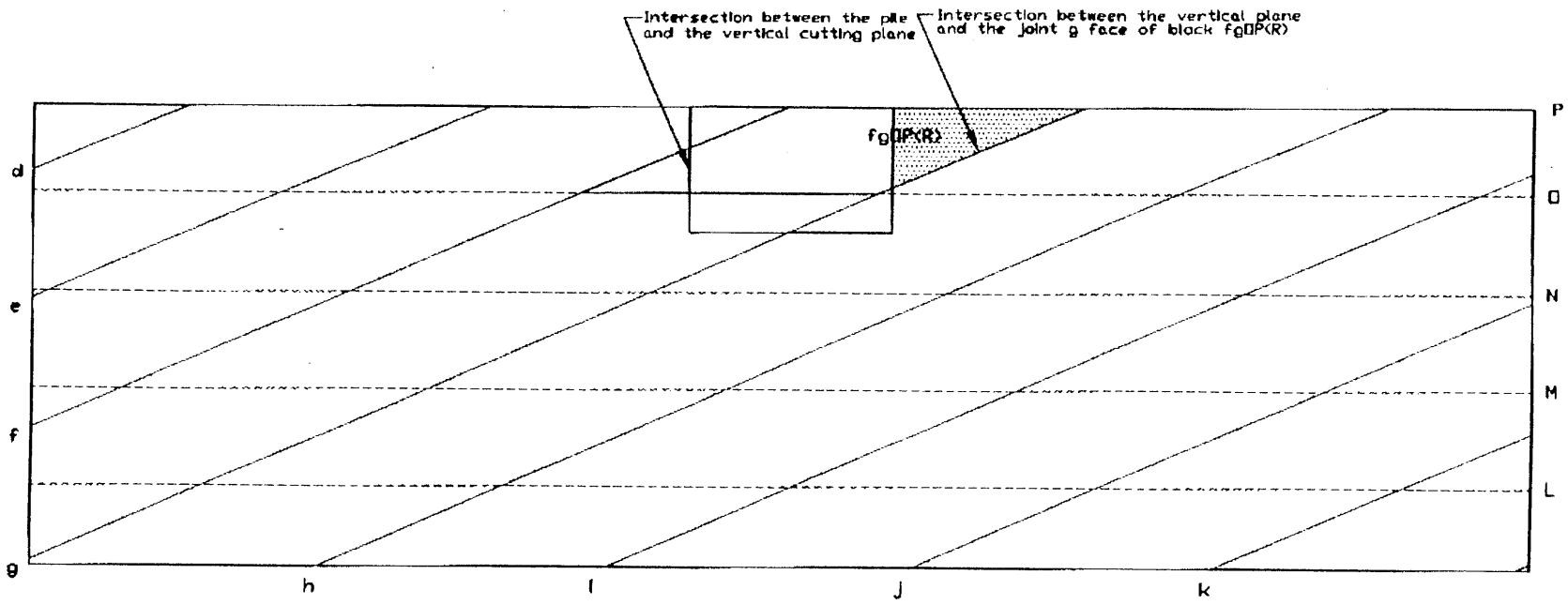

Figure 3.52 Joint Map of the 2nd and 3rd Joint Sets on a Cutting Plane

Since joint g face of the secondary wedge intersects both the pile and the vertical cutting plane, the joint map on the cutting plane is used to find d as shown in Figure 3.53 in order to find the area of the face. The d used to find area and to find volume is identical. The area of joint g face on this secondary wedge is obtained by simplifying equation (3.38) to

$$A = \sum_{j=1}^{q} \frac{d_j w_j}{2\sin\gamma} = \sum_{j=1}^{q} \left[\frac{d_j}{2\sin\gamma} \bullet \left\| \frac{s_j}{\sin(\beta_1 - \beta_2)} \right\| \right] \tag{3.40}$$

Joint O face and joint f face of the secondary wedge intersect the pile only, and thus the joint map on the pile is used to find H as shown in Figure 3.54 in order to find the area of the face. The area of joint O face and the area of joint f face on this secondary wedge are figured by simplifying equation (3.38) to

$$A = \sum_{i=1}^{p} \frac{H_i w_i}{\sin\gamma} = \sum_{i=1}^{p} \left[\frac{H_i}{\sin\gamma} \bullet \left\| \frac{s_i}{\sin(\beta_1 - \beta_2)} \right\| \right] \tag{3.41}$$

For this secondary wedge, the total A for joint set E-W, 60°W is the area of joint O face and the total A for joint set N45°E, N45°W is the sum of the area of joint f face and the area of joint g face as shown in Figure 3.48.

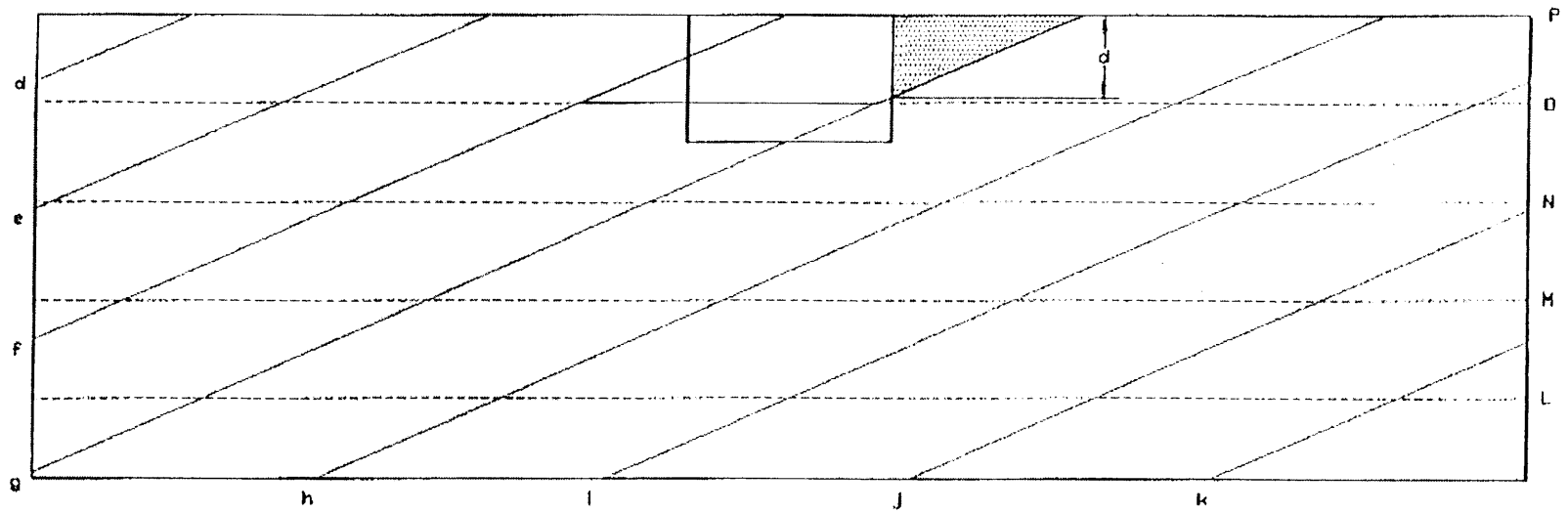

Figure 3.53 d of Grid fgOP(R) on a Joint Map on a Cutting Plane

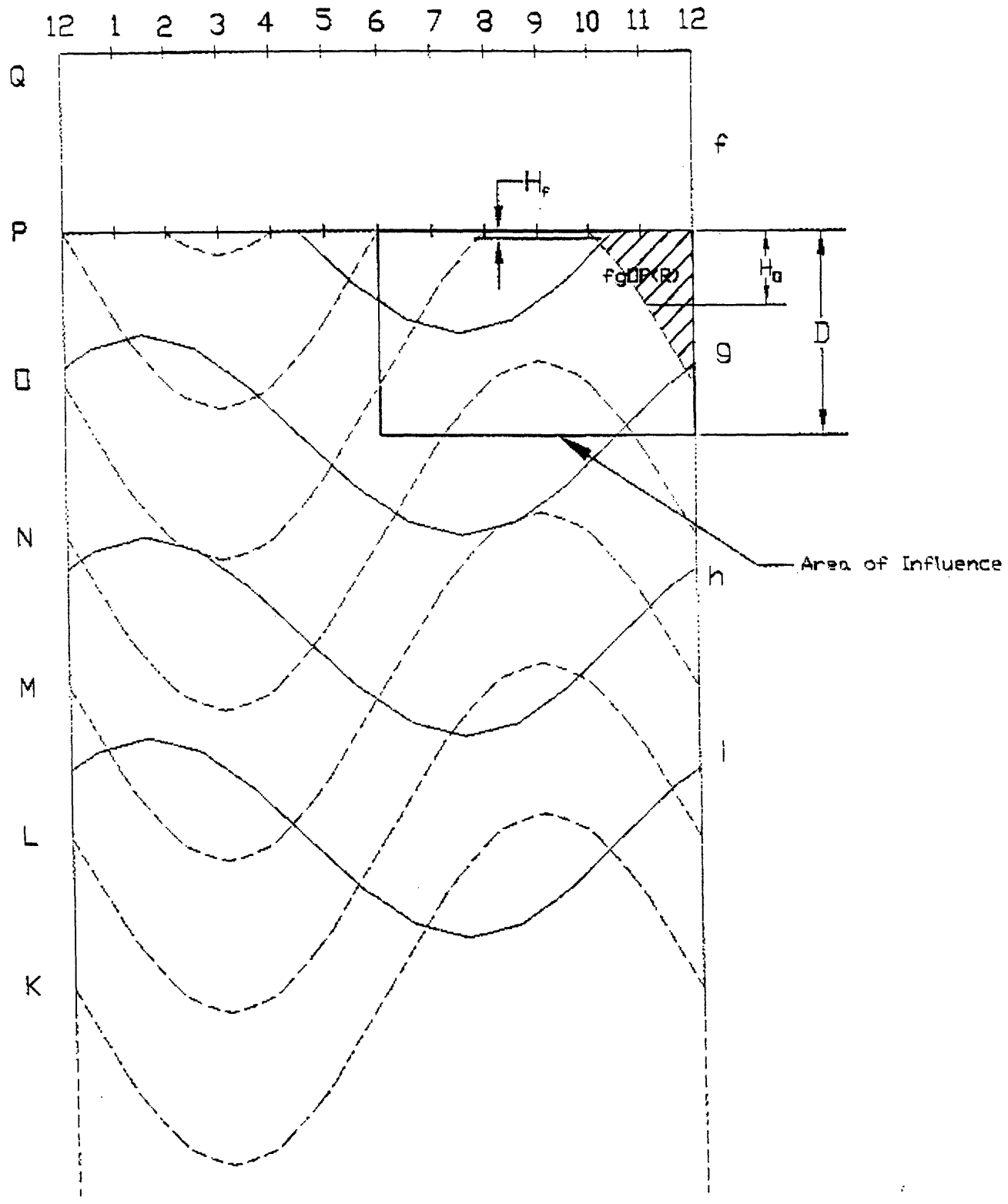

Figure 3.54 H's of Grid fgOP(R) on a Joint Map on a Pile

3.3.4 DEAD LOAD OF THE PILE

Finally, the expression for the Dead Load (P) of the pile on the primary wedge is:

$$\vec{P} = -P\hat{k} \tag{3.42}$$

This is different from the 2-joint-set system in which the dead load of the pile applies on any wedge. In a 3-joint-set system, the primary wedge encompasses most or all of the area that the pile sits on as shown in Figure 3.47. The secondary wedge encompasses little or none of the area that the pile sits on as shown in Figure 3.50. Therefore, only the primary wedge is considered for the dead load (P) of the pile.

3.3.5 SUMMARY OF FORCES

The forces in each direction (x, y, and z) are summarized in the table below:

Table 3.2 Summary of Forces in Each Direction

	X	Y	Z
Lateral Force	$F\cos\theta$	$F\sin\theta$	
Weight of Wedge			$-W$
Tangential Force of Joint Set #1	$R_1(-\sin\gamma_1\cos\beta_1\cos\gamma_2 + \cos\gamma_1\sin\gamma_2\cos\beta_2)$	$R_1(-\sin\gamma_1\sin\beta_1\cos\gamma_2 + \cos\gamma_1\sin\gamma_2\sin\beta_2)$	$R_1(-\sin\gamma_1\sin\gamma_2 \sin(\beta_1-\beta_2))$
Normal Force of Joint Set #1	$N_1\sin\gamma_1\sin\beta_1$	$-N_1\sin\gamma_1\cos\beta_1$	$N_1\cos\gamma_1$
Tangential Force of Joint Set #2	$R_2(-\sin\gamma_1\cos\beta_1\cos\gamma_2 + \cos\gamma_1\sin\gamma_2\cos\beta_2)$	$-R_2(-\sin\gamma_1\sin\beta_1\cos\gamma_2 + \cos\gamma_1\sin\gamma_2\sin\beta_2)$	$R_2(-\sin\gamma_1\sin\gamma_2 \sin(\beta_1-\beta_2))$
Normal Force of Joint Set #2	$N_2\sin\gamma_2\sin\beta_2$	$-N_2\sin\gamma_2\cos\beta_2$	$N_2\cos\gamma_2$
Dead Load of the Pile			*-P for primary wedge* *0 for secondary wedge*

3.3.6 CALCULATING THE LATERAL LOAD CAPACITY

Substitute R with $cA + N\tan\phi$. the equation in x-direction becomes

$$F\cos\theta+c_1A_1(-\sin\gamma_1\cos\beta_1\cos\gamma_2+\cos\gamma_1\sin\gamma_2\cos\beta_2)+N_1\tan\phi_1(-\sin\gamma_1\cos\beta_1\cos\gamma_2+\cos\gamma_1\sin\gamma_2\cos\beta_2)+N_1\sin\gamma_1\sin\beta_1+c_2A_2(-\sin\gamma_1\cos\beta_1\cos\gamma_2+\cos\gamma_1\sin\gamma_2\cos\beta_2)+N_2\tan\phi_2(-\sin\gamma_1\cos\beta_1\cos\gamma_2+\cos\gamma_1\sin\gamma_2\cos\beta_2)+N_2\sin\gamma_2\sin\beta_2=0 \quad (3.43)$$

Rearrange terms:

$$(\sin\gamma_1\sin\beta_1-\tan\phi_1\sin\gamma_1\cos\beta_1\cos\gamma_2+\tan\phi_1\cos\gamma_1\sin\gamma_2\cos\beta_2)N_1+(\sin\gamma_2\sin\beta_2-\tan\phi_2\sin\gamma_1\cos\beta_1\cos\gamma_2+\tan\phi_2\cos\gamma_1\sin\gamma_2\cos\beta_2)N_2+(\cos\theta)F=c_1A_1\sin\gamma_1\cos\beta_1\cos\gamma_2-c_1A_1\cos\gamma_1\sin\gamma_2\cos\beta_2+c_2A_2\sin\gamma_1\cos\beta_1\cos\gamma_2-c_2A_2\cos\gamma_1\sin\gamma_2\cos\beta_2 \quad (3.44)$$

For the equation in y-direction:

$$F\sin\theta+c_1A_1(-\sin\gamma_1\sin\beta_1\cos\gamma_2+\cos\gamma_1\sin\gamma_2\sin\beta_2)+N_1\tan\phi_1(-\sin\gamma_1\sin\beta_1\cos\gamma_2+\cos\gamma_1\sin\gamma_2\sin\beta_2)-N_1\sin\gamma_1\cos\beta_1+c_2A_2(-\sin\gamma_1\sin\beta_1\cos\gamma_2+\cos\gamma_1\sin\gamma_2\sin\beta_2)+N_2\tan\phi_2(-\sin\gamma_1\sin\beta_1\cos\gamma_2+\cos\gamma_1\sin\gamma_2\sin\beta_2)-N_2\sin\gamma_2\cos\beta_2=0 \quad (3.45)$$

Rearrange terms:

$$(-\sin\gamma_1\cos\beta_1-\tan\phi_1\sin\gamma_1\sin\beta_1\cos\gamma_2+\tan\phi_1\cos\gamma_1\sin\gamma_2\sin\beta_2)N_1+(-\sin\gamma_2\cos\beta_2-\tan\phi_2\sin\gamma_1\sin\beta_1\cos\gamma_2+\tan\phi_2\cos\gamma_1\sin\gamma_2\sin\beta_2)N_2+(\sin\theta)F=c_1A_1\sin\gamma_1\sin\beta_1\cos\gamma_2-c_1A_1\cos\gamma_1\sin\gamma_2\sin\beta_2+c_2A_2\sin\gamma_1\sin\beta_1\cos\gamma_2-c_2A_2\cos\gamma_1\sin\gamma_2\sin\beta_2 \quad (3.46)$$

For the equation in z-direction:

$$-W-c_1A_1\sin\gamma_1\sin\gamma_2\sin(\beta_1-\beta_2)-N_1\tan\phi_1\sin\gamma_1\sin\gamma_2\sin(\beta_1-\beta_2)+N_1\cos\gamma_1-c_2A_2\sin\gamma_1\sin\gamma_2\sin(\beta_1-\beta_2)-N_2\tan\phi_2\sin\gamma_1\sin\gamma_2\sin(\beta_1-\beta_2)+N_2\cos\gamma_1-P=0 \quad (3.47)$$

Rearrange terms:

$$(\cos\gamma_1-\tan\phi_1\sin\gamma_1\sin\gamma_2\sin(\beta_1-\beta_2))N_1+(\cos\gamma_2-\tan\phi_2\sin\gamma_1\sin\gamma_2\sin(\beta_1-\beta_2))N_2+(0)F=W+P+c_1A_1\sin\gamma_1\sin\gamma_2\sin(\beta_1+\beta_2)+c_2A_2\sin\gamma_1\sin\gamma_2\sin(\beta_1-\beta_2) \quad (3.48)$$

Once again. remember that P for the secondary wedge is 0. N_1, N_2, and F can be computed by solving these three equations. These three equations can be put into matrix form and then can be easily solved with math programs such as Matlab. The matrix can

$$\begin{bmatrix} A_{11} & A_{12} & A_{13} \\ A_{21} & A_{22} & A_{23} \\ A_{31} & A_{32} & A_{33} \end{bmatrix} \begin{bmatrix} N_1 \\ N_2 \\ F \end{bmatrix} = \begin{bmatrix} B_{11} \\ B_{21} \\ B_{31} \end{bmatrix} \quad (3.49)$$

be set up as follows:

$$Af=B \quad (3.50)$$

where

$A_{11}=\sin\gamma_1\sin\beta_1-\tan\phi_1\sin\gamma_1\cos\beta_1\cos\gamma_2+\tan\phi_1\cos\gamma_1\sin\gamma_2\cos\beta_2$

$A_{12}=\sin\gamma_2\sin\beta_2-\tan\phi_2\sin\gamma_1\cos\beta_1\cos\gamma_2+\tan\phi_2\cos\gamma_1\sin\gamma_2\cos\beta_2$

$A_{13}=\cos\theta$

$B_{11}=c_1A_1\sin\gamma_1\cos\beta_1\cos\gamma_2-c_1A_1\cos\gamma_1\sin\gamma_2\cos\beta_2+c_2A_2\sin\gamma_1\cos\beta_1\cos\gamma_2-c_2A_2\cos\gamma_1\sin\gamma_2\cos\beta_2$

$A_{21}=-\sin\gamma_1\cos\beta_1-\tan\phi_1\sin\gamma_1\sin\beta_1\cos\gamma_2+\tan\phi_1\cos\gamma_1\sin\gamma_2\sin\beta_2$

$A_{22}=-\sin\gamma_2\cos\beta_2-\tan\phi_2\sin\gamma_1\sin\beta_1\cos\gamma_2+\tan\phi_2\cos\gamma_1\sin\gamma_2\sin\beta_2$

$A_{23}=\sin\theta$

$B_{21}=c_1A_1\sin\gamma_1\sin\beta_1\cos\gamma_2-c_1A_1\cos\gamma_1\sin\gamma_2\sin\beta_2+c_2A_2\sin\gamma_1\sin\beta_1\cos\gamma_2-c_2A_2\cos\gamma_1\sin\gamma_2\sin\beta_2$

$A_{31}=\cos\gamma_1-\tan\phi_1\sin\gamma_1\sin\gamma_2\sin(\beta_1-\beta_2)$

$A_{32}=\cos\gamma_2-\tan\phi_2\sin\gamma_1\sin\gamma_2\sin(\beta_1-\beta_2)$

$A_{33}=0$

$B_{31}=W+P+c_1A_1\sin\gamma_1\sin\gamma_2\sin(\beta_1-\beta_2)+c_2A_2\sin\gamma_1\sin\gamma_2\sin(\beta_1-\beta_2)$

3.3.7 AN EXAMPLE ON CALCULATING THE LATERAL LOAD CAPACITY IN A 3-JOINT-SET SYSTEM

Joint Set Characteristics:
Joint Set N-S, 30°E:
$\phi_1=22.5^\circ$ ($\pi/8$)
$c_1=2$ psi
$\beta_1=90^\circ$ ($\pi/2$)
$\gamma_1=30^\circ$ ($\pi/6$)
$s_1=0.866 \cdot D$

Joint Set E-W, 60°S:
$\phi_2=15^\circ$ ($\pi/12$)
$c_2=3$ psi
$\beta_2=0^\circ$
$\gamma_2=60^\circ$ ($\pi/3$)
$s_2=0.433 \cdot D$

Joint Set N45°E, 45°NW:
$\phi_3=30^\circ$ ($\pi/6$)
$c_3=2$ psi
$\beta_3=225^\circ$ ($5\pi/4$)
$\gamma_3=45^\circ$ ($\pi/4$)
$s_3=D$

Force Direction:
$\theta=90^\circ$

Pile:
$l=D$

Rock Unit Weight:
$\gamma_r=2.75 \cdot 62.4$ lb/ft^3 = 171.6 lb/ft^3

Pile Diameter:
D=5ft

Dead Load of Pile:
P=1400k

From kinematics analysis, there are two possible removable combinations as shown in Figures 3.23 and 3.24 for a force pointing northward. Each possible combination is analyzed separately in the following.

1st Combination: Primary Wedge

Joint Set #1: N-S, 30°E
Joint Set #2: E-W, 60°S

The primary wedge of the first combination is shown on the joint mesh in Figure 3.55 and on the joint map on the pile in Figure 3.56.

Volume of Wedge:

Complete Method:
Use equation (3.30) to calculate the volume of the wedge.

$$V = \sum_{i=1}^{n} a_i h_{i\,(centroid)} - \frac{\pi D^2}{8} l$$

where
a_i=area of a block on the surface
$h_{centroid}$=height from the surface to the centroid of the area of intersection between the block and the vertical cutting plane
D=diameter of the pile
l=pile depth

$a_i = \| (s_1 \bullet s_2)/\sin(\beta_1-\beta_2) \| = \| (0.866D \bullet 0.433D)/\sin(90^\circ-0^\circ) \| = 0.375D^2$

As shown in Figure 3.57, h_1=0.375D, h_2=1.125D, and h_3=1.875D
$V=0.375D^2 \bullet (3 \bullet h_1+4 \bullet h_2+2 \bullet h_3) - \pi D^2 \bullet D/8$
$=0.375D^2 \bullet (3 \bullet 0.375D+4 \bullet 1.125D+2 \bullet 1.875D) - \pi D^3/8$
$=3.516D^3-\pi D^3/8$
$=3.123D^3=390.37\ ft^3$

Simplified Way:
Use equation (3.31) to quickly estimate the volume of the wedge.
$V=n \bullet a \bullet 0.5 \bullet b-\pi D^2 \bullet l/8$
where b is the height from the surface to the bottom of the wedge, and as shown in Figure 3.58, b=2.25D.

$V=9 \bullet 0.375D^2 \bullet 0.5 \bullet 2.25D-\pi D^2 \bullet D/8$
$=3.404D^3$
% Difference: $(3.404-3.123)/3.123 \bullet 100\% = 9.00\%$

$V=3.123D^3=390.375\ ft^3$
$W=\gamma_r \bullet V=171.6\ lb/ft^3 \bullet 390.375\ ft^3=66988.35\ lb$

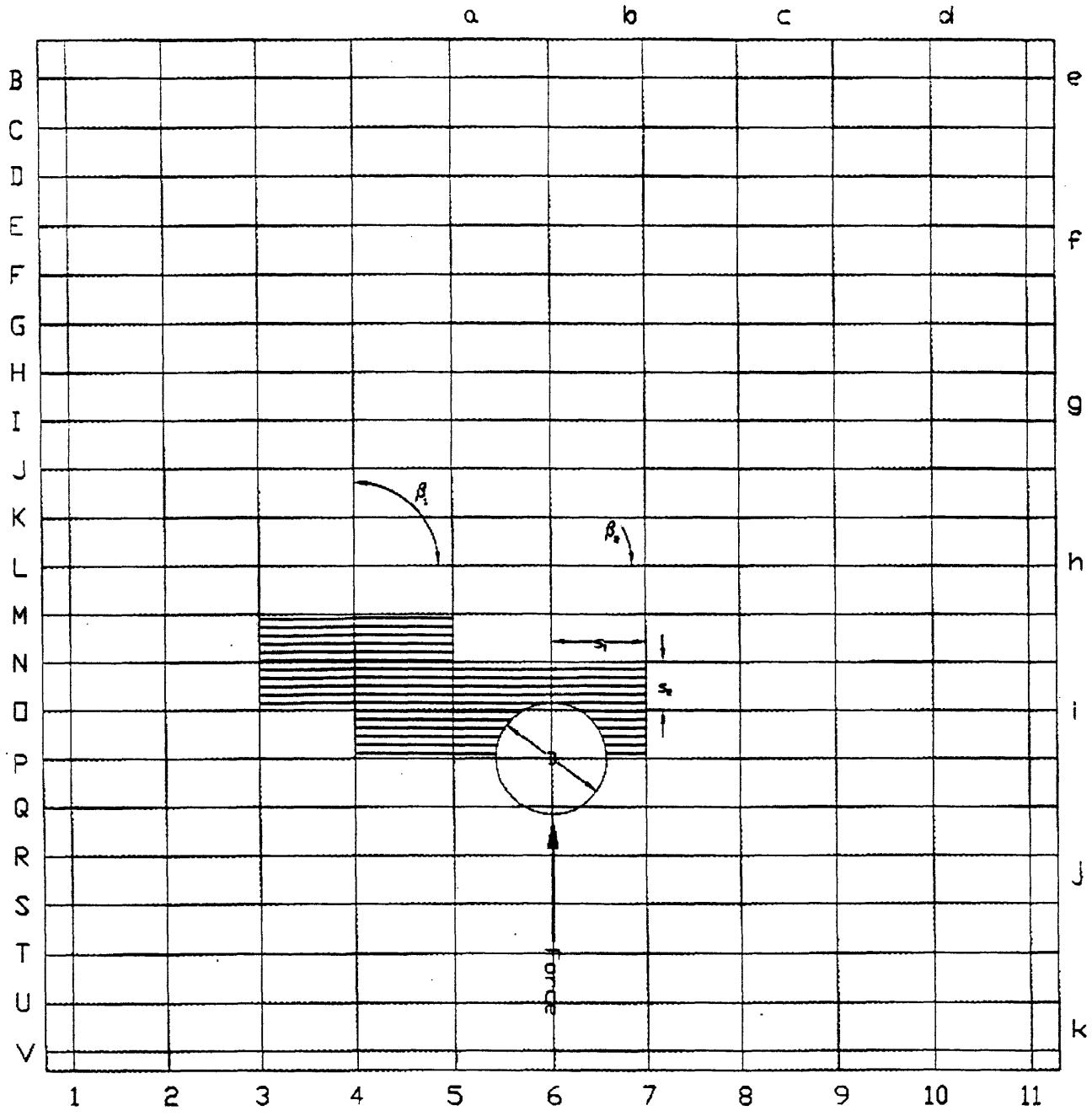

Figure 3.55 Primary Wedge of 1st Combination on the Joint Mesh

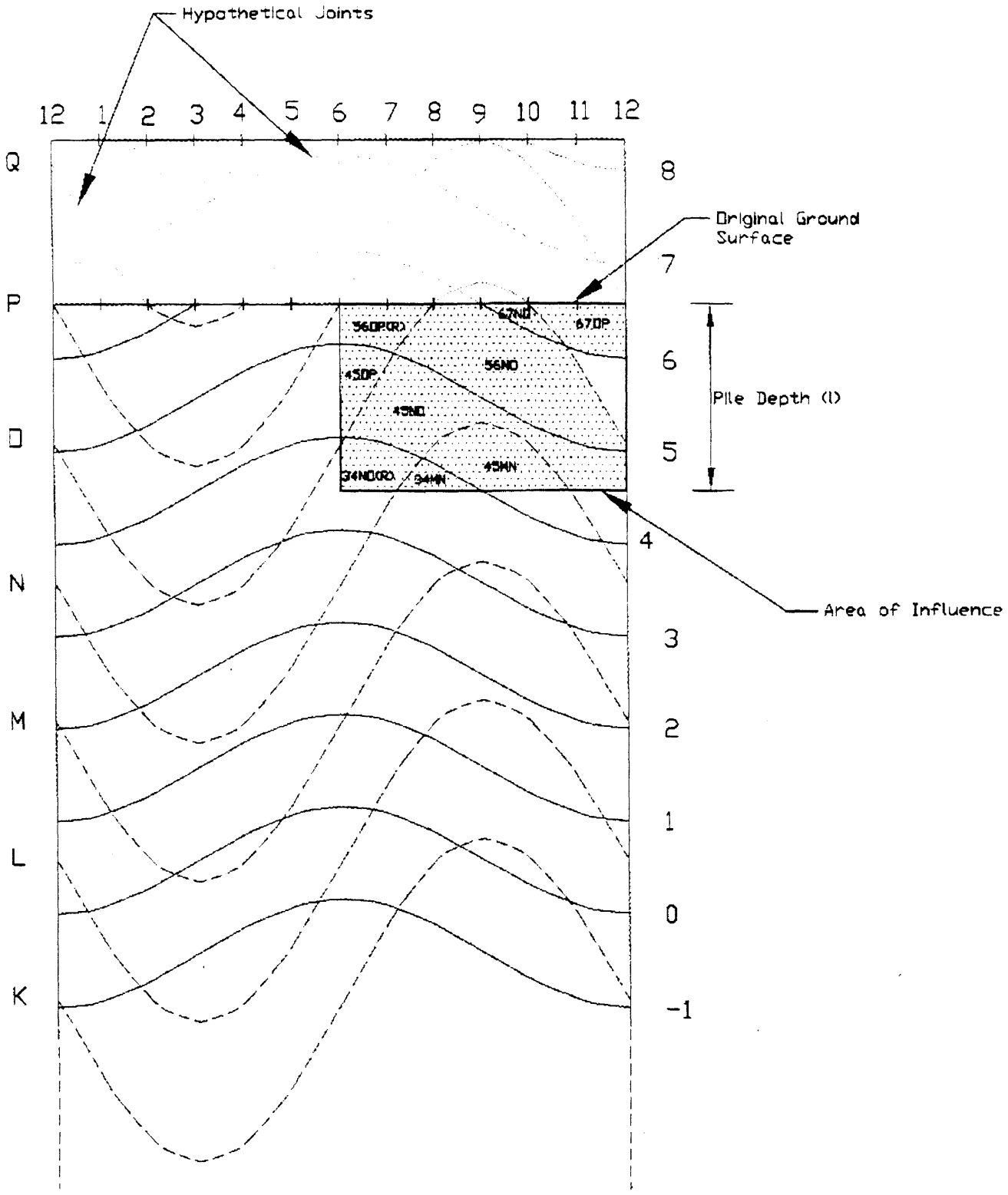

Figure 3.56 Primary Wedge of 1st Combination on the Joint Map

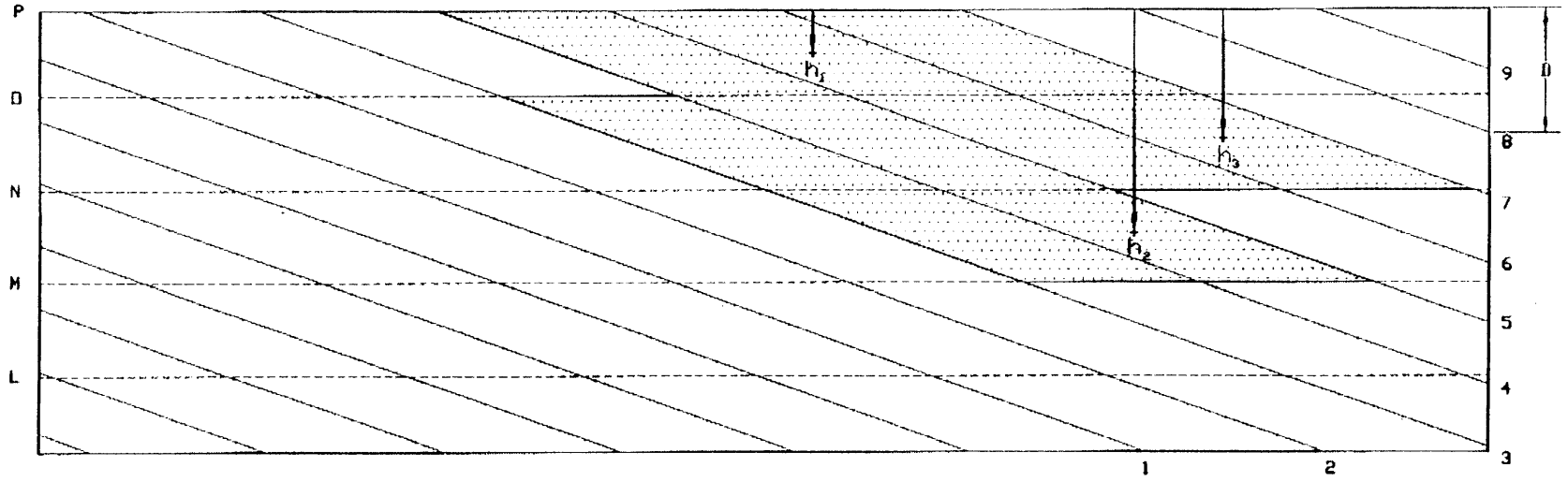

Figure 3.57 Typical h(centroid)'s for Various Blocks of the Primary Wedge

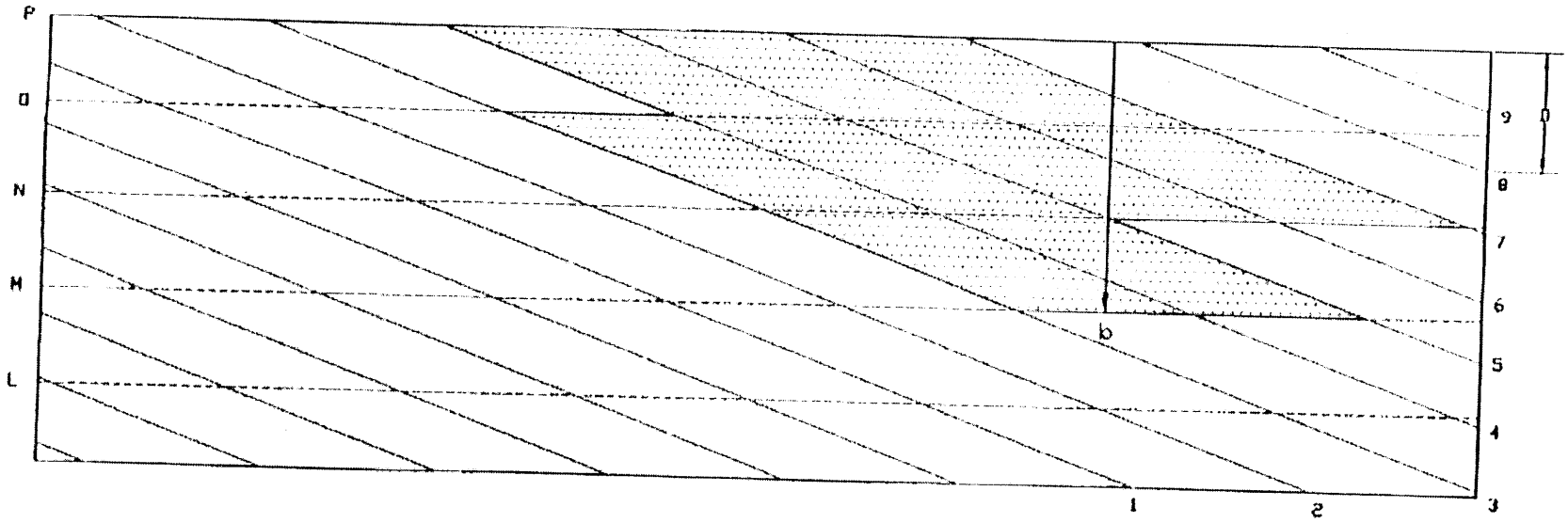

Figure 3.58 b, Height of the Wedge

Area of Faces:

Since the faces on this primary wedge intersect the vertical cutting plane only, use equation (3.39) to calculate the area of the faces for each joint set:

$$A = \sum_{i=1}^{p} \frac{H_i w_i}{\sin\gamma} = \sum_{i=1}^{p} \left[\frac{H_i}{\sin\gamma} \bullet \left\| \frac{s_i}{\sin(\beta_1 - \beta_2)} \right\| \right]$$

where

H_i=height of a face from the surface to the center of the edge that intersects the pile or the cutting plane

w_i=width of a face on the surface

γ=dip angle of the respective joint set

β=angle measured counterclockwise from the x-axis to the strike line of the respective joint set

s_i=the horizontal spacing of the other joint set

Since s and γ are the same for the faces of the same joint set, and thus

$$A = \frac{s}{\sin\gamma \cdot \left\| \sin(\beta_1 - \beta_2) \right\|} \sum_{i=1}^{p} H_i$$

For A_1 (joint set N-S, 30°E):

γ=30° for joint set N-S, 30°E

s_2=0.433D for joint set E-W, 60°S

β_1=90° for joint set N-S, 30°E

β_2=0° for joint set E-W, 60°S

As shown in Figure 3.59, H_1=0.375D, H_2=1.125D, H_3=1.875D, H_4=1.875D, H_5=1.125D, and H_6=0.375D:

$$\sum_{i=1}^{p} H_i = (H_1 + H_2 + H_3 + H_4 + H_5 + H_6)$$

$$= \sum_{i=1}^{p} H_i = (0.375D + 1.125D + 1.875D + 1.875D + 1.125D + 0.375D) = 6.75D = 33.75\,ft$$

$$A_1 = \frac{s}{\sin\gamma \cdot \left\| \sin(\beta_1 - \beta_2) \right\|} \sum_{i=1}^{p} H_i = \frac{0.433D}{\sin 30° \cdot \left\| \sin(90° - 0°) \right\|} \cdot 33.75\,ft = 146.14\,ft^2 = 21043.8\,in^2$$

For A_2 (joint set E-W, 60°S):
γ=60° for joint set E-W, 60°S
s_1=0.866D for joint set N-S, 30°E
β_1=90° for joint set N-S, 30°E
β_2=0° for joint set E-W, 60°S

As shown in Figure 3.60, H_7=0.75D, H_8=2.25D, H_9=2.25D, H_{10}=1.5D, and H_{11}=1.5D:

$$\sum_{i=1}^{p} H_i = (H_7 + H_8 + H_9 + H_{10} + H_{11})$$

$$= \sum_{i=1}^{p} H_i = (0.75D + 2.25D + 2.25D + 1.5D + 1.5D) = 8.25D = 41.25\,ft$$

$$A_2 = \frac{s}{\sin\gamma \cdot \left\|\sin(\beta_1 - \beta_2)\right\|} \sum_{i=1}^{p} H_i = \frac{0.866D}{\sin 60° \cdot \left\|\sin(90° - 0°)\right\|} \cdot 41.25\,ft = 206.24\,ft^2 = 29699.1\,in^2$$

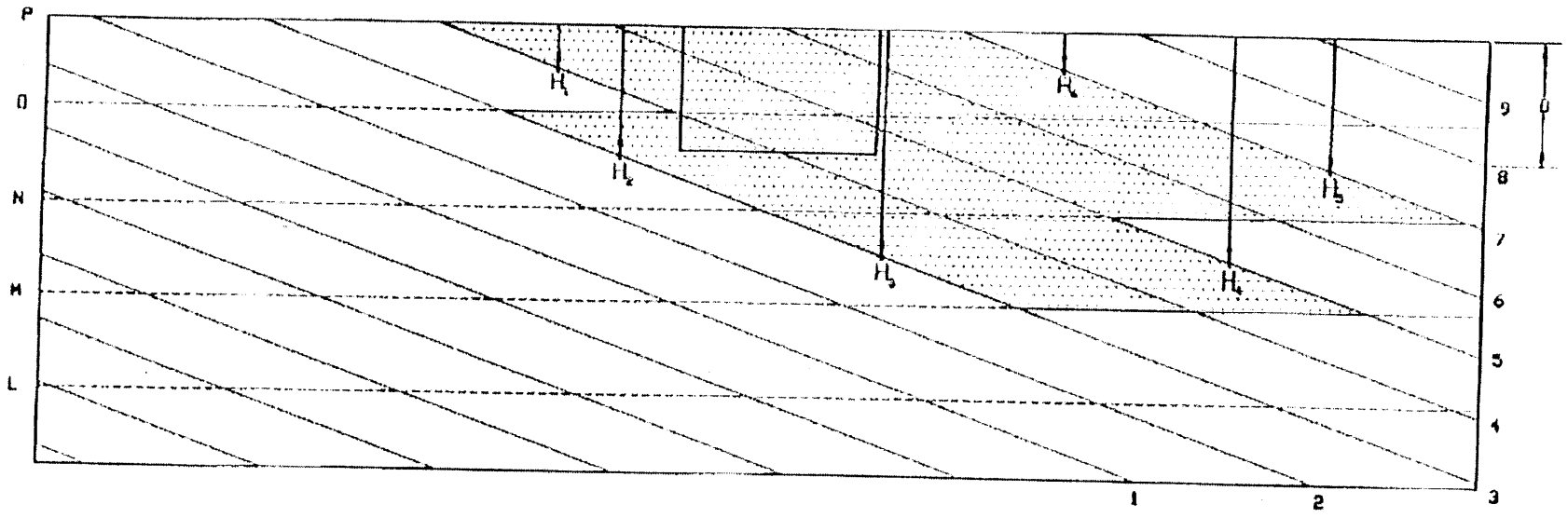

Figure 3.59 H's for Faces of Joint Set N-S, 30°E on the Primary Wedge

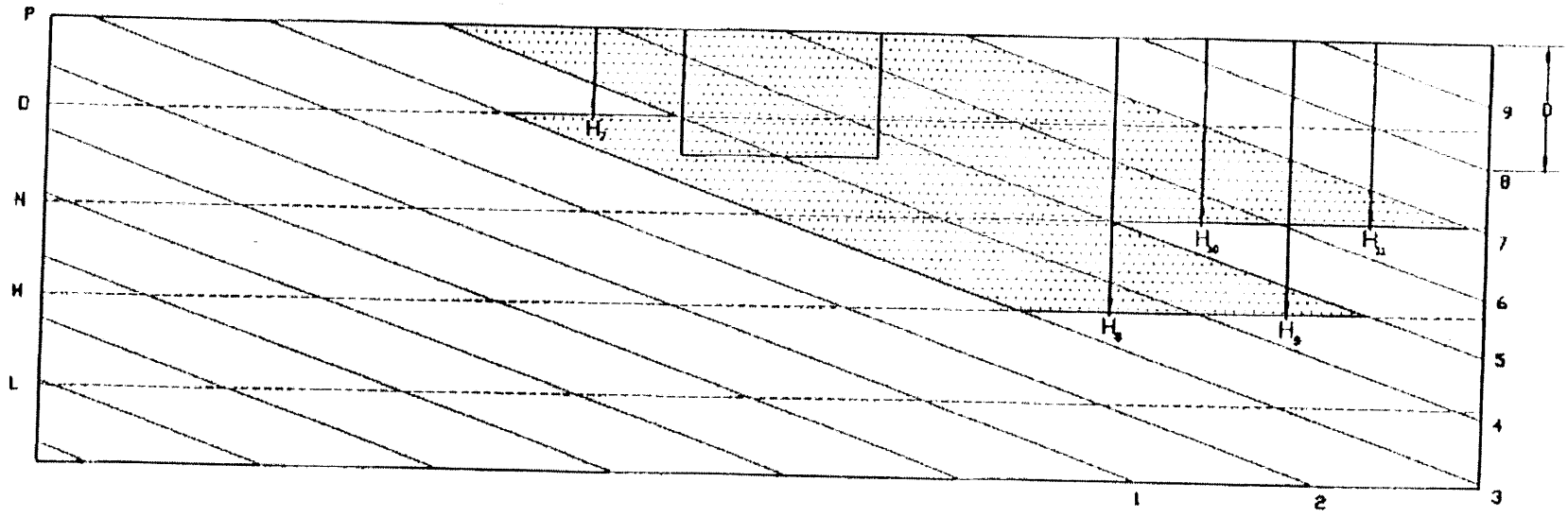

Figure 3.60 H's for Faces of Joint Set E-W, 60°S on the Primary Wedge

Limit Equilibrium:

In the x-direction:

$(\sin\gamma_1\sin\beta_1-\tan\phi_1\sin\gamma_1\cos\beta_1\cos\gamma_2+\tan\phi_1\cos\gamma_1\sin\gamma_2\cos\beta_2)N_1+(\sin\gamma_2\sin\beta_2-\tan\phi_2\sin\gamma_1\cos\beta_1\cos\gamma_2+\tan\phi_2\cos\gamma_1\sin\gamma_2\cos\beta_2)N_2+(\cos\theta)F=c_1A_1\sin\gamma_1\cos\beta_1\cos\gamma_2-c_1A_1\cos\gamma_1\sin\gamma_2\cos\beta_2+c_2A_2\sin\gamma_1\cos\beta_1\cos\gamma_2-c_2A_2\cos\gamma_1\sin\gamma_2\cos\beta_2$

$(\sin30^o\sin90^o-\tan22.5^o\sin30^o\cos90^o\cos60^o+\tan22.5^o\cos30^o\sin60^o\cos0^o)N_1+(\sin60^o\sin0^o-\tan15^o\sin30^o\cos90^o\cos60^o+\tan15^o\cos30^o\sin60^o\cos0^o)N_2+(\cos90^o)F=2\cdot21043.8\cdot\sin30^o\cos90^o\cos60^o-2\cdot21043.8\cdot\cos30^o\sin60^o\cos0^o+3\cdot29699.1\cdot\sin30^o\cos90^o\cos60^o-3\cdot29699.1\cdot\cos30^o\sin60^o\cos0^o$

$(0.811)N_1+(0.201)N_2+(0)F=-98,388.675$ [lb]

In the y-direction:

$(-\sin\gamma_1\cos\beta_1-\tan\phi_1\sin\gamma_1\sin\beta_1\cos\gamma_2+\tan\phi_1\cos\gamma_1\sin\gamma_2\sin\beta_2)N_1+(-\sin\gamma_2\cos\beta_2-\tan\phi_2\sin\gamma_1\sin\beta_1\cos\gamma_2+\tan\phi_2\cos\gamma_1\sin\gamma_2\sin\beta_2)N_2+(\sin\theta)F=c_1A_1\sin\gamma_1\sin\beta_1\cos\gamma_2-c_1A_1\cos\gamma_1\sin\gamma_2\sin\beta_2+c_2A_2\sin\gamma_1\sin\beta_1\cos\gamma_2-c_2A_2\cos\gamma_1\sin\gamma_2\sin\beta_2$

$(-\sin30^o\cos90^o-\tan22.5^o\sin30^o\sin90^o\cos60^o+\tan22.5^o\cos30^o\sin60^o\sin0^o)N_1+(-\sin60^o\cos0^o-\tan15^o\sin30^o\sin90^o\cos60^o+\tan15^o\cos30^o\sin60^o\sin0^o)N_2+(\sin90^o)F=2\cdot21043.8\cdot\sin30^o\sin90^o\cos60^o-2\cdot21043.8\cdot\cos30^o\sin60^o\sin0^o+3\cdot29699.1\cdot\sin30^o\sin90^o\cos60^o-3\cdot29699.1\cdot\cos30^o\sin60^o\sin0^o$

$(-0.104)N_1+(-0.933)N_2+(1)F=32.796.225$ [lb]

In the z-direction:

$(\cos\gamma_1-\tan\phi_1\sin\gamma_1\sin\gamma_2\sin(\beta_1-\beta_2))N_1+(\cos\gamma_2-\tan\phi_2\sin\gamma_1\sin\gamma_2\sin(\beta_1-\beta_2))N_2+(0)F=W+P+c_1A_1\sin\gamma_1\sin\gamma_2\sin(\beta_1-\beta_2)+c_2A_2\sin\gamma_1\sin\gamma_2\sin(\beta_1-\beta_2)$

$(\cos30^o-\tan22.5^o\sin30^o\sin60^o\sin(90^o-0^o))N_1+(\cos60^o-\tan15^o\sin30^o\sin60^o\sin(90^o-0^o)N_2+(0)F=66988.35+1,400,000+2\cdot21043.8\cdot\sin30^o\sin60^o\sin(90^o-0^o)+3\cdot29699.1\cdot\sin30^o\sin60^o\sin(90^o-0^o)$

$(0.687)N_1+(0.384)N_2+(0)F=1,523,793.08$ [lb]

Solve these three equations and obtain the results:

$N_1=-1985.3k$
$N_2=7518.7k$
F=6842.3k for the primary wedge of the 1st combination

1st Combination: Secondary Wedge

Joint Set #1: E-W, 60°S
Joint Set #2: N45°E, 45°NW

The secondary wedge of the first combination is shown on the joint mesh in Figure 3.61 and on the joint map on the pile in Figure 3.62.

Volume of Wedge:
Use equation (3.32) to calculate the volume of the wedge.

$V_{block} \approx V_{pyramid} = a \cdot d/3$

where
a=area of a block on the surface
d=height of the wedge

a is estimated as shown in Figure 3.63:

$$A_1 = \left\| \frac{s_1 \cdot s_2}{\sin(\beta_1 - \beta_2)} \right\| = \left\| \frac{0.433D \cdot D}{\sin(0° - 225°)} \right\| = 0.612D^2$$

$A_2=\pi r^2 \cdot 45°/360° = 0.098D^2$
$a=A_1-A_2=0.612D^2-0.098D^2=0.514D^2$

As shown in Figure 3.64, d=0.675D
V= a•d/3
$=0.514D^2 \cdot 0.675D/3=0.116D^3$
$=14.46\ ft^3$

$W=\gamma_r \cdot V=171.6\ lb/ft^3 \cdot 14.46\ ft^3=2481.34\ lb$

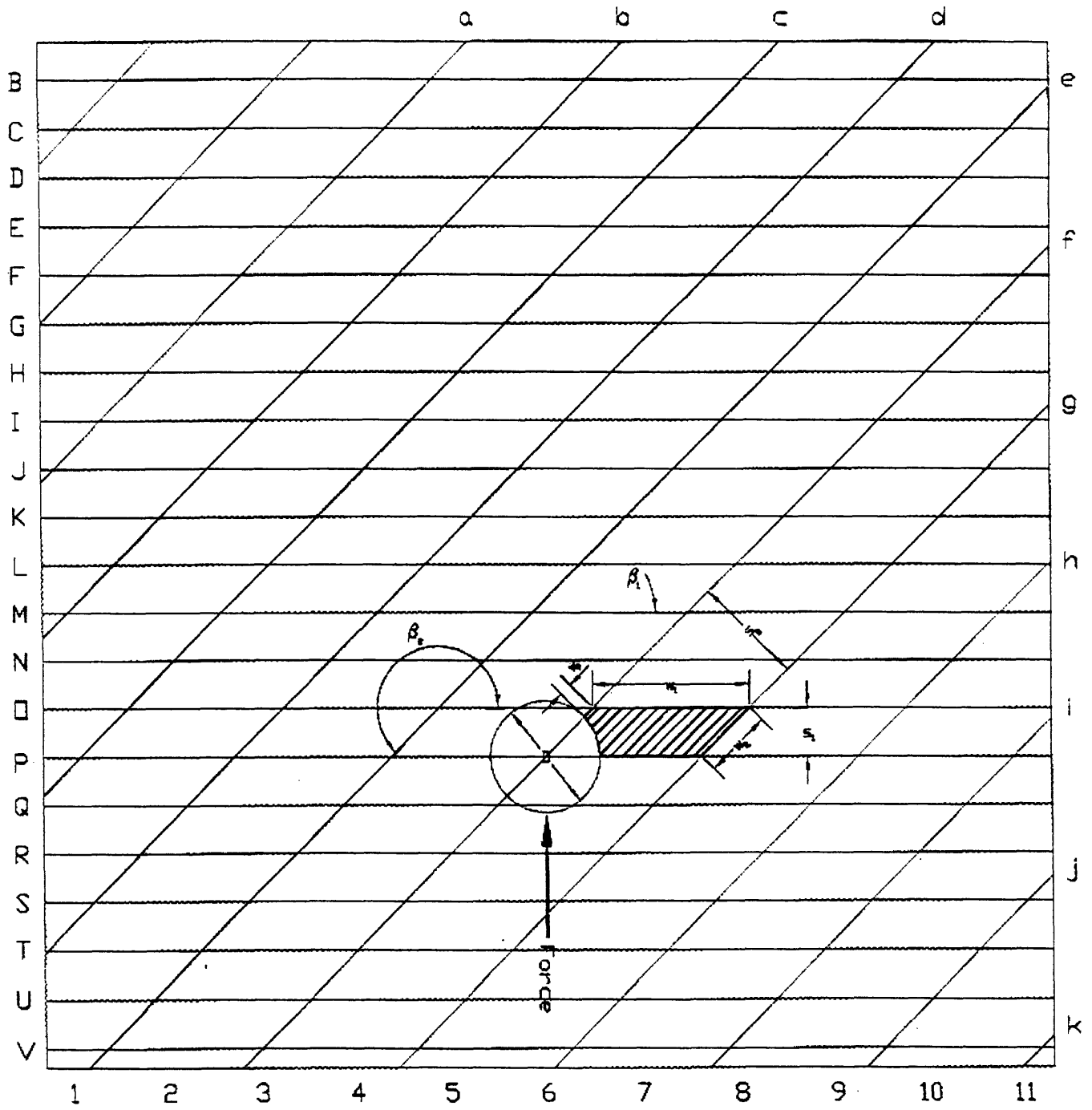

Figure 3.61 Secondary Wedge of 1st Combination on the Joint Mesh

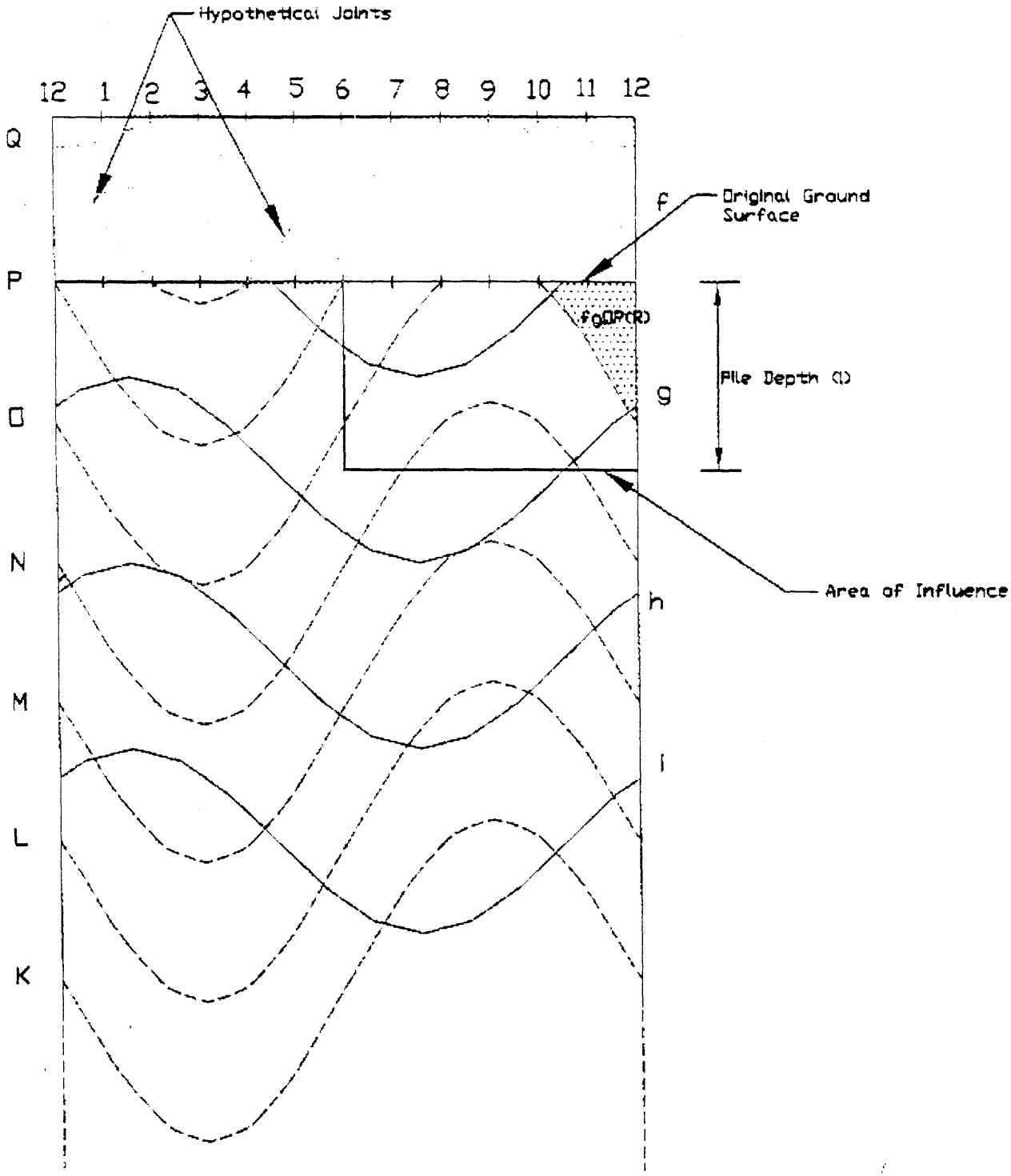

Figure 3.62 Secondary Wedge of 1st Combination on the Joint Map

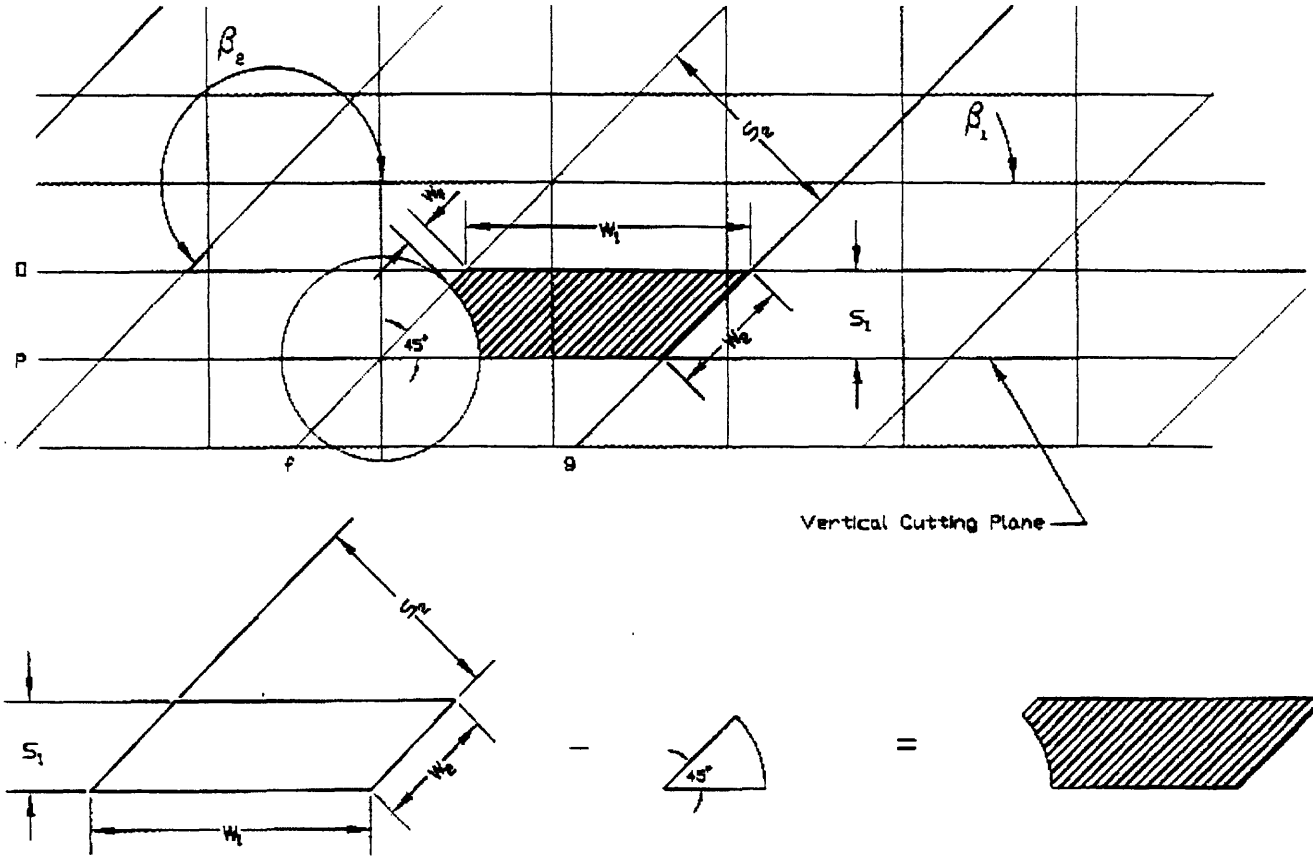

$$A_1 = w_1 \times S_1 = w_2 \times S_2 = \left\| \frac{S_1 \times S_2}{\sin(\beta_1 - \beta_2)} \right\|$$

$$A_2 = \pi(D/2)^2 \times 45^\circ/360^\circ$$

a

Figure 3.63 Estimation of Surface Area of Block fgOP(R)

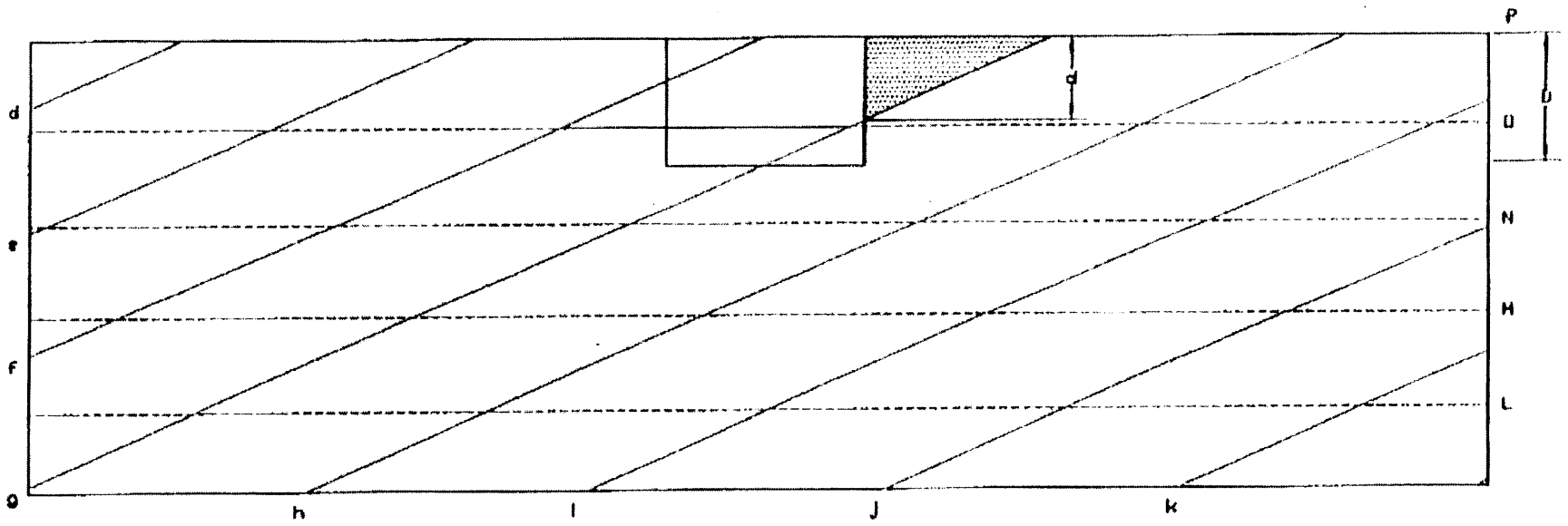

Figure 3.64 d of Grid fgOP(R) on a Joint Map on a Cutting Plane

Area of Faces:

Three faces on the secondary wedge, namely joint O, f, and g faces, need to be considered for shearing resistance. Joint g face on the secondary wedge intersects not only the pile as shown in Figure 3.65 but also the vertical cutting plane as shown in Figure 3.66. Joint O face and joint f face on the secondary wedge intersect the pile as shown in Figure 3.65, but they do not intersect the vertical cutting plane as shown in Figure 3.66.

Since joint O face on the secondary wedge intersects only the pile, use equation (3.41) to calculate its area:

$$A = \sum_{i=1}^{p} \frac{H_i w_i}{\sin\gamma} = \sum_{i=1}^{p} \left[\frac{H_i}{\sin\gamma} \bullet \left\| \frac{s_i}{\sin(\beta_1 - \beta_2)} \right\| \right]$$

where
H_i=height of a face from the surface to the center of the edge that intersects the pile or the cutting plane
w_i=width of a face on the surface
γ=dip angle of the respective joint set
β=angle measured counterclockwise from the x-axis to the strike line of the respective joint set
s_i=the horizontal spacing of the other joint set

Joint O face belongs to joint set #1 E-W, 60°S:
γ=60° for joint set E-W, 60°S
s_2=D for joint set N45°E, 45°NW
β_1=0° for joint set E-W, 60°S
β_2=225° for joint set N45°E, 45°NW

As shown in Figure 3.67, H_O=0.36D.

$$A_O = \frac{H_O}{\sin\gamma} \bullet \left\| \frac{s}{\sin(\beta_1 - \beta_2)} \right\| = \frac{0.36D}{\sin 60°} \bullet \left\| \frac{D}{\sin(0° - 225°)} \right\| = 0.588D^2 = 14.70 ft^2 = 2116.4 in^2$$

Since joint O face is the only face belonging to joint set E-W, 60°S on the secondary wedge, the total A for joint set #1 E-W, 60°S is A_1=A_O=2116.4in^2.

Since joint f face on the secondary wedge also intersects only the pile, use equation (3.41) again to calculate its area.

Joint f face belongs to joint set set #2 N45°E, 45°NW:
γ=45° for joint set N45°E, 45°NW
s_1=0.433D for joint set E-W, 60°S
β_1=0° for joint set E-W, 60°S
β_2=225° for joint set N45°E, 45°NW

H_f=0.030D as shown in Figure 3.67, and $w_f=w_2-D/2$ as shown in Figure 3.63

$$A_f = \frac{H_f \cdot w_f}{\sin\gamma} = \frac{H_f}{\sin\gamma} \bullet \left(w_2 - \frac{D}{2} \right) = \frac{H_f}{\sin\gamma} \bullet \left(\left\| \frac{s_1}{\sin(\beta_1 - \beta_2)} \right\| - \frac{D}{2} \right)$$

$$= \frac{0.030D}{\sin 45°} \bullet \left(\left\| \frac{0.433D}{\sin(0° - 225°)} \right\| - \frac{D}{2} \right) = 0.0048D^2 = 0.119ft^2 = 17.2in^2$$

Since joint g face on the secondary wedge intersects both the pile and the vertical cutting plane, use equation (3.40) to calculate its area:

$$A = \sum_{j=1}^{q} \frac{d_j w_j}{2\sin\gamma} = \sum_{j=1}^{q} \left[\frac{d_j}{2\sin\gamma} \bullet \left\| \frac{s_j}{\sin(\beta_1 - \beta_2)} \right\| \right]$$

where
d_j=height of a face from bottom to the top of the face
γ=dip angle of the respective joint set
w_i=width of a face on the surface
β=angle measured counterclockwise from the x-axis to the strike line of the respective joint set
s_j=the horizontal spacing of the other joint set

Joint g face belongs to joint set #2 N45°E, 45°NW:
γ=45° for joint set N45°E, 45°NW
s_1=0.433D for joint set E-W, 60°S
β_1=0° for joint set E-W, 60°S
β_2=225° for joint set N45°E, 45°NW

As shown in Figure 3.64, d=0.675D.

$$A_g = \frac{d}{2\sin\gamma} \bullet \left\| \frac{s}{\sin(\beta_1 - \beta_2)} \right\| = \frac{0.675D}{2\sin 45°} \bullet \left\| \frac{0.433D}{\sin(0° - 225°)} \right\| = 0.292D^2 = 7.31ft^2 = 1052.2in^2$$

The total A for joint set N45°E, N45°W is the sum of the area of joint f face and the area of joint g face: $A_2=A_f+A_g=17.2in^2+1052.2in^2=1069.4in^2$.

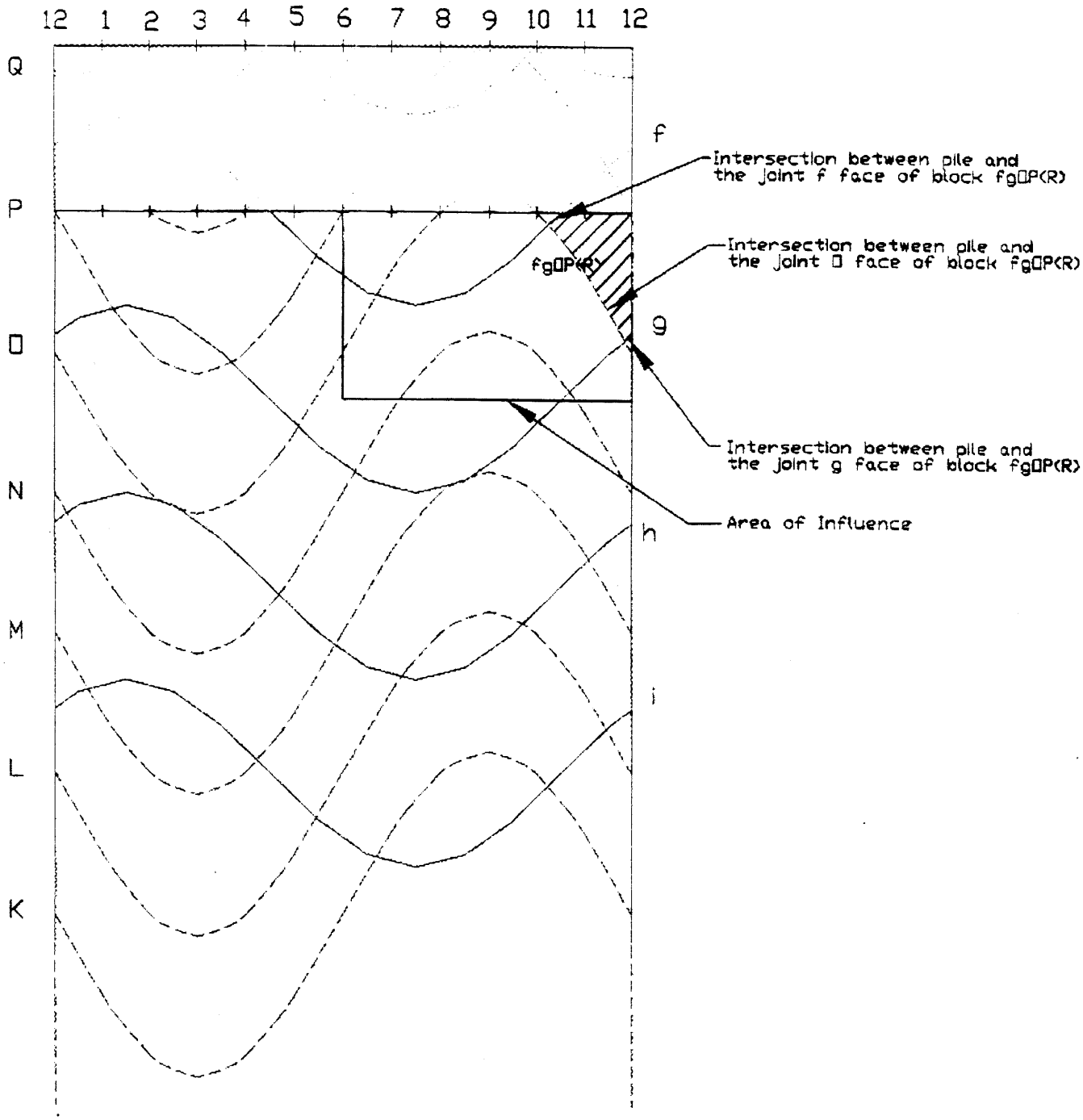

Figure 3.65 Grid fgOP(R) on a Joint Map on a Pile

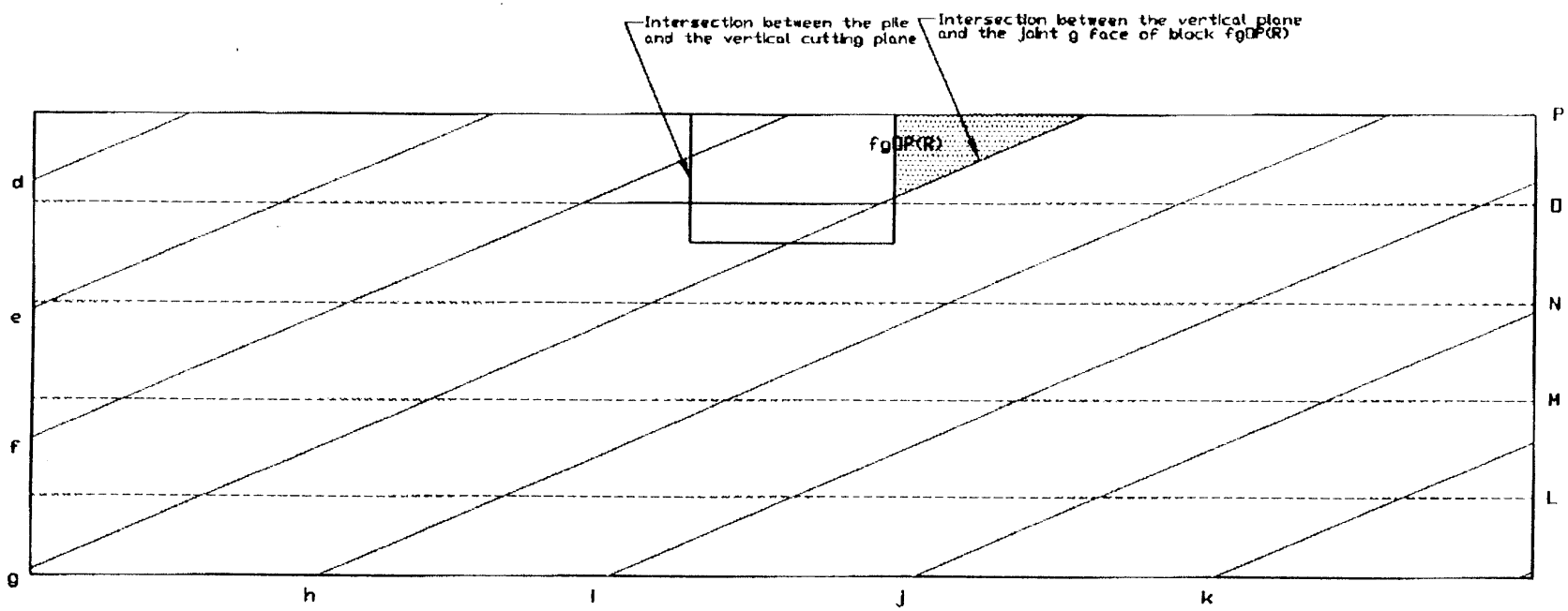

Figure 3.66 Grid fgOP(R) on a Joint Map on a Cutting Plane

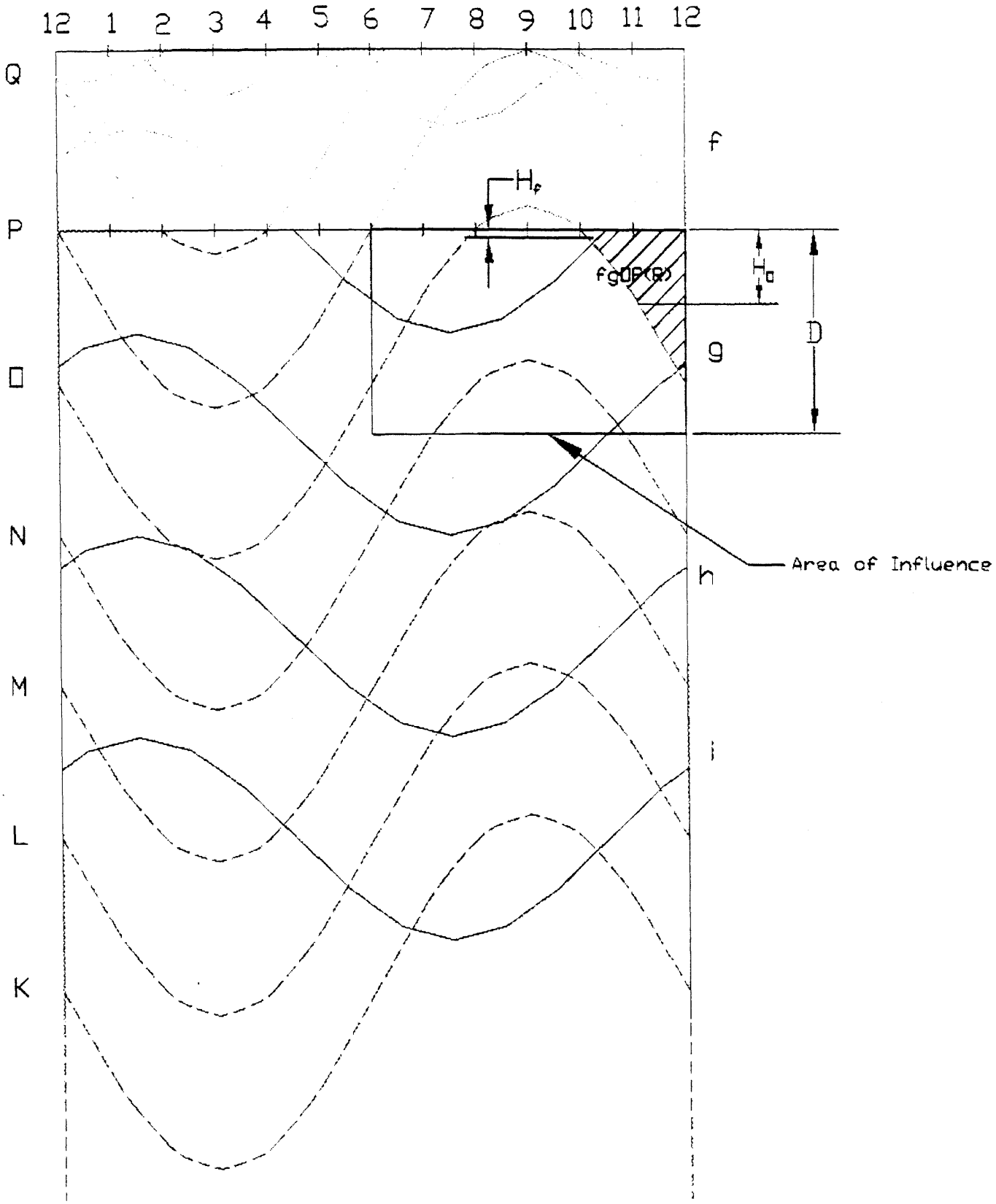

Figure 3.67 H's of Grid fgOP(R) on a Joint Map on a Pile

Limit Equilibrium:

In the x-direction:

$(\sin\gamma_1\sin\beta_1-\tan\phi_1\sin\gamma_1\cos\beta_1\cos\gamma_2+\tan\phi_1\cos\gamma_1\sin\gamma_2\cos\beta_2)N_1+(\sin\gamma_2\sin\beta_2-\tan\phi_2\sin\gamma_1\cos\beta_1\cos\gamma_2+\tan\phi_2\cos\gamma_1\sin\gamma_2\cos\beta_2)N_2+(\cos\theta)F=c_1A_1\sin\gamma_1\cos\beta_1\cos\gamma_2-c_1A_1\cos\gamma_1\sin\gamma_2\cos\beta_2+c_2A_2\sin\gamma_1\cos\beta_1\cos\gamma_2-c_2A_2\cos\gamma_1\sin\gamma_2\cos\beta_2$

$(\sin60^\circ\sin0^\circ-\tan15^\circ\sin60^\circ\cos0^\circ\cos45^\circ+\tan15^\circ\cos60^\circ\sin45^\circ\cos225^\circ)N_1+(\sin45^\circ\sin225^\circ-\tan30^\circ\sin60^\circ\cos0^\circ\cos45^\circ+\tan30^\circ\cos60^\circ\sin45^\circ\cos225^\circ)N_2+(\cos90^\circ)F=3\bullet2116.4\bullet\sin60^\circ\cos0^\circ\cos45^\circ-3\bullet2116.4\bullet\cos60^\circ\sin45^\circ\cos225^\circ+2\bullet1096.4\bullet\sin60^\circ\cos0^\circ\cos45^\circ-2\bullet1096.4\bullet\cos60^\circ\sin45^\circ\cos225^\circ$

$(-0.231)N_1+(-0.998)N_2+(0)F=7366.39$ [lb]

In the y-direction:

$(-\sin\gamma_1\cos\beta_1-\tan\phi_1\sin\gamma_1\sin\beta_1\cos\gamma_2+\tan\phi_1\cos\gamma_1\sin\gamma_2\sin\beta_2)N_1+(-\sin\gamma_2\cos\beta_2-\tan\phi_2\sin\gamma_1\sin\beta_1\cos\gamma_2+\tan\phi_2\cos\gamma_1\sin\gamma_2\sin\beta_2)N_2+(\sin\theta)F=c_1A_1\sin\gamma_1\sin\beta_1\cos\gamma_2-c_1A_1\cos\gamma_1\sin\gamma_2\sin\beta_2+c_2A_2\sin\gamma_1\sin\beta_1\cos\gamma_2-c_2A_2\cos\gamma_1\sin\gamma_2\sin\beta_2$

$(-\sin60^\circ\cos0^\circ-\tan15^\circ\sin60^\circ\sin0^\circ\cos45^\circ+\tan15^\circ\cos60^\circ\sin45^\circ\sin225^\circ)N_1+(-\sin45^\circ\cos225^\circ-\tan30^\circ\sin60^\circ\sin0^\circ\cos45^\circ+\tan30^\circ\cos60^\circ\sin45^\circ\sin225^\circ)N_2+(\sin90^\circ)F=3\bullet2116.4\bullet\sin60^\circ\sin0^\circ\cos45^\circ-3\bullet2116.4\bullet\cos60^\circ\sin45^\circ\sin225^\circ+2\bullet1096.4\bullet\sin60^\circ\sin0^\circ\cos45^\circ-2\bullet1096.4\bullet\cos60^\circ\sin45^\circ\sin225^\circ$

$(-0.933)N_1+(0.356)N_2+(1)F=2135.50$ [lb]

In the z-direction:

$(\cos\gamma_1-\tan\phi_1\sin\gamma_1\sin\gamma_2\sin(\beta_1-\beta_2))N_1+(\cos\gamma_2-\tan\phi_2\sin\gamma_1\sin\gamma_2\sin(\beta_1-\beta_2))N_2+(0)F=W+P+c_1A_1\sin\gamma_1\sin\gamma_2\sin(\beta_1-\beta_2)+c_2A_2\sin\gamma_1\sin\gamma_2\sin(\beta_1-\beta_2)$

$(\cos60^\circ-\tan15^\circ\sin60^\circ\sin45^\circ\sin(0^\circ-225^\circ))N_1+(\cos45^\circ-\tan30^\circ\sin60^\circ\sin45^\circ\sin(0^\circ-225^\circ)N_2+(0)F=2481.34+0+3\bullet2116.4\bullet\sin60^\circ\sin45^\circ\sin(0^\circ-225^\circ)+2\bullet1096.4\bullet\sin60^\circ\sin45^\circ\sin(0^\circ-225^\circ)$

$(0.384)N_1+(0.457)N_2+(0)F=6180.09$ [lb]

Solve these three equations and obtain the results:

$N_1=34.6k$

$N_2=-15.3k$

F=39.6k for the secondary wedge of the 1st combination

The ultimate lateral capacity (F_u) for the 1st removable combination is

F_u=6842.3k+39.6k=**6881.9k**

2nd Combination: Primary Wedge

Joint Set #1: E-W, 60°S
Joint Set #2: N45°E, 45°NW

The primary wedge of the second combination is shown on the joint mesh in Figure 3.68 and on the joint map on the pile in Figure 3.69.

Volume of Wedge:
Complete Method:
Use equation (3.30) to calculate the volume of the wedge.

$$V = \sum_{i=1}^{n} a_i h_{i\,(centroid)} - \frac{\pi D^2}{8} l$$

where
a=area of a block on the surface
$h_{centroid}$=height from the surface to the centroid of the area of intersection between the block and the vertical cutting plane
D=diameter of the pile
l=pile depth

$a_i = \| (s_1 \bullet s_2)/\sin(\beta_1-\beta_2) \| = \| (0.433D \bullet D)/\sin(0^\circ-225^\circ) \| = 0.612D^2$

As shown in Figure 3.70, h_1=0.375D, h_2=1.125D, and h_3=1.875D
$V=0.612D^2 \bullet (3 \bullet h_1+3 \bullet h_2+2 \bullet h_3)- \pi D^2 \bullet D/8$
$=0.612D^2 \bullet (3 \bullet 0.375D+4 \bullet 1.125D+2 \bullet 1.875D)- \pi D^3/8$
$=5.738D^3-\pi D^3/8$
$=5.345D^3=668.125\ ft^3$

Simplified Way:
Use equation (3.31) to quickly estimate the volume of the wedge.
$V=n \bullet a \bullet 0.5 \bullet b-\pi D^2 \bullet l/8$
where b is the height from the surface to the bottom of the wedge, and as shown in Figure 3.71, b=2.25D.

$V=8 \bullet 0.612D^2 \bullet 0.5 \bullet 2.25D-\pi D^2 \bullet D/8$
$=5.115D^3$
% Difference: $(5.345-5.115)/5.345 \bullet 100\%=4.30\%$

$V=5.345D^3=668.125\ ft^3$
$W=\gamma_r \bullet V=171.6\ lb/ft^3 \bullet 668.125\ ft^3=114650.25\ lb$

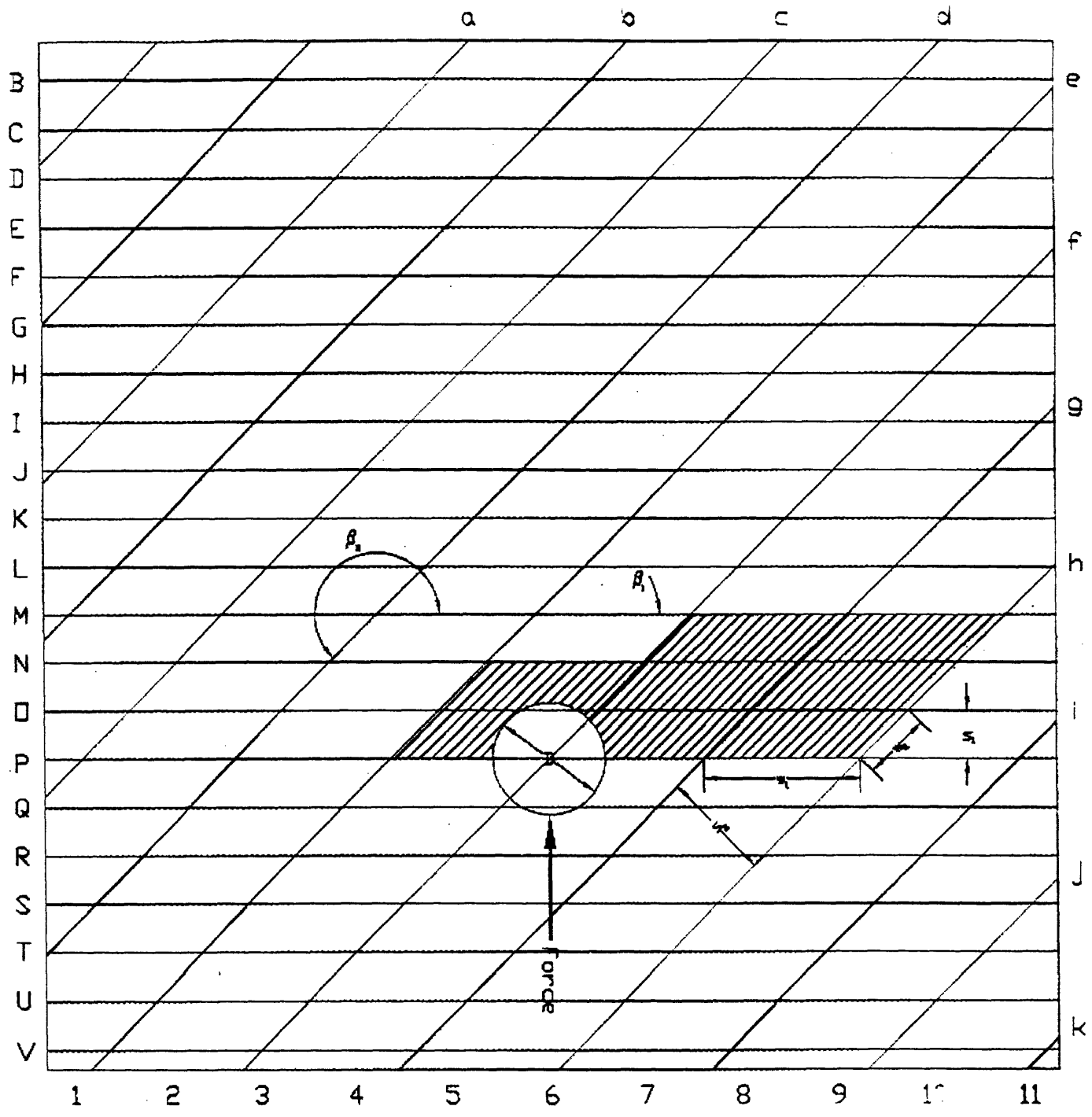

Figure 3.68 Primary Wedge of 2nd Combination on the Joint Mesh

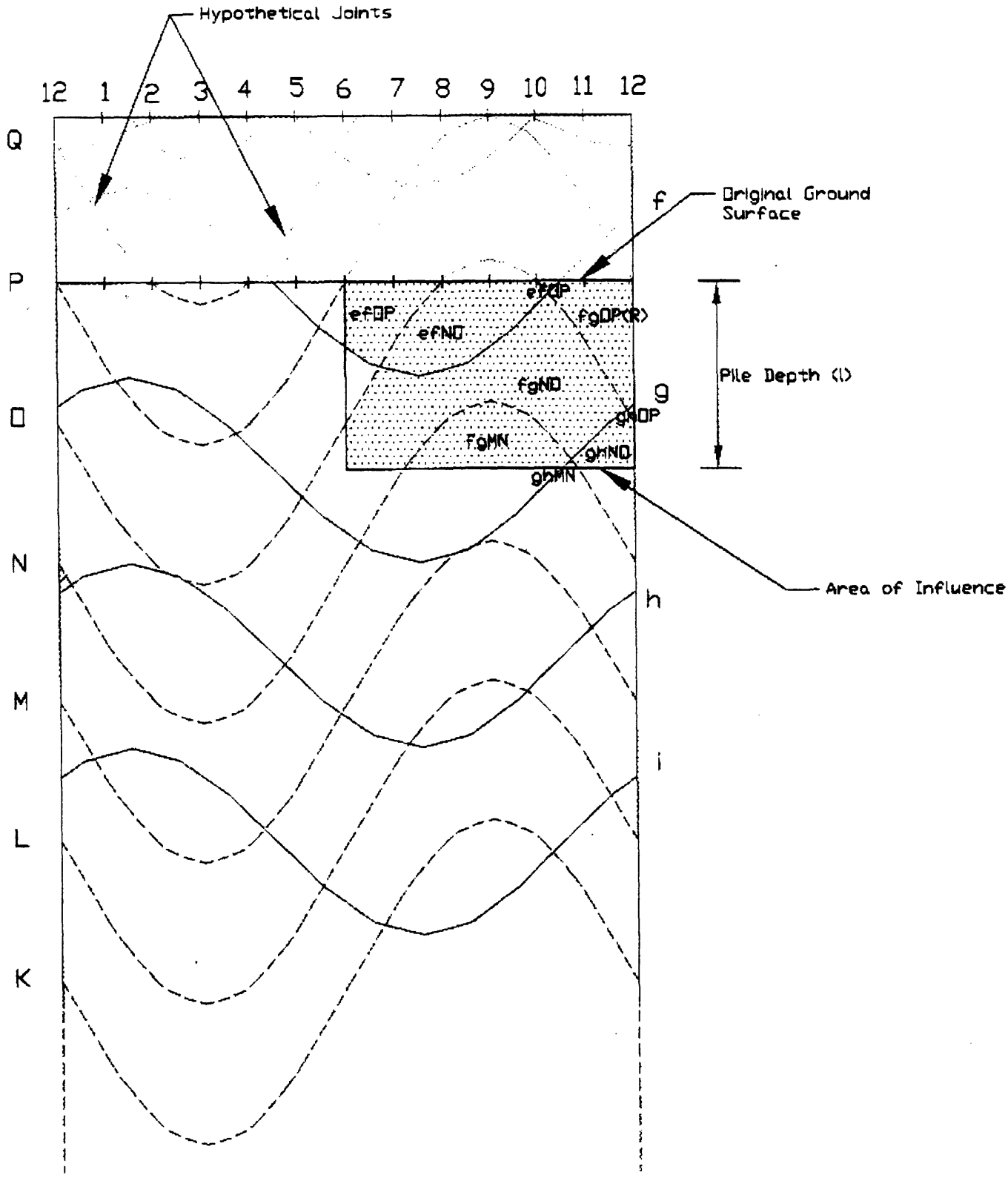

Figure 3.69 Primary Wedge of 2nd Combination on the Joint Map

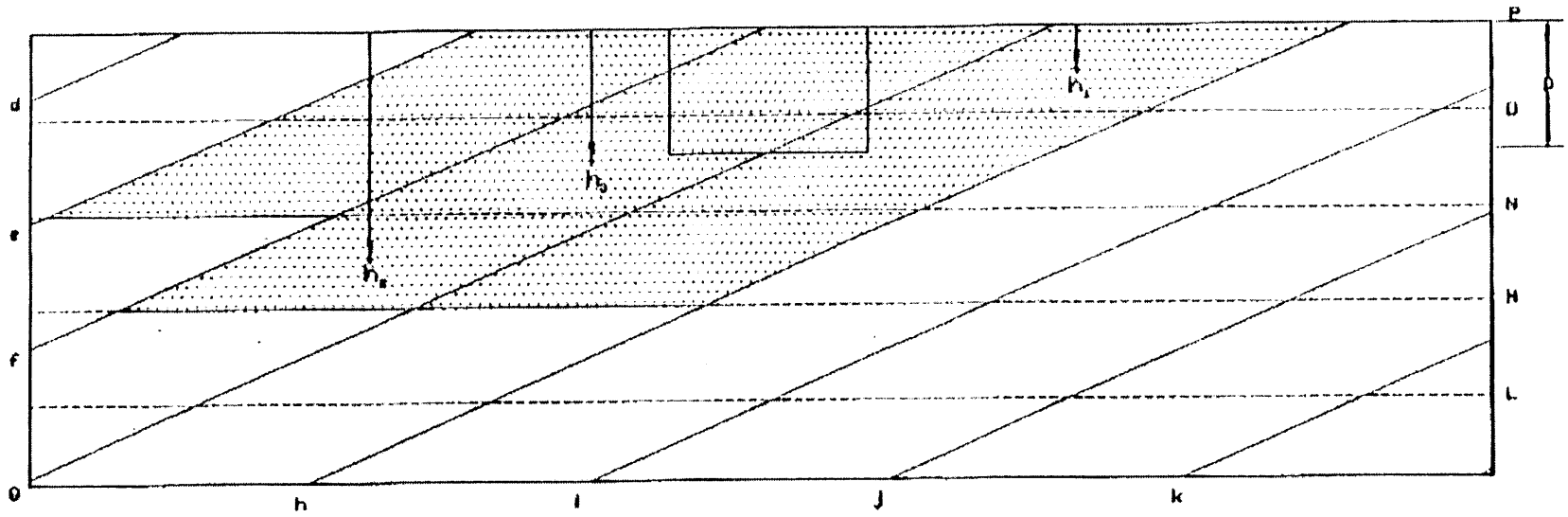

Figure 3.70 Typical h(centroid)'s for Various Blocks of the Primary Wedge

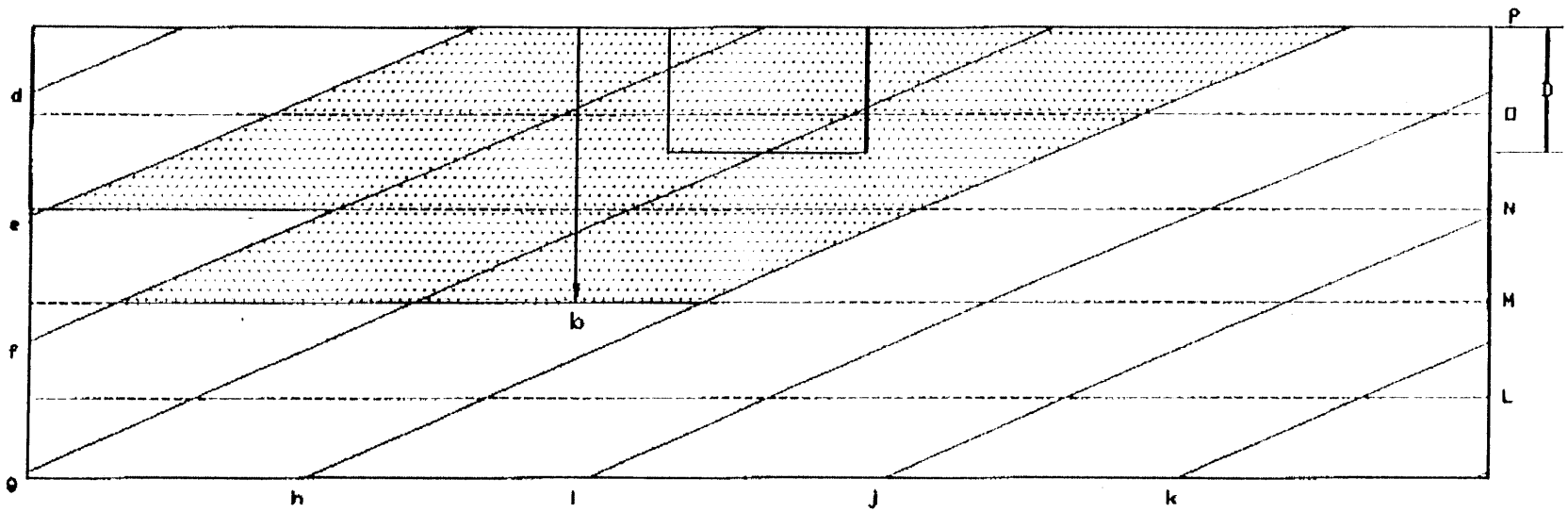

Figure 3.71 b, Height of the Wedge

Area of Faces:

Since the faces on this primary wedge intersect the vertical cutting plane only, use equation (3.39) to calculate the area of the faces for each joint set:

$$A = \sum_{i=1}^{p} \frac{H_i w_i}{\sin\gamma} = \sum_{i=1}^{p} \left[\frac{H_i}{\sin\gamma} \bullet \left\| \frac{s_i}{\sin(\beta_1 - \beta_2)} \right\| \right]$$

where

H=height from the surface to the center of the edge that intersects the pile or the cutting plane

γ=dip angle of the respective joint set

β=angle measured counterclockwise from the x-axis to the strike line of the respective joint set

s=the horizontal spacing of the other joint set

Since s and γ are the same for the faces of the same joint set and thus

$$A = \frac{s}{\sin\gamma \cdot \left\|\sin(\beta_1 - \beta_2)\right\|} \sum_{i=1}^{p} H_i$$

For A_1 (joint set E-W, 60°S):

γ=60° for joint set E-W, 60°S

s_2=D for joint set N45°E, 45°NW

β_1=0° for joint set E-W, 60°S

β_2=225° for joint set N45°E, 45°NW

As shown in Figure 3.72, H_1=1.5D, H_2=2.25D, H_3=2.25D:

$$\sum_{i=1}^{p} H_i = (H_1 + H_2 + H_3)$$

$$= \sum_{i=1}^{p} H_i = (1.50D + 2.25D + 2.25D) = 6.00D = 30.00\,ft$$

$$A_1 = \frac{s}{\sin\gamma \cdot \left\|\sin(\beta_1 - \beta_2)\right\|} \sum_{i=1}^{p} H_i = \frac{D}{\sin 60° \cdot \left\|\sin(0° - 225°)\right\|} \cdot 30.00\,ft = 244.95\,ft^2 = 35272.7\,in^2$$

For A_2 (joint set N45°E, 45°NW):
γ=45° for joint set N45°E, 45°NW
s_1=0.433D for joint set E-W, 60°S
β_1=0° for joint set E-W, 60°S
β_2=225° for joint set N45°E, 45°NW

As shown in Figure 3.73, H_4=0.375D, H_5=1.125D, H_6=1.875D, H_7=1.875D, H_8=1.125D, and H_9=0.375D:

$$\sum_{i=1}^{p} H_i = (H_4 + H_5 + H_6 + H_7 + H_8 + H_9)$$

$$= \sum_{i=1}^{p} H_i = (0.375D + 1.125D + 1.875D + 1.875D + 1.125D + 0.375D) = 3.375D = 16.875\,ft$$

$$A_2 = \frac{s}{\sin\gamma \cdot \left\|\sin(\beta_1 - \beta_2)\right\|} \sum_{i=1}^{p} H_i = \frac{0.433D}{\sin 45° \cdot \left\|\sin(0° - 225°)\right\|} \cdot 16.875\,ft = 73.07\,ft^2 = 10521.9\,in^2$$

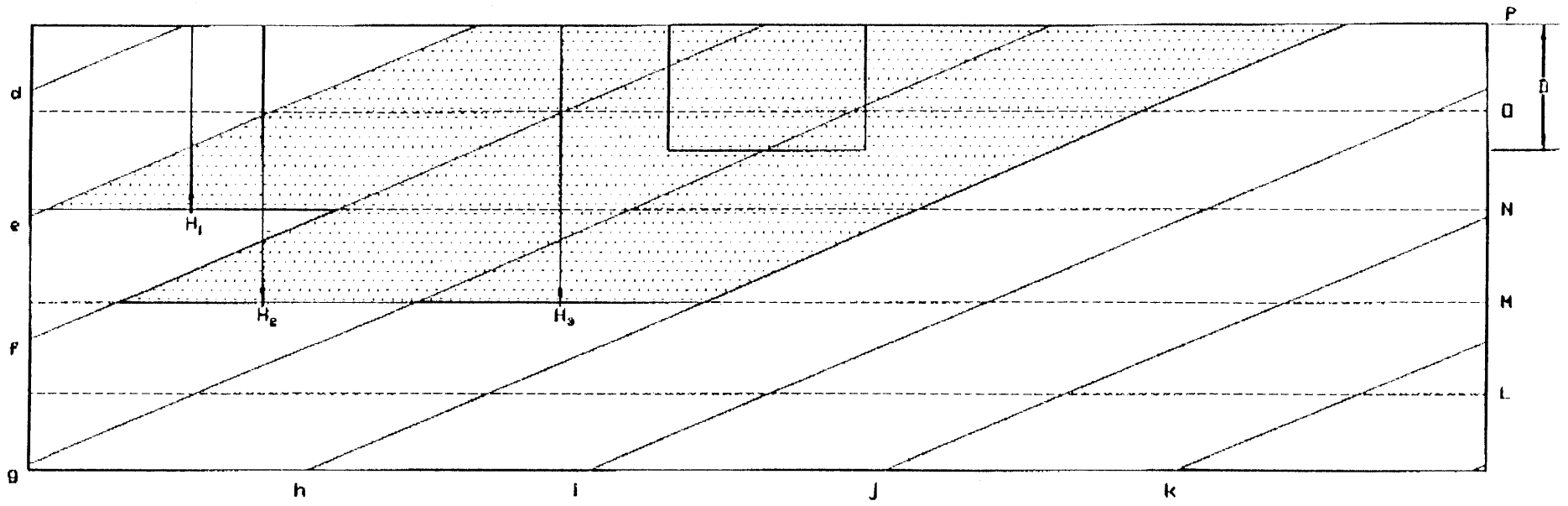

Figure 3.72 H's for faces of Joint Set E-W, 60°S on the Primary Wedge

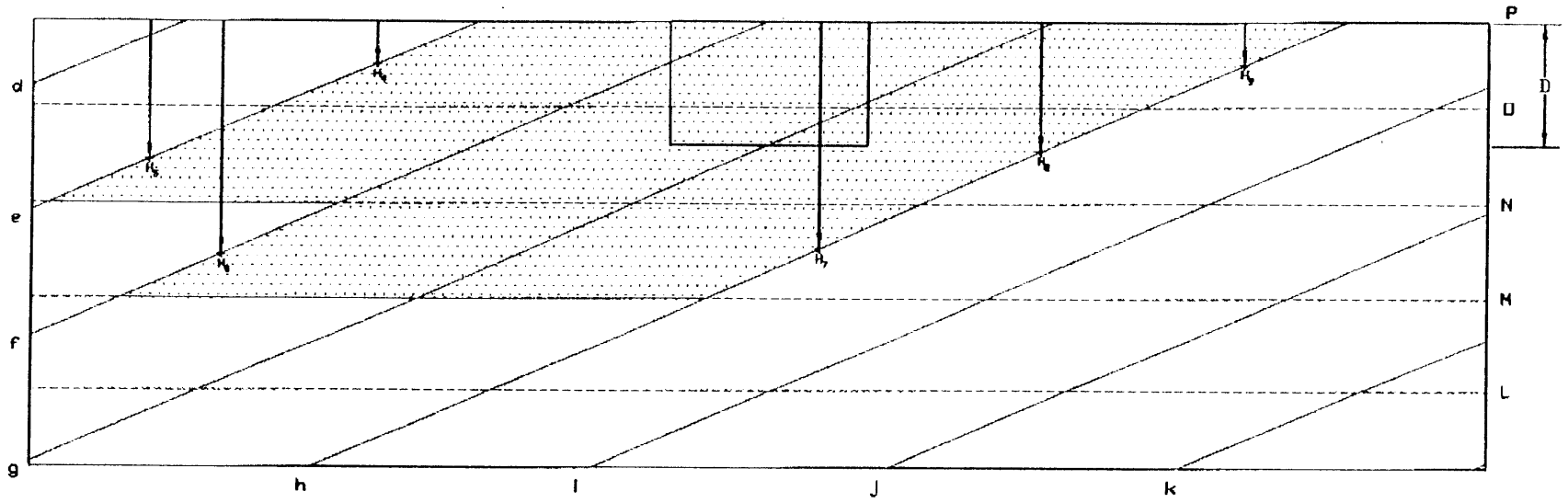

Figure 3.73 H's for Faces of Joint Set N45°E, 45°NW on the Primary Wedge

Limit Equilibrium:

In the x-direction:

$(\sin\gamma_1\sin\beta_1-\tan\phi_1\sin\gamma_1\cos\beta_1\cos\gamma_2+\tan\phi_1\cos\gamma_1\sin\gamma_2\cos\beta_2)N_1+(\sin\gamma_2\sin\beta_2-\tan\phi_2\sin\gamma_1\cos\beta_1\cos\gamma_2+\tan\phi_2\cos\gamma_1\sin\gamma_2\cos\beta_2)N_2+(\cos\theta)F=c_1A_1\sin\gamma_1\cos\beta_1\cos\gamma_2-c_1A_1\cos\gamma_1\sin\gamma_2\cos\beta_2+c_2A_2\sin\gamma_1\cos\beta_1\cos\gamma_2-c_2A_2\cos\gamma_1\sin\gamma_2\cos\beta_2$

$(\sin60^o\sin0^o-\tan15^o\sin60^o\cos0^o\cos45^o+\tan15^o\cos60^o\sin45^o\cos225^o)N_1+(\sin45^o\sin225^o-\tan30^o\sin60^o\cos0^o\cos45^o+\tan30^o\cos60^o\sin45^o\cos225^o)N_2+(\cos90^o)F=3\cdot35272.7\cdot\sin60^o\cos0^o\cos45^o-3\cdot35272.7\cdot\cos60^o\sin45^o\cos225^o+2\cdot10521.9\cdot\sin60^o\cos0^o\cos45^o-2\cdot10521.9\cdot\cos60^o\sin45^o\cos225^o$

$(-0.231)N_1+(-0.998)N_2+(0)F=109402.21$ [lb]

In the y-direction:

$(-\sin\gamma_1\cos\beta_1-\tan\phi_1\sin\gamma_1\sin\beta_1\cos\gamma_2+\tan\phi_1\cos\gamma_1\sin\gamma_2\sin\beta_2)N_1+(-\sin\gamma_2\cos\beta_2-\tan\phi_2\sin\gamma_1\sin\beta_1\cos\gamma_2+\tan\phi_2\cos\gamma_1\sin\gamma_2\sin\beta_2)N_2+(\sin\theta)F=c_1A_1\sin\gamma_1\sin\beta_1\cos\gamma_2-c_1A_1\cos\gamma_1\sin\gamma_2\sin\beta_2+c_2A_2\sin\gamma_1\sin\beta_1\cos\gamma_2-c_2A_2\cos\gamma_1\sin\gamma_2\sin\beta_2$

$(-\sin60^o\cos0^o-\tan15^o\sin60^o\sin0^o\cos45^o+\tan15^o\cos60^o\sin45^o\sin225^o)N_1+(-\sin45^o\cos225^o-\tan30^o\sin60^o\sin0^o\cos45^o+\tan30^o\cos60^o\sin45^o\sin225^o)N_2+(\sin90^o)F=3\cdot35272.7\cdot\sin60^o\sin0^o\cos45^o-3\cdot35272.7\cdot\cos60^o\sin45^o\sin225^o+2\cdot10521.9\cdot\sin60^o\sin0^o\cos45^o-2\cdot10521.9\cdot\cos60^o\sin45^o\sin225^o$

$(-0.933)N_1+(0.356)N_2+(1)F=31715.48$ [lb]

In the z-direction:

$(\cos\gamma_1-\tan\phi_1\sin\gamma_1\sin\gamma_2\sin(\beta_1-\beta_2))N_1+(\cos\gamma_2-\tan\phi_2\sin\gamma_1\sin\gamma_2\sin(\beta_1-\beta_2))N_2+(0)F=W+P+c_1A_1\sin\gamma_1\sin\gamma_2\sin(\beta_1-\beta_2)+c_2A_2\sin\gamma_1\sin\gamma_2\sin(\beta_1-\beta_2)$

$(\cos60^o-\tan15^o\sin60^o\sin45^o\sin(0^o-225^o))N_1+(\cos45^o-\tan30^o\sin60^o\sin45^o\sin(0^o-225^o)N_2+(0)F=114{,}650.25+1{,}400{,}000+3\cdot35272.7\cdot\sin60^o\sin45^o\sin(0^o-225^o)+2\cdot10521.9\cdot\sin60^o\sin45^o\sin(0^o-225^o)$

$(0.384)N_1+(0.457)N_2+(0)F=1569583.06$ [lb]

Solve these three equations and obtain the results:

$N_1=5823.6k$

$N_2=-1458.1k$

F=5983.8k for the primary wedge of the 2nd combination

2nd Combination: Secondary Wedge

Joint Set #1: N-S, 30°E
Joint Set #2: E-W, 60°S

The secondary wedge of the second combination is shown on the joint mesh in Figure 3.74 and on the joint map on the pile in Figure 3.75.

Volume of Wedge:

Use equation (3.32) to calculate the volume of the wedge.

$V_{block} \approx V_{pyramid} = a \cdot d/3$

where
a=area of a block on the surface
d=height of the wedge

As shown in Figure 3.74, the area of the block on the surface is just a rectangle, and thus

$$a = \left\| \frac{s_1 \cdot s_2}{\sin(\beta_1 - \beta_2)} \right\| = \left\| \frac{0.866D \cdot 0.433D}{\sin(90° - 0°)} \right\| = 0.375D^2$$

As shown in Figure 3.76, d=0.75D
V= a•d/3
=0.375D^2•0.75D/3=0.09375D^3
=11.72 ft^3

W=γ_r•V=171.6 lb/ft^3•11.72 ft^3=2010.94 lb

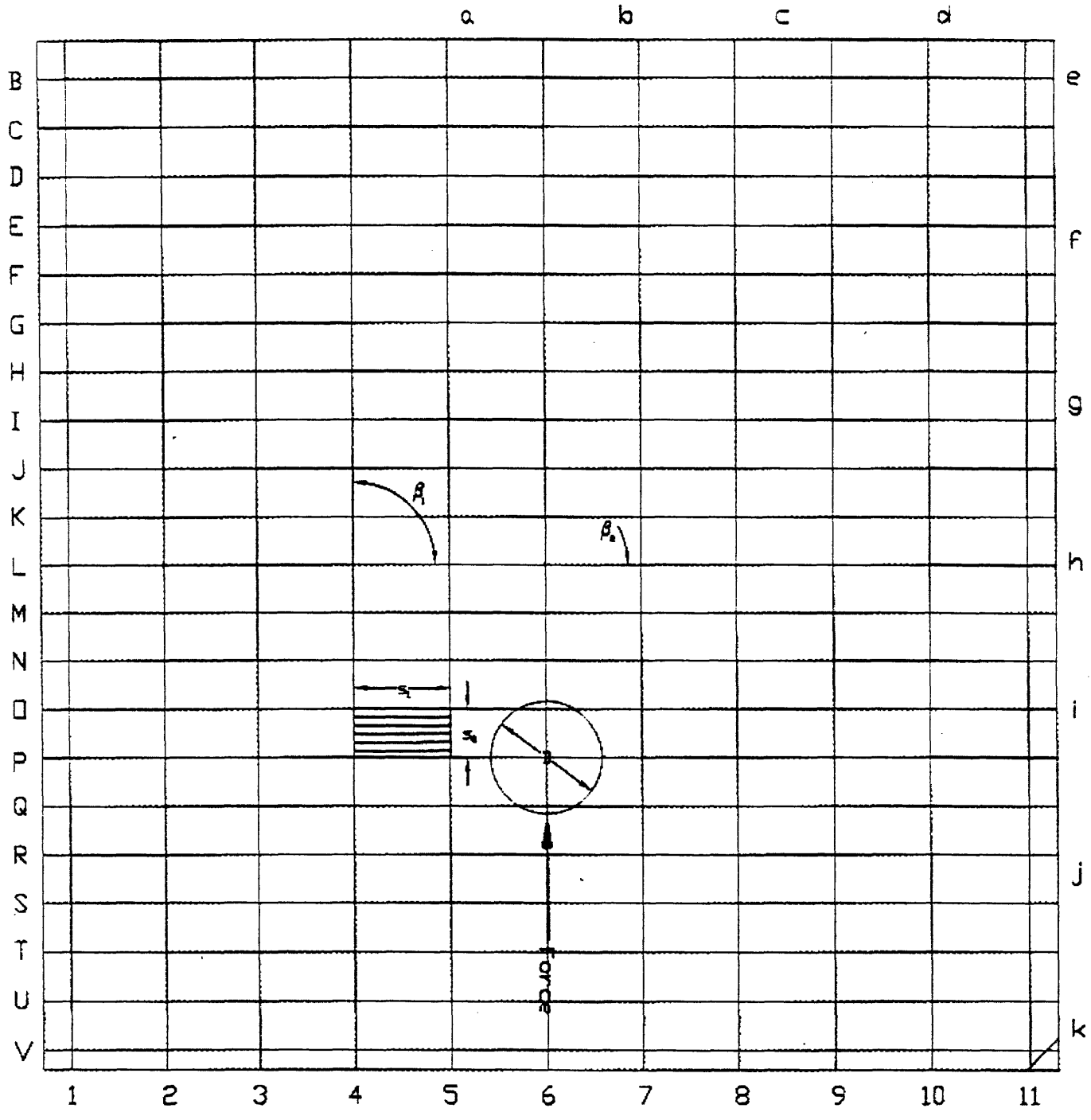

Figure 3.74 Secondary Wedge of 2nd Combination on the Joint Mesh

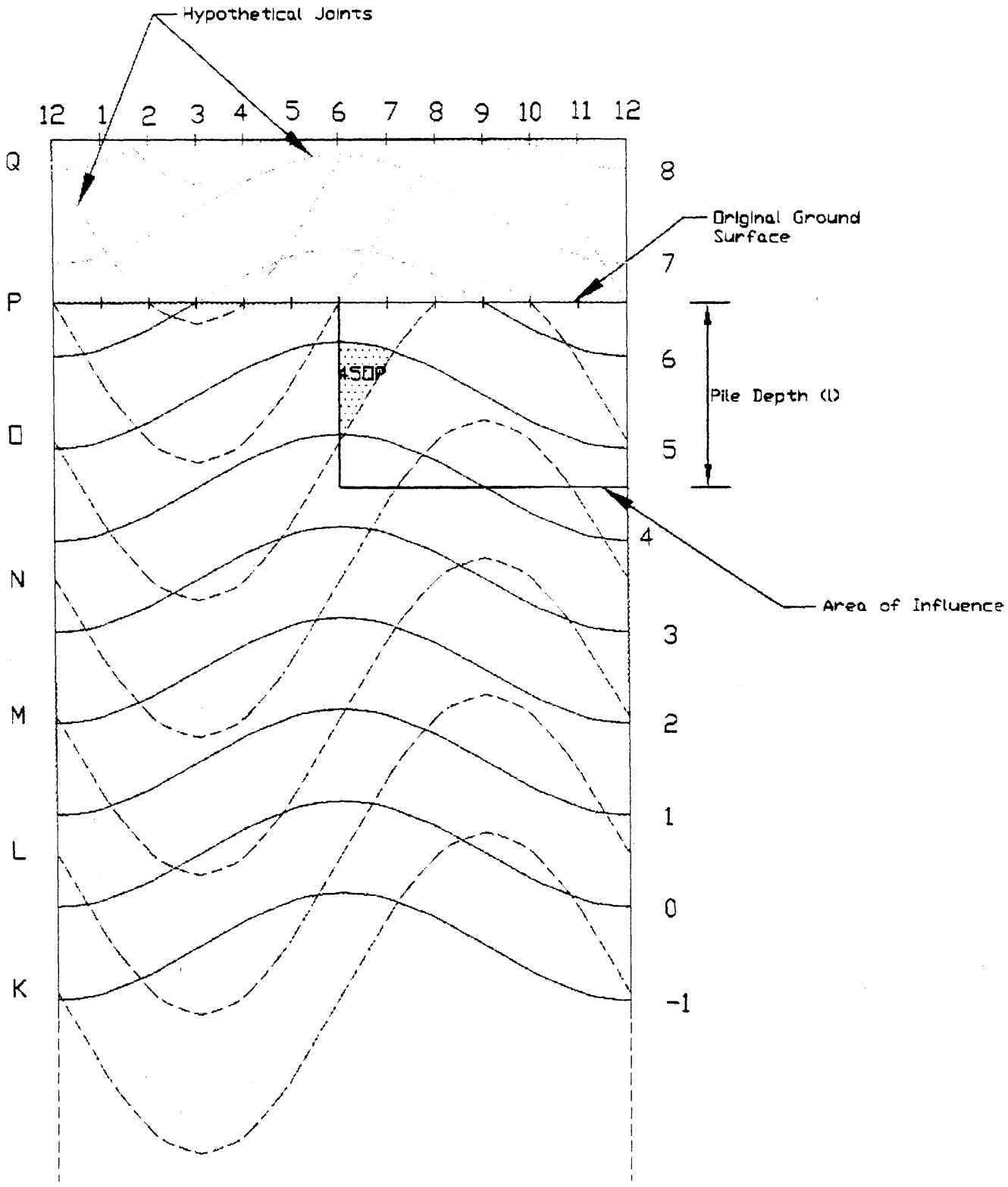

Figure 3.75 Secondary Wedge of 2nd Combination on the Joint Map

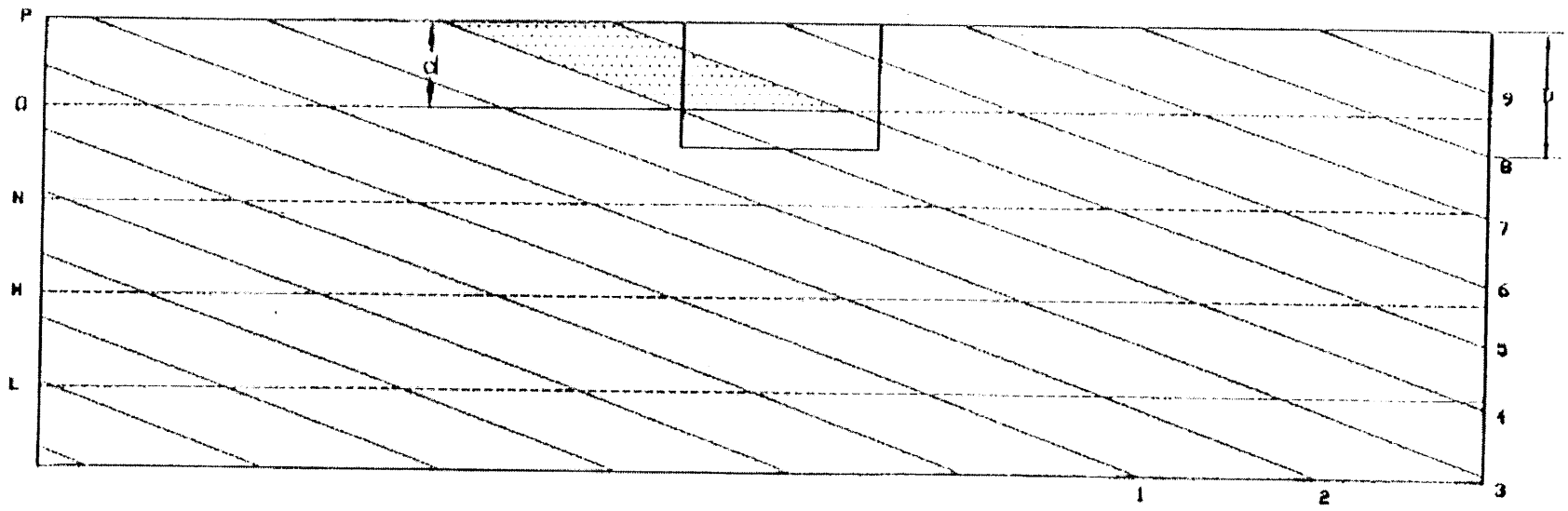

Figure 3.76 d's of Joint Faces of Block 45OP on a Joint Map on a Cutting Plane

Area of Faces:

Three faces on the secondary wedge, namely joint 4, 5, and O faces, need to be considered for shearing resistance. All three faces on the secondary wedge intersect not only the pile as shown in Figure 3.77 but also the vertical cutting plane as shown in Figure 3.78. Therefore, only equation (3.40) is necessary to calculate the area of these faces for each joint set:

$$A=\sum_{j=1}^{q}\frac{d_j w_j}{2\sin\gamma}=\sum_{j=1}^{q}\left[\frac{d_j}{2\sin\gamma}\bullet\left\|\frac{s_j}{\sin(\beta_1-\beta_2)}\right\|\right]$$

where
d_j=height of a face from bottom to the top of the face
γ=dip angle of the respective joint set
w_i=width of a face on the surface
β=angle measured counterclockwise from the x-axis to the strike line of the respective joint set
s_j=the horizontal spacing of the other joint set

For A_1 (joint set N-S, 30°E):
$\gamma=30°$ for joint set N-S, 30°E
$s_2=0.433D$ for joint set E-W, 60°S
$\beta_1=90°$ for joint set N-S, 30°E
$\beta_2=0°$ for joint set E-W, 60°S

As shown in Figure 3.79, $d=d_1=0.75D$ for joint 4 face and $d=d_2=0.21D$ for joint 5 face.

$$A_1=\frac{d_1}{2\sin\gamma}\bullet\left\|\frac{s_2}{\sin(\beta_1-\beta_2)}\right\|+\frac{d_2}{2\sin\gamma}\bullet\left\|\frac{s_2}{\sin(\beta_1-\beta_2)}\right\|$$

$$=\frac{0.75D}{2\sin 30°}\bullet\left\|\frac{0.433D}{\sin(90°-0°)}\right\|+\frac{0.21D}{2\sin 30°}\bullet\left\|\frac{0.433D}{\sin(90°-0°)}\right\|=0.416D^2=10.39ft^2=1496.4in^2$$

For A_2 (joint set E-W, 60°S):
$\gamma=60°$ for joint set E-W, 60°S
$s_1=0.866D$ for joint set N-S, 30°E
$\beta_1=90°$ for joint set N-S, 30°E
$\beta_2=0°$ for joint set E-W, 60°S

As shown in Figure 3.79, $d=d_1=0.75D$ for joint O face.

$$A_2=\frac{d_1}{2\sin\gamma}\bullet\left\|\frac{s_1}{\sin(\beta_1-\beta_2)}\right\|=\frac{0.75D}{2\sin 60°}\bullet\left\|\frac{0.866D}{\sin(90°-0°)}\right\|=0.375D^2=9.37ft^2=1350.0in^2$$

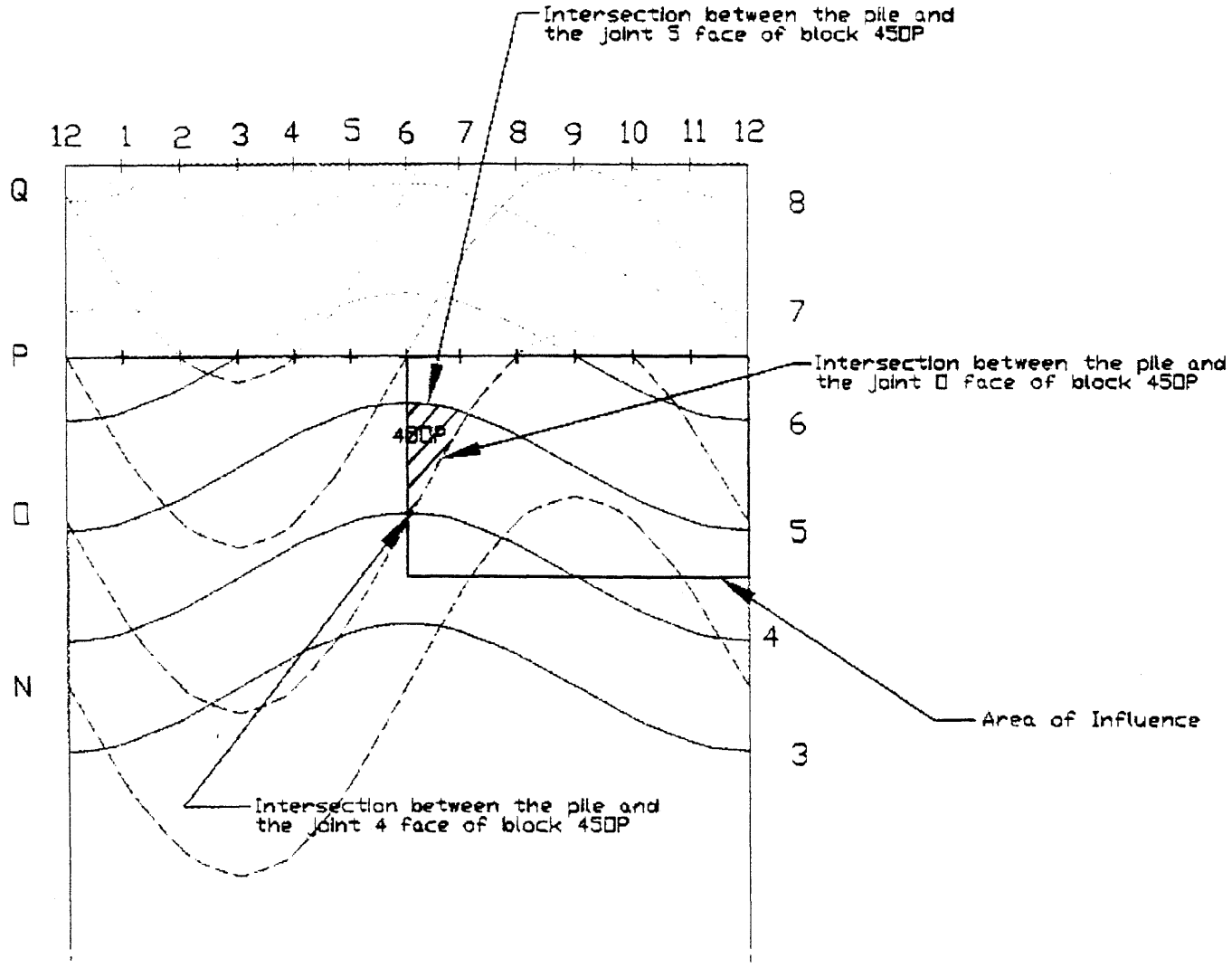

Figure 3.77 Block 45OP on a Joint Map on a Pile

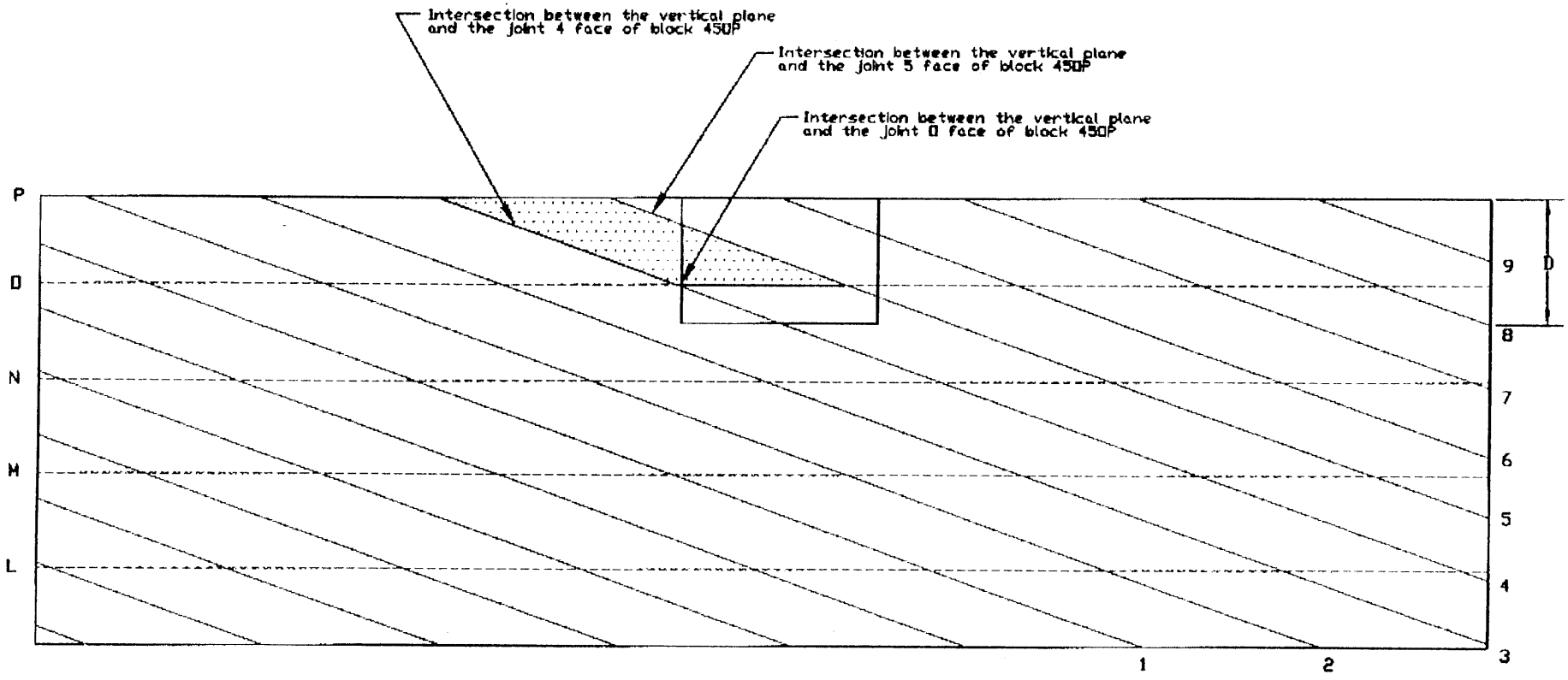

Figure 3.78 Grid 45OP on a Joint Map on a Cutting Plane

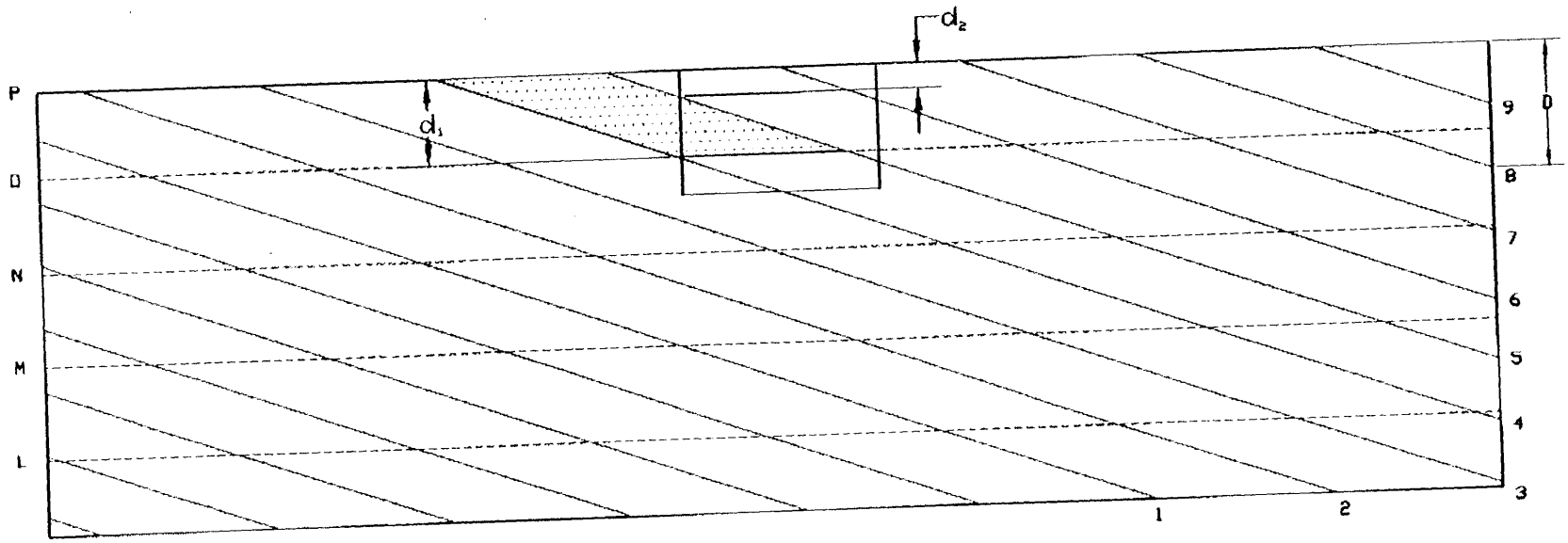

Figure 3.79 d's of Joint Faces of Block 45OP on a Joint Map on a Cutting Plane

Limit Equilibrium:

In the x-direction:

$(\sin\gamma_1\sin\beta_1-\tan\phi_1\sin\gamma_1\cos\beta_1\cos\gamma_2+\tan\phi_1\cos\gamma_1\sin\gamma_2\cos\beta_2)N_1+(\sin\gamma_2\sin\beta_2-\tan\phi_2\sin\gamma_1\cos\beta_1\cos\gamma_2+\tan\phi_2\cos\gamma_1\sin\gamma_2\cos\beta_2)N_2+(\cos\theta)F=c_1A_1\sin\gamma_1\cos\beta_1\cos\gamma_2-c_1A_1\cos\gamma_1\sin\gamma_2\cos\beta_2+c_2A_2\sin\gamma_1\cos\beta_1\cos\gamma_2-c_2A_2\cos\gamma_1\sin\gamma_2\cos\beta_2$

$(\sin30^\circ\sin90^\circ-\tan22.5^\circ\sin30^\circ\cos90^\circ\cos60^\circ+\tan22.5^\circ\cos30^\circ\sin60^\circ\cos0^\circ)N_1+(\sin60^\circ\sin0^\circ-\tan15^\circ\sin30^\circ\cos90^\circ\cos60^\circ+\tan15^\circ\cos30^\circ\sin60^\circ\cos0^\circ)N_2+(\cos90^\circ)F=2\bullet1496.4\bullet\sin30^\circ\cos90^\circ\cos60^\circ-2\bullet1496.4\bullet\cos30^\circ\sin60^\circ\cos0^\circ+3\bullet1350.0\bullet\sin30^\circ\cos90^\circ\cos60^\circ-3\bullet1350.0\bullet\cos30^\circ\sin60^\circ\cos0^\circ$

$(0.811)N_1+(0.201)N_2+(0)F=-5282.10$ [lb]

In the y-direction:

$(-\sin\gamma_1\cos\beta_1-\tan\phi_1\sin\gamma_1\sin\beta_1\cos\gamma_2+\tan\phi_1\cos\gamma_1\sin\gamma_2\sin\beta_2)N_1+(-\sin\gamma_2\cos\beta_2-\tan\phi_2\sin\gamma_1\sin\beta_1\cos\gamma_2+\tan\phi_2\cos\gamma_1\sin\gamma_2\sin\beta_2)N_2+(\sin\theta)F=c_1A_1\sin\gamma_1\sin\beta_1\cos\gamma_2-c_1A_1\cos\gamma_1\sin\gamma_2\sin\beta_2+c_2A_2\sin\gamma_1\sin\beta_1\cos\gamma_2-c_2A_2\cos\gamma_1\sin\gamma_2\sin\beta_2$

$(-\sin30^\circ\cos90^\circ-\tan22.5^\circ\sin30^\circ\sin90^\circ\cos60^\circ+\tan22.5^\circ\cos30^\circ\sin60^\circ\sin0^\circ)N_1+(-\sin60^\circ\cos0^\circ-\tan15^\circ\sin30^\circ\sin90^\circ\cos60^\circ+\tan15^\circ\cos30^\circ\sin60^\circ\sin0^\circ)N_2+(\sin90^\circ)F=2\bullet1496.4\bullet\sin30^\circ\sin90^\circ\cos60^\circ-2\bullet1496.4\bullet\cos30^\circ\sin60^\circ\sin0^\circ+3\bullet1350.0\bullet\sin30^\circ\sin90^\circ\cos60^\circ-3\bullet1350.0\bullet\cos30^\circ\sin60^\circ\sin0^\circ$

$(-0.104)N_1+(-0.933)N_2+(1)F=1760.70$ [lb]

In the z-direction:

$(\cos\gamma_1-\tan\phi_1\sin\gamma_1\sin\gamma_2\sin(\beta_1-\beta_2))N_1+(\cos\gamma_2-\tan\phi_2\sin\gamma_1\sin\gamma_2\sin(\beta_1-\beta_2))N_2+(0)F=W+P+c_1A_1\sin\gamma_1\sin\gamma_2\sin(\beta_1-\beta_2)+c_2A_2\sin\gamma_1\sin\gamma_2\sin(\beta_1-\beta_2)$

$(\cos30^\circ-\tan22.5^\circ\sin30^\circ\sin60^\circ\sin(90^\circ-0^\circ))N_1+(\cos60^\circ-\tan15^\circ\sin30^\circ\sin60^\circ\sin(90^\circ-0^\circ)N_2+(0)F=2010.94+0+2\bullet1496.4\bullet\sin30^\circ\sin60^\circ\sin(90^\circ-0^\circ)+3\bullet1350.0\bullet\sin30^\circ\sin60^\circ\sin(90^\circ-0^\circ)$

$(0.687)N_1+(0.384)N_2+(0)F=5060.56$ [lb]

Solve these three equations and obtain the results:

$N_1=-17.6k$

$N_2=44.6k$

F=41.6k for the secondary wedge of the 2nd combination

The ultimate lateral capacity (F_u) for the 2nd removable combination is

F_u=5983.8k+41.6k=**6025.4k**

The 2nd removable combination has lower ultimate lateral capacity (F_u=6025.4k).

As mentioned before, a math program can be used to solve the equations and to manipulate inputs and outputs easily. Matlab is run to solve the problem above, and the program for solving the matrix, inputs, and outputs are attached in the Appendix.

CHAPTER 4
SUMMARY, CONCLUSIONS, AND RECOMMENDATIONS

4.1 SUMMARY AND CONCLUSIONS

The analysis of the lateral load capacity of drilled shafts in jointed rock is divided into two parts: kinematics and kinetics. In kinematics, a removability theorem for a non-convex block by a pile was developed based on the block theory (Goodman and Shi, 1985). Then, the removability theorem of a combination of blocks by a pile was developed. A combination of blocks that is removable can then be selected for kinetic analysis. However, it is very difficult and time-consuming to check the removability of each individual block, and it is not easy to gain complete geological information around a pile. Therefore, it is assumed that joint sets are persistent and parallel to each other and have the same spacing. With these assumptions, a two-dimensional graphical method was developed to select possible combinations of removable blocks in a rock mass with two and three joint sets. This 2-D graphical method can easily be implemented with CAD programs such as AutoCAD or spreadsheet programs such as Excel.

In kinetics, the stability of a removable combination of blocks was analyzed with the limit equilibrium approach. Although the analysis is similar to slope stability analysis, it is made more complicated by the addition of a lateral force exerted by the pile and the vertical pile load exerted on the wedge. The analysis also considers the weight of the wedge, the shear resistance along the joints, and the vertical pile load exerted on the wedge. Analytical relations were developed to solve for ultimate lateral load capacity. These equations can be put into matrix form and can be easily solved by hand calculations or with math programs such as Matlab.

4.2 CONTRIBUTIONS

The major contributions of this thesis to the design of laterally loaded shafts in jointed rock are

1. A discontinuum model for analyzing laterally loaded shafts in jointed rock was developed: such a model did not exist so far.
2. Only easily constructed 2D figures are needed to solve the 3-dimensional design problem without changing the 3D nature of the problem.
3. Equations with few parameters can be solved easily to obtain the ultimate lateral load capacity.

4.3 RECOMMENDATIONS FOR FUTURE RESEARCH

Further work can be performed to advance the discontinuum model:

1. Tests should be run on laterally loaded shafts in jointed rock until failure to a) obtain results for comparison with the discontinuum model, b) find out the critical pile depth to diameter ratio (l/D) for which the pile behaves like a rigid body, and c) observe the failure mode to prove the validity of the model.
2. It is desirable to also solve design problems in a rock mass with more than three joint sets with techniques presented in the thesis, but this needs additional investigations.
3. Deformability of the rock mass and pile, the moment applied on the pile, and non-persistent, non-parallel, and randomly spaced joints might also be incorporated into the discontinuum model.
4. Stereonets might be used to determine if a removable combination of blocks is stable for a given force direction before kinetic analysis. This technique may save much time by reducing the number of removable combinations necessary for kinetic analysis.

APPENDIX

COMPUTATIONS BY MATLAB:

```
----------------------
Matrix:
----------------------
A(1,1)=sin(g1)•sin(b1)-tan(p1)•sin(g1)•cos(b1)•cos(g2)+
       tan(p1)•cos(g1)•sin(g2)•cos(b2)
A(1,2)=sin(g2)•sin(b2)-tan(p2)•sin(g1)•cos(b1)•cos(g2)+
       tan(p2)•cos(g1)•sin(g2)•cos(b2)
A(1,3)=cos(t)
B(1,1)=-(c1)•(A1)•sin(g1)•cos(b1)•cos(g2)-(c1)•(A1)•cos(g1)•sin(g2)•cos(b2)-
       (c2)•(A2)•sin(g1)•cos(b1)•cos(g2)-(c2)•(A2)•cos(g1)•sin(g2)•cos(b2)

A(2,1)=-tan(p1)•sin(g1)•sin(b1)•cos(g2)+tan(p1)•cos(g1)•sin(g2)•sin(b2)-
       sin(g1)•cos(b1)
A(2,2)=-tan(p2)•sin(g1)•sin(b1)•cos(g2)+tan(p2)•cos(g1)•sin(g2)•sin(b2)-
       sin(g2)•cos(b2)
A(2,3)=sin(t)

B(2,1)=(c1)•(A1)•sin(g1)•sin(b1)•cos(g2)-(c1)•(A1)•cos(g1)•sin(g2)•sin(b2)+
       (c2)•(A2)•sin(g1)•sin(b1)•cos(g2)-(c2)•(A2)•cos(g1)•sin(g2)•sin(b2)

A(3,1)=cos(g1)-tan(p1)•sin(g1)•sin(g2)•sin((b1)-(b2))
A(3,2)=cos(g2)-tan(p2)•sin(g1)•sin(g2)•sin((b1)-(b2))
A(3,3)=0
B(3,1)=W+P+(c1)•(A1)•sin(g1)•sin(g2)•sin((b1)-(b2))+
       (c2)•(A2)•sin(g1)•sin(g2)•sin((b1)-(b2))

f=A\B

end
```

Two-Joint-Set System:
Joint Set N-S, 30°E
Joint Set E-W, 60°S

Inputs:

```
clear
t=pi

p1=pi/8
g1=pi/6
c1=2
b1=pi/2

p2=pi/6
g2=pi/3
c2=3
b2=0

P=1400000

A1=20264.4
A2=16199.5

W=53925.3

end
```

Outputs:

A =

0.8107	0.4330	-1.0000
-0.1036	-1.0104	0.0000
0.6867	0.2500	0

B =

1.0e+06 *

-0.0668

0.0223
1.4925

f =

1.0e+06 *

2.2662
-0.2543
1.7938

Three-Joint-Set System:
Joint Set N-S, 30°E
Joint Set E-W, 60°S
Joint Set N45°E, 45°NW

Primary Wedge of the 1st Combination:
Joint Set #1: N-S, 30°E
Joint Set #2: E-W, 60°S

Inputs:

```
clear
t=pi/2

p1=pi/8
g1=pi/6
c1=2
b1=pi/2

p2=pi/12
g2=pi/3
c2=3
b2=0

P=1400000

A1=21043.8
A2=29699.1

W=66988.35

end
```

Outputs:

A =

0.8107	0.2010	0.0000
-0.1036	-0.9330	1.0000
0.6867	0.3840	0

B =

1.0e+06 *

-0.0984
0.0328
1.5238

f =

1.0e+06 *

-1.9853
7.5187
6.8423

Secondary Wedge of the 1st Combination:
Joint Set #1: E-W, 60°S
Joint Set #2: N45°E, 45°NW

Inputs:

```
clear
t=pi/2

p1=pi/12
g1=pi/3
c1=3
b1=0

p2=pi/6
g2=pi/4
c2=2
b2=5*pi/4

P=0

A1=2116.4
A2=1096.4

W=2481.3
```

```
end


--------------------
Outputs:
--------------------

A =

   -0.2311   -0.9979    0.0000
   -0.9330    0.3557    1.0000
    0.3840    0.4571         0


B =

   1.0e+03 *

    7.3664
    2.1355
    6.1801


f =

   1.0e+04 *

    3.4353
   -1.5337
    3.9642
```

Primary Wedge of the 2nd Combination:
Joint Set #1: E-W, 60°S
Joint Set #2: N45°E, 45°NW

Inputs:

```
clear
t=pi/2

p1=pi/12
g1=pi/3
c1=3
b1=0

p2=pi/6
g2=pi/4
c2=2
b2=5*pi/4

P=1400000

A1=35272.7
A2=10521.9

W=114650.25

end
```

Outputs:

A =

-0.2311	-0.9979	0.0000
-0.9330	0.3557	1.0000
0.3840	0.4571	0

B =

1.0e+06 *

```
   0.1094
   0.0317
   1.5696


f =

   1.0e+06 *

   5.8236
  -1.4581
   5.9838
```

Secondary Wedge of the 2nd Combination
Joint Set #1: N-S, 30°E
Joint Set #2: E-W, 60°S

```
--------------------
Inputs:
--------------------

clear
t=pi/2

p1=pi/8
g1=pi/6
c1=2
b1=pi/2

p2=pi/12
g2=pi/3
c2=3
b2=0

P=0

A1=1496.4
A2=1350.0

W=2010.94

end
```

Outputs:

A =

0.8107	0.2010	0.0000
-0.1036	-0.9330	1.0000
0.6867	0.3840	0

B =

1.0e+03 *

-5.2821
1.7607
5.0606

f =

1.0e+04 *

-1.7574
4.4607
4.1560

REFERENCES

Amir, J. M. (1986). *Pilling in Rock*, A. A. Balkema Publishers, Rotterdam, Netherlands.

Gabr, M. A. (1993). Discussion on "Analysis of laterally loaded shafts in rock." *J. Geotech. Engrg.*, ASCE, 119(12), 2015-2018.

Goodman, R. E. (1980). *Introduction to Rock Mechanics*, Wiley, New York.

Goodman, R. and Shi, G. (1985). *Block Theory and Its Application to Rock Engineering*, Prentice-Hall, Inc., Englewood Cliffs, New Jersey.

Hoek, E. and Bray J. (1981). *Rock Slope Engineering*, Institution of Mining and Metallurgy, London.

Matlock, H. (1970). "Correlations for design of laterally loaded piles in soft clay." *Proc., 2nd offshore Technol. Conf.*, Offshore Technology Conference, Houston, Tex., 1, 577-594.

Matlock, H., and Reese, L. C. (1960). "Generalized solutions for laterally loaded piles." *J. Soil Mech. Found. Div.*, ASCE, 86(5), 63-91.

Matlock H., and Ripperberger, E. A. (1958). "Measurement of soil pressure on a laterally loaded pile." Proc. ASTM, 58, 1245-1259.

Pare, E. G. (1965). *Descriptive Geometry*, Macmillan, New York.

Shi, G. (1982). "A geometric method of stability analysis of discontinuous rocks," *Scientia Sinica*, Vol. XXV, No. 1, pp. 125-143.

Shi, G. and Goodman, R. (1981). "A new concept for support of underground and surface excavations in discontinuous rocks based on a keystone principle," *Proc. 22nd U.S. Symposium on Rock Mechanics*, Massachusetts Institute of Technology, Cambridge, Mass., pp. 290-296.

Wyllie, D. C. (1992). *Foundations on Rock*, E & FN SPON.